

# STUDIES ON CHROMIUM WHITE CAST IRONS

THE THESIS SUBMITTED FOR  
THE AWARD OF THE DEGREE  
OF

DOCTOR OF PHILOSOPHY  
IN  
ENGINEERING

BY  
N. S. POONAWALA

METALLURGICAL ENGINEERING DEPARTMENT  
INDIAN INSTITUTE OF TECHNOLOGY  
KHARAGPUR - 721302 INDIA

1991

CERTIFICATE

This is to certify that the thesis entitled "STUDIES ON CHROMIUM WHITE CAST IRONS" being submitted by Shri Nirav S Poonawala for Ph.D. degree (Engineering), is a record of bonafide research work carried out by him in the Metallurgical and Mechanical Engineering Departments at the Indian Institute of Technology, Kharagpur, under our guidance and supervision. In our opinion, the work fulfils the requirement for which it is being submitted.

The work incorporated in this thesis has not been submitted to any other University or Institute for the award of degree or diploma.

*A.K. Chakraborty* 30.12.91.

Dr. A.K. Chakraborty  
Professor  
Metallurgical Engg. Deptt.  
I.I.T., Kharagpur

*Chattopadhyay* 30.12.91

Dr. A.B. Chattopadhyay  
Professor  
Mechanical Engg. Deptt.  
I.I.T., Kharagpur

Place: IIT, KHARAGPUR  
Dated: 27 December 1991

## ACKNOWLEDGEMENTS

Coming for research work at Kharagpur (Eastern India) from Bombay (Western India) was an experience in itself, like an East-West cultural encounter. Kharagpur has an advantage of having in its vicinity, major steel plants, metallurgical industries and National Laboratories.

I am thankful to the Principal and Management of my parent organisation, Victoria Jubilee Technical Institute (VJTI) as well as Ministry of H.R.D (QIP programme), Govt. of India for giving me this opportunity of research work for the Ph.D under QIP.

I wish to convey my heartiest thanks to Prof. Dr. A.K.Chakraborty and Prof. Dr. A. B. Chattopadhyay (Mechanical Engg.), not only for constantly guiding me but encouraging and giving me moral support throughout my work. They supported me by their trinity of qualities of Guide, Friend and Philosopher. Throughout my work, I got friendly cooperation from Prof. U.K.Chatterjee, Late Prof. S. C. Sircar, Prof. P.G.Mukunda, Dr. S.B.Sarkar, Prof. M. Chakraborty, Dr. A. Basak, Dr. S.C.Panigrahi, Dr. K.K.Roy and many other colleagues of this and other departments.

I am thankful to all the staff members of Metallurgical & Mechanical Engineering Departments for their kind cooperation; particularly to Kamalda, Mr. Samanta, Ashok Jha, Mr. Pattanayak, Mr. Sripadababu, Mr. Karmakar, Mr. Jena, Mr. Banerjee, Kalaambabu, Mr. Mahato, Baghbabu, Bhuniyababu etc. Thanks are due to Dineshbabu, Sealbabu and Khudiram for their

help. The support of Mr. Lakshmanan and Mr. Sudhir Datta and others of CWISS was valuable. I got able support of staff from Machine Training Shop/Welding Shop during cutting trials.

CRF(Central Research Facility) was my workplace for a long time during my stay at IIT, Kharagpur. The friendly co-operation I received from Mitra Babu, Das brothers, Mr. Mirdyya and others can not be expressed in words.

I wish to convey my sincere thanks to Mr. V.S.Parikh and Dr. R.H.G.Rao of Mukand Ltd. (Bombay) for the help in spectrographic analysis; Dr. B. Prasad of Research and Development Center for Iron and Steel of SAIL (Ranchi) for nitrogen analysis and Dr. Paramguru of Regional Research Laboratory (Bhubaneswar) for potentiostatic studies. Assistance rendered by Dr. Anjan Pradhan and Mr. Sukomal Ghosh, Scientists of National Metallurgical Laboratory (Jamshedpur) in XRD and other analysis work were most valuable and is gratefully acknowledged.

Mr. Banerjee and others of QIP office were always ready in helping. Mr. Jana, Mr. Bera, Mr. Prasad and Mr. Sardar of our office were quite cordial. I owe much thanks to all of them.

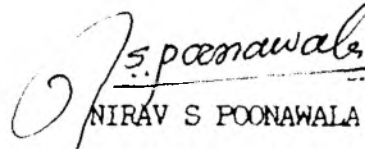
There were many Research Scholar friends who without any reluctance, extended their helping hands in my experimental work. I can not miss to mention Mr. Soumitra Pal, Mr. Chandan Sikdar, Mr. Sharad Babu, Mr. Kalyan

Chakraborty, Mr. Jib Nath Jha, Mr. Pattanayak, and others.

Thanks are due to Mr. Ashis for computer typing and Mr.C.Mukherjee for neat drafting work.

We were fortunate to have many good friends in and around IIT, who made our stay a pleasant and memorable experience. I am specially thankful to Mr. G.C.Jana and his family members, Mr. Kamran and family and Prof. Barve and his family members for their homely support.

My wife Reshma, son Adil, daughter Alisha and housemaid TataAnna kept me in good mood. God's grace and Bahauallah's blessings were all the time with me; I must confess.

  
NIRAV S POONAWALA

IIT, KHARAGPUR

DATED:30 Dec.1991

## PREFACE

"My best is none too good" said Don Coppel\*.

The work attempted here also indicates this point and proves that it is possible to do the job in a better way.

One can go into more depth in a narrower area of the research presented here. For better quality management; quantitative analysis is a must. Though the present research is more qualitative in nature, attempts have been made to present quantitative data wherever possible.

The best final product\* requires the complete integration of the design (mechanical as well as material), manufacturing and management by a total system approach. This may be true even in the development of a new material, such as, in the present case. Whatever shortcomings are found, may be attributed to the lack in the above factors; in present case, precisely to the personal constraints. The suggestions to improve are most welcome.

\* From the "Handbook of Product Analysis" by N S Poonawala, published by JEMECONS (Bombay) in August 1986.

## BIODATA

Name : Nirav S. Poonawala

Born on : 3rd June 1945 at Godhra(Gujrat)

Qualification : B.E.(Metallurgical Engg.), Poona University, 1967.  
M.E.(Foundry Research), Poona University, work carried out at R&D Centre of Mukand Iron & Steel Works Ltd. Bombay, 1977.

Affiliations : Member, ISME (Indian Society of Manufacturing Engineers); SME(USA) ISTE, PMAI, ISTD.

Presently : Asst. Professor in the Faculty of Production Engineering, V.J.T.I. (Bombay) and Consulting Industrial Engineer.

Experience : 24 years' combined teaching, consultancy and industrial experience in the production, R&D, product development and marketing etc.  
  
Worked in the C.I/Malleable/Steel Foundries of Powermaster engg./ Bombay Malleables/KT Steel founders. Training in Godrej & Boyce, Garlick Engg., Precision Bearings, Sandvik Asia etc.

Publications : Handbook of Product Analysis published by 'Jemecons' in August 1986. Various articles published in industrial journals.

Seminars/  
Conferences : Presented papers/lectures in various seminars/societies and Institutions.

Areas of interest: Composite Materials, Coatings, Entrepreneurship, Product Management, Quality with Economy.

## ABSTRACT

The effects of alloying 12% chromium cast irons with nitrogen alone as well as with nitrogen and titanium together on the as cast microstructure, phase transformations during heat treatment, abrasive wear resistance and its performance as cutting tools have been investigated. Nitrogen was added both as nitrided manganese and nitrided chromium. The experimental techniques used included hardness and microhardness measurements, light, scanning and transmission electron microscopy, electron microprobe analysis, TMA, X-ray diffraction analysis, corrosion tests, sliding abrasive wear test against a bonded alumina wheel under load, and machining trials with chromium cast iron turning tools.

In half of the fourteen experimental alloy irons, the Cr/C ratio ranged between 2.9 to 3.6. In the remaining half, the Cr/C ratio was between 4.1 to 4.6. Nitrogen and titanium additions to the group of alloys having lower Cr/C ratio (2.9-3.6) partially modified the eutectic carbide morphology into discontinuous rods, although other types of eutectics were also observed. Nitrogen stabilised a high volume fraction of retained austenite in irons with relatively higher Cr/C ratio (4.1 and above), but did not modify their carbide morphology appreciably. In the sand cast alloys of the former group, both  $\text{Cr}_7\text{C}_3$  and  $\text{Cr}_{23}\text{C}_6$  carbides were detected. On raising the Cr/C ratio to 4.1 and above, the eutectic carbide became primarily  $\text{Cr}_7\text{C}_3$  type. On destabilisation of the retained austenite, mainly  $\text{Cr}_{23}\text{C}_6$  type carbide precipitated in either group of chromium cast irons.

In a chill cast nitrogenated alloy of Cr/C ratio  $\approx 4.1$ , a transition from  $Cr_{23}C_6$  to  $Cr_7C_3$  type carbide was found to occur on prolonged homogenisation at  $900^{\circ}C$ . In general, the retained austenite content in as quenched nitrogenated samples increased on extending the soaking period in the temperature range  $900-950^{\circ}C$ . Nitride and carbonitride precipitates were detected in alloys with both high and low Cr/C ratios. During isochronal and isothermal tempering of both as cast and as quenched samples containing N +Ti or N+Al, secondary hardening occurred at  $600^{\circ}C$ . This was caused by the precipitation of  $Ti_2N$  or AlN as the case may be.

The corrosion resistance of as cast austenitic chromium cast irons containing nitrogen alone or nitrogen and titanium together were found to be only marginally inferior to a plain pearlitic chromium cast iron in both 1N HCl and 1M NaCl solutions. The effect of nitrogen and titanium additions on wear resistance however depended upon the retained austenite content and the applied load. A high retained austenite content ( $\approx 40\%$ ) increased wear appreciably, while low levels of retained austenite ( $\approx 10\%$ ) improved wear resistance considerably. In the intermediate ranges, workhardening of the retained austenite decreased wear rate, but ultimately the total wear depended upon the applied load and the actual retained austenite content.

Quenched and tempered chromium cast iron cutting tools prepared from sand cast alloys (Cr/C 4.10 and above) could machine a 0.25% C steel bar at a speed of 40m/min and feed of 0.12 mm/rev., but suffered brittle failure at higher speed-feed combinations. Alloying with nitrogen and titanium

improved their performance to some extent. Presence of microshrinkage pores was primarily responsible for premature failure of these tools. A chill cast tool of Cr/C ratio 4.1, however performed satisfactorily when its austenite content was controlled around 20%. This particular tool superseded the performance of a HSS tool at 50m/min speed and 0.16 mm/rev. feed rate.

Key words:

Wear resistance, corrosion, carbonitride, retained austenite, microshrinkage, work hardening.

## CONTENTS

Certificate	
Acknowledgements	i
Preface	iv
Biodata	v
Abstract	vi
Contents	ix
	Page Nos
Chapter one	
Introduction	1-3
Chapter two	
Literature Review	4-70
2.1 Introduction	4
2.2 Grades of Chromium White Cast Irons	6
2.3 The role of individual alloying elements	6
2.4 Substitute grade of CWCI	21
2.5 Solidification and Carbide Morphology	27
2.5.1 Solidification	27
2.5.2 Carbide morphology	34
2.5.3 Identification of carbides	40
2.6 Heattreatments, Microstructures and Hardenability	42
2.6.1 As cast microstructures	43
2.6.2 Microstructures after heattreatment	44
2.6.3 Hardenability	44
2.6.4 Cooling rate	47
2.6.5 Tempering	47
2.7 Retained austenite and its measurement	47

2.8 Wear studies	51
2.8.1 Introduction	51
2.8.2 Mechanisms of wear	56
2.9 Fracture toughness tests	61
2.10 Corrosion tests	66
2.11 CWCI as a cutting tool material	69

### Chapter three

Experimental Procedure	71-86
3.1 Melting and casting	71
3.2 Metallography and heattreatment	74
3.3 Thermo Mechanical Analysis(TMA)	77
3.4 X-ray diffraction analysis (XRD)	78
3.5 Transmission Electron Microscopy (TEM)	78
3.6 Wear Studies	79
3.7 Machining Trials	79
3.8 Scanning Electron Microscopy (SEM)	85
3.9 Corrosion tests	85

### Chapter four

Results	87-179
4.1 As cast structures and response to heat treatment	87
4.1.1 Nitrogen addition	87
4.1.2 As cast microstructure	87
4.1.3 X-ray diffraction analysis and microhardness	91
4.1.4 Scanning electron microscopy	99
4.1.5 Microprobe analysis (EDAX/EPM)	105

4.1.6 Quenching and tempering treatment and dilatometry (TMA)	107
4.1.7 Transmission Electron Microscopy (TEM)	123
4.1.8 Corrosion tests	131
4.2 Wear tests	138
4.3 Machining trials with Chromium White Cast Iron Tools	160
Chapter five	
Discussion	180-198
5.1 Metallurgical aspects	180
5.1.1 As cast microstructures and carbide morphology	180
5.1.2 Heattreatments	184
5.1.2.1 Destabilisation	184
5.1.2.2 Tempering	186
5.2 Corrosion characteristics	188
5.3 Wear behaviour	189
5.4 Evaluation of CWCI tools in turning experiments	194
Chapter six	
Conclusions	199-201
References	202-214
14th AIMTDR Conference Paper	

## INTRODUCTION

Chromium cast irons are extensively used for the manufacture of wear resistant components like grinding balls, liners etc. Among the various standard grades of chromium cast irons, the 12% Cr grade is the cheapest and is normally used for the manufacture of small diameter grinding balls used in less arduous working conditions. The present exercise was undertaken to examine the influence of alloying 12% Cr cast iron with nitrogen (added as nitrided manganese or nitrided chromium) alone or together with titanium on its metallurgical properties and wear resistance.

The concept of alloying chromium cast irons with manganese and titanium is not new. Manganese additions to chromium cast irons is known to increase the hardenability [129], while titanium forms hard carbides and carbonitrides [38] and refines austenite dendrites [48]. The principle of saturating the ferrous matrix with nitrogen to improve wear resistance has been in practice for a long time. The ageold processes of nitriding and carbonitriding are based on this principle. A relatively recent application of the nitride surface coating principle is the PVD or CVD coating of TiN on cutting tools and other substrates. Nitrogen has very limited solubility in  $\alpha$ -iron. Nitrogen diffusing into the matrix beyond the solubility limit usually precipitates out. The

common alloying elements present in nitriding grade steels are aluminium, chromium, and molybdenum which form hard finely dispersed nitrides and carbonitride precipitates. Titanium, though not commonly used, is almost as powerful a nitride former as aluminium. Because of the precipitation of such hard nitride and carbonitride particles the wear resistance of the nitrided surface is greatly increased. But the nitriding process is basically a solid state diffusion process. Hence the depth of the nitrided layer is usually of the order of few hundred microns. The vapour phase deposition of TiN is a costly process and in this case the nitride layer is of the order of few microns only. Because of these potential limitations of the solid state nitriding or vapour phase deposition processes, these processes have not found any application in the production of grinding balls, liners etc. which are exposed to highly abrasive wear situations. The powerful effects of a low cost alloying element like nitrogen nevertheless remains attractive. To overcome the limitations of solid state or vapour phase deposition processes, an attempt has therefore been made in the present exercise to add nitrogen to chromium cast irons in the melt itself in the form of nitrided manganese or nitrided chromium.

Nitrogen has long been used as an alloying element in chromium nickel stainless steels primarily as an austenite stabiliser. Of late, its beneficial effects in resisting sensitisation and improving corrosion resistance of stainless steels have come to light [141]. In grey cast irons, small doses of nitrogen addition have been observed to cause

compaction of graphite. In contrast, however, the effect of nitrogen on solidification, heat treatment and wear resistance of chromium cast irons has not received adequate attention of investigators. In one of the limited investigations carried out at IIT, Kharagpur [117], nitrogenated 12% chromium cast iron tools were found to possess better air hardenability and tool life than plain chromium cast irons tools. In view of such encouraging results, it was decided to explore the effect of nitrogen addition to chromium cast irons in greater details. Since titanium is a hard nitride former and also a grain refiner, it was further decided to add titanium in combination with nitrogen in some of the alloys. The specific objects of the present investigation were to study the effect of nitrogen addition alone as well as in combination with titanium to 12% chromium cast irons on

- (1) the austenite dendrite size and carbide morphology in as cast state;
- (2) the amenability of 12% Cr cast irons to hardening by forced air draft;
- (3) the phase transformations during conditioning treatment at 900°C and above, and on quench-temper treatment;
- (4) the abrasive wear resistance;
- (5) the performance of chromium cast irons as cutting tools;
- (6) corrosion resistance of nitrogenated austenitic chromium cast irons

## LITERATURE REVIEW

### 2.1 Introduction

White Cast Irons have traditionally been used for wear resistance applications, ~~since long~~. The carbides in the microstructure of White Cast Irons (WCI) depending on their type, morphology and volume fraction, provide the hardness required for crushing materials without degradation. The supporting matrix structure can be controlled by alloy content and/or heat treatment to develop pearlitic, bainitic, austenitic or martensitic structures to provide the most cost effective balance between abrasive wear resistance and toughness[1]. However, during 1920-30, alloy cast irons were developed to get improved mechanical properties like UTS, Y.S., Impact Strength etc. This process of search for new improved cast irons opened up a whole new field of alloy cast irons, and a series of new specifications for specific applications like heat resistance, corrosion resistance and wear resistance were developed.

To improve these WCI, Becket suggested a 27% Cr, 2.75% C, WCI. This alloy showed the structure of eutectic carbide in a matrix of 'sorbite' later claimed to be martensite. The microhardness of  $M_7C_3$  carbide was higher i.e. 1300-1800  $H_V$  compared to  $M_3C$  having 900-1000  $H_V$ . Thus this alloy WCI with

sorbitic matrix resulted in a more wear resistant WCI than unalloyed WCI.

Metallurgical work on Chromium White Cast Irons dates back to 1917, when the first patent was filed for a HCWCI (high chromium white C.I.) [2]. This alloy is extensively used in the mining & mineral processing industries and contains 25-30% Cr, 1.5-3.0% C, 0-3.0% Si in a Fe-base. In the 1960's Abex Corporation (USA) undertook an exhaustive series of alloying experiments to develop optimum abrasion resistance in HCWCI. They investigated Ni, Mo, Mn, Si & Cr as alloying elements and developed a patented alloy 'Paraboly'. However, original HCWCI still was widely used [3].

According to Dodd [4] and Durman [5], further improvement of CWCI was delayed by the development of a Ni-Cr martensitic WCI, Ni-hard I around 1930. Further development of wear-resistant alloy white irons occurred in the early 1950's with the advent of Ni-hard IV, also called Eutectic Ni-hard [6].

The development of the 27% Cr WCI was delayed by the requirement of electric melting. Moreover, this iron lacked hardenability, giving pearlitic matrix and shorter service life (compared to Ni-hard I). Mo was added to CWCI in the late 1930's, leading eventually to 15 Cr-3 Mo alloy, having better hardenability and comparable wear resistance. Later modifications resulted in the development of 20 Cr Mo irons in the later 1960's, including the 'Paraboly' [7] by Abex Corporation.

From the papers published in various journals and transactions, it seems that the interest in CWCI (Chromium

W.C.I) has not been reduced but more and more research continues in the field [8], primarily due to:

- (1) CWCI has offered an economic substitute for Hadfield steel and continues to be so.
- (2) the challenge of improved toughness and modification of carbide morphology still persists;
- (3) modifications in properties by the addition of inoculants in small amounts in the ladle, or microalloying offer a variety of interesting propositions and useful applications.

## 2.2 Grades of Chromium White Cast Iron (CWCI)

There are a few grades of CWCI used for abrasion resistance applications. Some of them are shown in table 2.1 and table 2.2.

## 2.3 The Role of Individual Alloying Elements

The Chemical composition plays an important role in case of abrasion resistant materials, the reason being that these materials require an optimum balance of abrasion resistance and toughness. The effects are described in tabular form (table No. 2.3) and further discussion follows.

The following properties needed in the final product must be kept in mind while selecting the composition.

- (1) Good abrasion resistance
- (2) Adequate toughness.
- (3) Sufficient hardenability for response to heat treatment

The effects of some of the important alloying elements have

Table 2.1 Ranges of alloy content for various types of abrasion resistant WCI

Description	Composition wt% (a)								
	Tc(b)	Mn	P	S	Si	Ni	Cr	Mo	Cu
Low C white iron(d)	2.2 to 2.8	0.2 to 0.6	0.15	0.15	1.0 to 1.6	1.5	1.0	0.5 (e)	
High-C, low Si white iron	2.8 to 3.6	0.3 to 2.0	0.30	0.15	0.3 to 1.0	2.5	3.0	1.0 (e)	
Malleable white iron	2.2 to 2.5	0.3 to 0.5	0.15	0.15	1.0 to 1.6	-	-	-	-
Martensitic nickel-chromium iron	2.5 to 3.7	1.3	0.30	0.15	0.8	2.7 to 5.0	1.1 to 4.0	1.0	-
Martensitic nickel, high-chromium iron	2.5 to 3.6	1.3	0.10	0.15	1.0 to 2.2	5 to 7	7 to 11	1.0	-
Martensitic chromium-molybdenum	2.0 to 3.6	0.5 to 1.5	0.10	0.06	1.0	1.5	11 to 23	0.5 to 3.5	1.2
High-chromium iron iron	2.3 to 3.0	0.5 to 1.5	0.10	0.06	1.0	1.5	23 to 28	1.5	1.2

TC = total carbon \* Cu may replace all or part of the Ni

Table 2.2 Mechanical Properties of Standard Martensitic  
WCI ( From ASTM A 532-75a)

Class	Type	Designation	Hardness, HB				Typical maximum section thickness	
			Min. values		Max. value		mm	in.
			Sand cast	Chill cast	Hardened	Annealed		
I	A	Ni-Cr-HC	550	600	--	--	200	8
I	B	Ni-Cr-LC	550	600	--	--	200	8
I	C	Ni-Cr-GB	550	600	--	--	75(b)	3*
I	D	Ni-Hi-Cr	550	500	600		300	12
II	A	12% Cr	550	--	600	400	25(b)	1*
II	B	15% Cr-Mo-LC	450	--	600	400	100	4
II	C	15% Cr-Mo-HC	550	--	600	400	75	3
II	D	20% Cr-Mo-LC	450	--	600	400	200	8
II	E	20% Cr-Mo-HC	450	--	600	400	300	12
III	A	25% Cr	450	--	600	400	200	8

\* Ball diameter

TABLE 2.3 - EFFECT OF ALLOYING ELEMENTS PREFERRED IN  
WHITE CAST IRONS/STEELS

ELEMENT	$\alpha$ - Ferrite Stabilizer	$\gamma$ - Austenite Stabilizer	Graphitizer	Carbide forming tendency	Hardena-bility	Partitions	Other Effects/Application
Cr	-	-	-	Strong	↑	Mostly to Carbide	(1) Eutectic C ↑ (2) T.S. ↑ (3) Hardness ↑ (4) Prevents free ferrite (5) Machinability ↑ (6) Resistant to corrosion ↑ (7) Refines pearlite and Hardens (8) Improves wear resistance (9) Resists oxidation at high temperatures.
Mn	-	Strong	-	Mild Cr > Mn > Fe	Markedly at low cost ↑	Non established. more in $\gamma$	(1) Deoxidizer (2) Retards $\gamma$ transformation (3) Refines pearlite and Hardens (4) Induces air hardening character (If > 1.8%) (5) Expected to improve wear resistance.
Cu	-	Mild	Mild (0.2 - 0.35 of Si)	-	When in solution ↑	Mostly to Austenite	(1) Solubility limited upto 3.5% (PPT if more) (2) Eutectic C ↓ (3) Refines Pearlite and Hardens (4) Fluidity ↓ (5) Ferrite Hardens (6) IS ↑ (7) Suppresses free ferrite formation (8) Resistant to Corrosion ↑ (9) Pearlite former and Stabilizer (10) Indirectly improves wear resistance

TABLE 2 (Contd..)

ELEMENT	$\alpha$ - Ferrite Stabilizer	$\gamma$ - Austenite Stabilizer	Graphitizer	Carbide forming tendency	Hardening	Partitions	Other effects/Application
Ni	-	Strong	Mild (0.3 of Si)	Less than Fe	Mild	Mainly to Austenite	(1) Fluidity $\uparrow$ (2) Eutectic C $\downarrow$ (3) Transformation rate $\uparrow$ (4) T S $\uparrow$ (5) Machinability improves (6) Refines pearlite and hardens (7) Free ferrite formation $\downarrow$ (8) Corrosion resistance $\uparrow$ (9) Hardness $\uparrow$ (10) Promotes pearlite formation (11) Improves wear resistance
Mo	$\checkmark$	-	-	Strong	$\uparrow$	Mostly to carbide	(1) Refines pearlite and hardens (2) Promotes formation of martensite (3) Suppresses pearlite formation (4) T S $\uparrow$ (5) Pearlite promoter (powerful) (6) Improves wear resistance
V	$\checkmark$	-	-	Very Strong	$\uparrow$	Mainly to Carbide	(1) Refines pearlite and hardens (2) Eutectic C $\uparrow$ (slightly) (3) Improves wear resistance (4) T S $\uparrow$ (5) Promotes pearlite formation
Si	$\checkmark$	-	Strong	Negative	$\downarrow$	Mainly to carbide	(1) Eutectic C $\downarrow$ (2) Fluidity $\uparrow$ (3) Promotes pearlite formation (4) Produces ferrite and softens
S	-	-	-	-	-	-	(1) Induces hot shortness (2) Lowers shock resistance (3) Should be low in abrasion resistant C.I.
P	-	-	Mild	Nil	$\uparrow$	-	(1) Phosphide eutectic induces embrittling effect (2) Toughness $\downarrow$ (3) Kept below 0.3% in white irons

TABLE 2 (Contd....)

ELEMENT	$\alpha$ -Ferrite Stabilizer	$\gamma$ -Austenite Stabilizer	Graphitizer	Carbide forming tendency	Hardenability	Partitions	Other Effects/Application
Ti	✓	-	-	Greatest	↑ (as dissolved)	Mainly to carbide	(1) Imparts secondary hardening (2) Prevents formation of austenite in high-Cr steels
Al	-	✓	✓	-	↑ (if dissolved in austenite)	to austenite	(1) Deoxidises efficiently (2) Restricts grain growth by forming dispersed oxides or nitrides. (3) alloying element in nitriding steel
W	✓	-	-	Strong	↑	to carbide	(1) Opposes softening by secondary hardening (2) Forms hard, abrasion-resistant particles in tool steels (3) Promotes hardness and strength at elevated temperature.
Co	-	✓	✓	-	↓	to austenite	(1) Contributes to red-hardness by hardening ferrite.

↑ - increases      ↓ - decreases

been summarised.

#### Carbon

1. Increase in C increases abrasion resistance but reduces toughness, as shown in Fig. 2.1 [9].
2. The alloying element which fixes C in the form of a carbide (different from cementite), with a higher hardness and more favourable morphology, and which reduces C of the matrix, allows the simultaneous improvement of both abrasion resistance and toughness. Cr is mostly used, however other carbide formers are also useful.
3. Normal range of C for unalloyed or low-alloy WCI is about 2.2 to 3.6 %. For HCWCI, the normal range is from about 2.5% to the C content of the eutectic composition (i.e. 3.15% C for 15% Cr and 2.5% C for 27% Cr) in accordance with the relation by Jackson [10].
4. Decreases hardenability
5. % Carbides  $\approx 12.33 (\% C) + 0.55 (\% Cr) - 15.2$  (after Maratray).

#### Chromium

1. Imparts abrasion, corrosion & high temperature oxidation resistance.
2. At Cr more than 10%, eutectic carbides of  $M_7C_3$  type are formed, rather than the  $M_3C$  type. The higher Cr changes solidification pattern and thus the final as cast structure also.
3. Hypoeutectic irons containing  $M_7C_3$  carbides are stronger and tougher than irons having  $M_3C$  carbides [4].

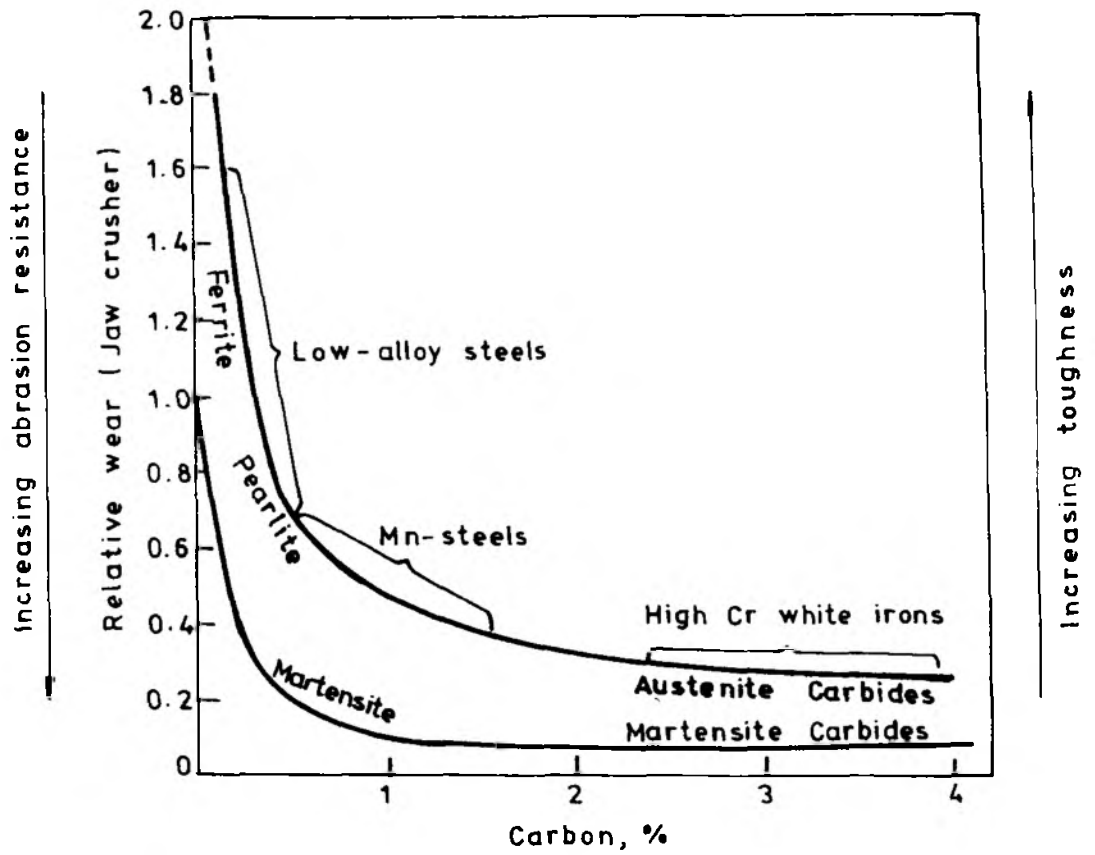


Fig. 2.1 Relation between the abrasion resistance, toughness and carbon content in ferrous alloys [9]

4. Cr prevents graphitisation and promotes carbide formation. The Cr equivalent is represented by the Rickett formula [11] as follows:
 
$$Cr_{\text{equ.}} = Cr + 2 Si + 1.5 Mo - 2 Ni - 1 Mn - 15N.$$
5. Cr contents in wear resistant WCI are in the range of 14-20% Cr with upto 3% Mo and 24-28 % Cr.

#### Chromium/Carbon ratio

1. This Cr/C ratio is important for ensuring sufficient quantity of carbides and some extra Cr for the matrix hardenability.
2. A Cr/C ratio of 4 and above are used in WCI.
3. Following compositions are used commercially with success.
  - (a) 25% Cr, 3% C in as cast or heat treated condition.
  - (b) 18% Cr, 2.5% C normally heat treated.
  - (c) 15% Cr, 3% C with 3% Mo in heat treated condition.
  - (d) 15% Cr, 1% C in the as cast condition.
4. The Fig. 2.2 gives relations between the C and Cr contents and the amount of carbides.

#### Nickel

1. With Cr, it has given a series of martensitic C.I. popularly known as Ni-hards (Ni-Cr martensitic irons) and Ni-resists (Ni-Cr austenitic irons). However, with Ni becoming scarce, the tendency is to reduce or eliminate its use.

#### Molybdenum

1. In WCI. Mo partitions between the carbides and the matrix.
2. 0.5 - 3.0% Mo in martensitic irons, suppresses pearlite

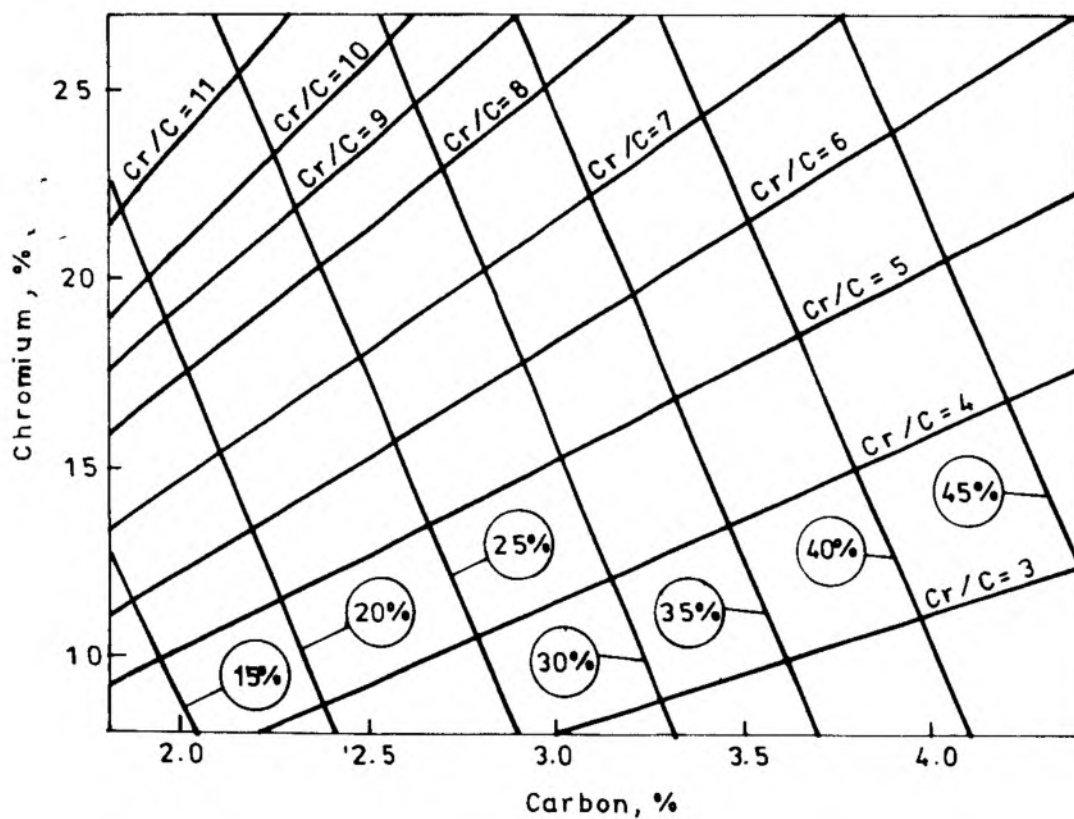


Fig. 2.2 Relations between the carbon and chromium contents and the amount of carbides [23]

formation and gives superior abrasion resistance even in heavy sections.

3. Mo alongwith appropriate Ni content can give austenitic, bainitic or martensitic and even stronger pearlitic WCI.
4. Can replace some of Ni in a value  $1 \text{ Mo} = 1.5\text{Ni}$  as it replaces W in H.S.S.
5. Forms special  $\text{M}_6\text{C}$  carbides.

#### Vanadium

1. In amounts of 0.1 to 0.5 refines the structure of the chill and minimizes coarse columnar grain structure.
2. Increases depth of chill.
3. At higher V content, forms VC carbides improving wear.

#### Titanium

1. In small percentages ( 0.1 - 0.5%) and with the presence of  $\text{N}_2$  and C, it forms very hard, strong, stable carbonitrides.
2. It has refining effect on microstructures and hence imparts better impact resistance.

#### Copper

1. Because of its limited solubility in austenite, Cu is limited to 2.5%.
2. In conjunction with 0.5 - 2.0% Mo, it is most effective in suppressing pearlite formation.
3. The hardenability of this combination (Cu-Mo) is surprisingly good, which indicates that there is synergistic effect.[12-15].

4. It enhances corrosion resistance.

#### Nitrogen

1. Can go into an alloy either, forming an interstitial solid solution (dissolved nitrogen) or forming nitride precipitates (undissolved nitrogen).
2. Dissolved nitrogen has double actions of strengthening the material by
  - (a) Solid solution strengthening.
  - (b) Grain size refining and hardening.
3. In Japan, recently nitrogen has been used to make tougher powder metallurgy H.S.S and cermets. In Russia, the work on W-free H.S.S has attempted to use nitrogen effectively.
4. Has limitations of solubility [16].(Fig.2.3)
5. Stabilises austenite in absence of strong nitride formers like Al,Ti.
6. Resists tempering by precipitation of carbonitrides [17].
7. Used as nitriding agent in salt baths, or in gaseous atmosphere to impart a hard wear resistant surface.
8. Introduced in surfaces by ion implantation, CVD or PVD (as TiN), imparts gold colour and enhances the performance.
9. Podrzucki [18] reports that nitrogen in C.I. increases the dispersion and the content of eutectic cementite hence causing elevated hardness of chilled layer.
10. In grey C.I., nitrogen increases hardness, T.S. and bending strength while deflection decreases. 120 ppm of nitrogen lowers wear by 15 - 25% [19], nitrogen in grey

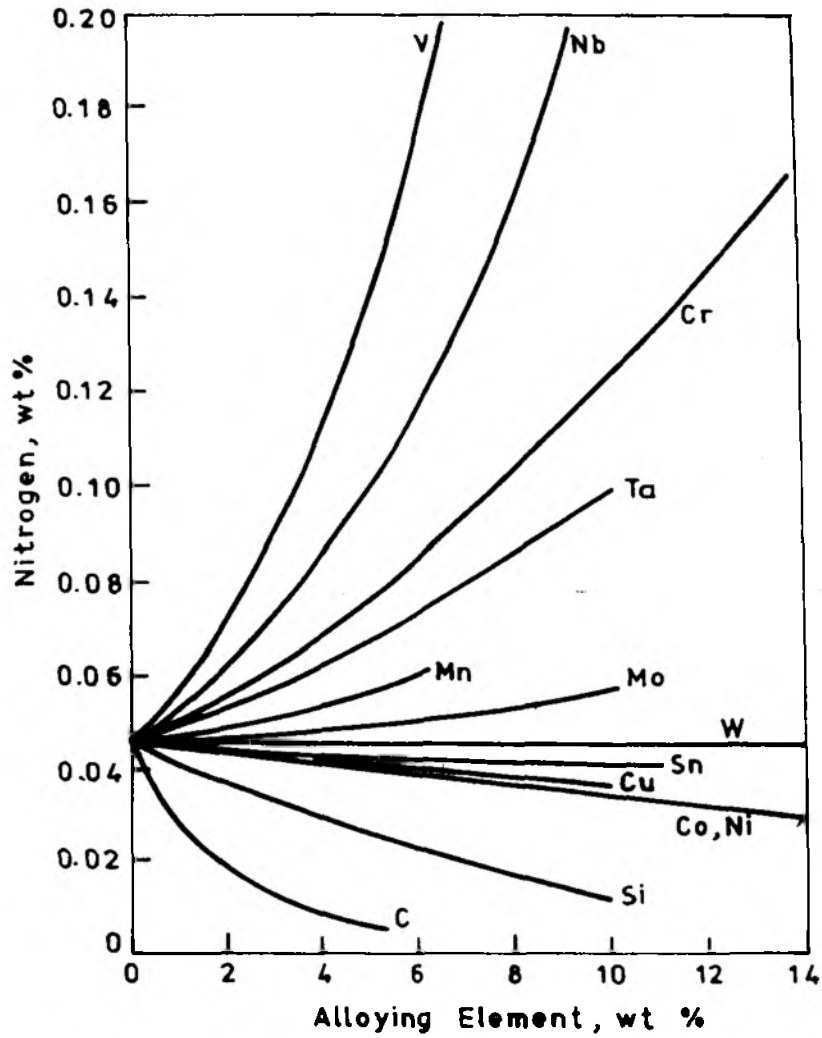


Fig. 2.3

Effect of alloying elements on the solubility of nitrogen (from Pehlke and Elliott) [16]  $1600^{\circ}\text{C}$ , 1 atmosphere pressure

irons is @ 0.005 - 0.012%.

11. The higher contents of nitrogen raise T.S. of hypo & Hypereutectic C.I effected by change in graphite structure.
12. Gilbert [20] examined the effect of nitrogen on stress-strain characteristics and found that total strain at failure was not much affected and that the increase in T.S. was by an increase in the stiffness. In another report, it was found that 10 ppm of nitrogen (over the range of 40-150 ppm) raises the T.S. by an average of  $7\text{N/mm}^2$  and hardness of  $3.5 H_B$  in inoculated irons having C.E. values between 3.8 and 4.5. The effect of nitrogen in S.G. irons has been discussed by Robinson [20].

#### Silicon

1. Improves the fluidity of liquid metal but reduces hardenability and abrasion resistance.
2. Limited to 0.6% in CWCI, however it can be increased to 1.0 - 1.2% in conjunction with a higher Mn level to compensate for the loss of hardenability.
3. Lower cost alloying element.

#### Manganese

1. Mn stabilises austenite when its percentage is about 3% and it has been used to improve the toughness of CWCI.[14]
2. Mn is kept below 0.7 % in martensitic irons.
3. Mn upto 1.5% increases retained austenite (R.A)and hence toughness in austenitic WCI.
4. One of the lowest cost alloying element.
5. Patwardhan et. al [12] have suggested use of Mn and Cu in place of Ni, to get the structures similar to Ni-hards.

6. Mn in excess of that required to combine with S, does not aid the formation of martensite. This contention is supported by Sandoz's microprobe studies.

#### Aluminium

1. In H.S.S. upto 1.5 Al has been added as a replacement for some W or Mo. However, its use at higher level is doubtful, because of its tendency of forming nitrides (AlN). [17]

#### Boron

1. In the range of 0.005 - 0.02% increases the strength and hardness.
2. Laird [3] has reported Day's work in which 0.2 - 0.4% B in eutectic composition resulted in globular instead of rod and blade shaped carbides. Day has hypothesized that B causes a rapid undercooling or shift in the kinetic transformation rate that favours nucleation rather than growth in the carbide phase, thereby causing a greater number of carbide particles of smaller size to develop. (Average carbide size = 4 $\mu$ m with the addition of B)
3. Costly alloying element.

#### Niobium

1. Nb is a carbide forming element.
2. In WC/Co, it affects the mechanical properties by influencing the matrix structure and the composition and the dispersion of carbide phases.
3. Forms extremely hard MC type (i.e. NbC) carbides and thus increases wear resistance of WC/Co.
4. Baik et al [21] have reported that with the increase in Nb content (from 0.63% to 2.13% Nb) there is a tendency for the NbC to change from a needle shape to a compact shape.
5. There is no partitioning of Nb to the austenite during solidification of these alloys and matrix structure would, therefore, not be affected by the addition of Nb.

6.  $K_{Nb} = 0 - 0.02$  shows that little Nb partitions in the primary austenite.

#### Tellurium

1. 5 gms/tonne or 5 ppm is extremely potent carbide inducing inoculant.

#### Bismuth

1. Has been used as an inoculant in the range of 50-100 ppm.

Optimization: Underalloying or Overalloying ?

#### Underalloying:

1. Results in low hardenability, a pearlitic structure and low abrasion resistance.

#### Overalloying

1. Affects the response to hardening treatments, reduces  $M_s$  temperature.
2. Increases amount of R.A. and lowers the hardness.
3. Lengthens the time required for sub-critical (cryogenic) treatments intended to eliminate R.A.

#### Optimum

Hence the concept of optimum "Lean Alloys" have been pursued [22].

#### 2.4 Substitute Grades of Chromium White Cast Iron (CWCI)

There are many grades of CWCI developed and used for a variety of applications. The research papers published on CWCI (see table no. 2.4) indicate continuous interest shown in these materials.

Recently, the microalloying concept have been applied both to the steels and cast irons, though much work has not

TABLE NO. 2.4 ' Some research papers published on Chromium White Cast Irons during 1965 - 1991'

Sl No	Author-s with reference number and year of publication	Composition tried ( weight percentages )					Heat treatment details and remarks (if any)
		C	Cr	Si	Mn	Others	
1.	Maratray[9],1980	0.5-4.0	1.2-20	2.5-4.3	1-14.0	Ni 0.3-10.0	Abrasion resistant austenitic alloys for hardfacing, Cr-Mn alloys and Mn Irons studied
2.	Srinivasan et.al. [12], 1977	3.13	7.45	1.68	1.98	(A) (B) + 1X Cu	Effects of Mn and Cu on microstructure CWCI studied.
3.	Sudan et.al. [13], 1980	3.34	6.97	1.53	0.68	S 0.10 Cu 0 - 3	Role of copper as an additive to CWCI was evaluated by producing a wear resistant microstructure.
4.	Chakraborty and Basak [14],1987	2.8	6.0	1.7	1 - 5		Ausaging 750-850-900°/1 hr. A.C. 800°C/1-3-4-5 hrs. A.C. Isochronal and isothermal tempering treatments carried out to investigate the effect of time and temperature on the behaviour of WCI(Cr-Mn-Cu) Effects of Mn and Cu on austenitic stability studied.
5.	Podrzucki et.al. [18],1985	3.5-3.6	N.R.	1.95-2.05	0.52	N 60-122 ppm P 0.08 S 0.075 Cr Cu and Mo constant (X not reported)	The influence of nitrogen in amount <sup>to</sup> up to 120ppm to improve the abrasion resistance of WCI was studied.
6.	Rongde et. al.[19] 1988	3.3-3-4	N.R	2.0-2.4	N.R.	C.E.3.95-4.1	Effects of nitrogen inoculation on the eutectic and eutectoid transformations of grey C.I. has been investigated using DFA techniques.
7.	Balk and Loper Jr.[21],1988	2.4-3.4	15	N.R.	N.R.	0-2.15 Nb	The influence of Nb on the structure, particularly carbide morphology of CWCI was studied by thermal analysis and metallographic techniques.

Table 2.4 (Contd..)

8. Dodd and Parks [22], 1980	2.4-3.0	15	N.R.	N.R.	Hypoeutectic Irons	Effects of C,Cr,Mn,Mo,Ni,Cu,Mn,Si,Ti and Al on the hardenability, toughness and abrasion resistance of CWCI in as-cast and heat-treated conditions evaluated.
9. Maratray [23], 1971	2-4.3	11-26	0.75	0.69	Mo 1.17-4.0 Cu 0.064 Ni 0.61	42 alloys with varying C,Cr and Mo contents studied to establish relationships between composition, microstructure and hardness Cr/C ratio varied between 3.5 and 10.2
10. Sawamoto et.al. [24], 1986	0.5-5.6	5 or 15	N.R.	N.R.	V 0-15 Nb 0-7.5 W 0-32	Unidirectional solidification for the simplification (-) of structures. Redistribution of alloying elements in primary and eutectic carbides evaluated by EPMA, VC and NbC nodularized.
11. Matsubara Et.al. [25,26], 1981	4.29-2.26	10-40	N.R.	N.R.		Eutectic solidification rates studied. Structures analysed quantitatively. Mechanism of eutectic growth studied.
12. Powell [32], 1980	Nihards	(I,II and IV)	and		15Cr-3 Mo 20 Cr-Mo, and 27 Cr.	Morphology of eutectic M <sub>3</sub> C and M <sub>7</sub> C <sub>3</sub> carbides in these WCIs studied
13. Sun and Loper [38], 1983	3.41-4.44	N.R.	2.48-3.51	.01-.09	Ti .039-.100 Ce .035 La .020 Mg .019 some alloys treated with rare earth silicides/ MnTiFeSi	The effects of Ti(C,N) as a nucleating agent studied in cast irons.
14. Hebbbar et. al. [45], 1991	3.06	25.8	0.26	0.40	S and P .03 each	900°C - 1125°C / 30 min - 240 mins. (900-975-1050-1125) / (30-60-120-140) - Air cooling - tempering 200-550°C/2-6 hrs

Influence of austenitising temperature and soaking time on hardness, wear loss and dynamic fracture toughness studied

Table 2.4 (Contd..)

15. Basak et. al. [47], 1988	2.3-2.7	10-12	<1	0.5-4.5	1100°C Isochronal tempering (1 hr) at various temps. Isothermal tempering at different temps.	O.Q.	(1) With increasing tempering temp. the time required to reach the peak hardness decreased (2) time required to reach the max. hardness decreased with increase in C content (3) Max. hardness was achieved at 500°C. (4) Most of the alloy carbides were of $M_7C_3$ type.	
16. Basak et. al. [48], 1982	2.54	11.6	0.47	4.4	S O.012, P O.029 without and with 0.35 Ti		Effect of Ti inoculation on wear resistance of Cr-Mn WCI studied.	
17. Fan et. al. [51], 1990	2.65	12	1.4	0.62	-		(A) (860°C/2hrs) O.Q. + (-196°C/30 min) + (250°C/2hrs) A.C. (B) (920°C/2hrs) O.Q. + (-196°C/30 min) + (250°C/2hrs) A.C. (C) (980°C/2hrs) O.Q. + (-196°C/30 min) + (250°C/2hrs) A.C. (D) (980°C/2hrs) O.Q. + (-40°C/30 min) + (250°C/2hrs) A.C. (E) (980°C/2hrs) O.Q. + R.T. + (250°C/2hrs) A.C.	
							(1)	Abrasion resistance and impact fatigue resistance evaluated (ii) with increasing re-austenitising temps. The bulk hardness and the microhardness of matrix increased (iii) with increasing R.A., both the bulk hardness and microhardness decreased. (iv) abrasion resistance increased with increasing C and with decreasing R.A. while impact fatigue resistance increased with decreasing C of the matrix and with decreasing R.A.

Table 2.4(Contd...)

18. Zumghar and Doane [52], 1980	1.4-3.9	11.6-25.7	0.6	1.5-1.6	Mo 2.39-2.45 Cu 1.24-0.76 Ni 0.02	Studies on optimization of fracture toughness and abrasion resistance in 12 Cr-Mo WCI carried out, with 7-45% carbide volume variations.
19. Subramanyam [60], 1985	2.69	18.7	0.75	0.69	Mo 1.17 Cu 0.064 Ni 0.61	(A) (1180°C/6hrs) A.C. + (230°C/4hrs) A.C. (B) (1100°C/2hrs) A.C. + (200°C/2hrs) A.C. (C) (1040°C/2hrs) A.C. + (230°C/2hrs) A.C. (D) (980°C/6hrs) A.C. + (230°C/4hrs) A.C. (-45°C/1hr)
						R.T + liquid N <sub>2</sub> soak 20 mins.
						(1) The effect of H.T. temps. on R.A. content determined (ii) R.A. was found to be sensitive to cooling rates (iii) magnetic method of R.A. measurement was proved quite reliable.
20. Watson et.al [69], 1980	2.7-3-46	2-27	0.3-3.0	0.45-0.85	Ni 0.06-5-50 Mo 0.01-2.85	Abrasive wear behaviour of 4 commercially significant WCIs examined
21. Pearce [70,71], 1984	(i) NiCr 1 and (iv) Cr 27 2.7-3.6 2.4-3.2	(ii) Ni Cr 4 1.5-10 1.4-28	(iii) Cr Mo 15.3 0.3-2.2 1.0	0.2-08 0.5-1.5	Ni 3-6 Mo 0.5 max Ni 0-1.5 Mo 0-3.0 Cu 0-1.2	(A) 900°C/1hr O.Q + 200°C/1hr A.C. (B) 900°C/1hr O.Q + 300°C/1hr A.C. (C) 800°C/1hr F.C. + 1025°C/1hr A.C + 450°C/1hr A.C. (D) 800°C/1hr F.C. + 1025°C/1hr A.C. (1) Wear due to cracking in eutectic carbides, (ii) high stress abrasion resistance depended on the level of support given by the matrix to the eutectoid carbides, (iii) work hardening was most significant in austenitic irons due to SiM (iv) thin foil TEM enabled identification of secondary carbide (v) Metallographic SEM, TEM studies to determine wear performance of CWCI.

Table 2.4(Contd...)

22. Crepeau et.al. [91], 1986	2-2.4	25-29	0.9-1.4	0.5-1.0	Ni 1.8 - 2.0	(A) Austenite destabilisation at 1050°C A.C (to martensite) (1) Fracture toughness was modelled for CWCI, having martensitic matrix and substantial amount of R.A.
23. Dupin and Schissler [118], 1984	2.6	20	0.8-2.6	0.82	0-1.0 Mo, Ni 1.2, V 0-1%, W 0 - 1.2%	The influence of Si, Mo, V and W on the as-cast structures of CWCI studied
24. Stefanescu et al. [119], 1976	3.0	15	0.7	0.5-5	2 - 5 % V	Structures of 15% Cr C.I. alloyed with upto 5% Mn or 5% V studied by dilatometry and diffractometry.
25. Durman and Elwell [120], 1985	2.4-3.6	11-28	1.0 max.	0.5-1.5	Ni 0.5 - 1.5 Mo 0 - 3.5 Cu 0 - 1.2 max.	Morphology of eutectic carbides in CWCI studied by SEM
26. Sentarli et. al. [121], 1985		N. R.				It was shown that by suspension casting technique, the dendrite became much refined and randomly oriented giving isotropic mechanical properties
27. Patwardhan and Jain [122], 1988	2.85-3.0	5	1.8-2.24	7.3-6.1	Cu 1.5 and 3.0 Mn 6 and 8 S 0.07 max. P 0.1 - 0.3 max.	A mathematical model developed for Fe-Mn-Cr-Cu WCI for corrosion resistant applications.
28. Sillman and Teikh [23], 1969	3.2-3.7	-	2.3-0.37	0.75-0.63	P 0.12, S 0.02 P 0.52, S 0.11	Effects of Mo, W, B and Ti on Grey and White CI's investigated.
29. Bunin et. al. [124], 1965.	4.3	Varying trace	.078		.016 Ni, 0.06 Cu .03 S, 0.014 P.	Effect of Cr on the structure of eutectic studied.
30. Garber et. al. [125], 1969	1.5-4.3	12-30	0.4-1.2	1.5-5	Mo 0 - 3	Effects of C, Cr, Si and Mo on the hardenability of CWCI studied.
31. Kontorovich et. al. [126], 1971	1.5-4.0	12-30	N.R.	N.R.	-	Optimal combination of C and Cr for the strength and wear resistance of WCI determined.
32. Pearce [127], 1983	2.44	30.6	0.71	0.21	0.17 Ni, 0.02 Mo 0.02 S and .04P	Thin foil TEM used to establish the occurrence of SIM (strain induced martensite) in austenitic CWCI.

been done on cast irons. The advantage of microalloying emerges from the fact that instead of substantial alloying, small additions of certain elements improve the property in economic way.

Many reports have recently been published on various alloy cast irons used for abrasive applications. The significant ones are by Dodd [22], Maratray [23], Jackson [10,11] and others e.g. A useful equation relating the Cr and carbide contents of the iron has been developed.

$$\% \text{ Carbide} = 11.3 (\text{C}\%) + 0.5 (\text{Cr}\%) - 13.4$$

$$\% \text{ Carbide} = 12.33 (\text{C}\%) + 0.55 (\text{Cr}\%) - 15.2 \text{ (By Maratray)}$$

A relationship developed by Jackson gives

$$\text{Eutectic Carbon} = 4.40 - 0.054 (\% \text{ Cr})$$

The work carried out on wear resistance, hardenability, toughness of these new CWCI is interesting and we shall discuss these in more details later.

## 2.5 Solidification and Carbide Morphology

### 2.5.1 Solidification

Solidification of CWCI follows the pattern of an eutectic alloy, though the compositions may be hypo-, hyper- or simply eutectic. The CWCI are distinguished by the presence of hard, relatively discontinuous  $M_7C_3$  primary or eutectic carbides or both.

Before discussing the solidification, it is necessary to study Fe-Cr-C ternary system. The figure 2.4 shows liquidus surface and resulting isotherms at  $1000^\circ\text{C}$  and  $700^\circ\text{C}$  [11]. From these, we could predict the types of phases which may be

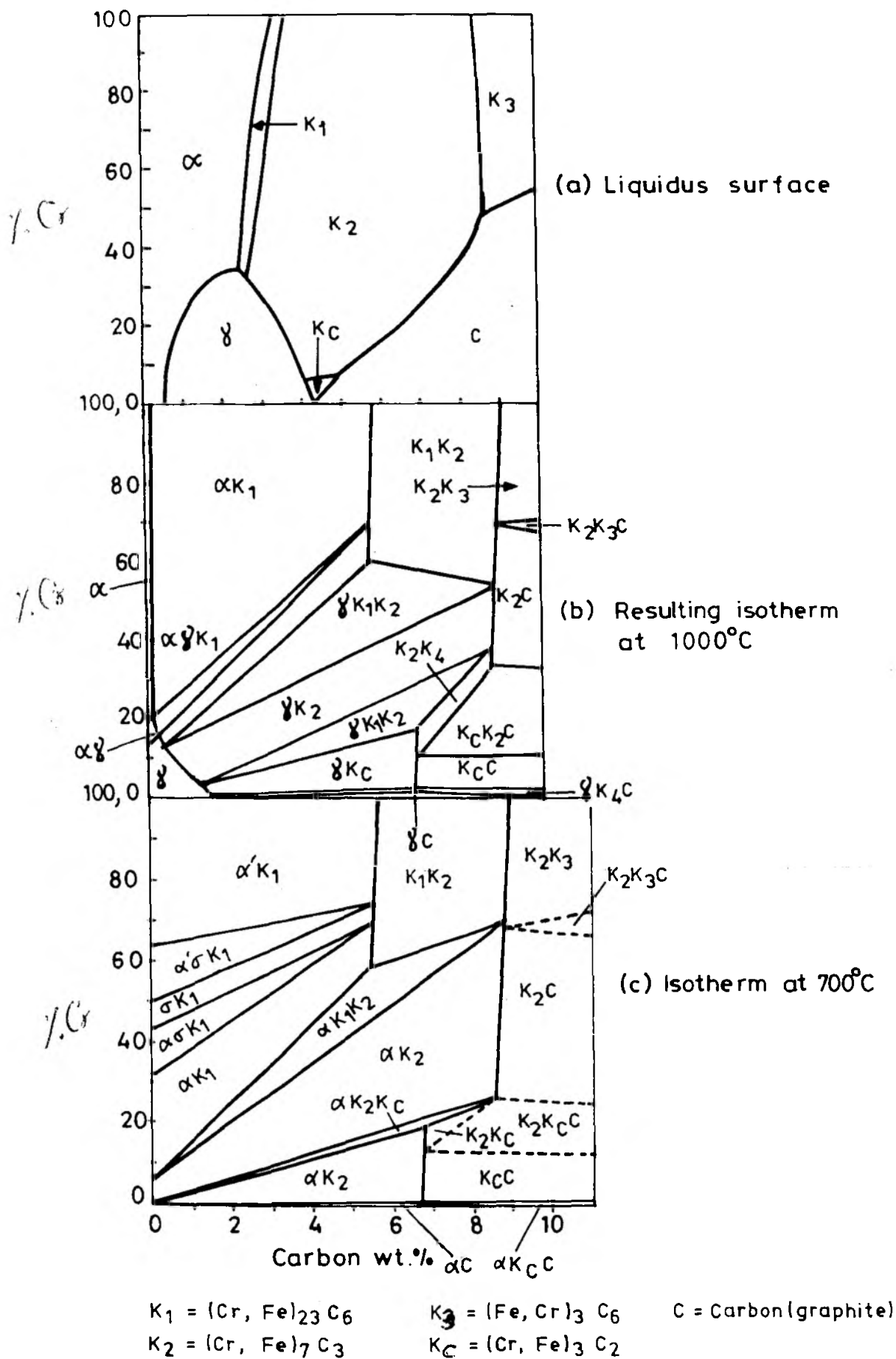


Fig. 2.4. Fe-C-Cr equilibrium diagram

present during and after the solidification.

Solidification in hypoeutectic alloys occur by the formation of austenite dendrites, followed by freezing of austenite and  $M_7C_3$  carbides simultaneously over a limited temperature range. Under non-equilibrium conditions, the austenite becomes supersaturated in C and Cr. This, alongwith other alloying elements like Mo, Mn, Ni, Cu, affect the transformation kinetics of austenite, resulting in retained austenite (R.A.) at room temperature. Particularly in thick sections, chemical composition and cooling rate determine whether during the solidification austenite will be retained, decompose partially or fully to ferrite-carbide products or transform to martensite.

Two basic requirements that must be fulfilled for the transformation of austenite to martensite to occur in CWCI are: First: The concentration of alloying elements in the matrix, particularly the C content must be lowered from the high levels present, following the solidification, and Second: There must be adequate hardenability to avoid the transformation of austenite to pearlite.

The first requirement involves the precipitation of secondary carbides either during slow cooling in the moulds or during a subsequent high temperature heat treatment. In most cases, martensitic structure in CWCI is obtained by a heat treatment called the "destabilisation" (by Maratray) or "conditioning".

Very interesting findings have been reported by A.Sawamoto et al [24] in which they studied the effects of V, Nb and W, all strong carbide forming elements, on the types,

amount, morphology and distribution of carbides in 5% and 15% Cr W.C.I.s. The variations studied were between 0.5 to 5.6%C, 0-15% V, 0-7.5% Nb and 0-32%W. The Cr contents (5% & 15%) were chosen as the typical irons in which  $Fe_3C$  and  $K_2$  carbide crystallized as primary and eutectic. The Ti was added in the range 0.01-0.3% to modify carbides, and to decrease the notch sensitivity of carbides, thus improving the toughness property.

Matsubara et. al.[25,26] have studied eutectic solidification of CWCI in a wide range of Cr (10-40% Cr) and various C levels. They have given the quantitative analysis and the mechanisms of eutectic growth. It was found that in the hypoeutectic iron (3.23% C, 19.20% Cr), the austenite<sup>e</sup> precipitated in the liquid first, and then austenite- $K_2$  eutectic nucleated in the liquid independently of the primary austenite dendrite and grew with a cellular interface. On the other hand, eutectic of hyper~~eutectic~~ eutectic iron (3.58 C, 18.78% Cr) grew radially with a cellular interface from the periphery of the hexagonal carbide, which had previously precipitated in the liquid as a primary crystallite. The primary carbide served as a nucleus of the austenite- $K_2$  eutectic. It was clear from the final structures that the eutectic finished solidifying as a colony structure. The quantitative analysis was carried out by measuring the colony diameter and the carbide spacing in the colony. In 10% Cr irons, the primary and eutectic carbides of both  $K_3=(M_3C)$  and  $K_2=(M_7C_3)$  type coexist, while in irons with 15% Cr and above, only the  $K_2$  type were present.

The eutectic carbides in the central region of the colony observed in the cross-section were of a fine globular shape and those developing from center to boundary were string-like or

granular and those at the boundary area were large massed grains. The string like carbides changed into globular ones with an increase in Cr content and the rate of eutectic solidification.

The eutectic solidification rates were represented by the following equations, which gave linear relations.

$$\text{For 15\% Cr irons, } y = 2.22 t - 0.43 \quad (1)$$

$$\text{For 20\% Cr, irons, } y = 2.28 t - 0.33 \quad (2)$$

$$\text{For 30\&40\% Cr irons, } y = 2.26 t - 0.01 \quad (3)$$

where  $y$  = distance (cm), from the chill face

$t$  = square root of time,  $t$ , mins, elapsed after pouring  
to the begining of the eutectic.

Differentiating  $y$  w.r.t.  $t$ , i.e.  $dy/dt$  gives the rate of eutectic solidification,  $R_E$ , cm/min. as follows:

$$\text{For 15\% Cr irons, } R_E = 1.11 . t^{-0.5} \quad (4)$$

$$\text{For 20\% Cr irons, } R_E = 1.14 . t^{-0.5} \quad (5)$$

$$\text{For 30\&40\% Cr irons } R_E = 1.13 t^{-0.5} \quad (6)$$

It is evident from these equations that the rate of eutectic solidification is reduced as the distance from the chill face increases. The  $R_E$  value becomes larger with the increase in Cr content.

The relation between the eutectic structure and the solidification rate was found to be

$$E_w = A . R_E^{-0.72} \quad (7)$$

where,  $E_w$  = Average colony diameter ( $\mu\text{m}$ )

$A$  = Positive constant, depends on the chemical composition.

$R_E$  = Rate of eutectic solidification (cm/min)

The influence of the eutectic solidification rate and the chemical composition on the carbide spacing at the central region of the eutectic colony and that at the boundary area had been established by the functional formula as follows:

$$F_a^c \cdot F_a^b = B \cdot R_E^{-0.5} \quad (8)$$

where,

$F_a^c$  = Average carbide spacing at the central region of colony ( $\mu\text{m}$ ).

$F_a^b$  = Average carbide spacing at the boundary region of colony ( $\mu\text{m}$ ).

B = Positive constant, depends on chemical composition.

$R_E$  = Rate of eutectic solidification (cm/min).

Both these spacings become smaller with an increase in the eutectic solidification rate, as in the case of colony diameter, it was reported.

The relation between the carbide spacing and the eutectic solidification rate seemed to agree well with that which Tiller [27] and Jackson et al [28] reported for nonferrous alloys.

It was established that the carbide spacing in the colony center was little affected by the Cr and C content, but the colony size and the carbide spacing at the colony boundary were greatly influenced by both the Cr and C content.

In another report, Matsubara et. al. [26] explained the mechanism of eutectic growth. It showed that

(i) The eutectic cell takes the shape of a slender bell

and the length of the eutectic cell projection becomes larger with an increase in the eutectic freezing range.

- (ii) The eutectic freezing range varies markedly with Cr content, and it has a maximum value of 65°C at 15% Cr and the minimum value of 21°C at 30% Cr.
- (iii) As the length of the eutectic cellular projection may determine the size of the eutectic cell, the size of the eutectic colony in the C.I. should also increase with an increase in the eutectic freezing range. The colony diameter ( $E_w$ ) can be expressed in terms of the eutectic freezing range ( $\Delta T_E$ ) at the same eutectic solidification rate of 1 cm/min.

$$E_w = 1.68 \times 10^{-3} \Delta T_E^{0.45} \quad (9)$$

where  $E_w$  is given in cm,  $\Delta T_E$  is in °C

- (iv) The rate of radial growth ( $R_r$ ) of the eutectic cell is high near the top of the cell, and it gradually decreases far away from the top of the cell to the cell boundary. In the neighbourhood of the cell boundary, the  $R_r$  value for 30% Cr iron is 4-5 times as large that for 15% Cr iron.

- (v) The carbide spacing near the colony boundary  $F_s^b$  can be expressed for the same eutectic solidification rate (1 cm/min)

$$F_s^b = 1.0 \times 10^{-5} \Delta T_E^{1.15} \quad (10)$$

where  $T_E$  is in °C and  $F_s^b$  in cm.

- (vi) The Cr concentration of the melt gradually decreases from the freezing front to the bottom of the cell boundary.

Eutectic solidification has been classified as follows [28].

- (i) Lamellar (nonfaceted - nonfaceted)  $\alpha < 2$
  - (ii) Faceted-nonfaceted and
  - (iii) Faceted - faceted
- $$\left. \begin{array}{l} \text{(ii) Faceted-nonfaceted and} \\ \text{(iii) Faceted - faceted} \end{array} \right\} \alpha > 2$$

This is on the basis of a phase being classified according to a dimensionless factor  $\alpha$ . A lamellar eutectic will form where both phases have an  $\alpha$  value less than 2. If a phase possesses a high  $\alpha$  value ( $>2$ ), its growth as a eutectic constituent will produce a faceted interface. Metal-metal carbide eutectics fall into the faceted-nonfaceted category (where metal is non-faceted phase and the carbide is faceted phase) where faceted phase could be modified.

Inferring the 3-dimensional morphology of a eutectic phase from optical micrograph can lead to errors. This point has been made by Chadwick [29] who concluded that the only family of truly discontinuous eutectics is that containing spheroidal graphite.

### 2.5.2 Carbide Morphology

In CWCI, the performance of the castings is governed by the factors that are applicable to other inherently brittle materials like WCI. Thus the Griffith's and Orowan's mechanisms will hold good even for CWCI. The following constituents exert maximum influence on the mechanical properties:

- (1) Carbides: As these CWCI are almost free from graphite, the type, amount, distribution size and the morphology of carbides play an important role in determining its resistance to abrasive wear, toughness etc. Essentially in

these brittle materials, the fracture mechanisms are governed by these hard, brittle constituents.

- (ii) Matrix: The matrix may consist of Pearlitic (or sorbitic/bainitic), martensitic (or troostitic) or austenitic, or combination of these structures. The amount of these phases influences the performance of the castings in terms of wear, impact, failure resistance etc.

The two most important aspects of WCWI which deserve detailed discussion are

- (a) Carbide morphology - Carbides of primary or eutectic type or secondary carbide precipitates.
- (b) Retained austenite - Its volume % and influence on various properties.

The earlier reports on carbide morphology may be summarised as follows:

- (1) In hypoeutectic WCI, the eutectic carbide morphology changes to platelike one on rapid quenching or on increasing considerably the degree of undercooling before carbide nucleation in a slow cooled sample[11].
- (2) Eutectic carbide is continuous in Ni-hard I & II but discontinuous in Ni-hard IV and HCWCI.
- (3) On increasing the Cr content of WCI over 10%  $(Fe,Cr)_7C_3$  carbide no longer forms the matrix but is itself contained in a pearlitic or austenitic-martensitic matrix. In this context, the matrix is the continuous phase [30].
- (4)  $M_7C_3$  eutectic is lamellar in eutectic Cr-Mo WCI, and forms radiating clusters between the dendrite arms in hypoeutectic irons [9].
- (5) Although heattreatment is rarely used to modify the

morphology of the eutectic carbide, one group of researchers reported globularisation of eutectic carbide in WCI by heattreatment. Majority of the researchers however believe that modification of carbide morphology must be obtained in the as cast state. Use of inoculants to nucleate carbide was suggested as a possible means of carbide morphology modification [31].

The earlier concepts of continuous or discontinuous nature of carbide morphology was largely changed when SEM investigations of the three dimensional morphology of carbide were carried out.

Powell [32] carried out detailed investigations on the carbide morphology in both unalloyed and alloyed WCI. His work on unalloyed iron confirmed earlier observations [33,34,35] that the morphology of  $Fe_3C$  changes from ledeburitic to plate like structure as the undercooling is increased. However, the apparently discontinuous platelike morphology appears as a continuous carbide network in three-dimensions under SEM.

The morphology of carbide<sup>of</sup> alloyed irons (27% Cr, 17% Cr - 1.5 Mo, Ni-hard Iv (8% Cr) and Ni-hard II (2% Cr)) was investigated in further details under SEM. He drew the following conclusions from his work.

- (1) Even in the alloy irons investigated, the carbide morphology is not truly discontinuous. In Ni-hard II the eutectic carbide is  $M_3C$  type and is usually of massive continuous form in sand cast samples. In highly alloyed irons (27% Cr, 17%cr-1.5Mo and Ni-hard IV) the eutectic carbide is predominantly  $M_7C_3$  type. The morphology of such eutectic carbide is one of hollow rods and blades.

- (2) In hardfacing weld deposits of 30-35% Cr-WCI the solidification rate is faster than that in a sand casting. Increase in growth rate changes the carbide morphology to rod type in such samples.
- (3) Since directionally solidified alloys of Fe-Cr-C and Co-Cr-C have been investigated as composite alloys for high temperature applications where strengthening is provided by the thermally stable  $M_7C_3$  fibres, it is unlikely that the morphology of the  $M_7C_3$  in alloy WCI can be appreciably changed by high temperature heattreatment, although coarsening will occur.

Since the toughness and service life of high chromium WCI depends appreciably on the composition (matrix) and dispersion of the carbide phases, the efforts to modify the carbide morphology is continuing till date. Baik and Loper [21] investigated the solidification process and resulting microstructures formed in Fe - 15% Cr alloys containing 2.4 to 3.4% C and upto 2.15% Nb. in castings and in samples quenched during the solidification of these alloys. Their important observations are as follows:

- (1) As the Nb content was increased, the amount of NbC carbide was increased with a corresponding decrease in the amount of  $M_7C_3$  carbide.
- (2) Four shapes of NbC were observed in this study:
- |                              |                    |
|------------------------------|--------------------|
| (i) Petal like carbides      | 82.97 - 90.70 % Nb |
| (ii) Hexagonal disc carbides | 84.35 - 89.92% Nb  |
| (iii) Nodular carbides       | 82.30 - 91.55% Nb  |
| (iv) Dendritic Carbides      | 85.73 - 91.76% Nb  |

The compact forms of these carbides were the hexagonal

disc and nodular carbides which appeared at intermediate Nb levels (greater than 0.64 % but less than 1.85% Nb).

The modification of the primary and eutectic carbide by the addition of 0.01 to 0.3% Ti (in the form of ferrotitanium) has been attempted by Sawamoto et. al [24,36]. As the Ti has very low solubility in molten C.I., the TiC precipitates at higher temperatures and initiates nodularisation of both primary and eutectic VC in Fe-Cr-V-C alloys containing 5-9% V (5&15% Cr). Thus TiC acts as an inoculant of VC. This view has further been supported [37,38], wherein it has been shown that Ti appears as TiC or Ti(C,N) i.e. Titanium carbonitride and nucleates the carbide in alloy C.I. Sun and Loper [38] have emphasised the fact that the growth conditions, impurities and the temperature of growth have marked influence on the crystal morphology.

It has been shown [39,40,41] that B could produce particulate or spheroidal carbide and thus increase wear resistance and toughness of WCI. This is because B and Si are dissolved in the melt and result in the dispersive precipitation of carbides. B also increases the entropy and the constitutional disorder of the melt, this causing kinetic undercooling of the melt. It is also reported that in China, nodular carbide was produced in low and medium alloy WCI by rare earth (RE) + Al complex modification and spheroidised by heat-treatment [42].

However, the roles of modifying additions and the mechanism of modification during the nucleation and growth of carbide has been studied by Chang et. al. [43]. They studied the effects of V content from 0 to 10% and rare earth (RE) or

RE + N complex addition on the carbide morphology of 2.65 - 2.85% C, 1.0 - 2.0 % Si and 0.6 - 0.8% Mn WCI to obtain spheroidal carbide. They explained the mechanism of spheroidising modification in the following way:

- (1) The first condition is the separation of primary VC from the melt with high V content, because it could grow freely in the melt and would further favour the divorced growth of eutectic VC.
- (2) Duplex heterogenous nuclei composed of TiN and CeS promotes growth of VC into spheroids. These elements come from complex RE + N. CeS nuclei forms first because of its higher negative value of free energy of formation. TiN precipitates on the CeS, and this in turn act as a nucleant for VC spheroids.
- (3) TiN is a better nucleating agent than VN.
- (4) Ratio of spheroidisation in RE+N modification is greater than that in Ti+N modification, because of the specific effects of RE.
- (5) RE modifier gives divorced eutectic growth because of its adsorbing and undercooling effect.
- (6) Purification of the melt from S and O by RE modifier prevents dendritic growth of VC. This is because purification increases the surface tension of the melt, favours the spheroidal growth and stabilises the spherical interface by preventing the growth of any microperturbation on the surface.
- (7) High cooling rate did not favour the formation of spheroidal carbide, since solute macrodiffusion in the melt

would be difficult, so that segregation of impurities was accentuated.

- (8) Spheroidal carbide could be formed only above the eutectic temperature (i.e.  $1400^{\circ}$  -  $1450^{\circ}$  C) at an appropriate cooling rate.

### 2.5.3 Identification of Carbides

In an effort to identify the carbides and to understand the sequence of transformations during solidification, carbides have been extracted by dissolving the matrix in acid and then subjected to XRD using iron-filtered Co-radiation. The results are as shown below:

Alloy	$(Cr,Fe)_7C_3$	$(Fe,Cr)_9C$
27% Cr	Strong	Weak
17% Cr - 1.5 Mo	Strong peak intensity	Weak peak intensity
Ni-hard IV	Medium	Strong
Ni-hard II	-	Strong

Maratray and Usseglio-Nanot [44] in an excellent work on 42 CWCI's have presented an invaluable atlas of data on transformation characteristics. They have suggested the method of carbide identification by means of their relative resistance to various etchants. This has been shown in Table 2.5.

The amount of carbides is determined by the linear intercept method, on the slices taken from the top, middle and bottom of the ingot. On each slice, five measurements are made

Table 2.5 Carbide Identification Chart

The carbides can be identified by means of their relative resistance to various etchants as indicated below:

Etchant	Composition		$M_3C_3$	$M_7C_7$	$M_{23}C_{16}$	$M_6C_6$	$M_2C_2$
alkaline picrate	picric acid sodium hydroxide water	2g 25g <sup>3</sup> 100cm <sup>3</sup>	A	NA*	NA*	NA*	A
Murakami	potassium ferricyanide potassium hydroxide water	10g 10g <sup>3</sup> 100cm <sup>3</sup>	NA	A	A	A	A
chromic acid electrolytic etch	chromic acid water	1g 100cm <sup>3</sup>	NA	A	NA	NA	A
sodium hydroxide saturated with potassium permanganate	4% sodium hydroxide solution saturated with potassium permanganate		NA	A	NA	A	A

A: attacked

NA: not attacked

\* lower chromium carbides are attacked

on each of five radii, near to the centre, at midradius and on the surface. This gives total of  $3 \times (5 \times 5) \times 3 = 225$  readings. The results are analysed by factorial method (statistical) which gives a confidence limit of 95% for the mean values of  $\pm 2.7\%$  carbides.

## 2.6 Heattreatments, Microstructures and Hardenability

CWCI have been used in the following conditions:-

- (1) As cast, metastable austenitic, which workhardens from  $H_V$  450 to  $H_V$  1000.
- (2) As cast, martensitic, not exploited fully.
- (3) Cast as pearlitic, hardened and tempered to  $H_V$  750-850.
- (4) Cast and heattreated to bainitic structure.

The CWCI for a long time have been used in the as-cast state, in applications where the impact resistance required were not very high. However, where higher impact strength are needed, CWCI have been heattreated by different treatments to various microstructures and properties, discussed later.

The typical hardness values of various micro-constituents are as follows [22]:

Carbides:	<u>VPN</u>
$M_3C$	840 -1100
$M_7C_3$	1200 -1800
$Mo_2C$	1500
Matrix	
Ferrite	70-200
Pearlite	300-460
Austenite (high Cr-iron)	300-600
Martensite	500-1000

In most cases, when martensite is required in CWCI, it is obtained by heattreatment.

After heating to a high temperature,  $950^{\circ}$  -  $1100^{\circ}\text{C}$  and precipitating secondary carbides in the matrix, a process termed "conditioning" or "destabilisation" (by Maratray), the austenite can transform to martensite on cooling (providing the iron has enough hardenability).

The response to heat/treatment, i.e. the  $M_s$  temperature, the amount of martensite formed (or alternatively the amount of austenite retained i.e. R.A) and the hardness, is affected by the time and temperature of the destabilisation treatment, chemical composition and cooling rate [45].

#### 2.6.1 As cast microstructures

In a thin (50 mm) and a thick (150mm) sections, the structures are different in CWCI of higher hardenability. The matrix microstructure of 50mm(thin) sections is predominantly austenite with a very small amount of pearlite and some martensite adjacent to the eutectic carbides. The microstructure in 150mm (thick) sections consists of greater amount of martensite in eutectic regions and precipitation of secondary carbides in the centre of austenite dendrites. In optical microscopy, these dark etching regions resemble pearlite, however on examination by TEM, it is observed that these areas are actually a dense precipitation of fine secondary carbides in an austenitic-martensitic matrix.

### 2.6.2 Microstructures after heattreatment

Heating the CWCI (thin-,thick-section) to high temperatures, usually in the range of  $950^{\circ}$  -  $1100^{\circ}$ C results in the precipitation of secondary carbides in irons which are predominantly austenitic in as-cast condition. Similarly, as-cast pearlitic irons transform to austenite and secondary carbides. Depending on chemical composition, hardenability and cooling rate, the austenite will transform on cooling to ferrite-cementitic-carbide constituents, martensite or mixtures of the two. Some austenite will be retained at room temperature.

The following regression equation is suggested for determining the minimum alloy content required to avoid pearlite formation when castings are cooled from the austenitising temperature [20].

$$\begin{aligned} \log \text{ Pearlite time(s)} = & 2.24 + 0.58 \text{ Mn}\% + 0.41 \text{ Mo}\% + 0.84 \text{ Ni}\% \\ & + 0.46 \text{ Cu}\% \end{aligned} \quad (11)$$

### 2.6.3 Hardenability

Dodd and Parks [22] have reported the following Multilinear Regression Analysis (MLRA) of Isothermal Transformation (IT) by Maratray.

$$\begin{aligned} \log (\text{Pearlite time}^*, \text{sec}) = & 2.61 - 0.51 (\% \text{C}) + 0.5 (\% \text{Cr}) \\ & + 0.37 (\% \text{Mo}) \end{aligned} \quad (12)$$

(\* indicates nose of s-curve)

No. of observations = 42

Composition range of the observations (weight %)

C = 1.95 - 4.31 %

Cr= 10.8 - 25.8 %

Mo= 0.02 - 3.8%

Maratray [44] and Cias [46] have derived an expression for the maximum diameter which could be air hardened without forming pearlite. The samples of 5 mm to 1000 mm dia which were austenitic in as-cast or after heating to 1100°C and quenching were heated to 1000°C for 20 minutes and subsequently cooled at different rates corresponding to that at the surface of air cooled rounds of above diameter.

$$\log_{10} \text{ max.dia. (mm) for air hardening on CCT} \\ = 0.32 + 0.158 \left( \frac{\%Cr}{\%C} \right) + 0.385 (\% Mo) \quad (13)$$

Both Maratray and Cias used dilatometric methods to determine Continuously Cooled Transformation (CCT) diagrams, although there were some differences in the alloys and experimental procedures employed.

The isothermal transformation characteristics of CWCI have been investigated by Maratray [44] and Klein [22]. Maratray's study included 42 irons with variations in C, Cr and Mo, and the kinetics of non-destabilised austenite (i.e. austenite present in as-cast condition or in case of as-cast pearlitic irons, after reaustenitizing above 1000°C and quenching) and for austenite that was destabilized at 1000°C for 20 mins. prior to isothermal transformation.

For Continuously Cooled Transformation (CCT) of the above composition range, with 42 observations made, the regression equation is somewhat similar to that for IT (eqn. no.12) of the same group of alloys.

$$\log (\text{Pearlite time, sec}) = 2.90 - 0.51 (\%C) + 0.05 (\%Cr) \\ + 0.38 (\% Mo) \quad (14)$$

Hardenability is also influenced by the time and temperature of the destabilisation treatment as reported by Maratray.

Basak et. al. [47,48] have suggested the following heat treatments:

- (i) Conditioning or Ausaging treatment
- (ii) Arrested cooling treatment

The ausaging treatment involves annealing in the  $\gamma$  + carbide region at the minimum possible temperature so that the equilibrium austenite contains minimum C and other alloying elements and hence  $M_s$  will be higher. During this treatment, a large amount of carbide is precipitated and on cooling a fully martensitic matrix is obtained. (This procedure is common for Ni-hard IV alloy). The temperature may be  $780^\circ - 850^\circ\text{C}$  and the time 12 hrs. and 8 hrs. respectively to get the maximum hardness.

The arrested cooling consists of soaking at the highest possible austenitisation temperature (say  $1100^\circ\text{C}$ ) followed by a subsequent annealing treatment at a lower temperature (usually @  $930^\circ\text{C}$ ) for about 1 hour, followed by air cooling. During the thermal arrest, an additional precipitation of carbides takes place. The carbides precipitated at a temperature  $>A_3$  are of  $M_7C_3$  type, while at a temperature between  $A_1$  &  $A_3$ , softer  $M_{23}C_6$  carbides are also precipitated alongwith. Hence, the temperature  $930^\circ\text{C}$  ( $>A_3$ ) is selected.

At the austenitising temperature of  $950^\circ - 1060^\circ\text{C}$ , castings which are largely austenitic as-cast, are generally held for 4 to 6 hours. Shorter times, about 3 hours are employed for castings with pearlitic microstructures in the

as-cast condition.

2.6.4 Cooling rate is as important factor, as the heating rate, because incorrect cooling rate can cause cracking in the castings. The accepted practice is adjusting the hardenability of iron to produce the desired martensitic structure on air cooling.

2.6.5 Tempering is carried out to improve toughness and to reduce retained austenite(R.A.) content. R.A. acts as a source of failure from spalling. The low temperature tempering at  $200^{\circ}\text{C}$  (similar to steel) improves the toughness, but it is too low for transforming R.A., therefore higher temperatures in the range of  $450^{\circ} - 525^{\circ}\text{C}$  have been employed for HCWCI. These  $450-525^{\circ}\text{C}$  treatments are also referred to as the subcritical treatments and eliminate R.A., and in some cases increase the hardness significantly.

At about  $600^{\circ}\text{C}$ , R.A. could be eliminated. However, it may cause loss in hardness due to transformation of the matrix to a spheroidized ferrite-carbide structure. Studies have shown that chemical composition, time and temperature and variations in the prior hardening treatment influence the response to subcritical treatment.

2.6.6 Subzero(Cryogenic) treatment is resorted to, to eliminate R.A. The castings after hardening are cooled to  $-80^{\circ}\text{C}$  or lower, in liquid nitrogen or other cooling/refrigeration media. A report [49] indicated that such a cryogenic treatment improved the tool life of dies and enhanced their performance.

## 2.7 Retained Austenite (R.A.) and its Measurement

It is important to understand the term properly. In case

of steels used for precision measuring instruments, the R.A. is not desirable, as it ages and changes the dimension. R.A. also affects various mechanical properties.

In case of CWCI, R.A. has different meaning and significance. Just in ADI, [50] the R.A. may be of two types:

- (i) Reacted Stable Austenite (~~RSA~~)
- (ii) Unreacted Metastable Austenite (~~UMA~~.)

Fan et. al [51] reports that there are contradictory opinions about austenite in literature.

The positive opinions are:

1. Austenite matrix exhibits a higher toughness against single blow impact, higher dynamic fracture toughness and better static fracture toughness. This is because of the good plasticity of the austenite which provides more resistance to crack propagation [52].
2. The binding force at the carbide-austenite interface is larger than that at the carbide-martensite interface. Austenite therefore reduces crack propagation.
3. When austenite transforms to martensite, by work hardening under an impact load, the transformation consumes energy, leaving less energy for crack propagation [22].
4. The presence of R.A. is a useful constituent for improving the wear resistance, particularly in conditions of high stress abrasion. Stress Induced Martensite (SIM) is produced which offers enhanced abrasive wear resistance [53,54].

The negative opinions are:

1. R.A. lowers the hardness of iron, and decreases its abrasion wear resistance.

2. R.A. causes spalling and even breakage of the balls [55-59].
3. It is reported that R.A. reduces wear resistance and it is always harmful to both 3-body abrasion and impact fatigue resistance [51].

The R.A. in case of CWCI was difficult to predict till Maratray et. al. [44] developed IT-OCT curves for a large number of CWCI's.

In any case, the measurement of R.A. content is necessary for evaluating its effect.

The methods suggested for R.A. measurement are [60]:

1. Microscopic method
2. XRD Analysis method
3. Magnetic flux method

The microscopic method is not very accurate as it is difficult to distinguish various phases accurately (particularly ferrite, austenite) in the metal.

The most commonly accepted way of measuring the absolute value of R.A. is XRD. Due to the frequent presence of solidification texture in castings, the technique developed by Miller [61] was modified by Kim [62] for use on CWCI. This method involves the simultaneous rotation and spinning of the sample to minimize orientation effects. However, XRD method involving the measurement of integrated intensity of the relevant lines, as used by Averbach and Cohen [63] still remains the reference method.

Because X-ray instrument is relatively expensive and not-so-portable, hence some NDT technique using magnetic principles have been developed, some instruments are available commercially and La Count [64] has evaluated some of them.

Subramanyam [60] used an instrument called Fischer Scope 'Magna' 460B and compared the results with those obtained by XRD. It showed that a linear relation exists between the results obtained by the above two methods. Hence by calibrating the 'Magna' with XRD, it could be used for production purposes.

There are difficulties in determining the R.A. in CWCI because of presence of eutectic and secondary carbides. Subramanyam has discussed the effects of surface roughness, cooling rate of castings, deformation and decarburization on the R.A. measurements. Durnin and Ridal [65] suggest that metallographic, dilatometric and saturation magnetization intensity methods can give reasonable measures of R.A. under favourable conditions. However, these methods become inaccurate when austenite content is less than 10% and are less reliable in high alloy steels and steels containing appreciable quantities of carbide.

Several investigation into the use of XRD measurements of R.A. have been made, by measuring the integrated intensity of relative lines with densitometer or planimeter. Averbach and Cohen found that with care, as little as 0.3% austenite could be measured.

Durnin and Ridal have determined the R.A. over a range of austenite contents down to low values by XRD and have compared with point counting and MSIM (Magnetic Saturation Intensity Measurements). They have discussed the theoretical considerations as well as the problems associated with the practice e.g. Intensity factors, specimen preparation, use of different radiations and diffraction planes, carbide interference and preferred orientation effects.

## 2.8 Wear Studies

### 2.8.1 Introduction

The wear processes are quite complex and their theories and practice have been discussed in many texts and papers [66-77,88]. Better known texts are by Czichos [66] Moore [67], Rabinowicz [68] etc. In a report, the theories and mechanisms of wear and the methods to reduce or prevent it have been summarised. Wear classification by Rabinowicz, Archard and Hirst and Burwell are described and oxidational theory of Quinn et. al. and Delamination theory by Suh et.al. have been explained. 'Design for wear resistance' from a system approach has been attempted [78].

As most of the wear tests are tailor-made we shall discuss only those used by a few researchers for CWCI.

In most of abrasion tests [71], one of the three basic forms of abrasive wear predominate-

- (i) Gauging abrasion usually associated with impact.
- (ii) High stress (grinding) abrasion.
- (iii) Low stress (erosion) scratching abrasion.

The following laboratory tests have been used to study the above types of abrasive wear:

- (1) Jaw crusher test [79] - for gauging wear
- (2) Pin-on-cloth (drum) test [80]- for high stress(grinding)wear,alternatively Specimen-on-track test.
- (3) Wet sand/Rubber wheel test [81] - for low stress (erosion) wear. High stress abrasion has been studied by Watso et. al. [69] using pin-On-cloth test. However, it is argued that this test gives only

2-body wear (cutting only). The specimen-on-track type of test [82,83,84] involves 3-body abrasion combining both deformation and cutting wear.

The principal features of each abrasion test (in comparison) are as follows:

	Gauging	High-stress	Low-stress
Abrasive size ( $\mu\text{m}$ )	$6 \times 10^4$	80 or 120	250
Abrasive hardness ( $H_V$ )	800-1100	1800 (1360 knoop)	900-1280
Nominal stress level (MPa)	250	2.1	0.6
Degree of impact	High	Low	Low

Some of the tests, used for the specific wear resistant materials have been described briefly here:

(1) High Stress-specimen-on-track test:

The specimens for wear test are sand cast into 50 mm x 30 mm x 15 mm blanks. The front and rear faces of the specimen are angled to ensure ease of entry and exit of the abrasive particles between the specimen and the wear track. Specimens are cast slightly oversize and then finish ground, removing 1 mm from the face to be abraded. The abrasive selected for the tests is clean washed silica sand with a mean particle size of 250  $\mu\text{m}$ . Two specimens are tested in each wear test using a specimen-on-track machine. Each test is of one hour duration after a short run-in period. The nominal compressive stress on each specimen is 0.12  $\text{N/mm}^2$  and the linear speed of the specimens over the track is 1.4 m/sec.

## (2) Low stress - Rubber Wheel Test

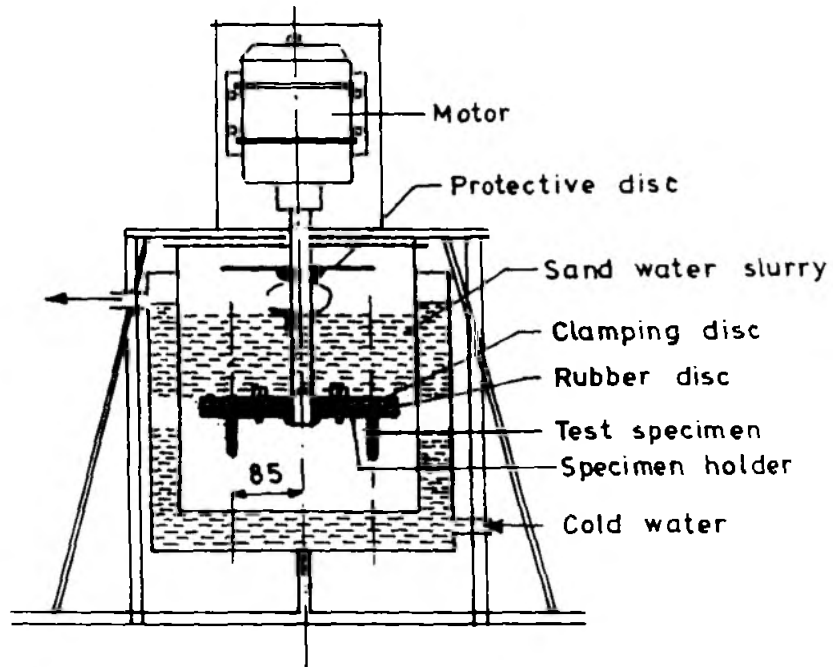
In the rubber wheel abrasion test [52] a specimen of known weight is pressed with a force of 222 N against a 178 mm dia rubber-rimmed steel wheel rotating at a speed of 240 RPM in a silica sand slurry. The slurry consists of 940 ml. of distilled water and 1500 gms. of sand (AFS 50-70 mesh). The used slurry is discarded after each test (5000 revolutions). After one run-in test, 3 tests are performed on each specimen with wheels of increasing rubber hardness (45, 55 & 65 shore durometer). For each test, the log of the weight loss is plotted against the hardness of rubber wheel, and a least-square line is fitted to three data points.

## (3) Cup-grinding Test (for corrosive-erosive wear)

A wear test equipment called 'cup-grinding' has been used by Basak et. al. [48] as shown in Fig. 2.5. In this, the specimens are used as stirring rods for vigorously stirring a sand-water slurry (3:2 by weight) in a water cooled, double walled closed vessel at about 1,000 RPM (linear speed 9 m/sec. or 540 m/min). Each wear test runs for 80 hours, with a break at the end of each 20 hours, for noting the wear loss of each specimen. Two standard samples of Ni-hard 4 are used alongwith for comparison.

## (4) Ball-on-ball Impact Test

Laird [3] used a ball-on-ball impact testing machine (Fig. 2.6) which facilitated multiple impacts of varying magnitudes on the balls within the J-tube section. This impact test is believed to simulate many field environments involving impact. Number of impacts-to-failure are measured in this test.

MAIN APPARATUS

Dimensions in mm

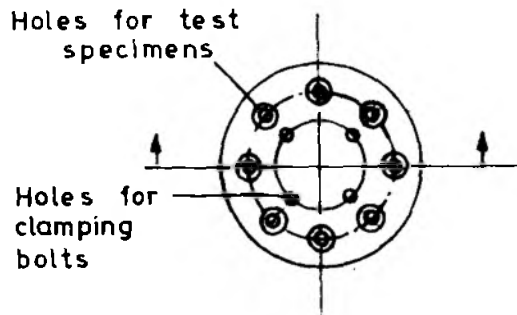
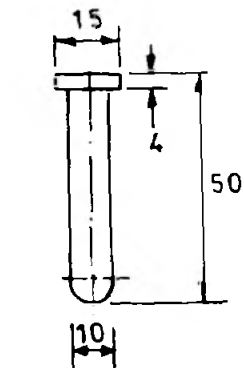
UPPER VIEW OF SPECIMEN HOLDERTEST SPECIMEN

Fig. 2.5 Apparatus for wear tests [48]

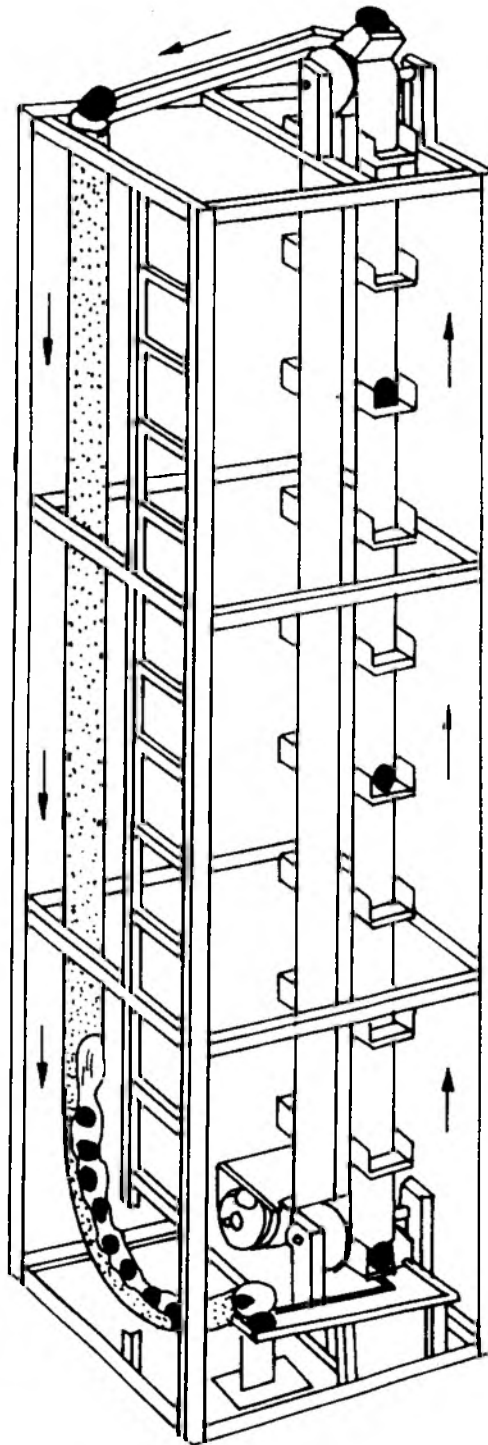


Fig. 2.6 Ball-on-ball impact wear testing machine [3]

About the composition-structure - abrasive wear property relations, various researchers [31,52,69,75,85-89] have done extensive work using different test methods, CWCI compositions; conditions (as cast or heattreated) and variety of abrasives. Their salient points of agreement and disagreement are summarised below.

### 2.8.2 Mechanisms of Wear

#### (1) Role of Carbides

Sare [88] concluded that, (1) low-stress abrasion resistance is controlled principally by the volume fraction and dispersion of hard carbides within the matrix, and the hardness of the matrix is of secondary importance. (2) Hardness of microstructurally heterogeneous solids is a poor indicator of low stress abrasion resistance.

Zungahr [75] discussed the influence of carbides in soft as well as in hard matrix and concluded that, (1) wear resistance increases with increasing carbide content in soft matrix. It suggested that wear resistance increases by decreasing mean free path ( $\lambda$ ), and carbide size ( $d$ ) in the equation

$$f^{1/2} = C(d/\lambda)$$

where  $f$  = volume fraction,

$d$  = particle diameter,

$\lambda$  = mean free path between the particles.

#### (2) Carbides in hard matrix behave as internal notches.

Pearce [70] reviewed the work of some researchers and concluded that (1) in austenitic materials, failure occurs by

cracking of eutectic carbides just ahead of fatigue cracks, cracking being initiated by a dislocation pile-up mechanism at the matrix-carbide interface. (2) In high C irons, the fracture paths follow the cleavage paths of the eutectic carbide, while in low C irons fracture paths in the austenite tend to follow through regions of strain induced martensite. (3) Martensitic irons give greater abrasion resistance than austenitic, when soft abrasives such as garnet and silica are used, maximum resistance being obtained with carbide volumes of 40-45%. (4) Austenitic irons give better abrasion resistance when hard abrasives such as alumina or silicon carbide are used, maximum resistance being obtained with carbide volume of 30%.

#### (2) Role of Retained Austenite

Sare [88] observed that the influence of austenite depends largely on its composition. When austenite retention is promoted by increasing its C or Cr content, an improvement in abrasion resistance is produced by the secondary carbide precipitation during subsequent heat-treatment. Strengthening of the austenite matrix can also occur by a work hardening mechanism in which metastable austenite undergoes a stress - induced transformation to martensite. According to Sare [88], Mn and Ni are austenite stabilizers and reduce the ability of austenite to work-harden by this mechanism. On the other hand, Cr and C tend to precipitate from solid solution, leaving the austenite in a metastable condition and able to transform.

Zungahr [75] reported that when retained austenite in a martensitic structure of a tool steel was reduced from 27% to 10% by refrigeration at  $-196^{\circ}\text{C}$ , hardness increased but wear

resistance decreased. This result is in stark contrast to the data for CWCI wherein it has been shown that wear resistance decreased with increasing retained austenite.

### (3) Modes of Wear Failures

Murray et. al. [86] gave a qualitative model and explained the relative role of cutting, ploughing and spalling (Fig. 2.7). It suggested that in case of high-stress abrasion, the wear mechanism was one of micromachining (i.e. predominantly cutting and ploughing), Hurricks [87] showed that relatively large increases in wear resistance occur when  $H/H_a$  is greater  $> 0.5 - 0.6$  (where  $H$  is the normal material hardness and  $H_a$  is the hardness of the abrasive. Hornbogen [89] explained that brittle materials like glasses, ceramics (exhibiting elastic fracture) are quite different from ductile metals (rigid-plastic). Brittle materials through cracking and spalling exhibit lower wear resistance than the ductile materials (Fig.2.8).

Pearce [70] conducted the specimen-on-track type wear tests on a series of chromium-containing white irons with chromium content ranging from 0-35%. The role of continuous ledeburitic  $M_9C$  type and fibrous  $M_7C_3$  type eutectic carbides during abrasion was examined. The relative effects of wear on pearlitic, austenitic, ferritic and martensitic matrix structures were also investigated. For the purpose of comparison of the relative wear resistance of the different alloys Pearce defined a parameter called Wear Index as given below:

$$\text{Wear Index} = \frac{\text{mean weight loss of white iron standard}}{\text{mean weight loss of alloy iron tested}}$$

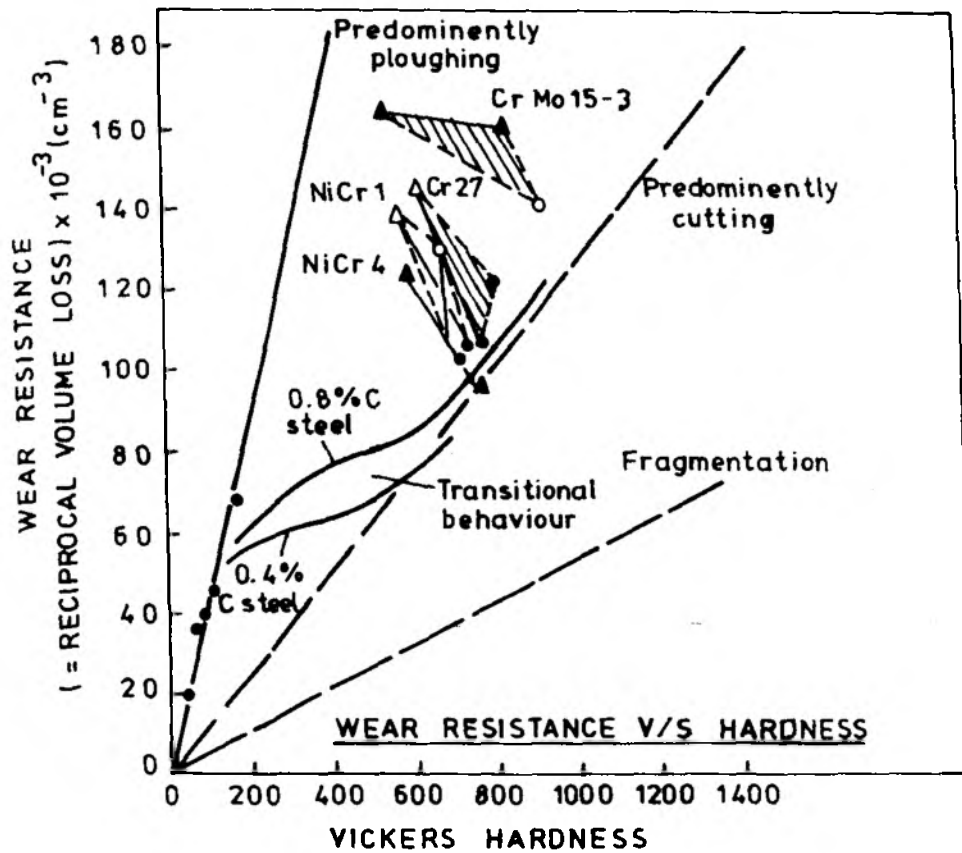


Fig. 2.7 Wear resistance of the white cast iron compared with quenched-and tempered carbon steels, pure metals and the wear regimes for cutting, ploughing and fragmentation suggested by Murray, Watson, and Mutton [86]

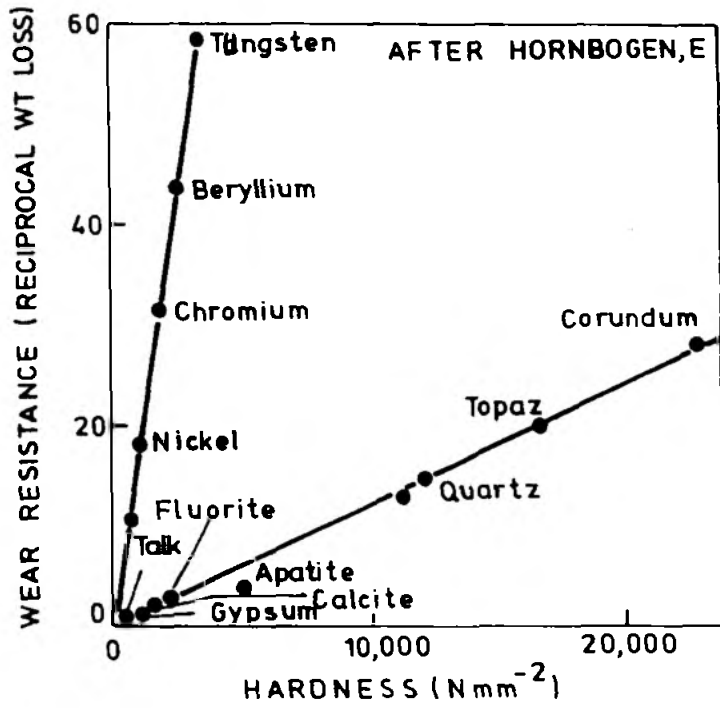


Fig. 2.8 The relationship between hardness and wear resistance for ductile materials (e.g. pure metals) and brittle materials (e.g. minerals) found by Hornbogen [89]

In all the irons examined by SEM and thin-foil TEM, the matrix and the eutectic carbides in the surface regions were distorted in the general wear direction. This caused deformation and cracking in the eutectic carbides and led to material removal by the detachment of the broken carbides from the matrix as well as penetration and cutting effects of the abrasive grits. Further, high stress abrasion resistance depends on the level of support given by the matrix to the eutectic carbides. Consequently, martensitic matrix structures gave greater abrasion resistance than austenitic or pearlitic structures.

## 2.9 Fracture Toughness Tests

The WCI being intrinsically brittle are poor in performance, where impact forces are encountered. Hence, attempts have been made to improve the toughness of these materials.

The conventional Charpy and Izod impacts tests can not give reliable results in case of WCI because these materials are hard, brittle and influenced by the carbides and matrix structures. They respond differently (not consistently) with notches and have poor sensitivity and lack reproducibility, hence impact tests are not very useful for WCI and CWCI. However, some work has been done on fracture-toughness (FT) of CWCI as evident from various papers published on the subject [52,88,90-91].

Pearce has attempted to establish relationship between structure, toughness and abrasive wear performance of CWCI. In general, impact tests show that WCI with the less continuous eutectic  $M_7C_3$  carbides absorb more energy in fracture than

irons with  $M_3C$  carbides, e.g. In impact fatigue, ball-drop tests, martensitic 18 Cr/2C withstood 20,000 drops, compared to about 3,000 drops for martensitic low alloy Ni-Cr irons.

However, for quantitative assessment of FT and for establishing its relationships with the structure, FT tests are necessary. These have enabled to determine the effects of carbide type, volume, morphology and the matrix on FT.

The level of both static ( $K_{Ic}$ ) and dynamic ( $K_{Id}$ ) F.T is reduced by increasing the volume of eutectic carbides present in the microstructure. At a given C level, increase in toughness can be obtained by refinement of eutectic carbides or by the reduction in the continuity of the carbide network. This involves decreasing the primary dendrite arm spacing, spheroidization of the as-cast carbides or hot-working of the cast structure [92].

Austenite dendrite refinement by increasing the cooling rate during solidification of a 15% Cr WCI gave a corresponding refinement of interdendritic carbides. Comparable increases could be made more easily by reducing C content by 0.4%. The use of die casting or hot working poses die material problems and would be limited to simple shapes [93,94].

Vacuum heat treatment at  $1180^\circ\text{C}$  produced spheroidization of the eutectic carbide lamellae in 15% Cr irons containing Mo or W, resulting in increase in toughness for austenitic matrix structures. After H.T. at  $1180^\circ\text{C}$ , the austenite matrix is stabilized and no benefit is gained if the iron is subsequently hardened since F.T. in martensitic irons containing secondary carbides are relatively independent of eutectic carbide morphology [95].

D.W.J. Elwell [96] has developed the short rod/short bar technique of fracture toughness determination. This avoids fatigue precracking and uses relatively simple test specimens, giving similar discrimination between different alloys to conventional testing.

ZumGahr and Doane [52] have described the dynamic fracture toughness ( $K_{I_d}$ ) testing of WC/Co. This is measured using an instrumented Charpy impact test machine. The standard size Charpy specimens 10 x 10 x 55mm were notched by EDM, a 0.2 mm radius slot 2 mm in depth. The hammer of the testing machine was released from a drop height, which produced a hammer velocity of 1.23 m/sec. at impact. Load and energy as a function of time were recorded during each test. The fracture load was used to calculate  $K_{I_d}$  values using the equation for bend specimens given in ASTM E 399-78. The testing was carried out in normal laboratory air with relative humidity of 50% and 21°C temp. (average).

The F.T. values as a function of volume of massive carbide, for a few WC/Co are as shown in Fig.2.9 F.T. v/s hardness relation is as shown in Fig. 2.10.

Sare [88] has suggested the double bend test (DTB) (in contrast to Compact Tension (CT) test which requires only a very simple specimen configuration, as shown in Fig.2.11 thereby eliminating the need for expensive and the time consuming specimen machining operations. The DTB test does not require a fatigue precrack (as a crack initiator) which is difficult to grow and measure its length.

In DTB, the only parameters to be measured are the specimen dimensions and the critical load  $P_c$ , for crack

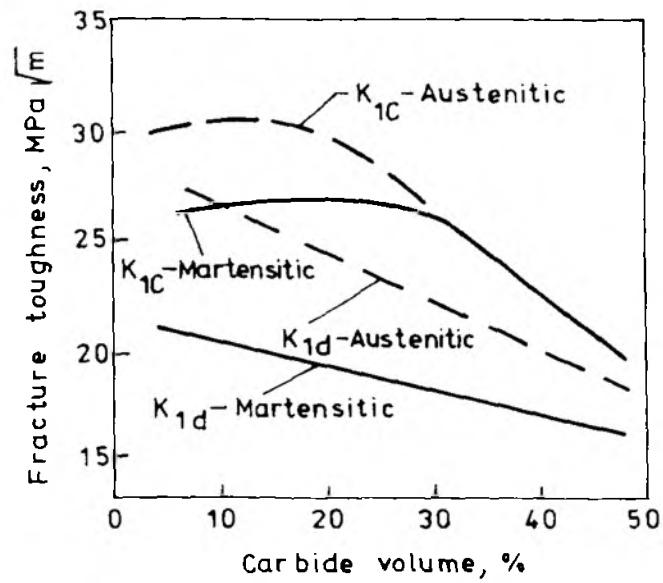


Fig. 2.9 Fracture toughness of Austenitic and Martensitic matrix irons as a function of volume of massive carbide (from Zum Gahr and Sholz) [67]

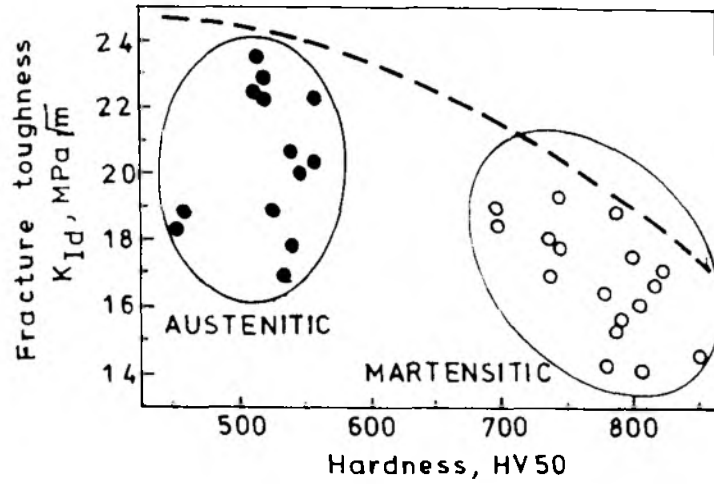


Fig. 2.10 Dynamic fracture toughness V/S hardness for WC1 subjected to various heat treatments . [52]

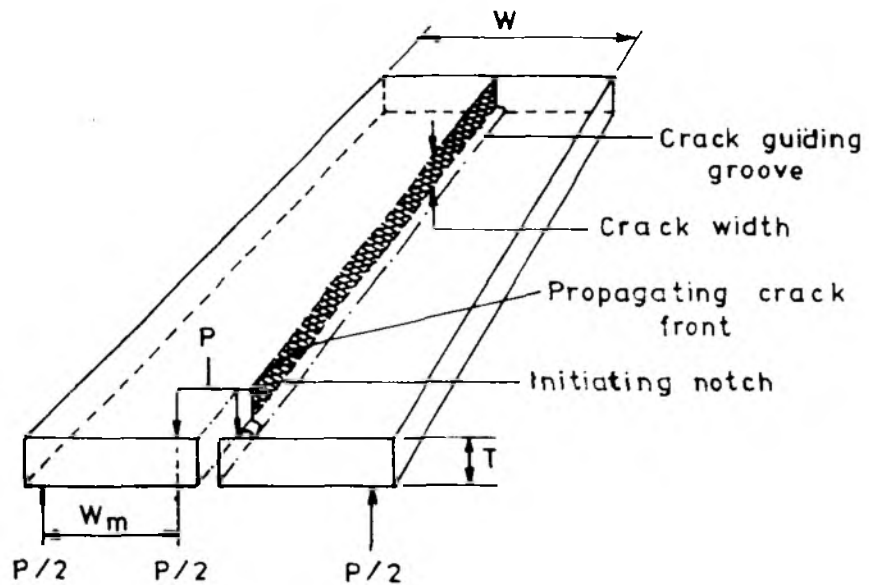


Fig. 2.11 Schematic diagram of double-torsion bend test specimen showing load application point [88]

propagation.  $K_{IC}$  is calculated from the equation

$$K_{IC} = PW_m \{ 3/[WT^3t(1-\nu)] \}^{1/2}$$

where P = critical load.

$W_m$ , W, T, t are as shown in the diagram.  $\nu$  is Poisson's ratio which is taken to be 0.3.

## 2.10 Corrosion Test

There are varieties of tests available for determining the corrosion characteristics of the alloy in question. However, these tests are quite time consuming, laborious and costly. Many of the traditional corrosion tests are field tests. An account of commonly used corrosion tests is given in the text book of Corrosion Engineering, [97].

However, based on the modern theory of electrochemical nature of corrosion, "electrode kinetics" has become a useful tool for the quick and quantitative determination of corrosion behaviour. The theory and applications of these techniques have been given by Fontanna [97].

Andrews, Buchanan and Gordon [98] used this technique called Anodic Polarization Measurements using a potentiostat and a polarization cell, described in detail by Thompson [99].

The polarization measurements are obtained using potentiostatic potential steps of 50 millivolts (mv) at 5 minute intervals and recording the corresponding current flow after each increment. The anodic polarization curves are plotted as potential versus log of the current density (All potentials are measured relative to a saturated calomel electrode - SCE).

The corrosion resistance is evaluated using one normal solution of sulphuric acid ( $1N H_2SO_4$ ) held at a temperature of  $21 \pm 1^\circ C$ . Oxygen is purged from the solution by bubbling purified nitrogen through the electrolyte for 15 minutes prior to placing the sample in the cell. The sample is allowed to stabilize for one hour in the cell before testing, and continuous purging is carried out during the stabilization and testing.

The pitting resistance is evaluated in a one normal sodium chloride solution ( $1N NaCl$ ) by the identical experimental procedure as mentioned above.

The important features of a typical P.A.P. curve for a passive alloy are as follows: (Fig. 2.12)

The X-axis records log current density  $I$  while Y-axis denotes the voltage (potential)  $E$ . In this plot, the potential is roughly equivalent to the oxidizing power of the solution while the current density is proportional to the corrosion rate. The critical current density  $I_c$ , indicates the degree of difficulty encountered in initially forming a passive film on an alloy. Low values of  $I_c$  are desirable since they indicate the ease of passive film forming. The potential which corresponds to the  $I_c$  is known as the passivation potential,  $E_{pp}$ . The minimum current density  $I_{min}$ , indicates the rate of corrosion with the passive film present. Low values of  $I_{min}$  are desirable. The breakdown potential,  $E_b$ , indicates the potential at which the passive film begins to breakdown. It is desirable to have high values of  $E_b$ . The portion of the curve between  $E_{pp}$  and  $E_b$  is known as the passive region. Thus good corrosion resistance is indicated by low values for  $I_c$ ,  $I_{min}$  and  $E_{pp}$

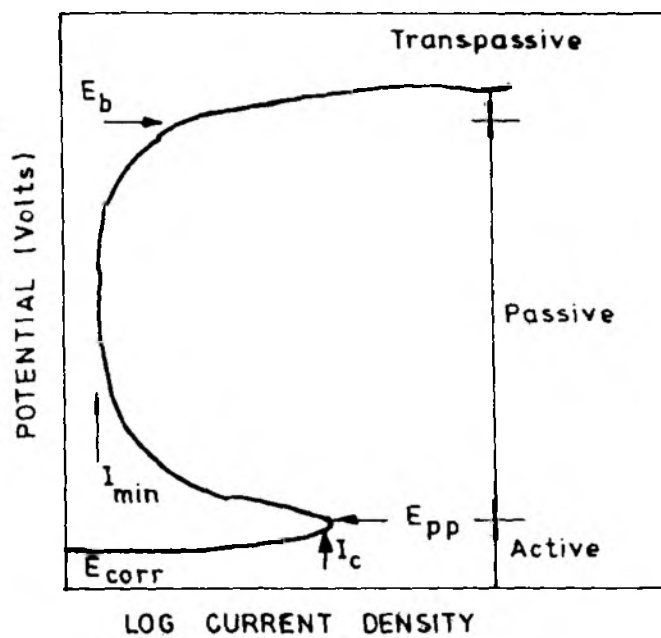


Fig.2.12 Anodic polarisation curve for cast and homogenized 304SS standard [98]

alongwith a high value for  $E_b$ .

Fig.2.12 shows a typical anodic polarization curve for cast and homogenized 304 S.S. standard. It shows  $I_c = 80 \mu A/cm^2$ ,  $I_{min} = 0.5 \mu A/cm^2$  (slightly lower than the  $1.0 \mu A/cm^2$  normally reported as typical for type 304 SS.).

## 2.11 Chromium White Cast Iron as a Cutting Tool Material

With the advent of newer work materials, there is demand for newer tool materials and hence research has been going on in this area. Alongwith the hardmetals (tungsten carbide) there are developments going on in ceramics, cermets (~~Ti-C-N~~<sup>(titanium carbonitride)</sup>), PCD, micrograin hardmetals & coated hardmetals [100-108]. But on the other hand, research has been directed to the developments of

(1) Tungsten-free High Speed Steels [108,109]

(2) Economic low-cost tools for small scale industries.[110-117].

Both these areas are of important to the country like India, where W is not found and there are plenty of small scale industries, which need economic cutting tool material.

Work on WCI as a cutting tool material has been reported first in 1979 [110] at IIT, Kharagpur, when forging of WCI was tried. Cold forging gave increased graphitisation of carbides and even fracturing. The strength and toughness were improved by hot forging, but not without the risk of crack formation. Even 50% reduction could not break the carbide network. Bhattacharyya [111] investigated the performance of a glass type very cheap tool material being developed by CGCRI (India) and reported the failure of these tools because of its brittleness and lack of toughness. It was reported that the

carbide network in WCI could be broken down and dispersed by hot rolling to improve its toughness. Chakraborty [112], Babu [113], and Rao [114] reported work on WCI as a cutting tool material. Mukherjee [115], Das [116] and Chakraborty [117] attempted further improvement by nitrogenating WCI tools by passing Nitrogen gas; using  $K_4Fe(CN)_6$  (potassium ferrocyanide) and Manganese nitride respectively and reported improvement.

However, the mechanisms of improvement were not reported and the physical metallurgy of structures were not fully understood.

## EXPERIMENTAL PROCEDURE

The procedures and techniques employed for the present research consisted of the following:

1. Melting and casting
2. Metallography and heattreatment
3. Dilatometry (TMA)
4. X-ray diffraction analysis(XRD)
5. Transmission Electron Microscopy (TEM)
6. Wear Studies (Abrasion)
7. Machining Trials (for flank wear, tool life and cutting force measurements)
8. Scanning Electron Microscopy (SEM)for carbide morphology,wear and tool failure studies.
9. Corrosion Tests (Potentiostatic)
10. Spectrography for Chemical Analysis in addition to wet methods and nitrogen analysis.
11. Photomicrographic support to the optical,SEM and TEM.
12. Hardness and Microhardness.

### 3.1 Melting and Casting

All the present alloys were prepared in an induction melting furnace (frequency 9.6 K Hertz and rating 20KW) in magnesia crucibles. The alloys were melted in 1.5 Kg. and 5.0 Kg. crucibles. The charges for melting consisted of carbon

steel scrap (C 0.5%) ferrosilicon, graphite and high carbon ferrochromium (60-65% Cr, 4-6% Si, 5-6% C). Nitrogen was added as nitrided manganese (nitrogen 6%) or nitrided chromium (5-6% N). The nitrided alloys were packed in mild steel capsules and plunged into the melts to ensure proper nitrogen pick up.

All charge calculations were made assuming ten percent loss of alloying elements during melting. The experimental samples were cast in the form of 15mm x 15mm x 150 mm square cross-section rods in dry sand moulds. Chill plates of mild steel of 5mm thickness and 50mm x 50mm cross-section were used at the bottom of the mould to promote directional solidification. A few samples were also cast in 12 x 12 mm square chill moulds. The melts were poured immediately after dissolution of the nitrided alloys into the melt to minimise loss of nitrogen. (Photograph 1)

The castings were allowed to cool in the mould itself upto room temperature, then the castings were taken out from the mould, the riser were cut off using abrasive cutters and the surfaces were dressed by grinding.

The alloys investigated and their chemical compositions are given in table 3.1. The alloys were of 11-12% Cr contents. The alloy A<sub>g</sub> was chill cast in 12mm x 12mm metallic mould. All other alloys were sand cast.



Photograph No.1 : CWCI molten metal being poured from induction furnace into a sand mould.

Table 3.1  
Chemical composition of various experimental alloys  
investigated

Alloy Designation	Chemical composition (wt%)						
	C	Cr	Mn	Si	Al	Ti	N(ppm)
A <sub>1</sub>	3.43	12.50	0.93	1.00	0.01	0.03	-
A <sub>2</sub>	3.30	12.00	2.45	0.98	0.01	0.03	300
A <sub>3</sub>	3.90	11.50	2.50	1.10	0.01	0.13	316
A <sub>4</sub>	3.34	12.00	2.50	1.10	0.08	0.03	348
A <sub>5</sub>	3.25	12.25	2.50	0.90	0.20	0.03	294
A <sub>6</sub> *	3.97	11.70	2.50	1.26	0.01	0.03	300
A <sub>7</sub> *	3.20	11.50	2.76	1.54	0.01	0.33	302
A <sub>B</sub> (chill cast)	3.35	13.86	2.60	1.02	0.01	0.032	300
B <sub>1</sub>	2.89	11.94	0.29	0.40	0.01	0.016	-
B <sub>2</sub>	2.70	11.50	1.77	0.41	0.01	0.013	319
B <sub>3</sub>	2.60	11.75	2.40	0.89	0.01	0.33	377
B <sub>4</sub>	2.50	11.60	2.40	0.89	0.01	0.39	395
C <sub>1</sub>	2.80	11.92	3.9	1.57	0.01	0.03	475
C <sub>2</sub>	2.85	12.00	3.8	1.62	0.01	0.92	.493

\* Nitrogen added as nitrided chromium. Nitrogen addition to other alloys was made as nitrided manganese.

### 3.2 Metallography and heat treatment

The as cast samples were first examined under a light microscope. The matrix in all the as cast samples were expected to contain varying amount of retained austenite. Heat treatment was carried out (a) to destabilise the retained austenite and (b) to harden and temper the matrix. The effect of transformation during heat treatment was evaluated primarily by hardness testing. However,

microstructure of representative specimens were also examined.

Initial soaking in the temperature range 900-950°C was carried out in a muffle furnace. The specimens were packed in charcoal to prevent decarburisation. Low temperature tempering at 200°C was done in an oven. Tempering at temperatures of 300°C and above was done in salt bath furnaces.

Different schedules of heat treatment cycles were initially tried on small metallographic samples for optimisation of the heat treatment procedure. The final heat treatment of test wear samples and test tool samples were conducted only according to selected schedules.

#### Phase - I

The heat treatment of the A-series (Table 3.1) samples was carried out in Phase I and the details are given below:

- (A) Ageing of as cast A-series samples for one hour at temperatures ranging from 200°C to 700°C at intervals of 100°C. The purpose of this heat treatment was to study the ageing response, if any, of samples containing N+ Al or N + Ti.
- (B) Austenitisation of A-series samples was initially carried out for one hour at 1100°C and 950°C respectively. The samples were then <sup>Water/Oil</sup> quenched and tempered. Two different soaking temperatures were used to study their effect, if any, on the as quenched hardness and subsequent tempering treatment. The samples <sup>Water</sup> quenched from 1100°C were tempered isochronally for one hour at temperatures

ranging from 200°C to 800°C at intervals of 100°C.

Oil

The samples quenched from 950°C were also tempered isochronally in the identical manner. In addition, these samples were also tempered isothermally at 300°C and 600°C respectively for periods of 15 minutes and 1 hour.

- (C) Austenitisation period at 950°C was varied for A series alloys for periods ranging from 1 hour to 5 hours, and it was followed by oil quenching. This was done to optimise the time of soaking required to develop the maximum as quenched hardness.
- (D) After the initial trials, heat treatment schedule finally adopted for hardening the wear test samples was soaking at 950°C for 2 hours followed by oil quenching and tempering at 200°C for 1 hour.

#### Phase - II

The heat treatment of B and C series samples (Table 3.1) was carried out in Phase II. These samples were used both as cutting tools as well as for abrasive wear tests. Initial exploratory trials indicated that forced air quenching from a soaking temperature of 900°C was adequate to harden the nitrogen bearing samples. By reducing the soaking temperature from 950°C to 900°C and by substituting oil quenching by forced air draft quenching, the incidence of quench crack formation was totally eliminated. The following heat treatment schedules were tried:

- (i) Soaking at 850°C for 1 hour, forced air draft quenching and tempering at 200°C.
- (ii) Soaking at 900°C for 1 hour, forced air draft

quenching and tempering at 200°C.

- (iii) Soaking at 900°C for 2 hours for B series samples and upto 8 hours for C series samples, forced air draft quenching and tempering at 200°C for 1 hour. Some of the B series samples were also cryotreated in liquid nitrogen (-196°C) after air quenching from 900°C and then tempered at 200°C.

The cutting tool and abrasion test samples were finally heat treated according to schedule (iii) only. B<sub>1</sub> was oil quenched. Adequate hardness could not be developed after quenching from 850°C and hence this heat treatment schedule was not finally tried.

The microstructures of the heattreated samples were also examined.

Microhardness readings on the matrix and the carbide phases were determined separately on a few as cast and heat treated samples. A LECO Hardness Tester (Model DM400) was used. For most of the samples loads of 25 gm for carbides and 10 gm for the matrix respectively were selected.

Photomicrographs of selected as cast and heat treated samples were also taken.

### 3.3 Thermo Mechanical Analysis (TMA)

To study the transformations taking place on heating and cooling, samples of A series alloys, were subjected to Thermo Mechanical Analysis (TMA) using a Shimadzu Thermal Analyzer DT-30. The heating rate employed was 30°C/min. Holding time was 5 hours at 950°C. The samples were cooled in-situ using a forced draft by a small fan. Some samples

were refrigerated in liquid nitrogen, and observed for any transformation taking place at the subzero temperatures. For this purpose, the alumina tube containing the experimental sample was dipped in liquid nitrogen kept in a polystyrene container. The graphical plots, gave information about the type of transformation (pearlitic, bainitic or martensitic) taking place during cooling. However, this was further confirmed by examination of the microstructures of the samples after conclusion of the tests.

### 3.4 X-ray Diffraction Analysis

The selected as cast, as quenched, quenched and tempered, and quenched cryotreated and tempered samples were studied on Philips X-ray Diffractometer. Molybdenum  $K_{\alpha}$  radiation was used for diffraction. The samples were scanned from  $15^{\circ}$  to  $45^{\circ}$  at a speed of  $1.2^{\circ}/\text{min}$ . The X-ray diffraction patterns were used to calculate retained austenite contents, using integrated intensities at  $32.5^{\circ}$ , (220) for austenite and  $35.7^{\circ}$  (112) for ferrite as at these angles, there was no interference of carbides. Carbides and other phases present in the samples were also identified by X-ray diffraction.

### 3.5 Transmission Electron Microscopy

A few heat treated samples were further examined under a Transmission Electron Microscope (Philips CM12) by replication technique. Since direct carbon extraction replicas of chromium cast irons could not be stripped even after persistent efforts by different techniques, it was decided to adopt two stage replicating technique. First a plastic replica of the etched surface was prepared using a

standard replicating tape. Next, carbon deposition was done on the plastic replica surface. The plastic base was next dissolved in acetone, the graphite replica was fished out, washed in water and examined in TEM.

### 3.6 Wear Studies

The wear tests were carried out using modified pin-on-disc machine. A laboratory polishing wheel was modified for the purpose, by fixing a 15 cm. dia alumina grinding wheel (grade A.60 QV) on the polishing wheel. The sample 15mm x 15mm x 50mm was clamped in a holder and was held against the rotating wheel under load rigidly. Three different loads were applied for the test : 0.5 Kg, 1 Kg, and 1.5 Kg [4.9N, 9.8N and 14.7N respectively] respectively. The spindle speed was 250 RPM, which at an average distance of 8 cm from the centre gave a linear speed of 120m/min (2m/sec). (Fig.3.1).[Photograph 2]

The loss in weight was measured at intervals of 10 minutes. The test was continued for 60 minutes. Cumulative weight loss per unit area was plotted against time. The weight loss per unit Load per unit distance travelled (wt. loss/N/m) gave a measure of the wear rate.

The abraded surfaces of the samples were studied under SEM for the probable wear mechanism. The wear behaviour of samples of A, B and C series were studied.

### 3.7 Machining Trials

To evaluate the usefulness of CWCI as a cutting tool material in turning, the 15mm x 15mm blanks were cut to

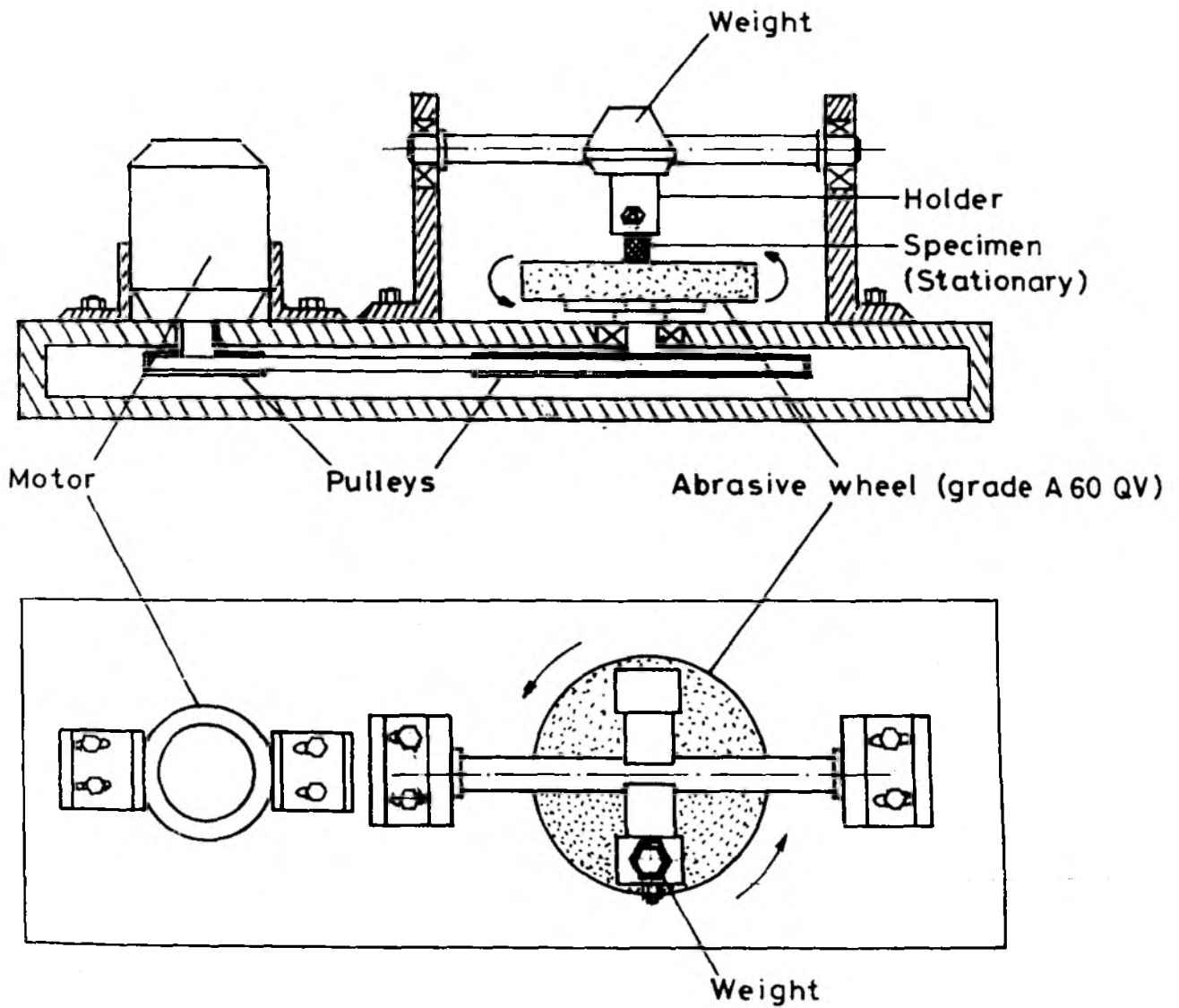


Fig. 3.1 Schematic diagram of Modified pin-on-disc Machine, used in the present study

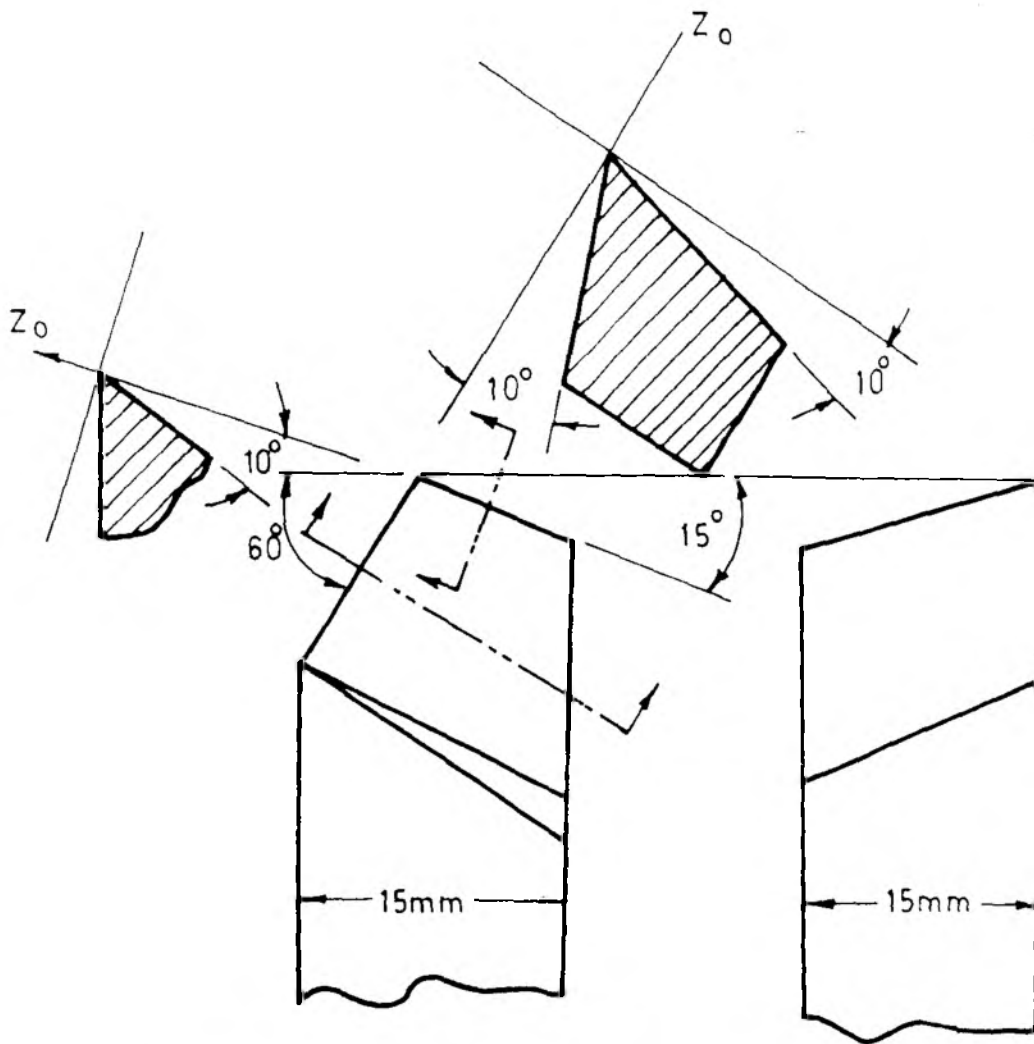


Photograph No.2 : Modified pin-on-disc machine for the abrasive wear tests.

a length of 70 mm. These blanks were shaped in a grinding wheel and then finish ground for desired geometry on a tool and cutter grinder to a geometry as shown in Fig. 3.2. Then tools thus made were tested for tool life (flank wear = 0.3 mm) at speeds of 40m/min and 50 m/min and feeds of 0.12 mm/revolution and 0.16 mm/revolution. The work piece material used was steel grade C<sub>25</sub> having the following composition C 0.25, Si 0.05, Mn 0.73, Cr and Ni 0.03 each, S and P < 0.03. A HSS tool was taken as a reference cutting tool.

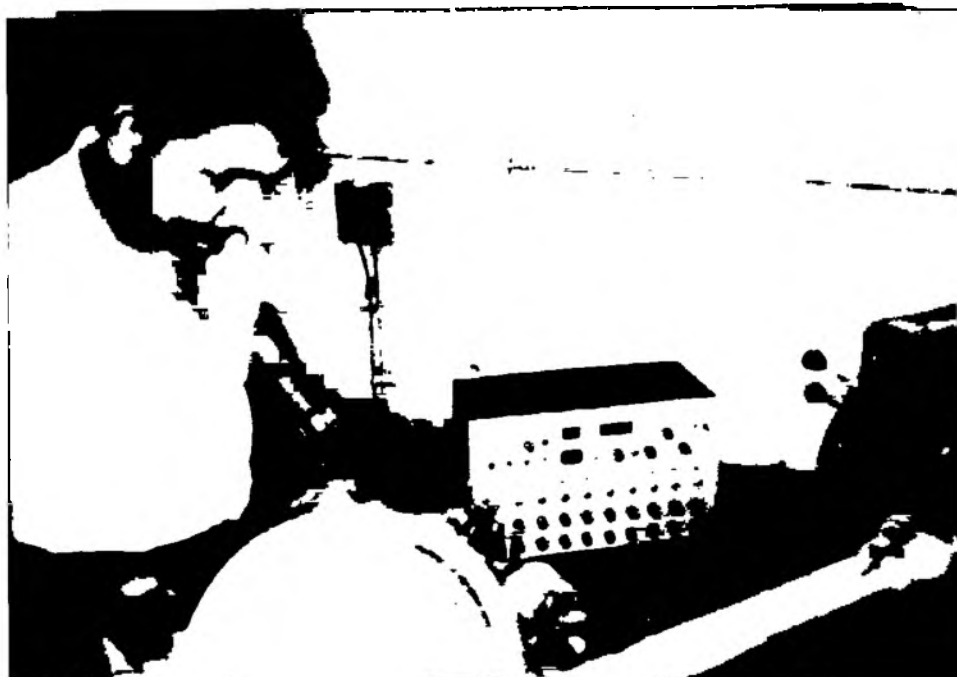
The main or tangential and the axial cutting forces were measured using a tool force dynamometer in conjunction with strain measuring instrument [Photograph 3]. During machining, the chips were collected after one minute, and the chip thickness were measured to calculate the value of chip reduction coefficient ( $\zeta$ ). The microhardness of the chips formed by different tools at similar speed-feed combinations was measured. The heattreatment given to the tool blanks was as follows: Soaking at 900°C for two hours, forced air draft cooling and then tempering at 200°C. Some of the tools were also cryotreated in liquid nitrogen before tempering. In case of only one tool (A 8, chill cast) the soaking time at 900°C was varied from 2 hours to 7 hours and the tempering was also done at 200°C and 150°C respectively. This was done primarily to study the effect of retained austenite content on the cutting efficiency.

$$\zeta = \text{Chip reduction coefficient} = \frac{\text{Chip thickness } (a_2)}{\text{thickness of uncut layer } (a_1)}$$



TOOL GEOMETRY :  $0^\circ, 10^\circ, 10^\circ, 10^\circ, 15^\circ, 60^\circ, 0$  (mm)  
(ISO)

FIG.3.2.GEOMETRY OF THE TOOLS TAKEN FOR INVESTIGATION



Photograph No.3 : Cutting force trial with tool dynamometer in progress. Strain measuring instrument is seen in the background.

but  $a_1 = S_o \sin\phi = \text{true feed}$

$$\therefore \zeta = \frac{a_2}{S_o} / \sin 60^\circ$$

For a particular feed,  $a_1$  was constant, and thus  $a_2/a_1$  gave chip reduction coefficient values.

The mode of failure of each tool and its life were noted under the preselected speed-feed conditions.

### 3.8 Scanning Electron Microscopy

Selected as cast samples were examined under SEM (Camscan) to study the carbide morphology. These samples were first deep etched in aqua regia, then treated with dilute HF solution to remove silica and then finally washed in water. The etched samples were gold coated by sputtering and then examined in SEM. For the purpose of determination of chromium partitioning between the matrix and the eutectic phases by EDAX, only normal etching was done.

The worn out tools and abrasive wear samples were also examined in SEM, both in unetched condition as well as after etching in 25% phosphoric acid to determine the wear pattern. The undersurface of chips formed during machining with standard HSS tools and chromium cast iron tools were also examined in SEM, to assess the crack density in the chips and metal flow pattern.

### 3.9 Corrosion Tests

The corrosion tests on samples  $C_1$ ,  $C_2$  and  $A_1$  were

carried out using EG and G Princeton Applied Research Model 362 Scanning potentiostat (with Model RE0092 X-Y recorder). The tests were carried out in both 1N HCl as well as 1 Molar NaCl solutions. Potentiostatic curves were plotted at 10 mV/sec scan rate, and the current range 0-1A. The curves plotted gave an idea about the passivation behaviour of these alloys.

## RESULTS

### 4.1. As Cast Structures and Response to Heat treatment

#### 4.1.1. Nitrogen addition

Nitrogen addition to the experimental chromium cast irons was made as 3 wt.% potassium ferrocyanide, nitrided manganese (5-6 wt %N) and nitrided chromium (5-6 wt.%N). The nitrogen pick up in 12% chromium cast irons containing a minimum of about 1.6% Mn is shown in Table 4.1.  $K_4Fe(CN)_6$  was equally effective as a nitrogen source like the nitrided chromium. However, after the first batch of experiments, its addition was discontinued due to the potential hazards. Nitrided manganese however, yielded higher nitrogen pick up. Increasing the quantity of nitrided manganese addition from 2 wt.% to 4 wt.% of the charge resulted in porosity in the castings. Nitrided chromium addition was also tried at three incremental doses - 2 wt%, 4 wt.% and 6 wt.% of the charge. In each case, the chromium percentage was adjusted around 12% and manganese around 2.0% by adjusting the amount of ferrochromium and ferromanganese additions respectively. The nitrogen pick up, however, did not increase with higher dose of nitrided chromium addition.

#### 4.1.2 As cast Microstructure

A comparison of the as cast structures of 12% Cr cast irons treated with nitrogen alone and nitrogen and

Table 4.1 Nitrogen pick up in trial samples

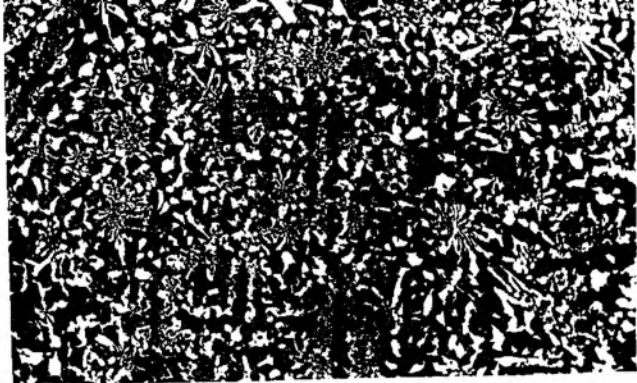
Sl No.	Method of Nitrogen addition	Nitrogen pickup in ppm	Chemical composition of the alloy					
			C	Cr	Si	Mn	Ti	Al
1.	3% $K_4Fe(CN)_6$	300	3.90	10.45	0.60	0.46	0.040	0.01
2.	2% Mn N	632	3.90	11.50	1.10	2.50	0.13	0.01
3.	2% CrN	316	3.00	11.00	1.30	0.45	0.66	0.01
4.	4% Cr N	294	2.90	10.50	1.60	0.50	0.22	0.01
5.	6% Cr N	310	2.90	10.65	1.80	0.60	0.33	0.01

titanium together were made by hardness and microhardness measurements, light microscopy, SEM and X-ray diffraction.

The microstructures of the A series alloys varied from hypoeutectic to near eutectic and slightly hypereutectic types due to differences in alloy composition and segregation of alloying elements. The microstructure of an alloy varied from section to section and even across a particular section. Hence the exact influence of nitrogen and titanium could not be assessed from the as cast microstructures examined under a light microscope. A series of photomicrographs of different alloys in as cast state are presented in Fig. 4.1 (a-f). From these photomicrographs, however, at least four different modes of growth of eutectic carbide in 12% Cr cast irons may be identified. The carbide morphology in Fig. 4.1a is the usual plate like. A typical colony structure is present in Fig. 4.1b. Unlike that in 4.1b the carbide plates in each of the eutectic colonies in 4.1c had grown from a hexagonal carbide in the core. Fig. 4.1d taken from the same section of the same alloy ( $A_1$ ) shows a typical platelike eutectic carbide growth. An example of interdendritic eutectic carbide growing in close proximity of primary carbide is illustrated in Fig. 4.1e. Simultaneous ledeburitic eutectic growth may occur along with other modes of eutectic growth. This may be noted from Fig. 4.1b. The chill cast sample  $A_6$  had a completely eutectic structure. Fig. 4.1f presents an apparent case of divorced eutectic growth of carbide rods. In all these samples the matrix was mainly pearlitic. The photomicrograph in 4.1b was actually taken from a quenched and tempered sample of  $A_2$  to illustrate that the eutectic structure is not affected by heattreatment.



(a) X 152



(b) X 152



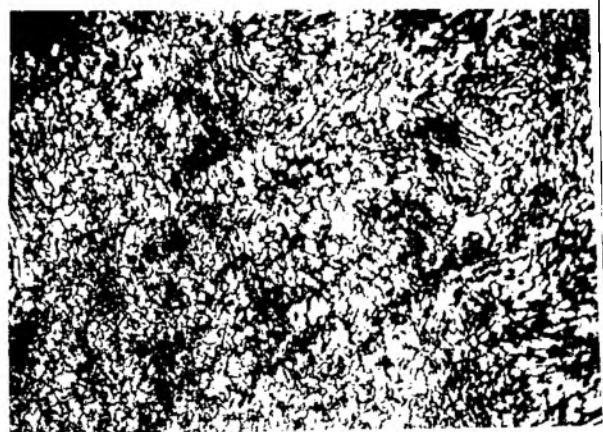
(c) X 152



(d) X 152



(e) X 152



(f) X 152

Fig.4.1 : Morphology of eutectics in A-series alloys (a-f).

- (a) Plate like eutectic ( $A_1$ )
- (b) Colony type and ledeburitic eutectic
- (c) Eutectic colony growth from a hexagonal ( $A_2$ ) primary carbide ( $A_7$ )
- (d) Plate like eutectic in the same samples as of 4.1(c) ( $A_7$ )
- (e) Interdendritic eutectic in close proximity of primary carbide ( $A_3$ )
- (f) Divorced eutectic carbide in a chill cast sample ( $A_4$ )

The as cast microstructures of the B-series alloys were more diverse. There was a gradual transition from predominantly pearlitic matrix in as cast  $B_1$  &  $B_2$  [Fig. 4.2(a-b)] to pearlite + stabilised austenite matrix in  $B_3$  (Fig. 4.2c) to almost completely austenitic matrix in  $B_4$  sample (Fig. 4.2d). In the nitrogen bearing samples containing higher amount of manganese [ $C_1$  and  $C_2$ ], the matrix was largely austenitic (Fig. 4.3). All these alloys were of hypoeutectic composition. X-ray diffraction data of all the samples, however, indicate the presence of considerable amount of the ferrite (or martensite) as well (Table 4.2). The relatively high microhardness of the matrix of particularly  $B_1$  and  $B_2$  also suggests partial transformation of austenite to martensite. The microstructure of the base alloy  $B_1$  shows the usual type of platelike carbide. In other alloys, the plate morphology was less prominent. Apparently, some globularisation of carbides had occurred in  $B_4$  and  $C_2$ .

The phases present in the as cast and heat treated alloys of both A and B series were determined by X-ray diffraction analysis. The microhardness of the bulk phases were also determined. These data are tabulated in Table 4.2. The microhardness values of the carbide phases and matrix varies widely in each of the alloy. Hence, no attempt has been made to calculate the average microhardness of the carbide phase and the matrix separately. Instead, the microhardness values have been presented as such in Table 4.2.

#### 4.1.3 X-ray Diffraction analysis and Microhardness in as cast alloys

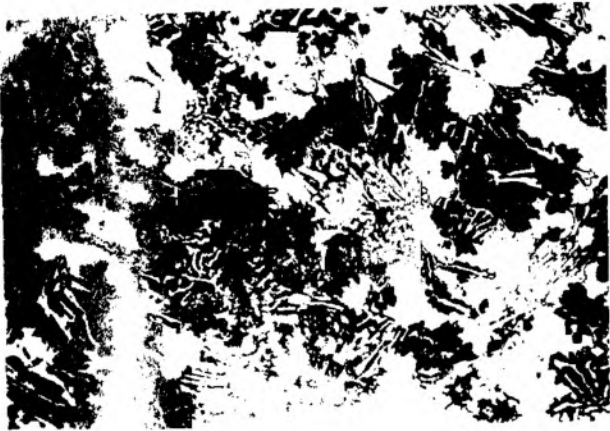
The presence of  $Fe_3C$  type carbide is likely, but some of



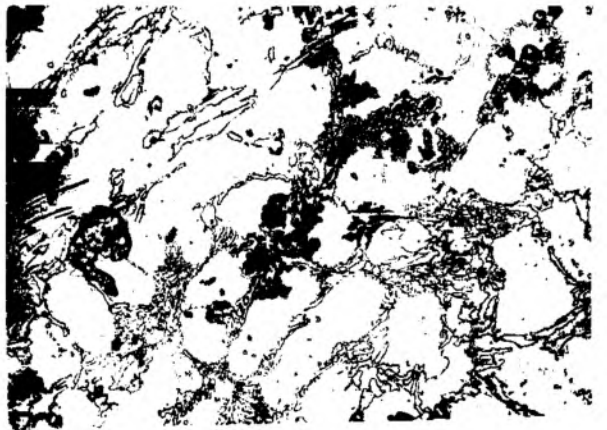
(a) X 132



(b) X 132



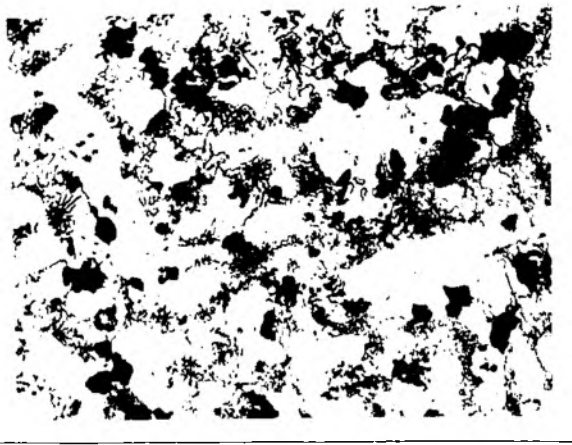
(c) X 132



(d) X 132

Fig.4.2 : As cast microstructure of B-series alloys.

- |                          |   |                        |
|--------------------------|---|------------------------|
| (a) alloy B <sub>1</sub> |   | Pearlitic              |
| (b) alloy B <sub>2</sub> |   |                        |
| (c) alloy B <sub>3</sub> | - | Pearlitic + austenitic |
| (d) alloy B <sub>4</sub> | - | Austenitic             |



X 152

Fig.4.3 : As cast microstructure of alloy C<sub>2</sub>

Table 4.2 Hardness, Microhardness and Phases Present in various alloys

Sample Designation	Hardness (R <sub>c</sub> )		Microhardness (VPN)		Phases Present	
	As cast	Quenched & tempered	(10 gms load)		As cast	As Quenched and tempered
						Carbide Matrix
A <sub>1</sub>	52	59	1003 1103 1390 1284 1051	509 549 482 453 401	$\alpha, \nu, Cr_7C_3$  $Cr_{23}C_6$  $(Cr, Fe)_7C_3$  $Fe_3C$ and $Cr_2C$  also likely	$\alpha, \gamma, Cr_3C_2, Cr_7C_3$  $Cr_{23}C_6, Mn_5C_2$  $Mn_{23}C_6$
A <sub>2</sub>	51	62	-	-	$\alpha, \nu, Fe_3C, Cr_7C_3, Cr_{23}C_6, (Cr, Fe)_7C_3$ $\gamma$ content more and $\alpha$ content less than that in A <sub>1</sub> (Likely other phases $(Cr, Fe)_7C_3, Fe_3C, (Cr_{0.62}Cr_{0.35}N_{0.03})$	$\alpha, \nu, Mn_{23}C_6, Mn_5C_2$ $Cr_7C_3, Cr_{23}C_6$ $Cr_{0.62}C_{0.35}$ $N_{0.03} Cr_2CN$
A <sub>3</sub>	52	64	-	-	$\alpha, \gamma, Cr_7C_3, Cr_{23}C_6, Fe_3C, (Cr_{0.62}C_{0.35}, Mn_{23}C_6, N_{0.03})(Cr, Fe)_7C_3$ AlN also likely Ti <sub>2</sub> N	$Cr_{23}C_6, Cr_7C_3$ $(Cr, Fe)_7C_3$ $Cr_{0.62}C_{0.35}$ On tempering at $N_{0.03} 600^\circ C / 1$ hr, precipitation of $Ti_2N, Cr_2C$ also noted.
A <sub>4</sub>	52	64	1392 1103 1392 1077 1519	358 389 401 395 407	$\alpha, \gamma, Cr_{23}C_6, (Cr, Fe)_7C_3, Cr_{0.62}C_{0.35}N_{0.3}, TiC$	$\alpha, \gamma, Cr_7C_3, Cr_{23}C_6, Cr_{0.62}C_{0.35}, N_{0.03}$
A <sub>5</sub>	55	66	-	-	$\alpha, \gamma, Cr_{23}C_6, Cr_7C_3, Fe_7C_3$ and $(Cr_{0.62}C_{0.35}N_{0.03})$	On tempering at $600^\circ C / 2$ hr AlN precipitation occurred.

A <sub>6</sub>	55	64	1051	467	Cr <sub>7</sub> C <sub>3</sub> , Fe <sub>7</sub> C <sub>3</sub> ,	α, γ, Mn <sub>23</sub> C <sub>6</sub> .	
			1251	432	(Cr, Fe) <sub>7</sub> C <sub>3</sub> ,	Mn <sub>5</sub> C <sub>2</sub> , Cr <sub>23</sub> C <sub>6</sub>	
			1514	348	Cr <sub>2</sub> C, Fe <sub>3</sub> C,		
			1319	348	Cr <sub>7</sub> C <sub>3</sub> ,	Fe <sub>7</sub> C <sub>3</sub> ,	
			1131	302	Cr <sub>0.62</sub> C <sub>0.35</sub> N <sub>0.03</sub>	(Cr, Fe) <sub>7</sub> C <sub>3</sub>	
		1392	430		Cr <sub>0.62</sub> C <sub>0.35</sub> N <sub>0.03</sub> , Cr <sub>2</sub> CN (Cr <sub>23</sub> C <sub>6</sub> peak intensity much greater than that of Cr <sub>7</sub> C <sub>3</sub> )		
A <sub>7</sub>	53	58	1051	363	Cr <sub>7</sub> C <sub>3</sub> , Fe <sub>7</sub> C <sub>3</sub> ,	Mn <sub>23</sub> C <sub>6</sub> , Fe <sub>0.4</sub> , Cr <sub>7</sub> C <sub>5</sub>	
			1392	373	Cr <sub>23</sub> C <sub>6</sub> , Cr <sub>3</sub> C <sub>2</sub> , Cr <sub>2</sub> C,		
			980	467	Cr <sub>0.62</sub> C <sub>0.35</sub>	Mn <sub>9.6</sub> C, Mn <sub>5</sub> C <sub>2</sub>	
			1355	301		Cr <sub>23</sub> C <sub>6</sub> , Ti <sub>12</sub> N, Cr <sub>7</sub> C <sub>3</sub> , Fe <sub>7</sub> C <sub>3</sub> ,	
			1392			Fe <sub>3</sub> C, Mn <sub>23</sub> C <sub>6</sub> , Mn <sub>5</sub> C <sub>2</sub> , (Cr, Fe) <sub>7</sub> C <sub>3</sub> , Cr <sub>2</sub> CN, Cr <sub>0.62</sub> C <sub>0.35</sub> N <sub>0.03</sub> , Ti <sub>12</sub> N	
B <sub>8</sub>	62	64	1869	1003	α, γ, Cr <sub>7</sub> C <sub>3</sub> . No	Cr <sub>7</sub> C <sub>3</sub> is the	
			1604	1003	evidence of	major type of	
			chill	2131	1003	Cr <sub>23</sub> C <sub>6</sub> type	carbide. Eviden-
			cast	1703		carbide	ce of Cr <sub>0.62</sub> ,
			sample	2060			C <sub>0.35</sub> , N <sub>0.03</sub> and Ti <sub>12</sub> N also exist Cr <sub>7</sub> C <sub>3</sub> intensity very weak
B <sub>1</sub>	52	61	1059	613	α, γ, Cr <sub>7</sub> C <sub>3</sub>	α. martensite	
			1051	729	(Cr, Fe) <sub>7</sub> C <sub>3</sub>	γ. dendrite	
			1514	561		reduced. New	
			1819			peaks indica-	
			958			ting precipi-	
				tation of Cr <sub>23</sub> C <sub>6</sub> (Fe, Cr) <sub>7</sub> C <sub>3</sub> and Cr <sub>2</sub> C observed			
B <sub>2</sub>	51	61	1703	699	α, γ, (Fe, Cr) <sub>7</sub> C <sub>3</sub>	α martensite	
			1027	727		Reduction of	
			1077	522	Cr <sub>7</sub> C <sub>3</sub>	γ content.	
			1319			Precipitation	
			1558			of Cr <sub>23</sub> C <sub>6</sub> .	
				Evidence of precipitation of (Cr <sub>0.60</sub> , Fe <sub>0.95</sub> , N <sub>0.03</sub> ) & Cr <sub>7</sub> C <sub>3</sub>			

B <sub>3</sub>	52	62	1219	432	$\alpha, \gamma, \text{Cr}_7\text{C}_3$ (Cr <sub>0.62</sub> C <sub>0.35</sub> N <sub>0.03</sub> ) CrCN	Reduction in $\gamma$ content, Cr <sub>23</sub> C <sub>6</sub> and Ti <sub>2</sub> N precipi- tation detected
			1251	471		
			1558	307		
			1077	384		
			1284			
B <sub>4</sub>	41	62	1027	515	$\alpha, \gamma, (\text{Cr, Fe})_7\text{C}_3$ , Fe <sub>3</sub> C, Fe <sub>7</sub> C <sub>3</sub> , Cr <sub>0.62</sub> C <sub>0.35</sub> N <sub>0.03</sub>	$\gamma$ content reduced. Precipitation of Cr <sub>23</sub> C <sub>6</sub> , Cr <sub>3</sub> C, Cr <sub>3</sub> C <sub>2</sub> and Ti <sub>2</sub> N phases indicated.
			1027	542		
			936	368		
			1431	446		
			1703	407		
C <sub>1</sub>	48	60	1051	419	$\alpha, \gamma, (\text{Cr, Fe})_7\text{C}_3$ , Fe <sub>3</sub> C, Fe <sub>7</sub> C <sub>3</sub> , Cr <sub>7</sub> C <sub>3</sub> , Cr <sub>0.62</sub> C <sub>0.35</sub> N <sub>0.03</sub>	$\gamma$ reduced. Evidence of Cr <sub>23</sub> C <sub>6</sub> precipitation.
			1003	419		
			1027	401		
			1251			
			980			
C <sub>2</sub>	50	62	1319	334	$\alpha, \gamma, \text{Cr}_7\text{C}_3$ (Cr, Fe) <sub>7</sub> C <sub>3</sub> Cr <sub>0.62</sub> C <sub>0.35</sub> N <sub>0.03</sub> , Cr <sub>2</sub> CN	$\gamma$ reduced Evidence of Cr <sub>3</sub> C and Ti <sub>2</sub> N <sub>6</sub> precipitation
			980	293		
			980	368		
			1051			
			958			

the 'd' values of  $\text{Fe}_3\text{C}$  are very close to those of other carbides. However, lower microhardness values of the order of 950 to 1050 VPN matches with the hardness of  $\text{Fe}_3\text{C}$  type carbide. Hence the presence of certain vol.% of such carbide also can not be ruled out. A scrutiny of the X-ray diffraction analysis data reveal that the predominant carbide phase in the A series cast alloys was  $\text{Cr}_7\text{C}_5$  type. Some  $\text{Cr}_{23}\text{C}_6$  type carbide was also present. In the nitrogenated alloys low intensity peaks of a complex nitrides and carbonitrides were also detected. In the B series alloys,  $\text{Cr}_{23}\text{C}_6$  type carbide was generally not present in appreciable quantity in the as cast state.

The actual volume % of retained austenite in the as cast and heat treated alloys were calculated from the XRD patterns and are given in Table 4.3. It may be noted that the retained austenite percentage increased on alloying with nitrogen. Increasing the  $\text{Cr/C}$  ratio to 4.0 and above along with addition of nitrogen and 0.2-0.6 % Ti caused a very high degree of stabilisation of retained austenite. In this respect, the high retained austenite contents in alloys  $\text{B}_3$ ,  $\text{B}_4$ ,  $\text{C}_1$  and  $\text{C}_2$  are particularly noteworthy. Chill casting promoted hardening of the matrix in Alloy  $\text{A}_8$ , although retained austenite was still present in it. It had a much higher as cast hardness (Rc 62) than the sand cast alloys. Microhardness data in Table 4.2 show that the hardness of both the matrix and the carbide phases were greater in the chill cast alloy. X-ray diffraction analysis of the chill cast alloy indicated that the carbide phase was predominantly  $\text{Cr}_{23}\text{C}_6$  type.

Table 4.3. Retained austenite content in as cast  
and heat treated samples matrices  
(excluding the primary carbide)

Sample designation	Retained austenite content (vol.%)		
	As cast	Soaked at 950°C/1 hr, oil quenched and tempered at 200°C for 1 hour	Soaked at 950°C for 3 hrs. oil quenched and tempered at 200°C for 1 hr.
A <sub>1</sub>	21	12	20.00
A <sub>2</sub>	30	14	16.00
A <sub>3</sub>	23	11	-
A <sub>4</sub>	17	10	25.00
A <sub>6</sub>	20.00		11.00
A <sub>7</sub>	4.00		44.00
A <sub>8</sub>	28	55.00*	29.00**

	As cast	Soaked at 900°C/2 hour oil quenched and tempered at 200°C for 1 hour.	Soaked at 900°C for 2 hrs. oil quenched, cryotreated in liq. N <sub>2</sub> and tempered at 200°C for 1 hour.
B <sub>1</sub>	8	6	2
B <sub>2</sub>	8	6	2
B <sub>3</sub>	16	10	6
B <sub>4</sub>	30	21	6
C <sub>1</sub>	47	39	15
C <sub>2</sub>	53	37	20

\* homogenised 4 hours at 900°C

\*\* homogenised 7 hours at 900°C

B<sub>1</sub> - Oil quenched;  
B<sub>2</sub>, B<sub>3</sub>, B<sub>4</sub>,  
C<sub>1</sub>, C<sub>2</sub> - Air quenched

#### 4.1.4 Scanning electron microscopy

The carbide morphology in the A series irons was examined in greater details under SEM. The matrix surrounding the carbide phase was removed partially or completely by deep etching. Consequently, the carbide morphology was revealed in the secondary electron image. The SEM photographs indicate that the carbide morphology in chromium cast irons was modified partially by the addition of nitrogen and titanium. In plain 12% Cr cast iron, the eutectic carbide exists in three dimensions as a continuous phase. In cast irons treated with nitrogen alone or nitrogen and titanium together, the carbide morphology was refined at places into rods and blades. Two photographs (Fig. 4.4 & 4/5) of alloys A<sub>6</sub> and A<sub>7</sub> respectively, showing alignment of rods in two direction are presented consecutively. The rods, however are observed to be partially connected among themselves, and thereby produce a semidiscontinuous network. Two adjacent rods may be connected at the tip and intermediate positions to develop a single rod. In alloy A<sub>4</sub>, where nitrogen and aluminium were added together, the carbide phase was largely discontinuous (Fig. 4.6a). A higher magnification view (Fig. 4.6b) shows that the eutectic carbide in this area consists mainly of rods and blades. The blades themselves are formed by coalescence of adjacent rods. The rod morphology was also very prominent in the chill cast alloy A<sub>8</sub>, having much lower titanium content than A<sub>7</sub>. The cross-sections of rods and blades are clearly revealed after partial etching of the matrix (Fig. 4.7). A closer examination of the colony structure is possible in Fig. 4.8. In each eutectic colony, plates shot out from a common nucleus. These plates ofcourse

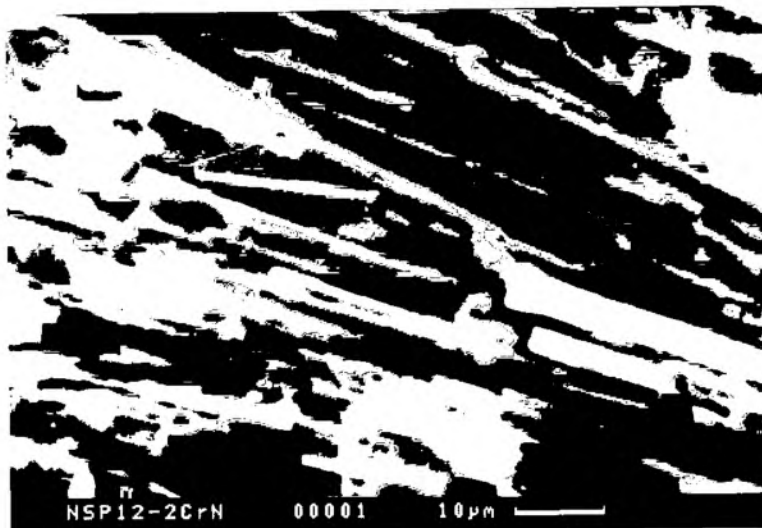


Fig. 4.4       $\times 1200 X$



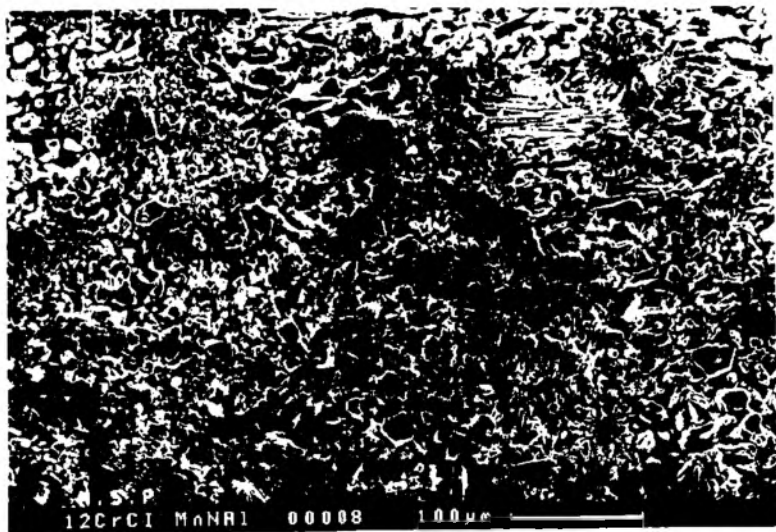
Fig. 4.5       $1400 X$

Fig.4.4 : SEM photograph of A<sub>6</sub> showing carbide rods.

Fig.4.5 : SEM photograph of A<sub>7</sub> showing carbide rods.

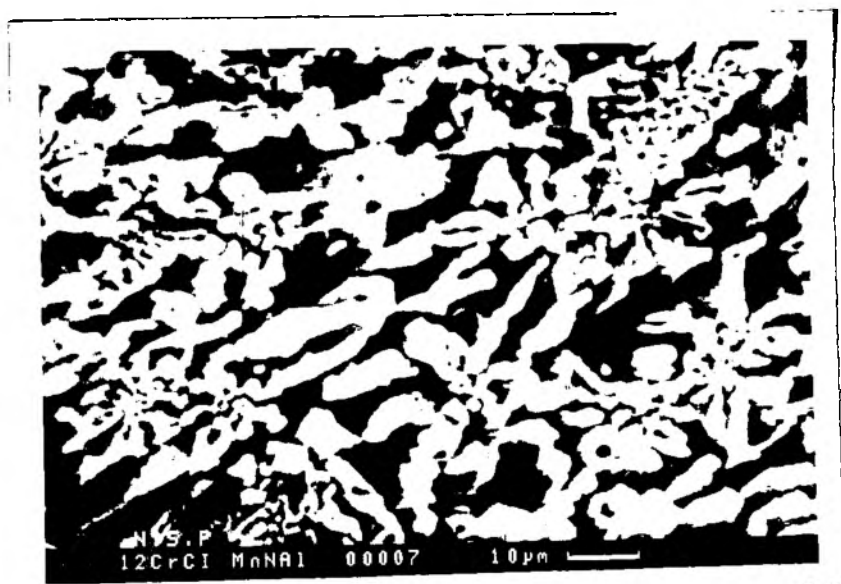
1607

669.734  
P00/S  
N91



(a)

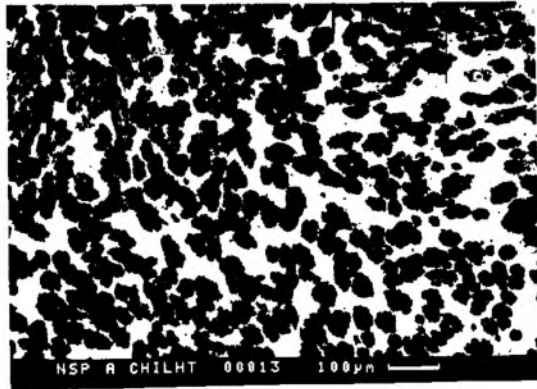
170X



(b)

950X

Fig.4.6 : SEM photograph of A<sub>4</sub> alloy.  
(a) at lower magnification  
(b) at higher magnification.



70X

Fig.4.7

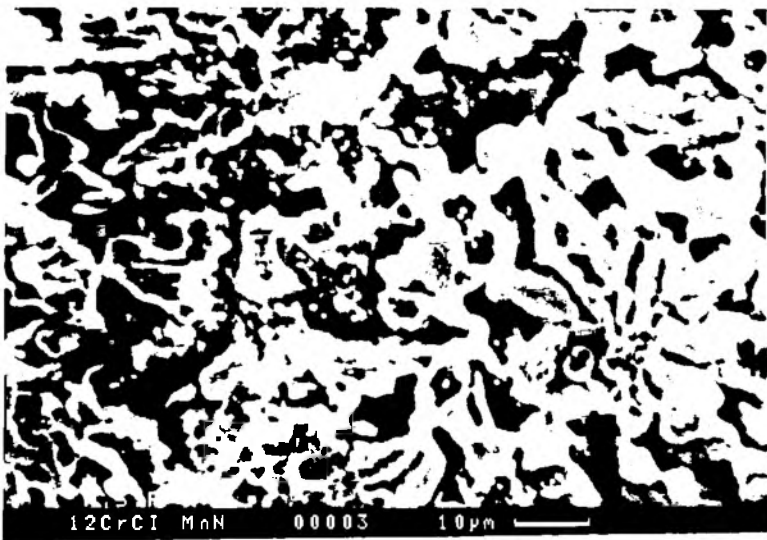


Fig.4.8

1000X

Fig.4.7 : SEM photograph of  $A_8$  showing cross sections of rods and blades.

Fig.4.8 : SEM photograph of  $A_2$  showing eutectic colonies.

are interconnected within a colony by dendritic branching. This growth morphology is very similar to the one visible in the light microscope photograph presented earlier.

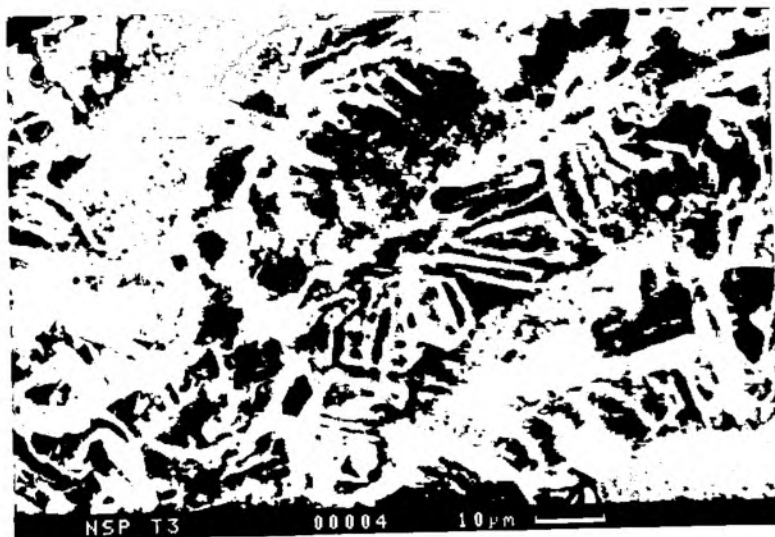
In the B series, rod like carbide morphology could not be detected in any of the alloys. Fig. 4.9a shows a typical petal like dendritic branching of carbide plates in B<sub>9</sub>. Each petal has distinct crystalline facets. These arms are of course ~~are~~ connected to the arms of the adjacent dendrites, so that in lower magnification (4.9b) a continuous carbide skeleton of interconnected dendrites is clearly observed. Although an apparent modification of the morphology in B<sub>4</sub> and C<sub>2</sub> was indicated by light micrograph in Fig. 4.3, the actual morphology in these samples turned out to be completely continuous in deep etched section under SEM.

The SEM micrographs of B<sub>1</sub>, B<sub>2</sub> and B<sub>3</sub> at an identical magnification (Fig. 4.10 a-c) are presented together. The photographs show a tendency towards dendritic to equiaxed transition on addition of nitrogen and titanium.

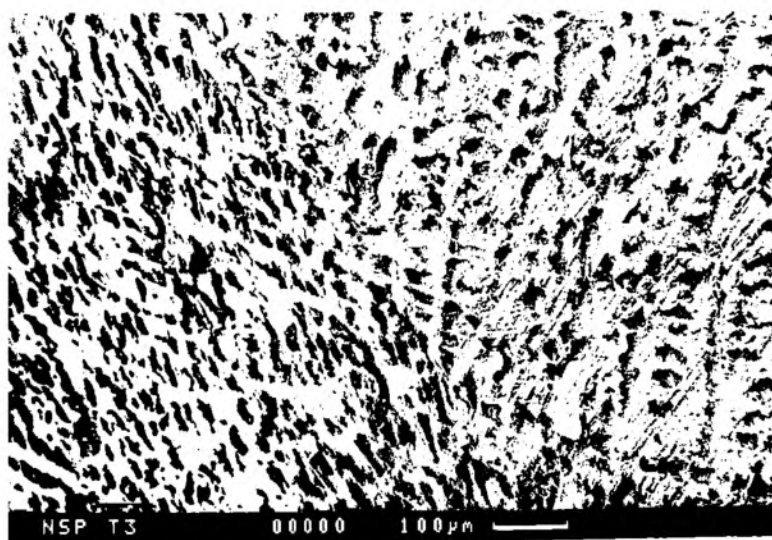
#### 4.1.5 Microprobe analysis(EDAX/EPMA)

Chromium segregation in selected samples was examined by spot analysis in EDAX. Representative data for chromium distribution in the transformed austenite and in the eutectic carbide are presented in Table 4.4.

Distribution of different phases in as cast alloy B<sub>2</sub> and B<sub>4</sub> were investigated separately in a JEOL Microprobe Analyser. The Secondary Electron Images, line profiles and x-ray  $k\alpha$  maps for the different elements are given in Fig. 4.11. for the samples B<sub>2</sub> and B<sub>4</sub>. In sample B<sub>2</sub>, the nitrogen



(a) 950X

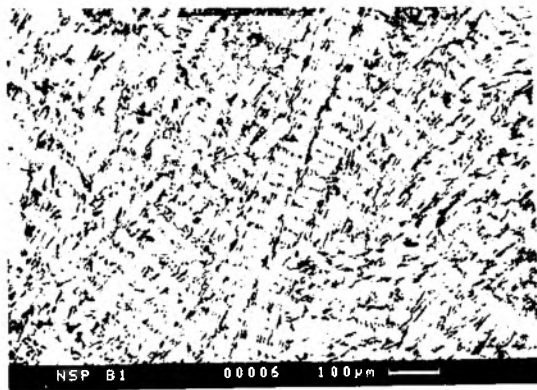


(b) 100X

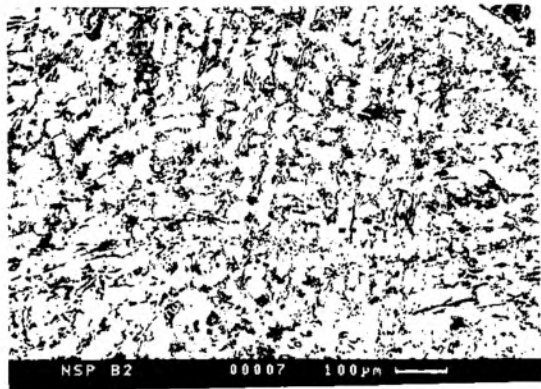
Fig.4.9 : Carbide morphology in alloy B<sub>3</sub> (SEM)

(a) higher magnification

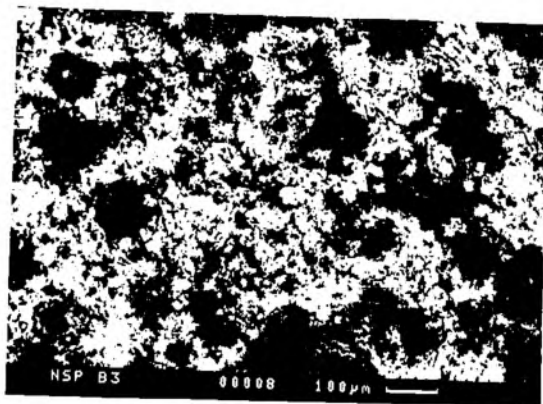
(b) lower magnification



(a) 70X



(b) 70X



(c) 70X

Fig.4.10 : SEM photographs of as cast B-series alloys.

(a) B<sub>1</sub> (b) B<sub>2</sub> (c) B<sub>3</sub>

Table 4.4 Partitioning of alloying elements in  
carbide and matrix phases (EDAX)

Sample No.	% Concentrations in carbide			% Concentrations in Matrix		
	%Cr	%Mn	%Si	%Cr	%Mn	%Si
A1	31.013	1.132	0.140	17.928	1.748	0.687
	16.628	1.281	0.987	8.259	0.964	1.152
	30.085	1.087	0.205	12.059	1.261	1.120
A2	28.947	5.262	0.150	13.225	3.955	0.806
	19.991	5.387	0.294	7.512	3.377	1.027
	17.193	4.796	0.461	12.788	3.986	0.898
A3	19.620	0.288	0.378	21.177	11.031	2.518
	31.648	0.406	0.169	12.696	0.348	0.794
	17.838	7.154	3.709	12.745	2.962	0.827
A4	15.018	3.320	1.708	13.240	3.120	1.503
	31.216	3.375	0.040	9.843	2.783	1.795
	32.354	2.981	0.127	17.851	2.967	1.577

concentration seemed to be more in the matrix than that in the eutectic phase (Fig. 4.11 A (ii)). Manganese distribution also appeared to be very non uniform (Fig. 4.11 A(iii)).

In the  $B_4$ , the nitrogen and titanium  $\kappa\alpha$  map and line profiles revealed an identical distribution pattern of the two elements. The peak positions of Ti tallied exactly with those of nitrogen. These evidences strongly suggests, precipitation of a compound of titanium and nitrogen (such as TiN or Ti(C,N)). A typical cellular distribution of nitrogen and titanium throughout the matrix also suggests segregation of these elements at grain boundaries or sub grain boundaries (Fig. 4.11B). Manganese was distributed preferentially in the dendritic regions (Fig. 4.11B).

#### 4.1.6 Quenching and tempering treatment and dilatometry

As cast samples contained retained austenite which was determined by X-ray diffraction analysis. The samples were heated at  $950^\circ\text{C}$  for periods of one hour to five hours to destabilise the retained austenite and to develop maximum possible hardness on oil quenching. The hardness of the oil quenched samples ( $A_1, A_2, A_3$  and  $A_4$ ) are plotted as a function of time in Fig. 4.12. The hardness plots show that as quenched hardness increased gradually on increasing the soaking period to three hours. Thereafter there was no further increase in hardness. The as quenched samples were also subjected to XRD. The data in Table 4.3 indicate that retained austenite content decreased on destabilisation at  $950^\circ\text{C}$  for 1 hour. Similar trends were observed in case of all other alloys. The representative XRD pattern of alloy  $A_6$  given in Fig. 4.13 (a&b) clearly shows that  $\text{Cr}_{23}\text{C}_6$  type carbide precipitated during



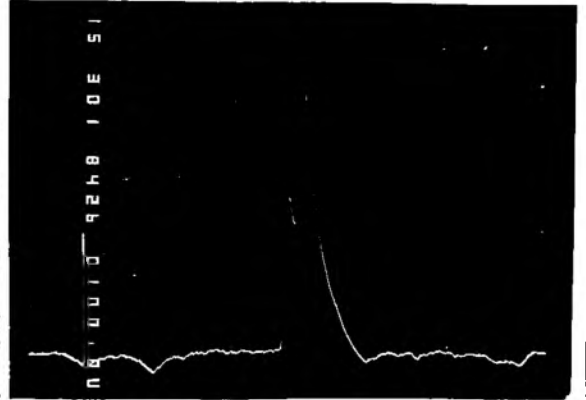


300X

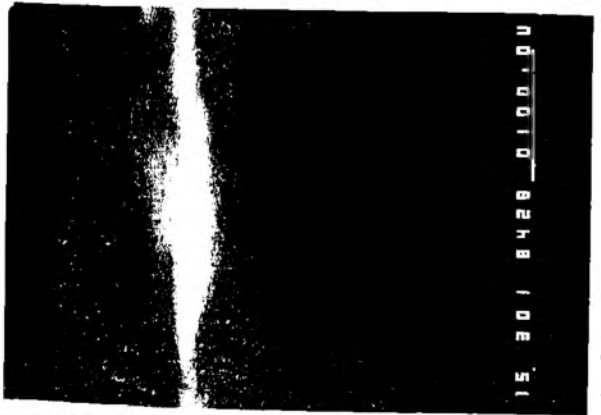
(i)



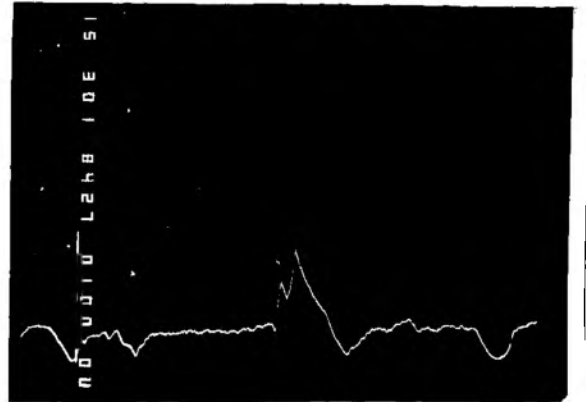
(ii)



13441



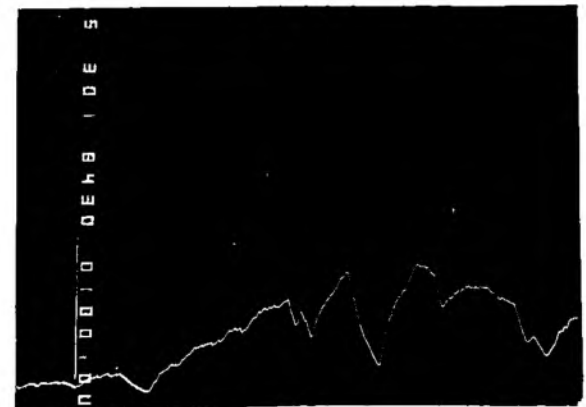
(iv)



(v)



(vi)



(vii)

(B) - Sample B4

Fig. 4.11.5

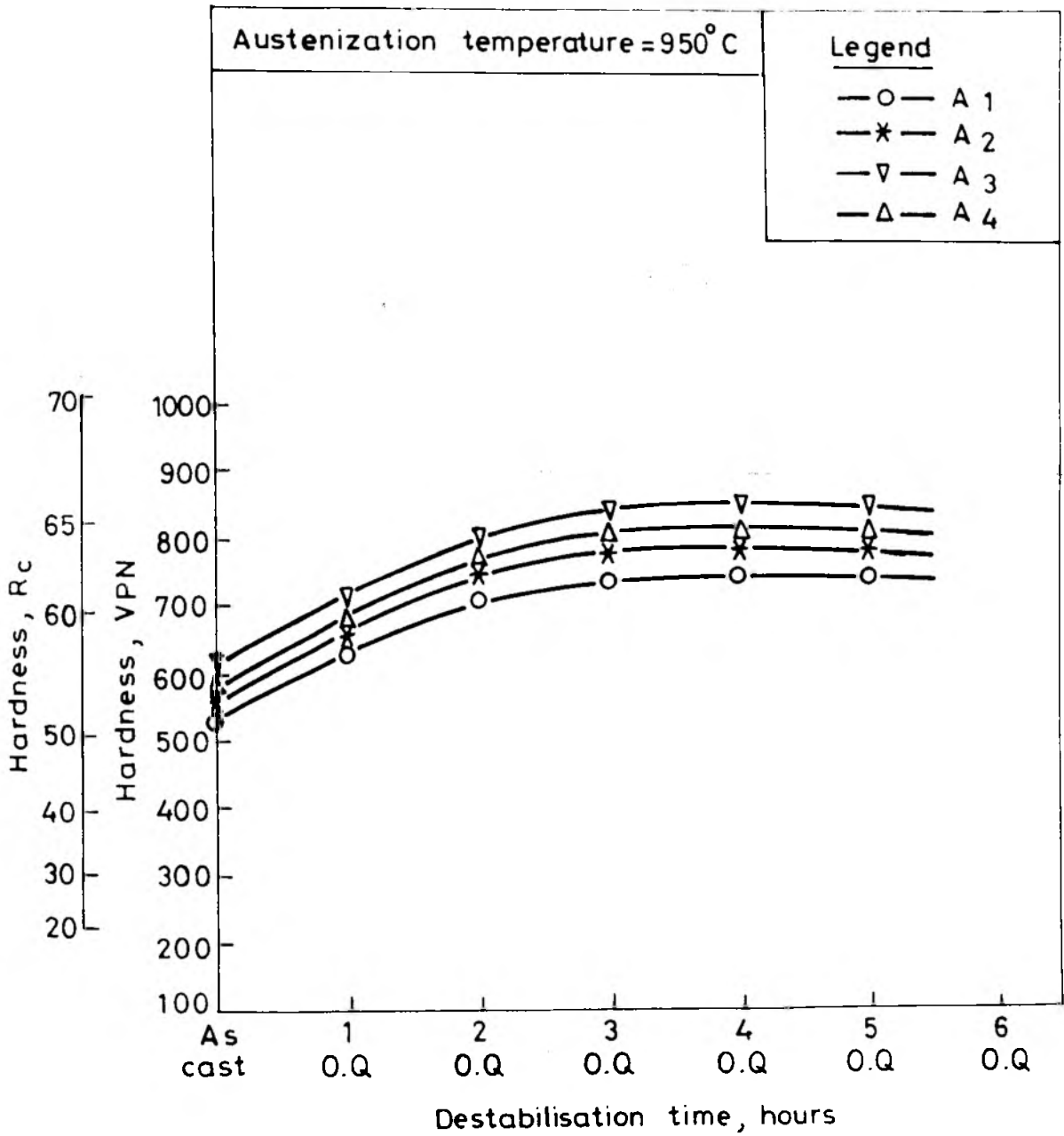


Fig. 4.12. Effect of destabilisation of Austenite time on the hardness of oil quenched samples

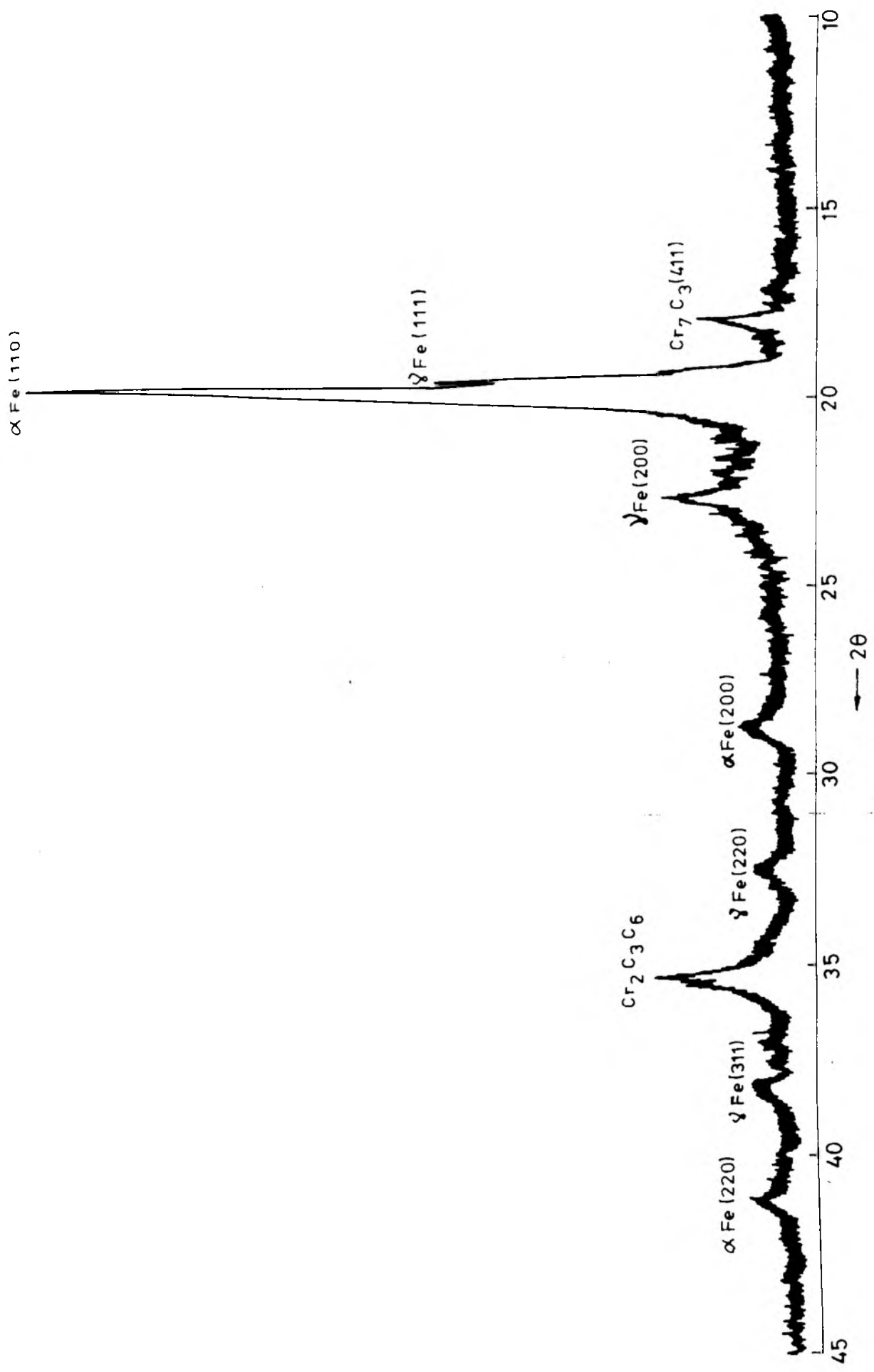


Fig. 4.13(a). XRD pattern of A6 as cast

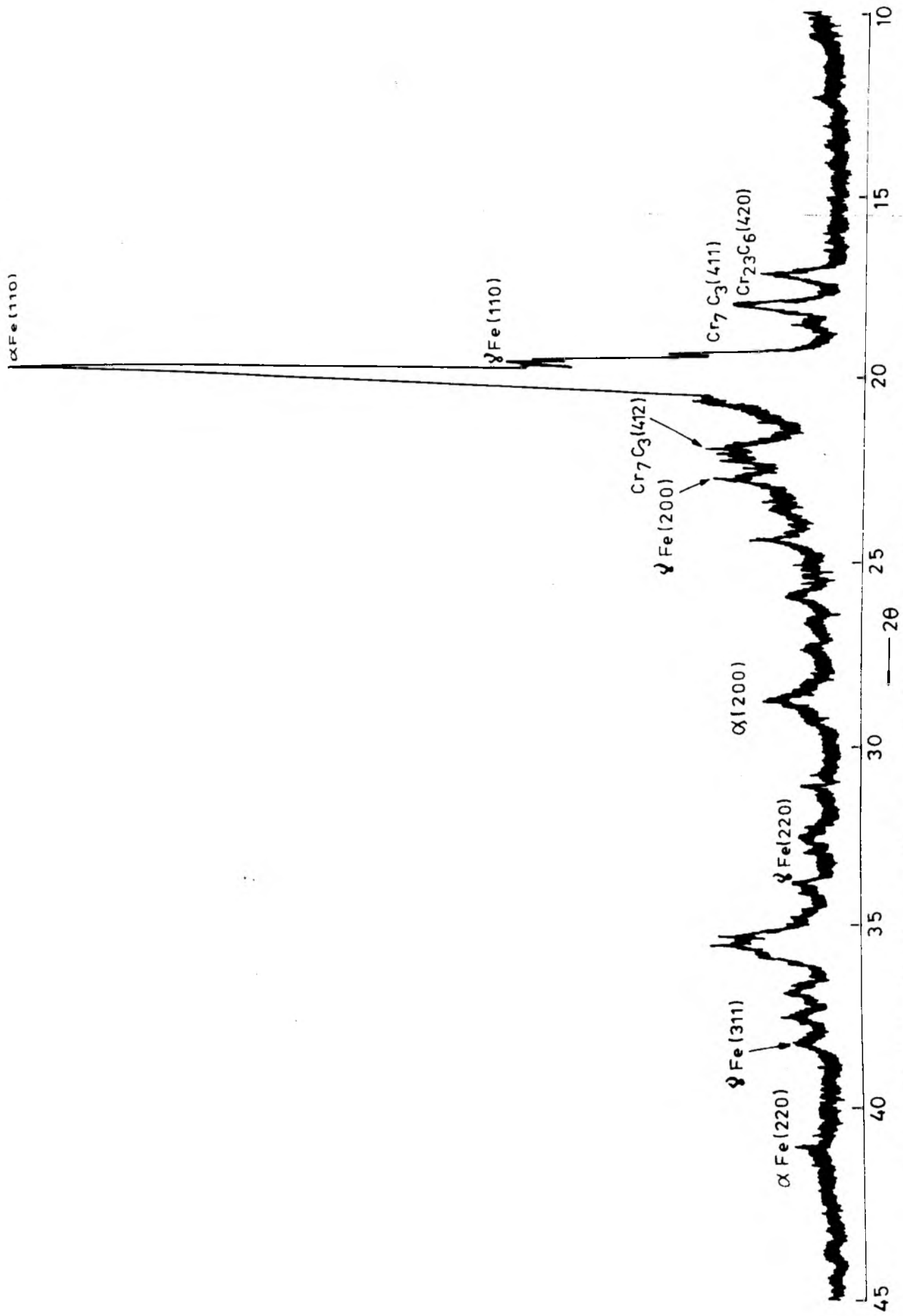


Fig. 4.13(b). XRD pattern of A6 quenched and tempered

destabilisation heat treatment. Prolonged soaking at  $950^{\circ}\text{C}$ , however, increased the retained austenite content in alloy  $A_7$ , which contained both nitrogen and titanium. The XRD patterns of alloy  $A_7$  in Fig. 4.14 (a&b) illustrates this point. The XRD patterns of  $A_8$ , in Fig. 4.15(a-c) indicate that the retained austenite content first increased on soaking  $900^{\circ}\text{C}$  for 4 hrs and then it decreased on further soaking upto 7 hours. These patterns also indicate transition of  $\text{Cr}_{23}\text{C}_6$  carbides into  $\text{Cr}_7\text{C}_3$  type.

The B series alloys had lower carbon contents. These alloys were destabilised at  $900^{\circ}\text{C}$  upto 2 hours only. The data on retained austenite content in the B series alloys are also given in Table 4.3. The same table also presents data on the retained austenite content after cryotreatment in liquid nitrogen. Appreciable retained austenite remained in the high manganese samples ( $C_1$  and  $C_2$ ), even after cryotreatment. The differences in the areas under the austenite peaks in the XRD plots of alloy  $C_2$  in as cast and as oil quenched and tempered conditions (Fig. 4.16 a,b) illustrate difference in the austenite contents before and after heat treatment.  $\text{Cr}_{23}\text{C}_6$  carbide precipitation during destabilisation is also indicated in the XRD pattern.

The effect of soaking temperature and quenching medium on the response to hardening of alloys  $A_1$ - $A_4$  was investigated by water quenching from  $1100^{\circ}\text{C}$  and oil quenching from  $950^{\circ}\text{C}$ . As water quenched (from  $1100^{\circ}\text{C}$ ) hardness was lower than the as oil quenched (from  $950^{\circ}\text{C}$ ) samples in all the alloys. Table 4.5 provides a comparison of these hardness values. The same table also compares the hardness of the

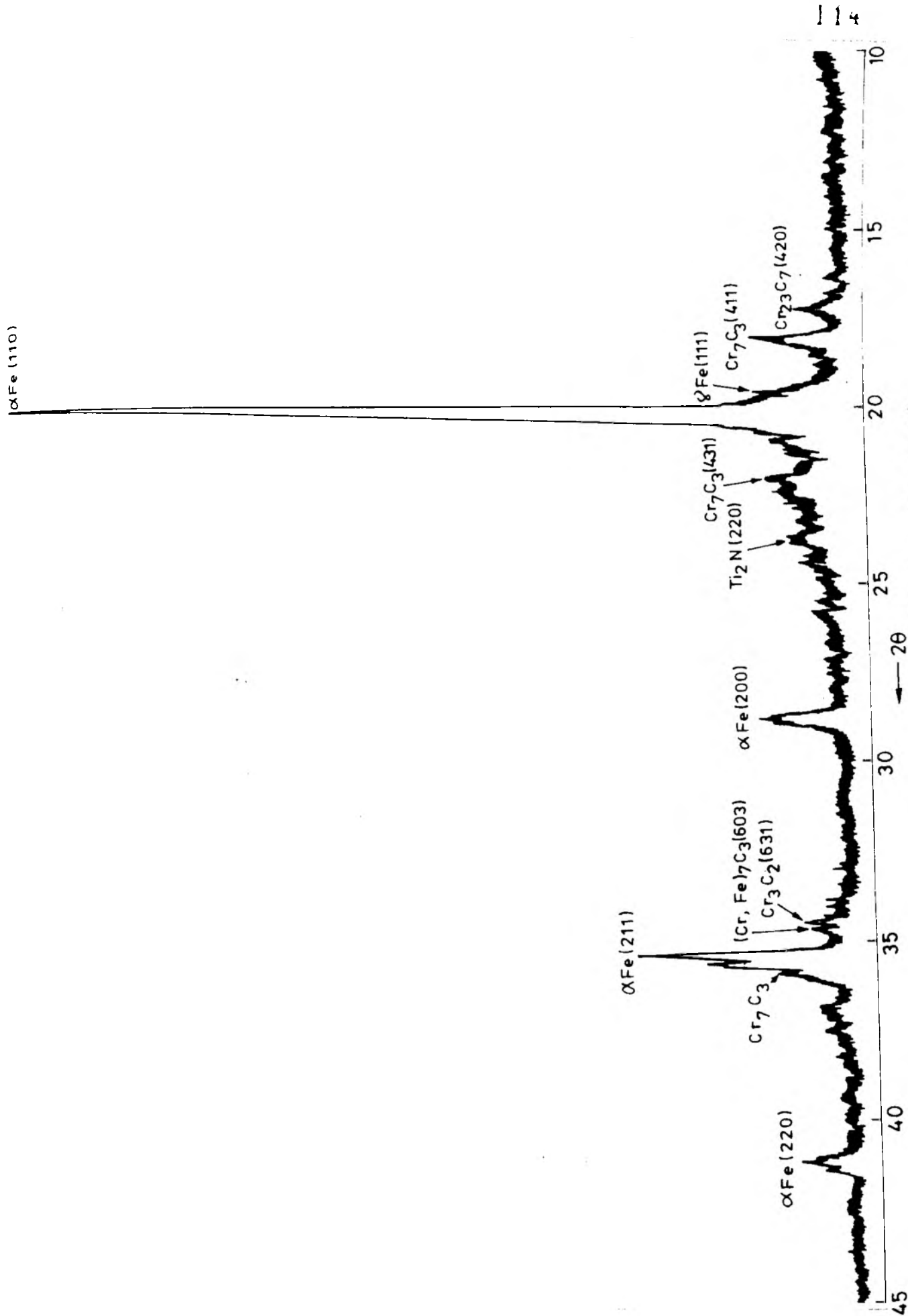


Fig. 4.14 (a). XRD pattern of A7 as cast

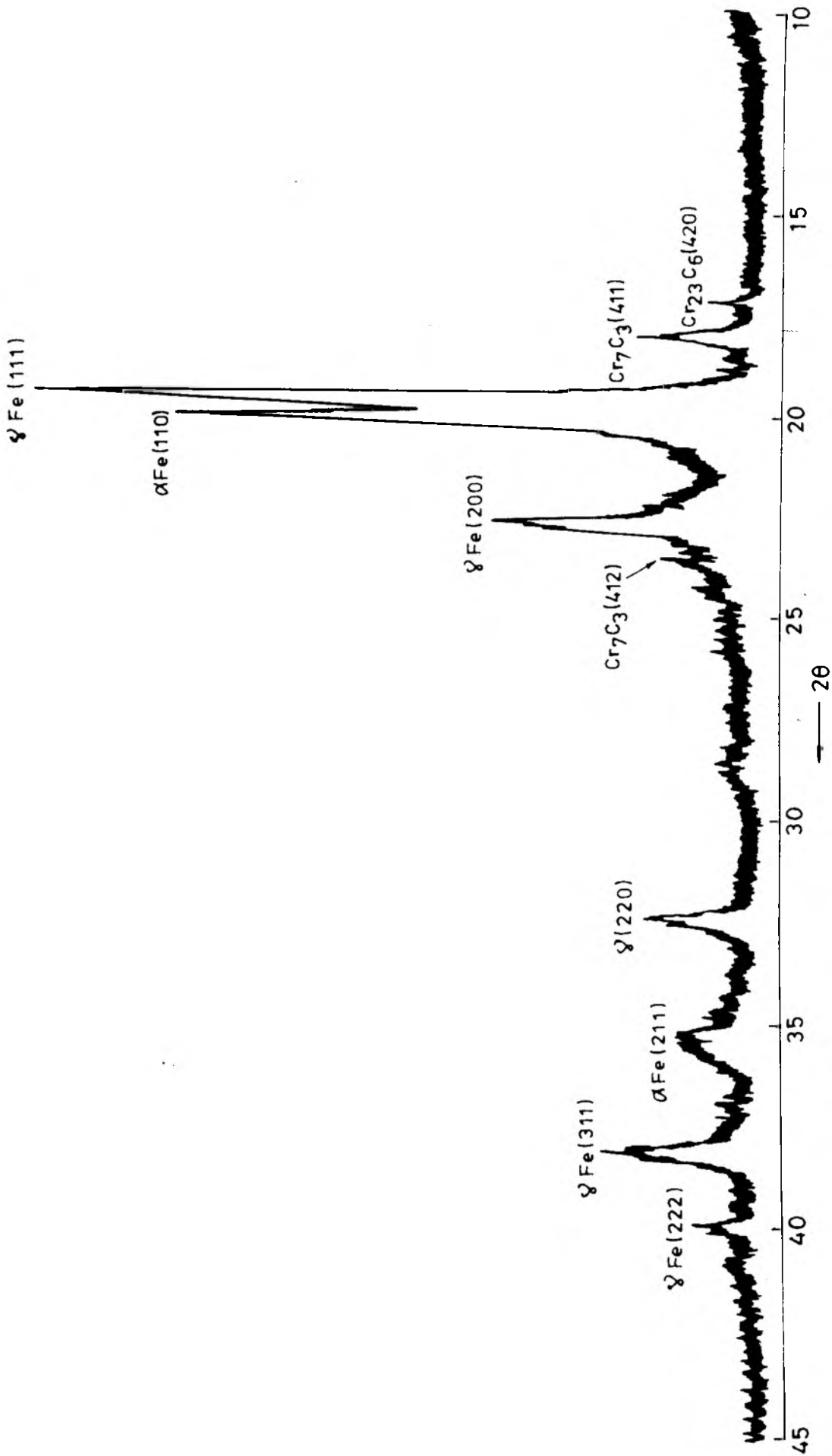


Fig. 4.14(b). XRD pattern of A7 heat treated

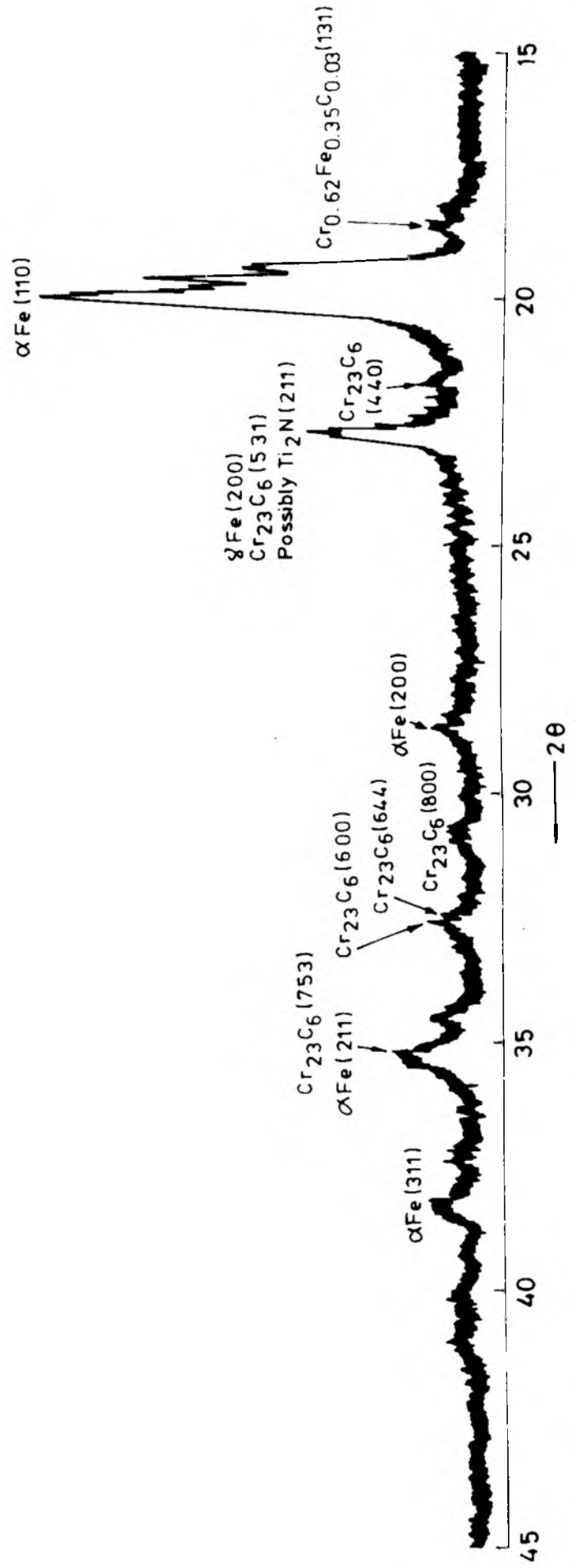


Fig. 4.15(a). XRD pattern of Ag chill cast (as cast)

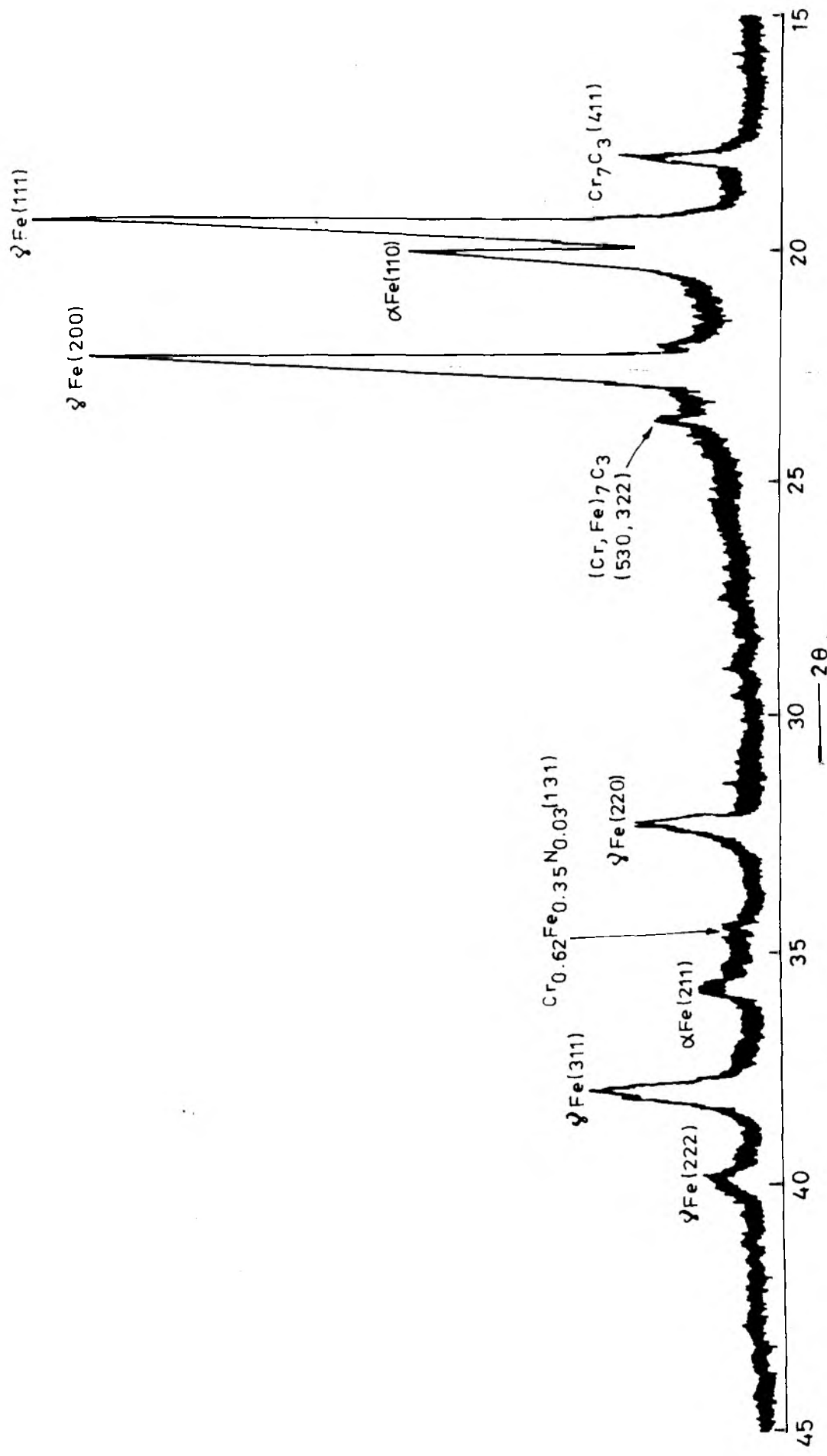


Fig. 4.15 (b). XRD pattern of Ag chill cast (H.Td. 900°/4hrs. — A.Q.)

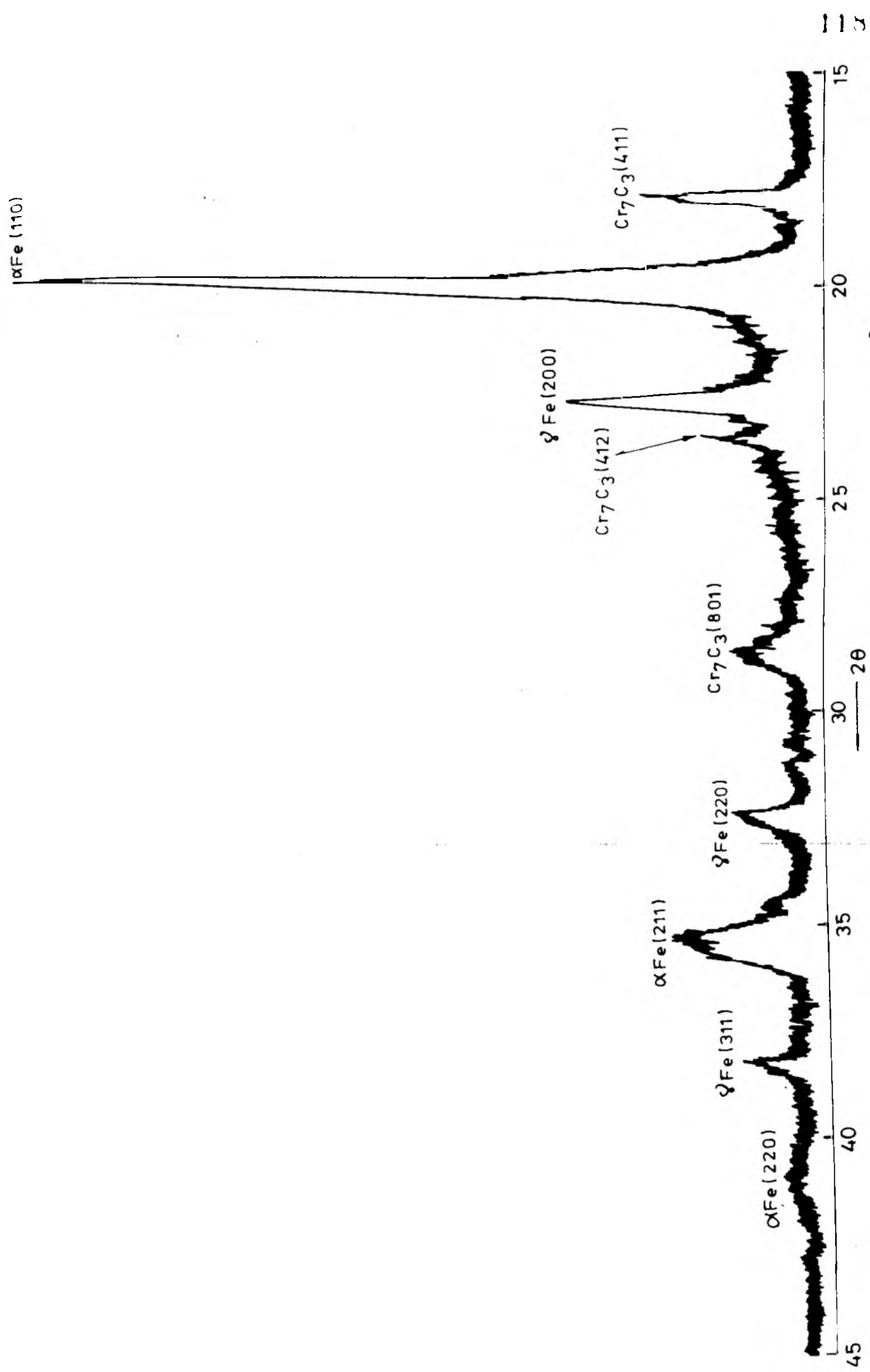


Fig. 4.15 (c). XRD pattern of Ag chill cast (H.Td. 900°/7hrs. -> A.Q.)

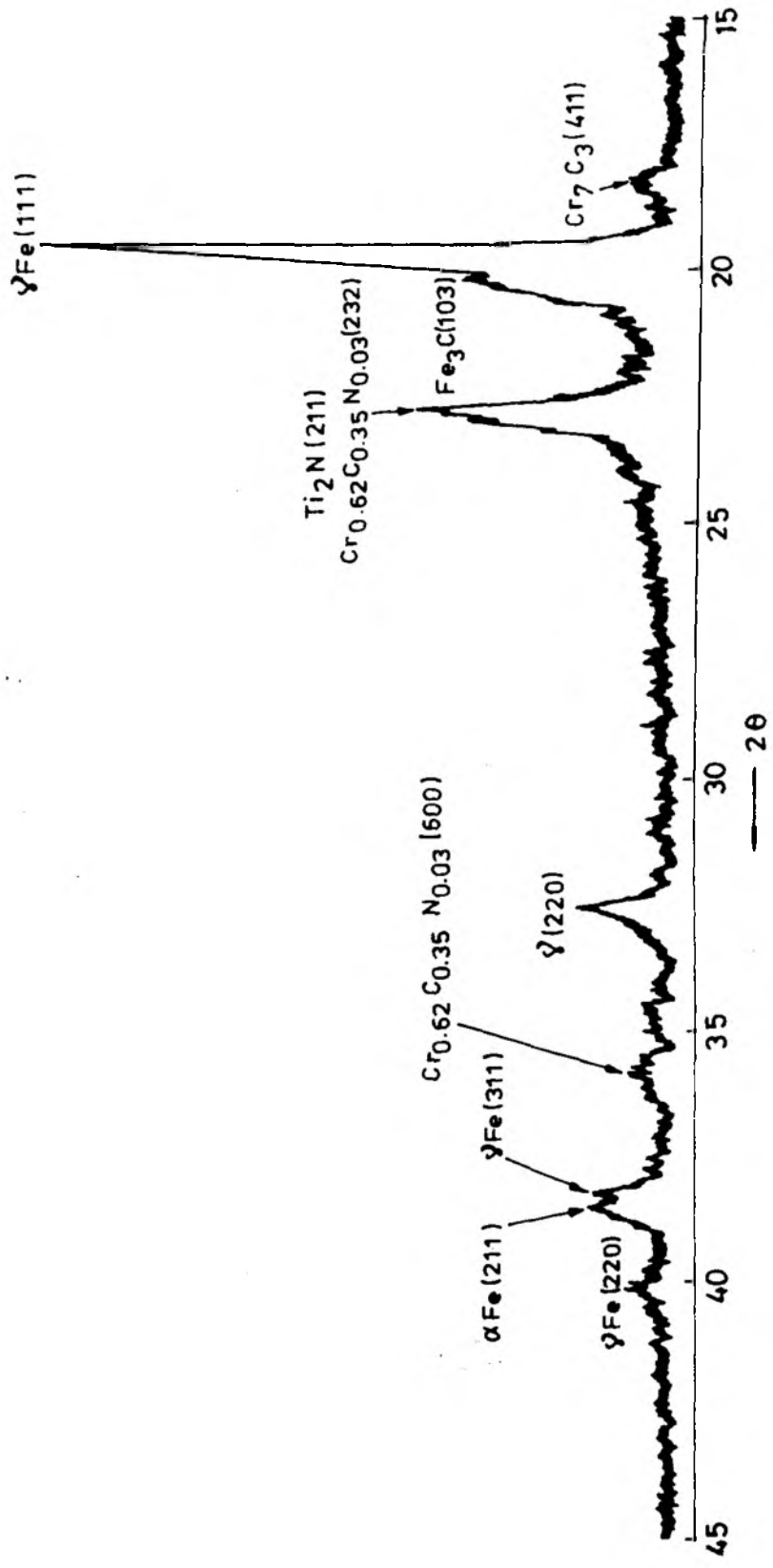


Fig. 4.16(a). XRD pattern of C2 as cast

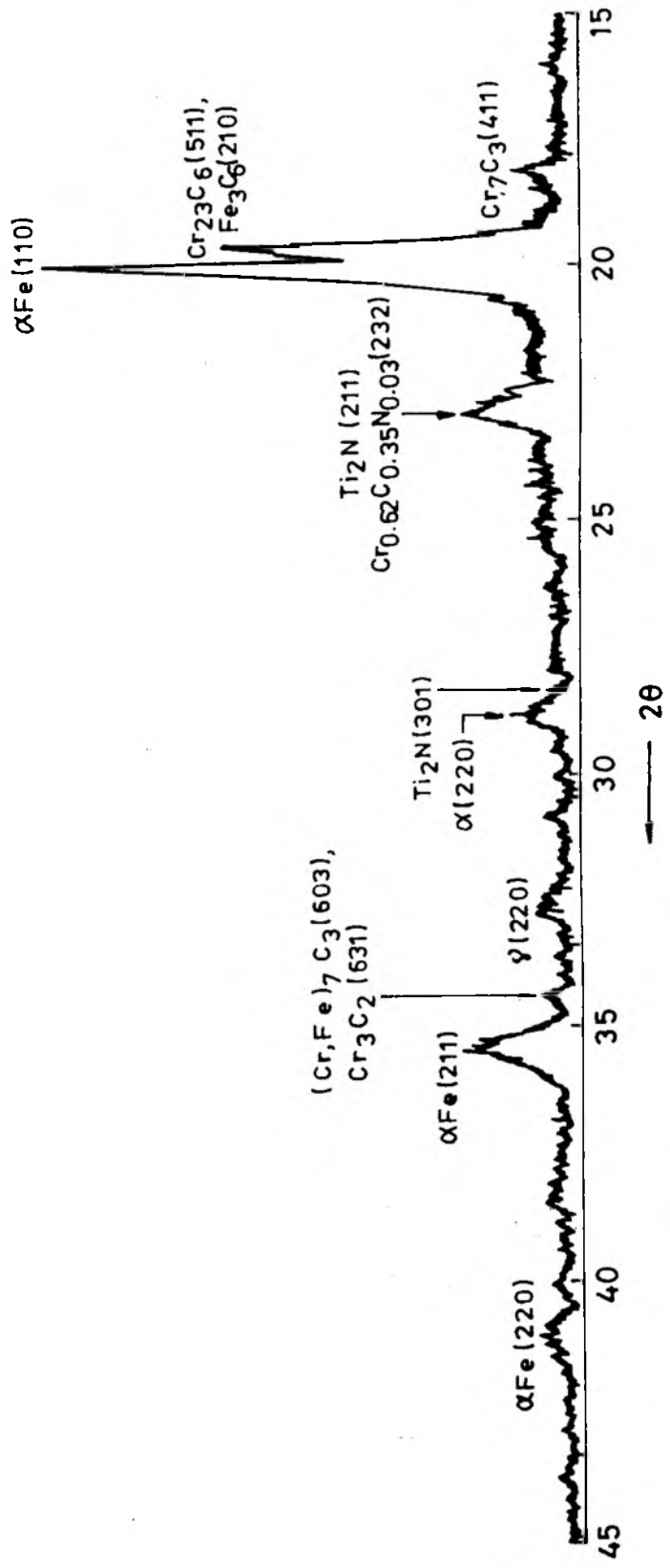


Fig.4.16(b). XRD pattern of C<sub>2</sub> quenched and tempered

differential thermal analysis samples, subjected to slow heating within the refractory specimen tube to  $950^{\circ}\text{C}$ , holding at  $950^{\circ}\text{C}$  for 5 hours followed by rapid cooling, by application of forced air draft on the specimen tube and cryotreatment. The hardness of the DTA samples were more or less similar to that of the oil quenched samples of  $A_2$  to  $A_4$ . The hardness of  $A_1$  was lower. The representative DTA plots of  $A_1$  and  $A_3$  are given in Fig. 4.17(a-b). The sample of alloy  $A_1$  did not record any transformation on cryotreatment. The effect of heat treatment on the hardness and retained austenite content of the chill cast alloy  $A_3$  is summarised below:

Sample History	Hardness	Retained austenite content (vol%)	Remarkable phase changes if any
As cast	62	28.4	$\text{Cr}_{23}\text{C}_6$ type carbide only
Soaked at $950^{\circ}\text{C}$ for 4 hours, forced air quenched, tempered at $150^{\circ}\text{C}$ for 1 hour	58	33.4	$\text{Cr}_7\text{C}_3$ , $(\text{Cr},\text{Fe})_7\text{C}_3$ type carbide appears, $\gamma$ content increased.
Soaked at $950^{\circ}\text{C}$ for 7 hours, forced air quenched, tempered at $150^{\circ}\text{C}$ for 1 hour	64	21.7	Only $\text{Cr}_7\text{C}_3$ type carbide detected. (Fig. 4.15 a, b&c)

The tempering behaviour of the as cast and as quenched chromium cast irons was followed by hardness measurement and X-ray diffraction analysis. Tempering curves are given in Fig. 4.18-4.20. Both the as cast and as quenched

Table 4.5 Comparison of the Hardness Values of  
water quenched, oil quenched and air quenched  
and cryotreated samples of A<sub>1</sub> - A<sub>4</sub>

Specimen designation	Hardness (Rc)			Remarks
	W.Q. from 1100°C, soaking period 1 hour	Oil quenched from 950°C soaking period 1 hour	Forced air draft quenched from 950°C, soaking time 5 hrs. cryo-treatment in liquid N <sub>2</sub>	
A <sub>1</sub>	56	58	49	only Cr <sub>7</sub> C <sub>3</sub>  carbide detected by XRD in the DTA sample retained austenite 3.0%
A <sub>2</sub>	57	60	63	--
A <sub>3</sub>	58	62	62	--
A <sub>4</sub>	59	63	62	In addition to Cr <sub>7</sub> C <sub>3</sub> , Cr <sub>23</sub> C <sub>6</sub> and Ti <sub>2</sub> N phases  also detected in the DTA sample, retained austenite 5.8%.

samples containing titanium and aluminium along with nitrogen ( $A_3 - A_5$ ) showed a secondary hardening peak at  $600^\circ\text{C}$  on isochronal tempering for 1 hour. The samples, water quenched from  $1100^\circ\text{C}$  (Fig. 4.18(b)) and those oil quenched from  $950^\circ\text{C}$  (Fig. 4.19) showed an identical response in this respect. This type of secondary hardening peak was not observed in other samples. Slight hardening at lower temperature upto  $300^\circ\text{C}$  in the water quenched samples and upto  $200^\circ\text{C}$  in the oil quenched samples could however be noted in all the samples. Alloys  $A_3$  and  $A_4$  exhibited characteristic secondary hardening peaks which appeared only after isothermal tempering for 60 mins. Shorter tempering periods of 15 mins. did not develop such peaks (Fig. 4.20). Fig. 4.21 (a,b) compares the hardness of samples tempered at  $300^\circ\text{C}$  and  $600^\circ\text{C}$  for 1 hour, from various starting states. Air quenched and tempered samples are only marginally softer than the samples tempered after oil or water quenching.

A comparison of the X-ray diffraction data on cast, and quenched and tempered sample, as given in Table 4.2, suggests precipitation of  $\text{AlN}$  and  $\text{Ti}_2\text{N}$  after tempering at  $600^\circ\text{C}$ .

#### 4.1.7 Transmission electron microscopy (TEM)

Selected as cast, as quenched and quenched and tempered samples of the alloys were further examined in TEM by the two stage replication technique to find out, whether nitrogen and titanium additions to chromium cast irons produced any changes in their microstructures. In the two stage replication process, some of the smaller particles were extracted out of the sample, into the final replica. However, the bigger particles were not usually extracted. Hence

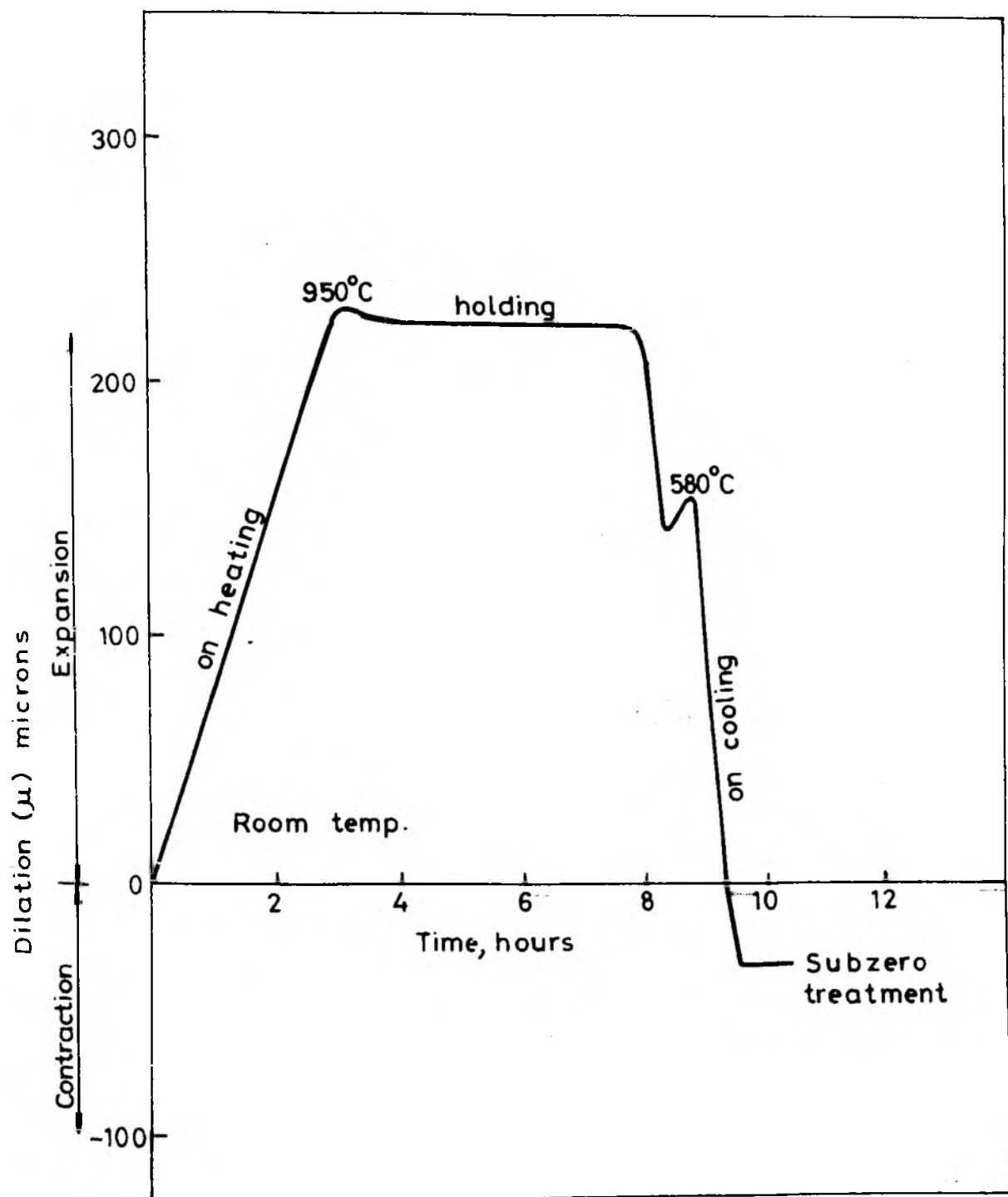


Fig. 4.17(a). Dilatometric curve of sample A<sub>1</sub>

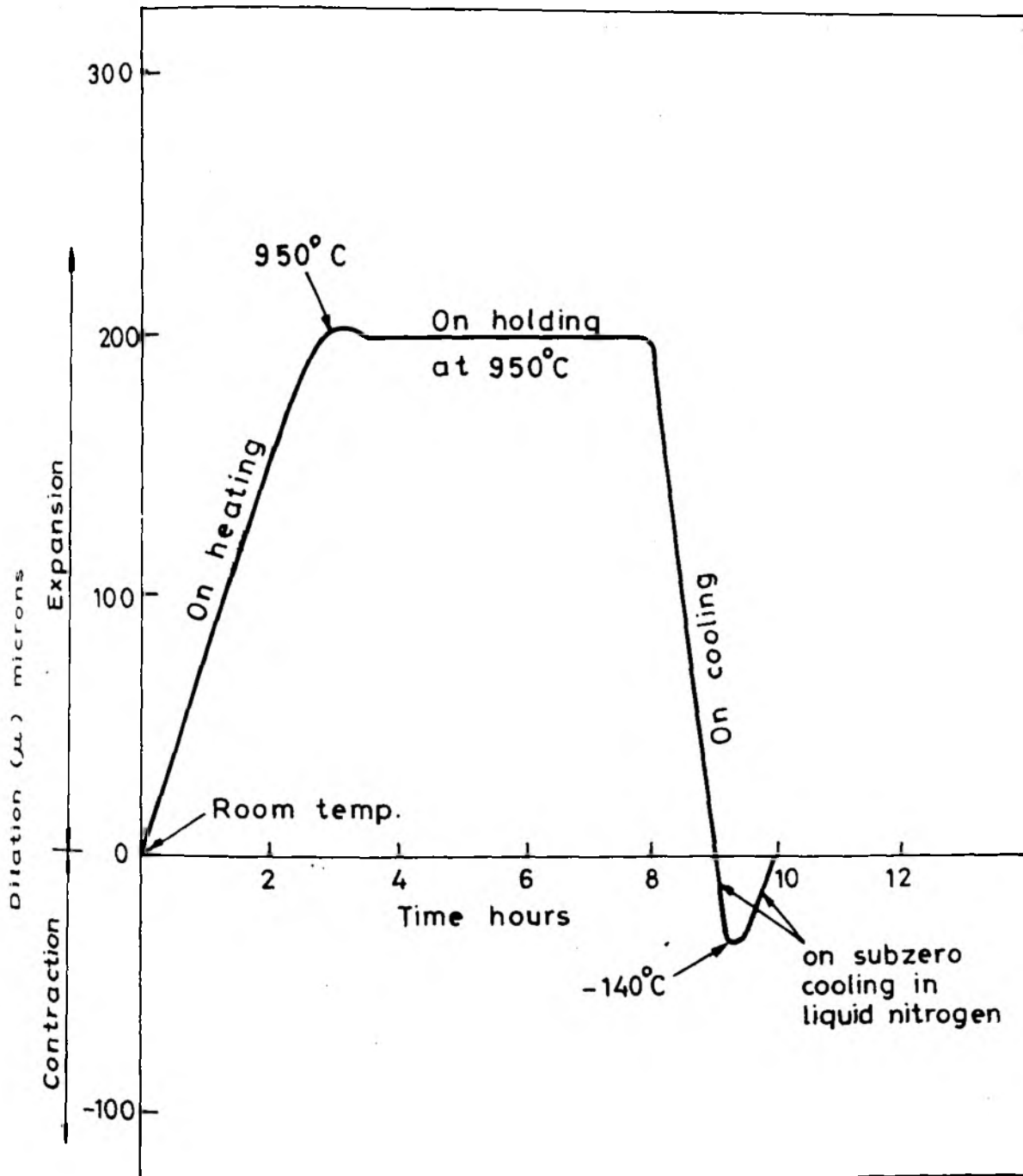


Fig. 4.17(b). Dilatometric curve of sample A<sub>3</sub>

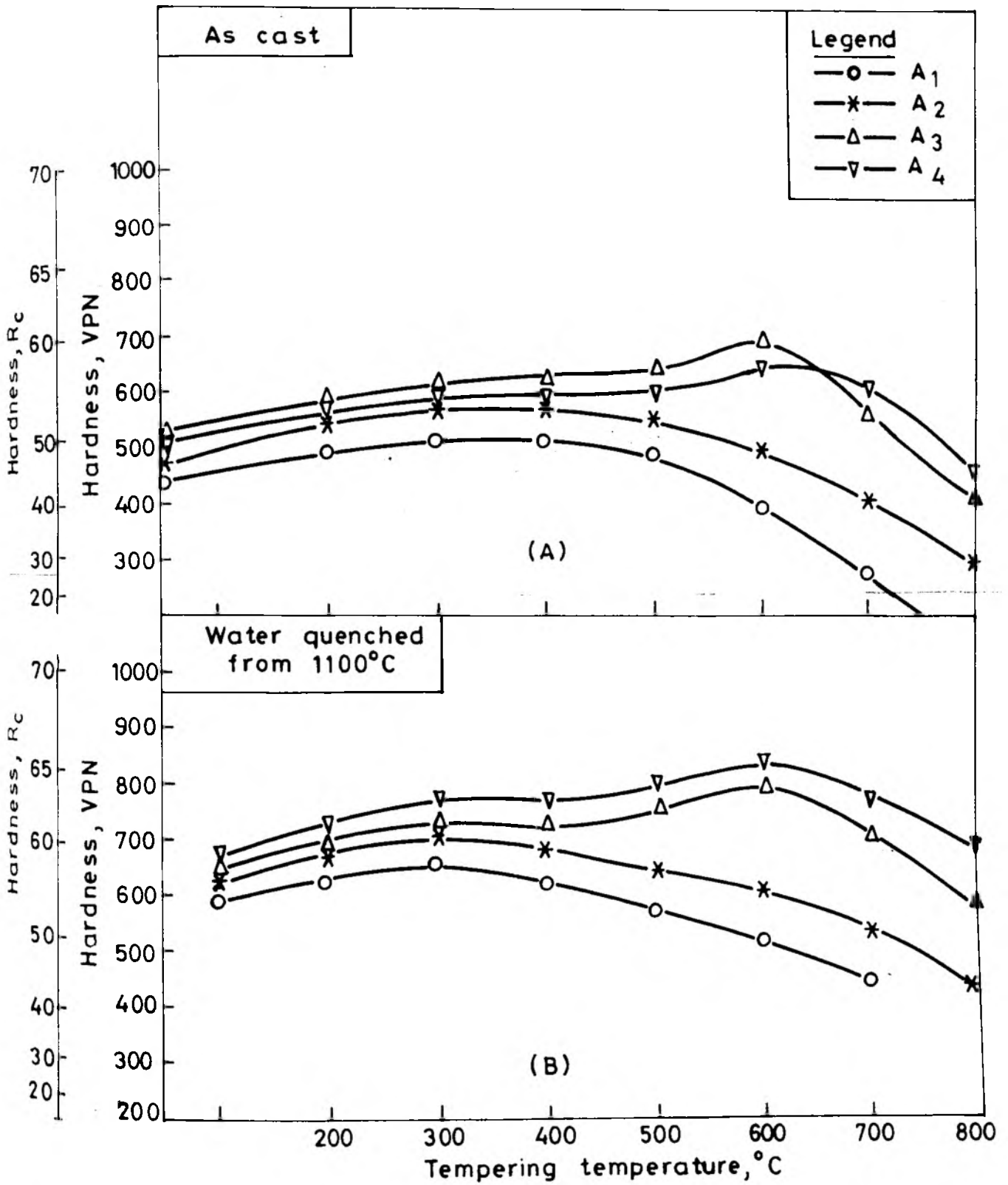


Fig. 4.18. Isochronal Tempering (1 hour) curves for (A) As cast and (B) As water quenched samples.

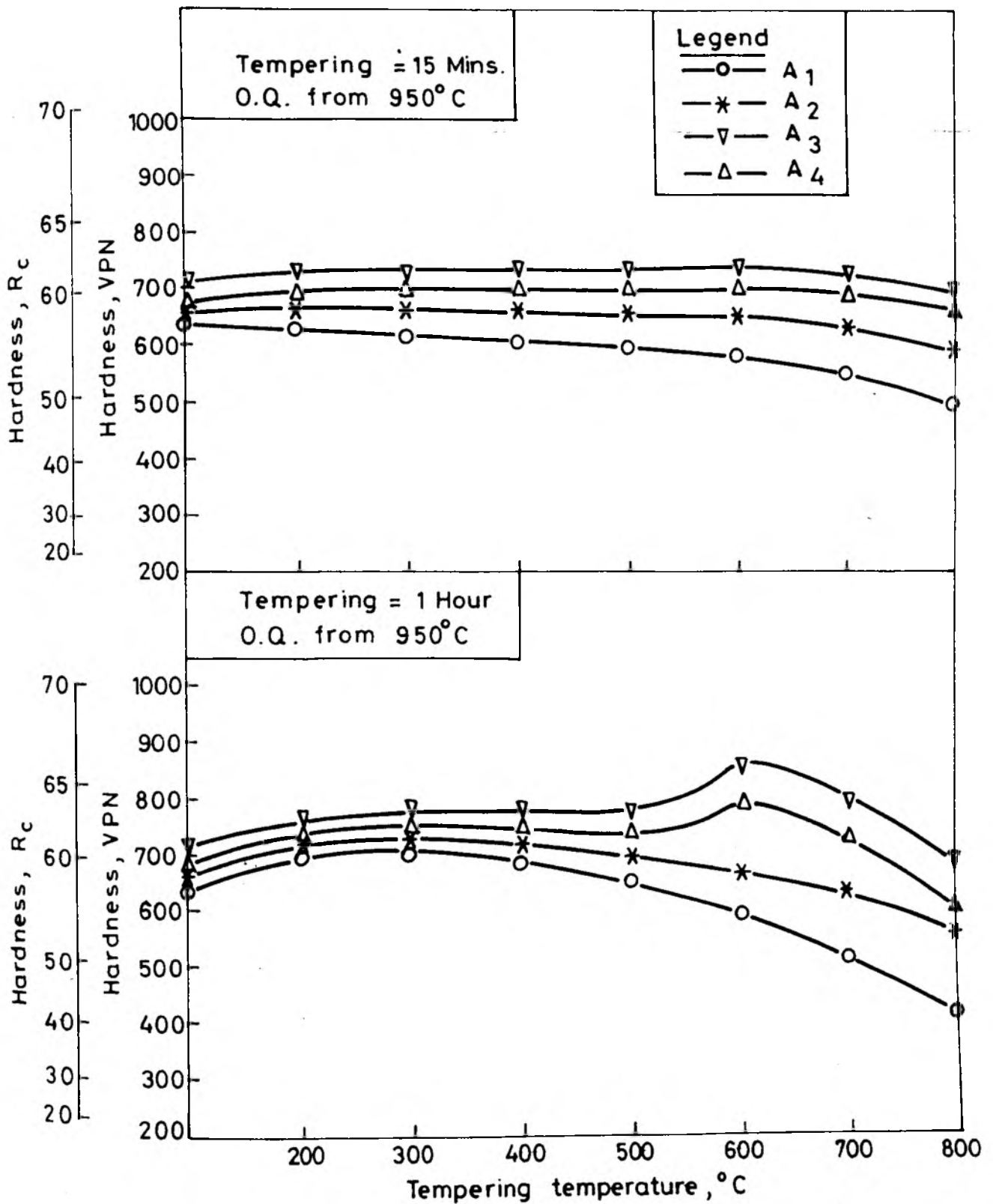


Fig. 4.19. Isochronal Tempering (A = 15 minutes, B = 1 hour) curves for as quenched (oil quenched from 950°C) samples for various temperatures.

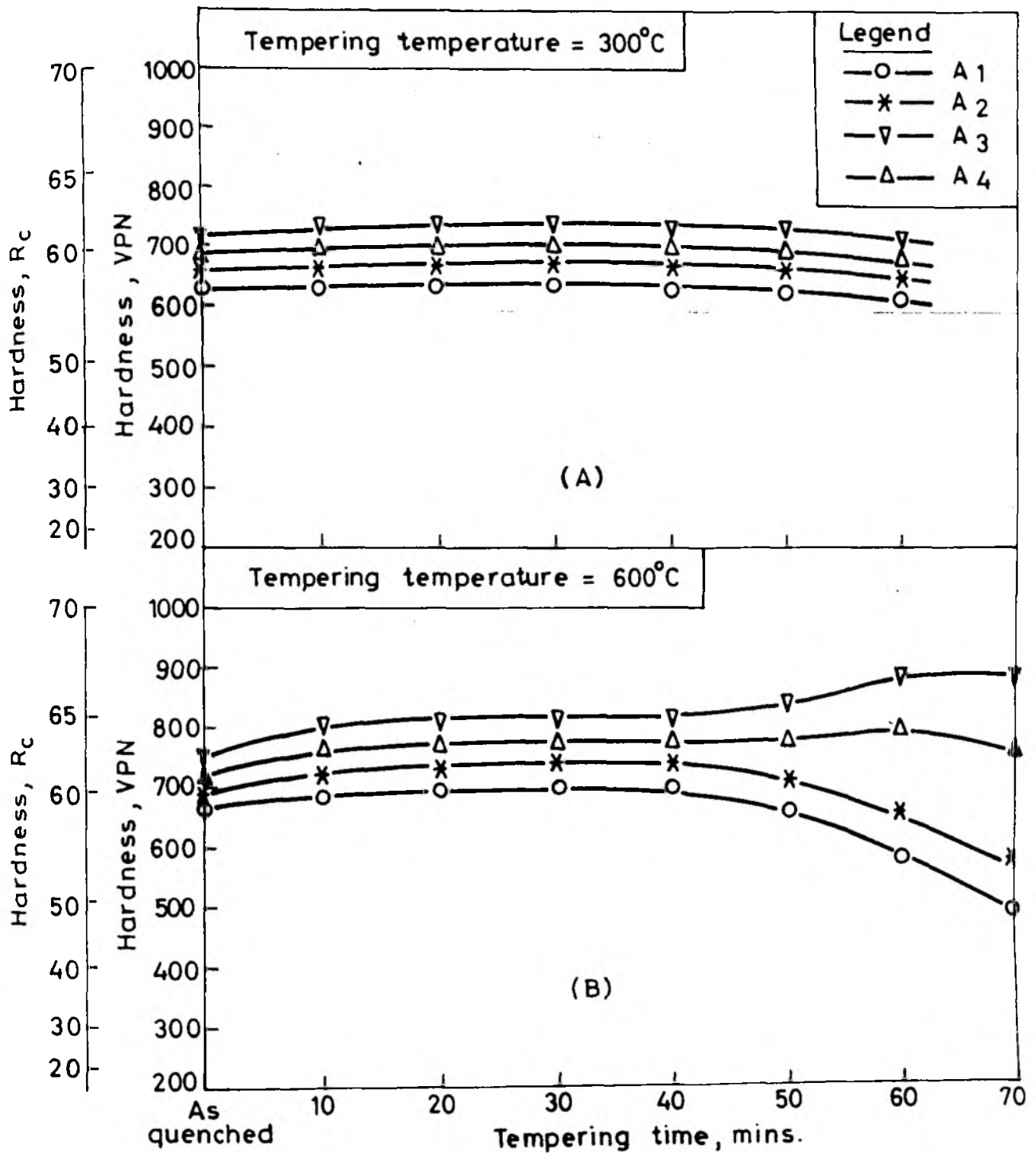


Fig. 4.20. Isothermal tempering (A=300°C, B=600°C) of samples oil quenched from 950°C for varying time)

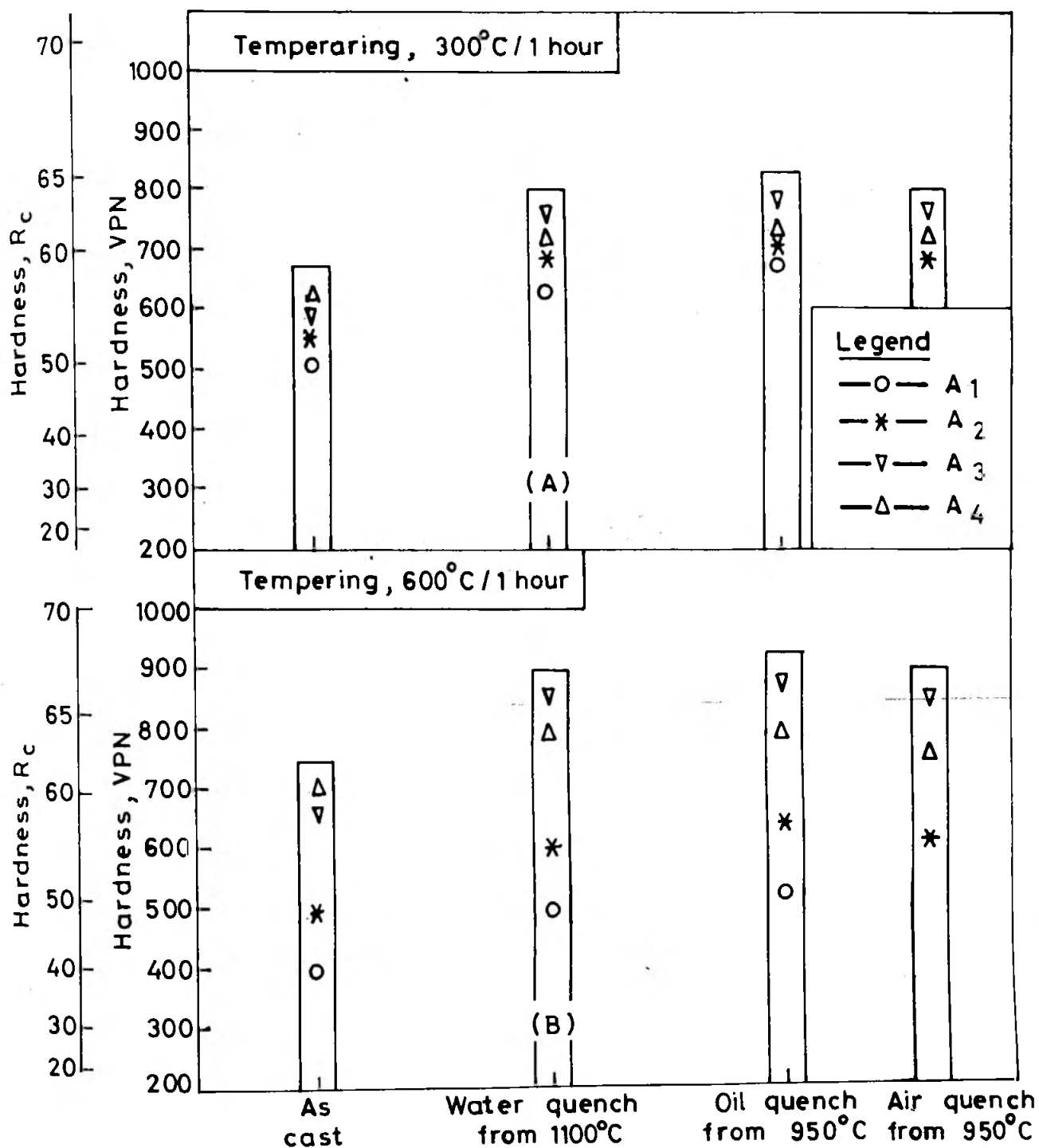


Fig. 4.21. Tempering characteristics of various samples in As cast, Water quenched (1100°C) and Oil quenched (950°C) at A = 300°C / 1 hour and B = 600°C / 1 hour

identification of the precipitate phases could not be done systematically. The present report will, therefore, highlight basically the details of the microstructural features.

The electromicrograph (Fig. 4.22a) of the as quenched sample of alloy  $A_4$  clearly reveals the distribution of the secondary carbide precipitated during soaking at  $950^\circ\text{C}$ . In addition, some extracted particles (dark particles) are also seen. The martensitic structure is not distinct in this photograph. In the as quenched and cryotreated structure of  $A_4$  (Fig. 4.22b) the secondary carbide particles were not readily visible. After tempering of this alloy ( $A_4$ ) at  $200^\circ\text{C}$ , finely dispersed precipitates formed (Fig. 4.22c). The bright rounded impressions of precipitates are likely to be those of secondary carbides. Finely dispersed precipitates could be noted in the oil quenched and tempered (at  $200^\circ\text{C}$ ) sample of  $A_7$  as well. (4.22d). It was found difficult to characterise the martensite morphology clearly from two stage replica electron micrographs. The high magnification micrograph (Fig. 4.22e) of the oil quenched and tempered (at  $200^\circ\text{C}$ ) samples of  $A_4$  reveal certain morphology which apparently does not look like one of tempered martensite.

Fig. 4.23(a-c) show details of the microstructures of samples oil quenched from  $950^\circ\text{C}$  and tempered at  $600^\circ\text{C}$ . Fig. 4.23a shows the morphology of carbide particles in  $A_7$  at various stages of growth. The impressions of secondary carbides (bright rounded spots) which are distinctly visible in Fig. 4.23a indicate that the carbides were much larger in size than the precipitates formed on tempering. In the higher magnification view in Fig. 4.23b, it may be further noted that

the secondary carbide particles had a duplex structure. A layer of a second phase with different contrast may be seen around the bright carbide phase. In addition, some rod shaped precipitates which extended over both the austenite and carbide phases could be seen in this sample (Fig. 4.23b) as well as in all samples containing titanium. The oil quenched and tempered at  $600^{\circ}\text{C}$  structure of  $A_4$  (Fig. 4.23c) however did not show any such rod shaped precipitate.

Numerous fine precipitate particles were observed in the as cast sample of  $B_9$ , particularly in the transformed austenite phase (Fig. 4.24 a&b). In  $B_1$  however, such precipitates were not visible (Fig 4.24 c&d). But in both these samples, the primary carbide appeared to be of duplex composition. This is suspected from the presence of a layer of another phase of different contrast around the primary carbide phase. Comparatively the chill cast sample of  $A_8$  contained few precipitate particles. The rod shaped particles, as reported earlier was visible in plenty (4.24e). Martensite laths were also visible. The oil quenched, cryotreated and tempered (at  $200^{\circ}\text{C}$ ) structures of  $B_1$  and  $B_9$  differed considerably. In  $B_1$ , coarse precipitates of definite geometric configurations, which were mostly extracted into the replicas could be seen (Fig. 4.25a). In  $B_9$ , the precipitates were finer, of irregular configuration and more evenly dispersed (Fig. 4.25b).

#### 4.1.8 Corrosion tests

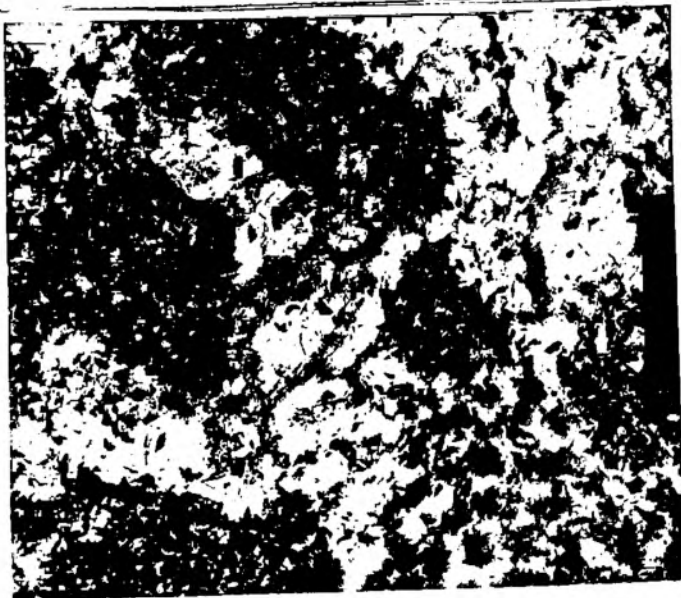
Corrosion tests were carried out by the potentiostatic technique in both 1N NaCl as well as 1 molar HCl solutions relative to tungsten cathode. The corrosion behaviour



(a)



(b)



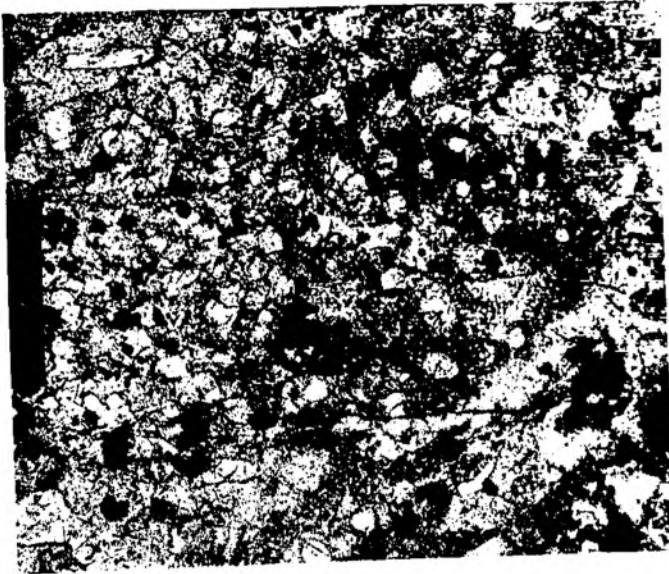
(c)

Fig.4.22 : Transmission Electron Micrographs of

(a)  $A_1$  as quenched, 23,000X

(b) TMA -  $A_4$  as quenched, 30,00 X

(c)  $A_1$  as quenched and tempered, 23000X



(a)

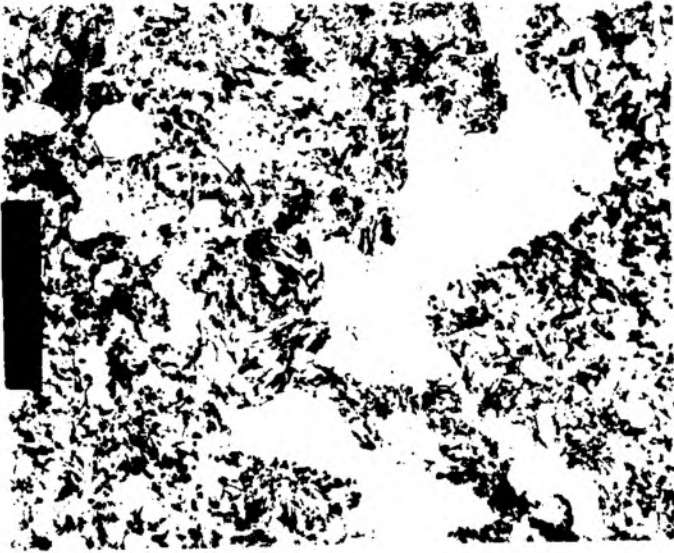


(e)

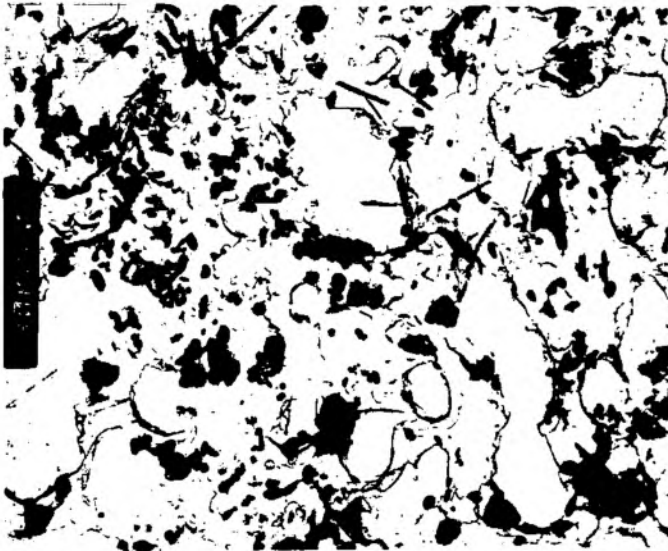
Fig.4.22 : Transmission Electron Micrographs of samples  
oil quenched from  $950^{\circ}\text{C}/3$  hrs. + tempered  
 $200^{\circ}\text{C}/1$  hr.

(d) 23,100X, A<sub>7</sub>

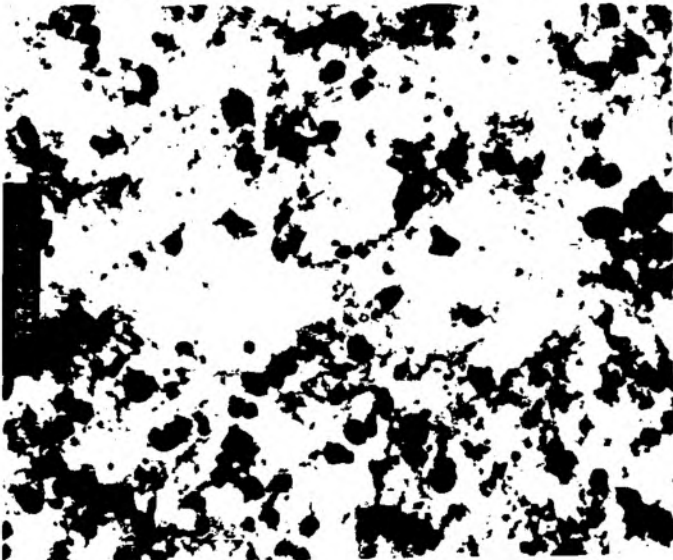
(e) 35,000X, A<sub>4</sub>



(a)

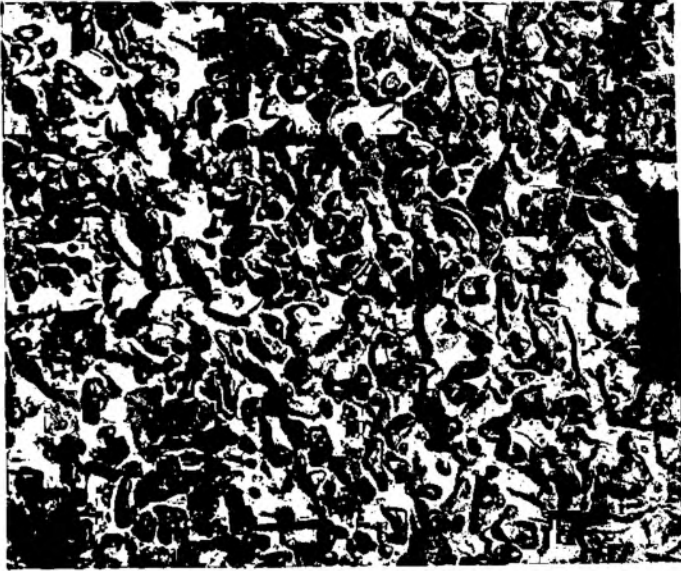


(b)

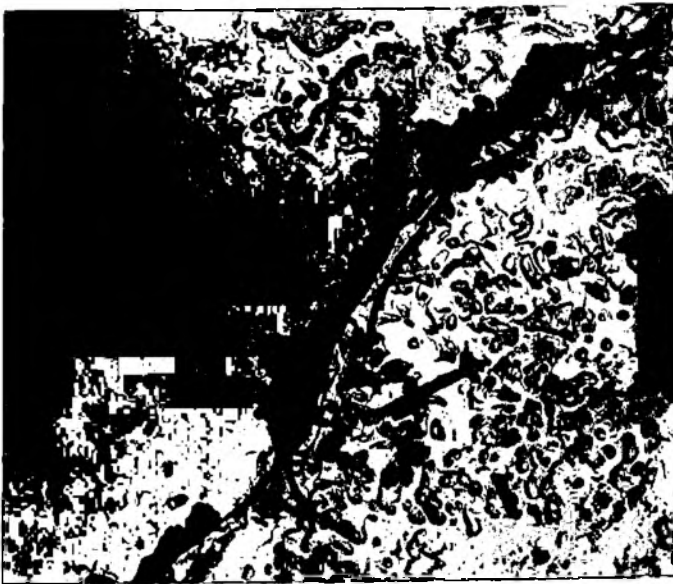


(c)

Fig.4.23 : Transmission Electron Micrographs of samples oil quenched and tempered at 600°C.  
(a) A<sub>7</sub>, 2000X, (b) A<sub>7</sub>, 30000X,  
(c) A<sub>4</sub>, 70000X



(a)



(b)

Fig.4.24 : Transmission Electron Micrographs of  $B_3$  as cast  
(a&b) 50,000X



(c)



(d)

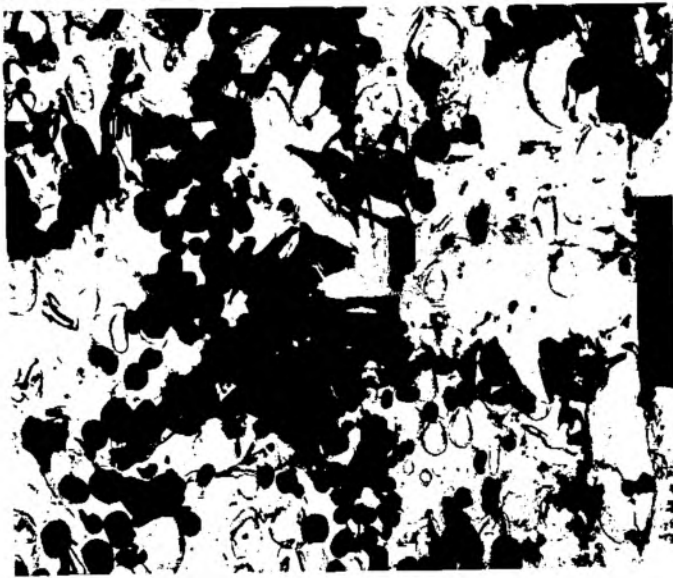


(e)

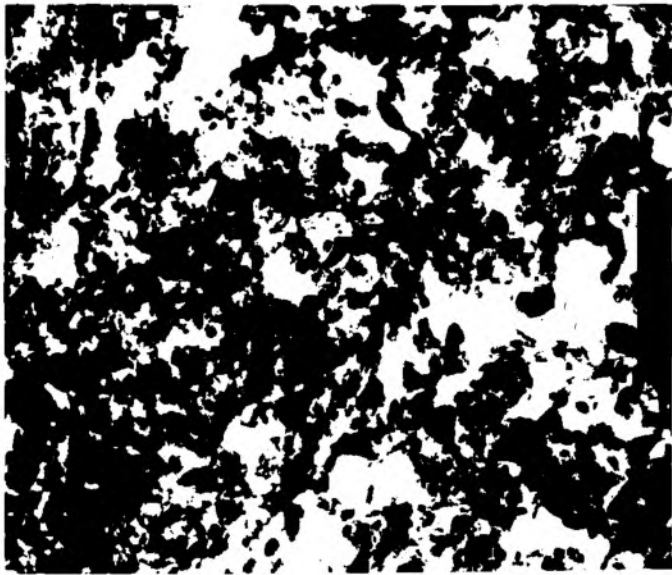
Fig.4.24 : Transmission Electron Micrographs of samples

(c&d)  $B_1$  as cast 30,000X

(e)  $A_8$  chill cast 30,000X



(a)



(b)

Fig.4.25 : Transmission Electron Micrographs of samples  
oil quenched and tempered at 200°C

(a) B<sub>1</sub>, 22000X

(b) B<sub>3</sub>, 15,000X

of the base alloy  $A_1$  was compared with that of the austenitic alloys  $C_1$  and  $C_2$ . The applied potential (mV) versus current (mA) plots are given in Figs. 4.26 (a,b). The exposed area of all samples was 1cm x 1.5cm. The plots indicate that the corrosion resistance of the chromium cast irons deteriorated in the order  $A_1 \rightarrow C_2 \rightarrow C_1$ .

#### 4.2 Wear Tests

Wear tests were conducted on alloys  $A_1, A_2, A_6, A_7, B_1-B_3, C_1$  and  $C_2$ . The experimental specimens abraded against a rotating bonded alumina wheel at a uniform speed of 120 ~~mm~~ min. The test specimens were pressed against the wheel under load. The test condition was one of high stress abrasion. The cumulative wear data are presented in Figs. 4.27 - 4.33. Wear rates ( $\text{gm/N/m}$ ) were computed from the cumulative wear data corresponding to a particular load and the <sup>sliding</sup> distance ~~slided~~ at such constant load (Fig. 4.34 - 4.40). The wear behaviour varied appreciably from alloy to alloy. In  $A_1$  the total wear increased consistently with increase in load. In  $A_2$ , however, total wear increased initially on increasing the load from 4.9N to 9.8N. Thereafter it decreased again. In  $A_6$  the total wear under 4.9N and 9.8N loads were nearly equal. It increased appreciably under 14.7N load. In  $A_7$  the total wear actually dropped slightly on increasing the load from 4.9N to 9.8N. On increasing the load to 14.7N, the total wear increased sharply. In fact, the wear in  $A_7$  under 14.7N load was highest among the A series alloys.

Alloys  $B_1$  to  $B_3$  were tested at only 14.7N load. In both ~~oil~~ quenched and tempered condition as well as in oil quenched, cryotreated and tempered condition total wear

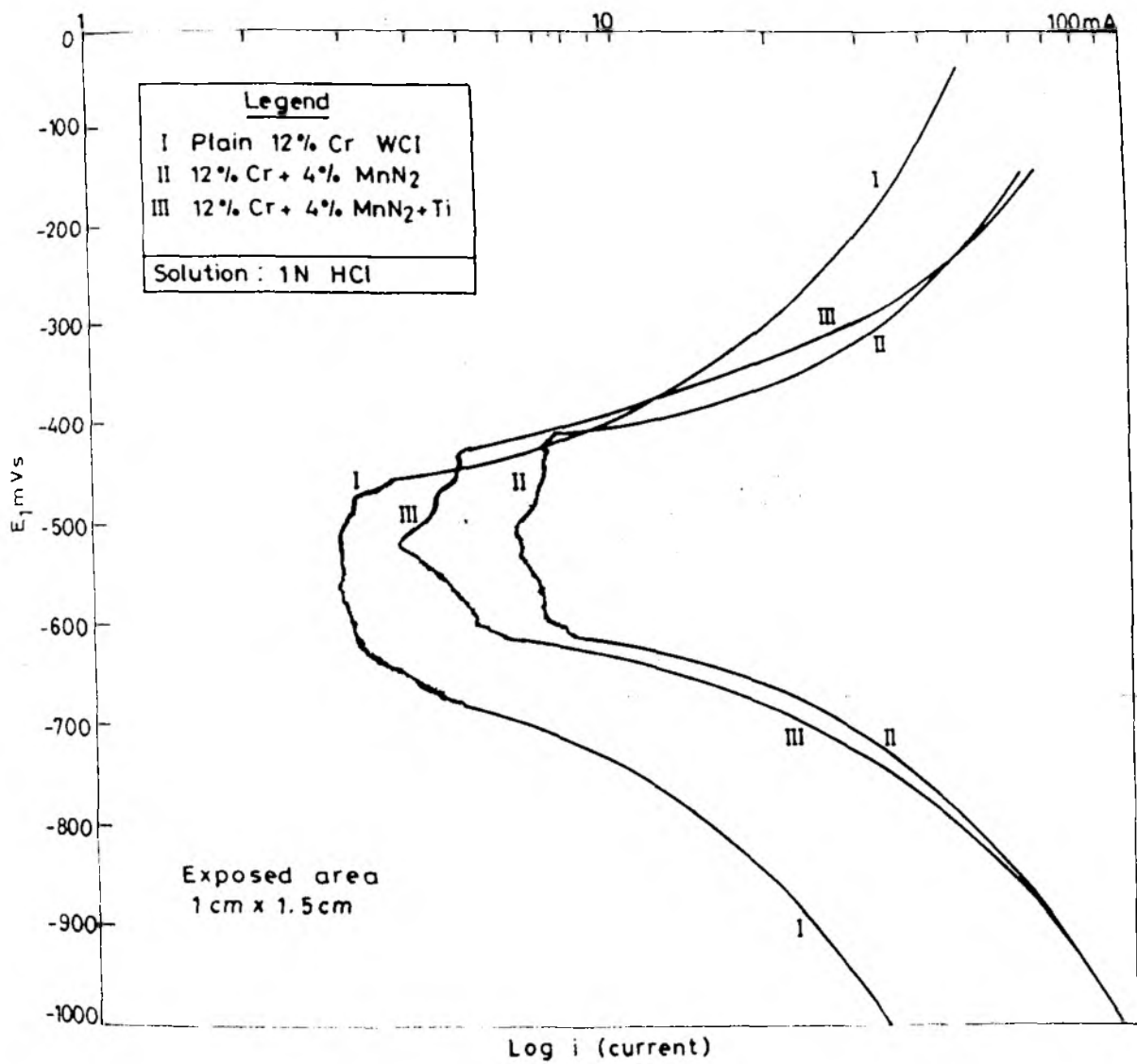


Fig. 4.26 (a). Polarization curves (Potentiostatic) in 1N HCl solution

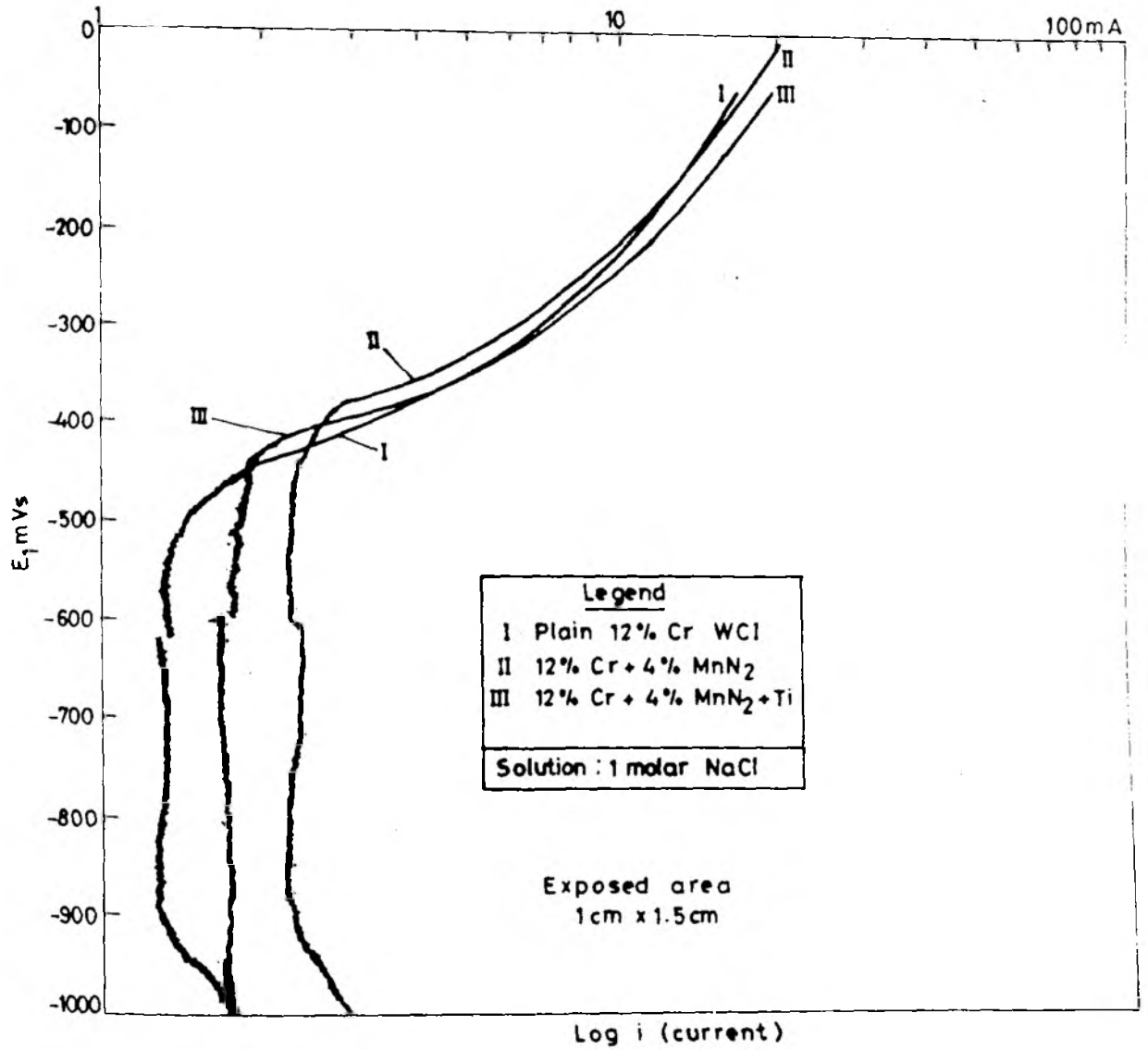


Fig. 4.26(b). Polarization curves (Potentiostatic) in 1 molar NaCl solution

decreased in the order  $B_1 \rightarrow B_2 \rightarrow B_3$ . Among the cryotreated and noncryotreated samples, the total wear was less in the former. In  $C_2$ , a drop in total wear occurred on enhancement of load from 4.9N to 9.8N. It increased again under 14.7N load. Among all the samples tested, the highest total wear was noted in case of  $C_2$ . The cumulative wear curves show the usual trend of running in and equilibrium wear although complete equilibrium wear state was not attained within the experimental period in several cases.

The wear rate (gm/N/M) plots differentiates the wear behaviour of the experimental alloys more explicitly. The wear rate in most cases decreased appreciably in the initial period of sliding. Thereafter the wear rate decreased either slowly or became constant. The effect of load on wear rate however varied from alloy to alloy. While in  $A_4$  and  $A_7$  wear rate increased consistently with increasing load, in  $A_2$  it decreased. In  $A_6$ ,  $C_1$  and  $C_2$  wear rate dropped initially but it rose again on increasing the load to 14.7N. Cryotreatment of alloys  $B_1$ - $B_3$  resulted in a drop in wear rate (Fig. 4.38 a,b).

The abraded samples of the B series alloys were examined in SEM after etching. A comparison of the wear tracks in samples of  $B_1$ - $B_3$  tested under 14.7N was made in SEM. The differences in the depth of abrasion marks between the base alloy  $B_1$  and the other alloys can be noted in Fig. 4.41 (a-c). The wear tracks were still shallower in the cryotreated samples. During wear tests bulging and cracking of the wear surface could be noted (Fig. 4.42). Such cracks had propagated both through the matrix as well as through the carbide phase. Fig. 4.43 shows bending of carbide plates in the sliding

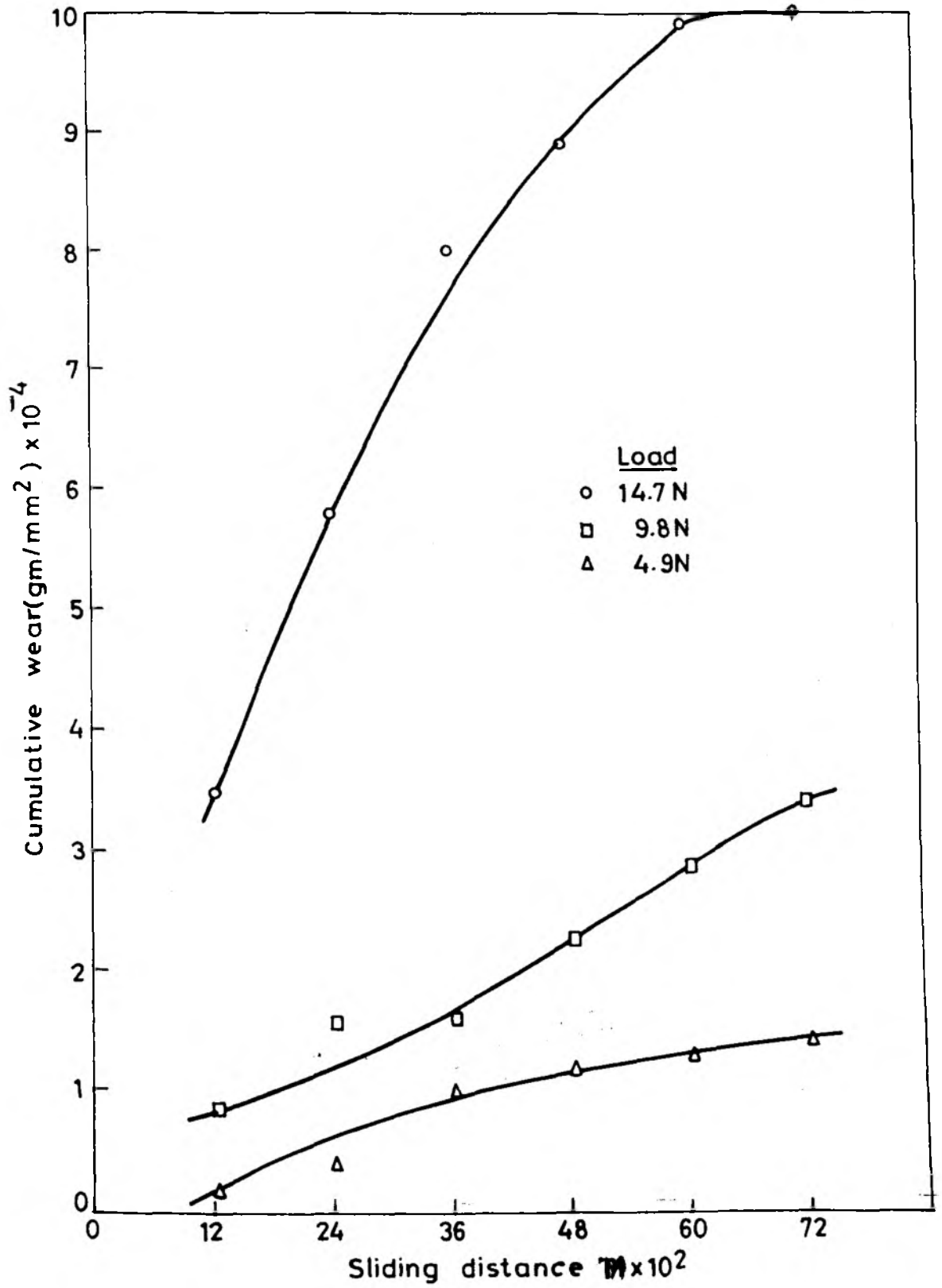


Fig. 4.27. Cumulative wear versus sliding distance [Sample A<sub>1</sub>]

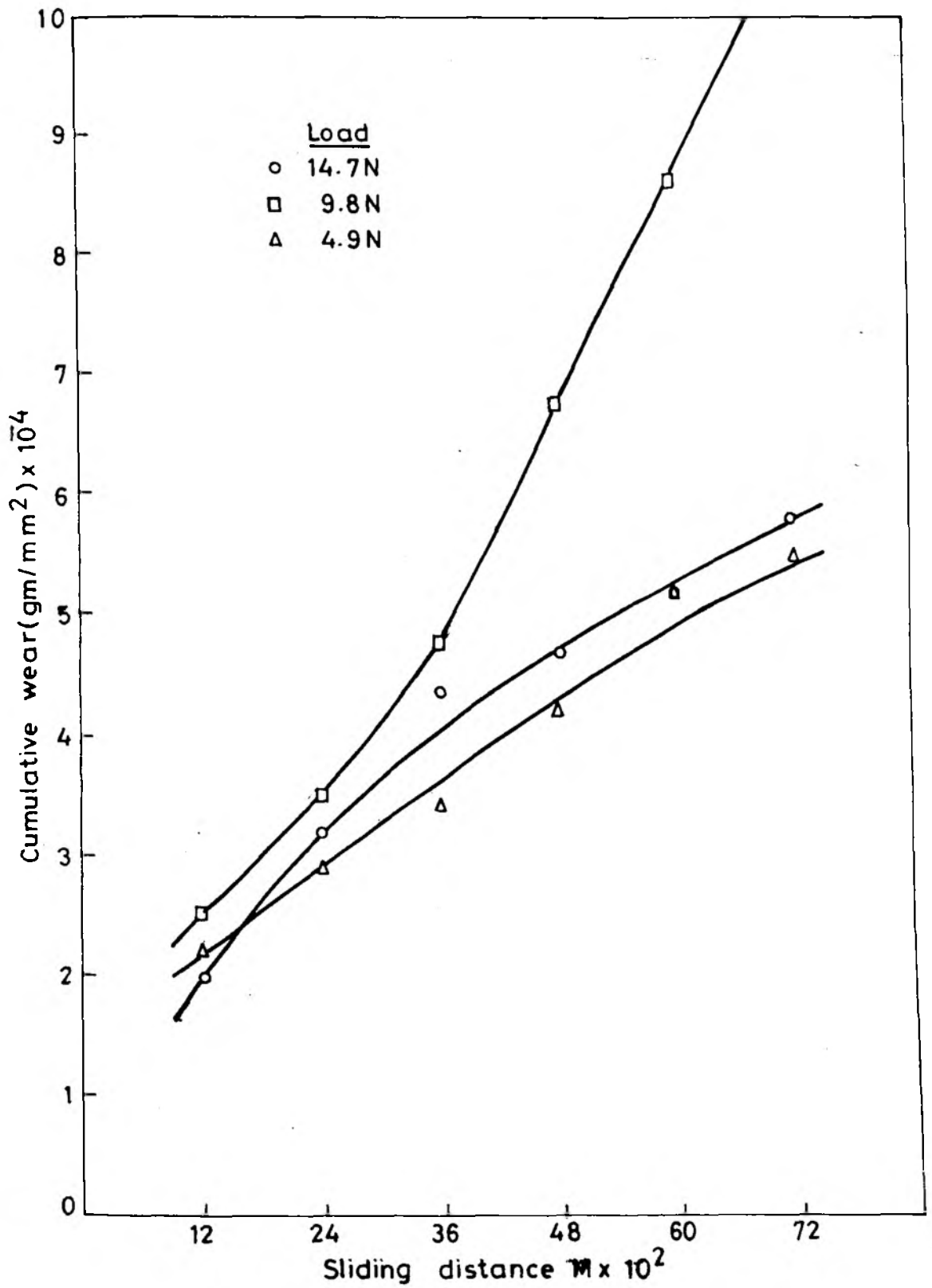


Fig. 4.28. Cumulative wear versus sliding distance  
[Sample A<sub>2</sub>]

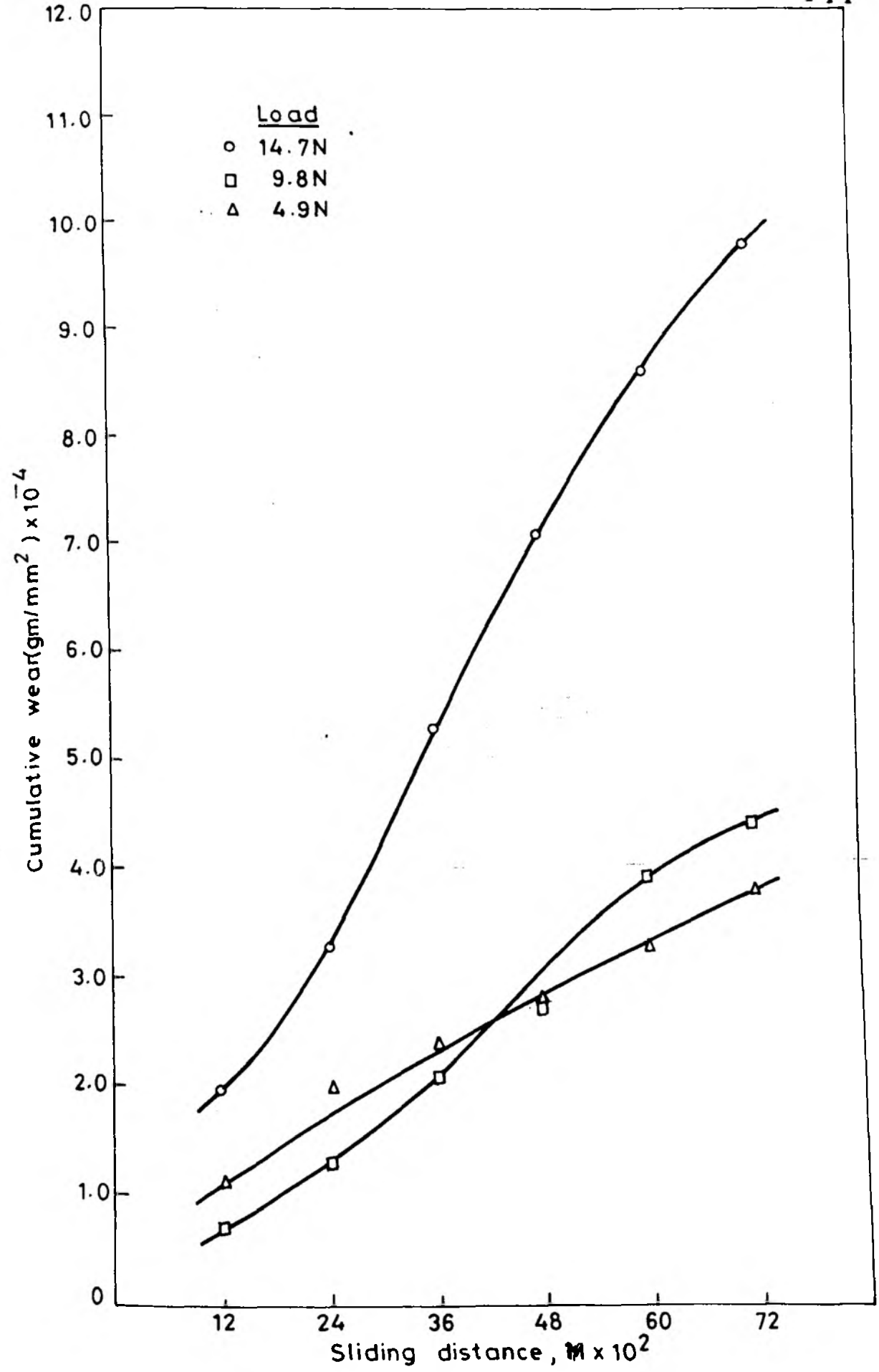


Fig. 4.29. Cumulative wear versus sliding distance [Sample A<sub>F</sub>]

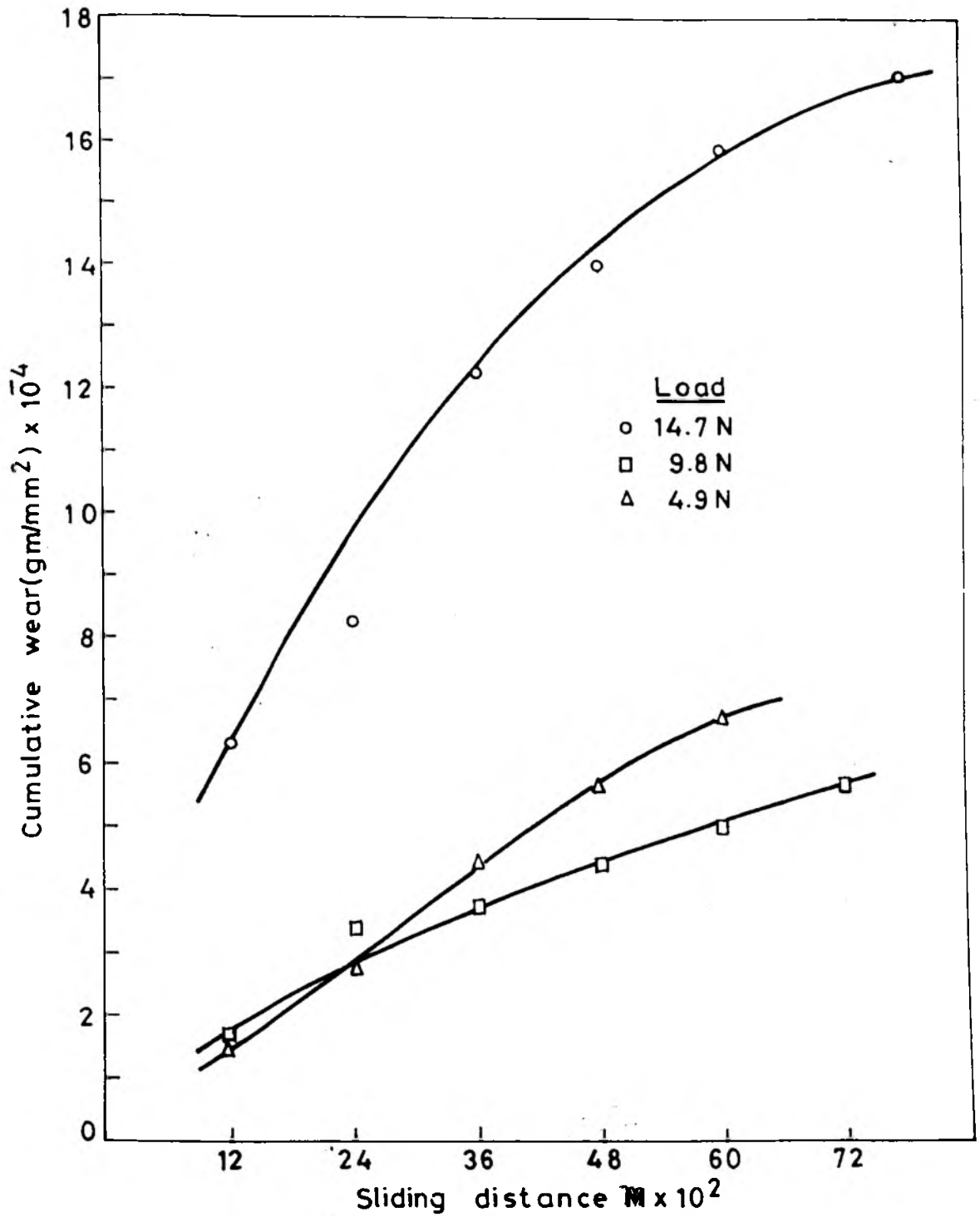


Fig. 4.30. Cumulative wear versus sliding distance  
[Sample A7]

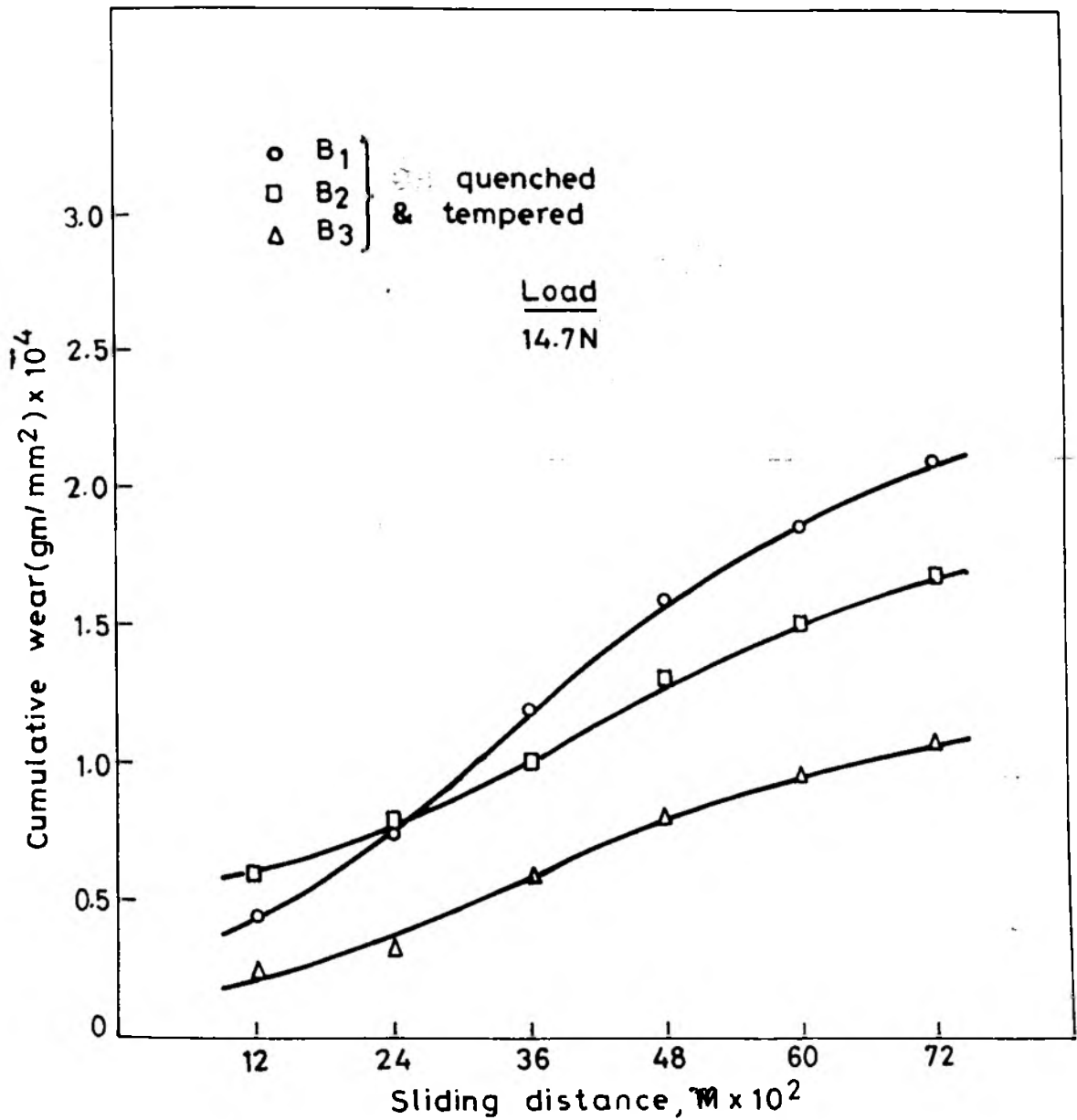


Fig. 4.31(a). Cumulative wear versus sliding distance.  
 Samples B<sub>1</sub>, B<sub>2</sub>, B<sub>3</sub>

ORDINARY HEATTREATMENT  
 Oil/Air quenched from 900°C,  
 and tempered at 200°C for  
 one hour

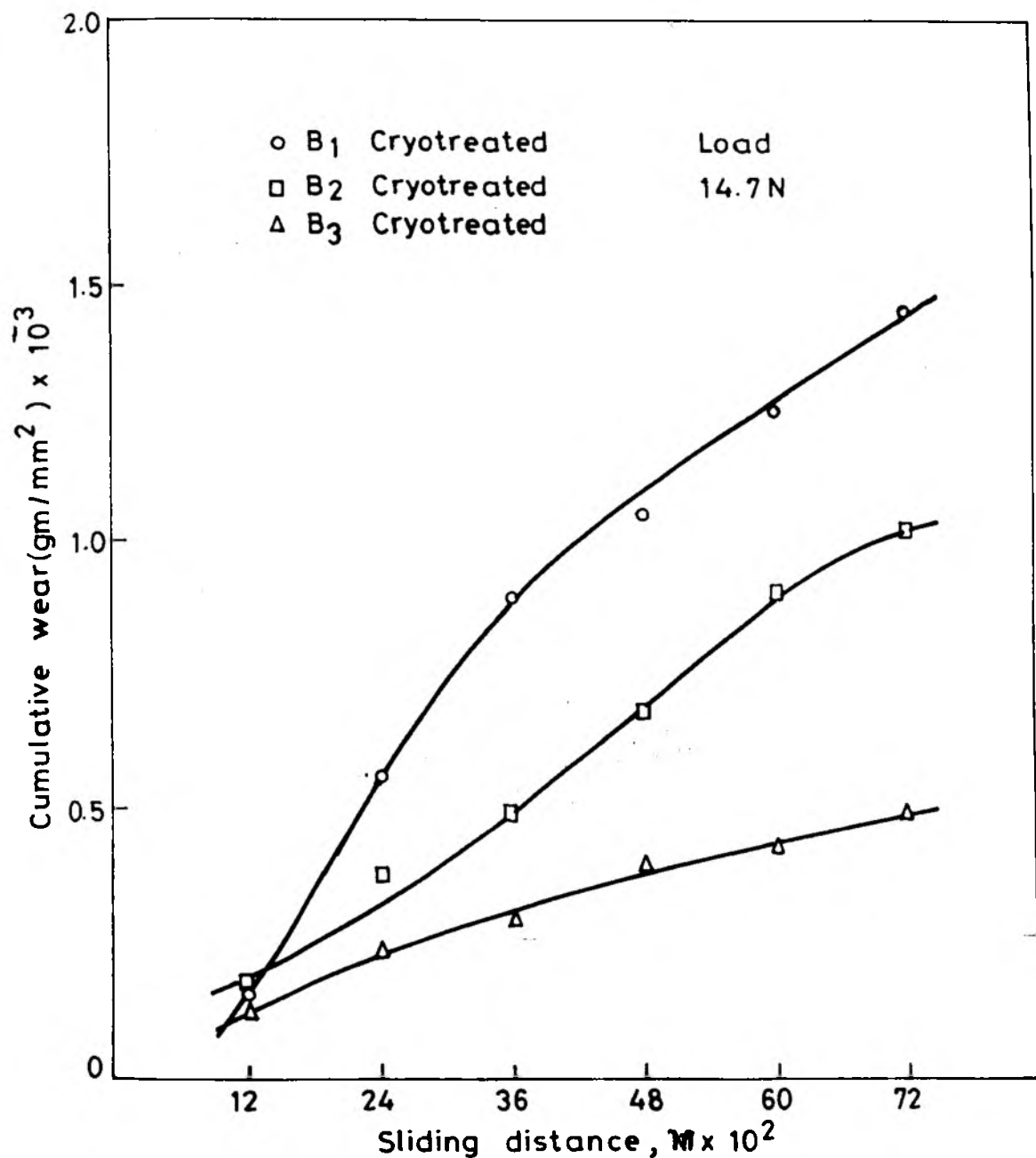


Fig. 4.31(b). Cumulative wear versus sliding distance  
Samples B<sub>1</sub>, B<sub>2</sub>, B<sub>3</sub>

CRYOTREATMENT  
 Oil/Air quenched from 900°C,  
 cryotreated in liquid N<sub>2</sub> and  
 tempered at 200°C for one hour

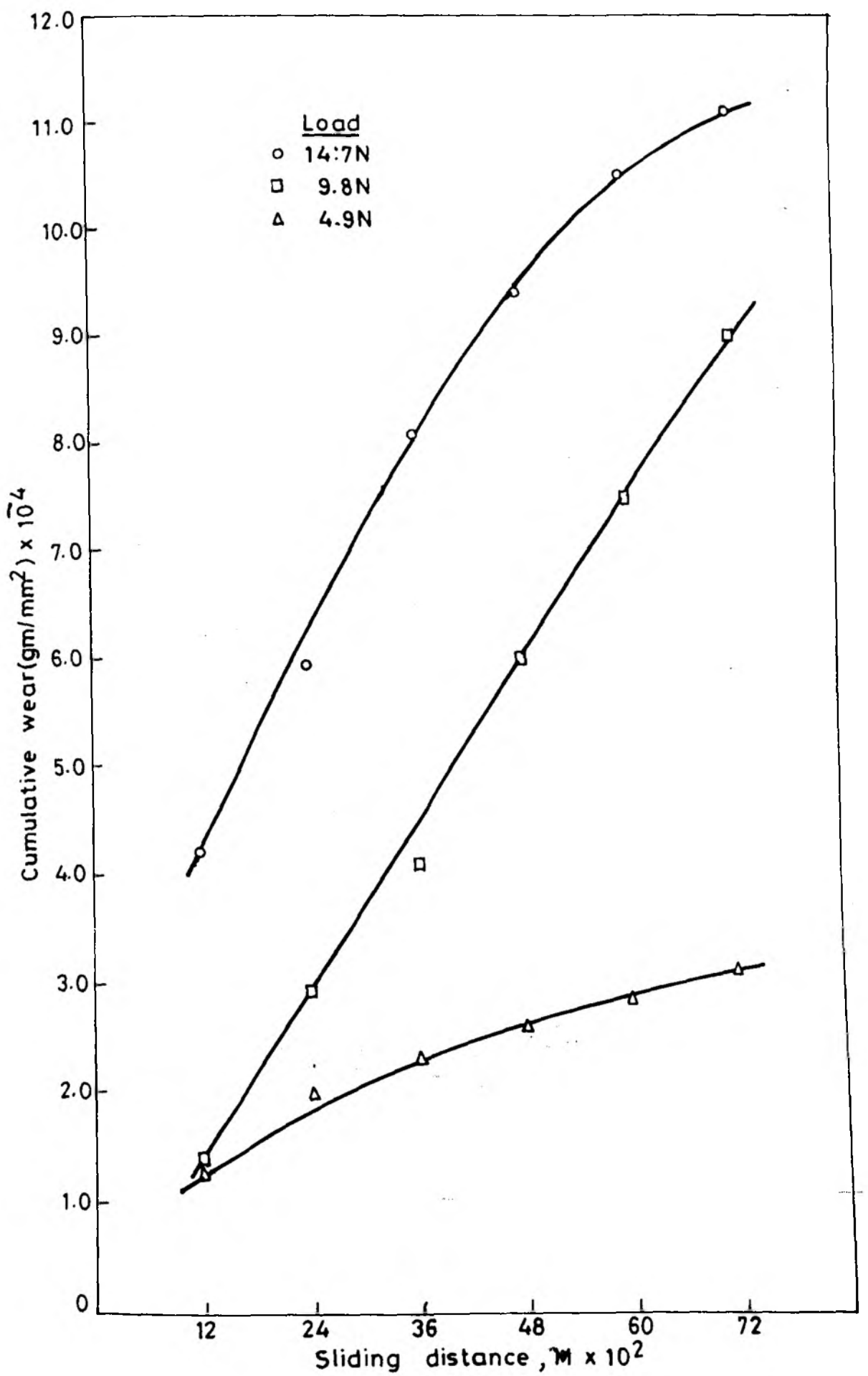


Fig. 4.32. Cumulative wear versus sliding distance. [Sample C<sub>1</sub>]

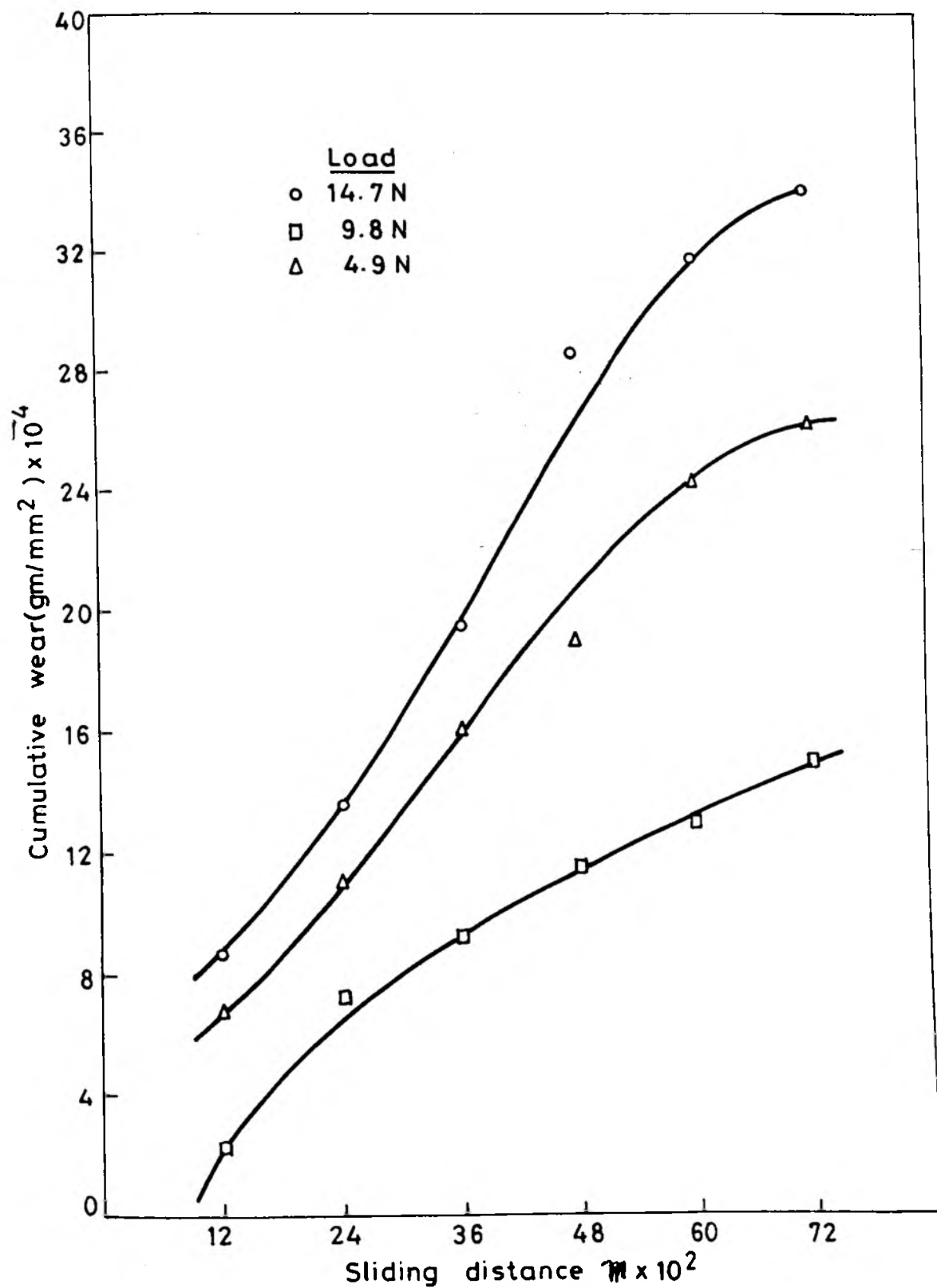


Fig. 4.33. Cumulative wear versus sliding distance [Sample C<sub>2</sub>]

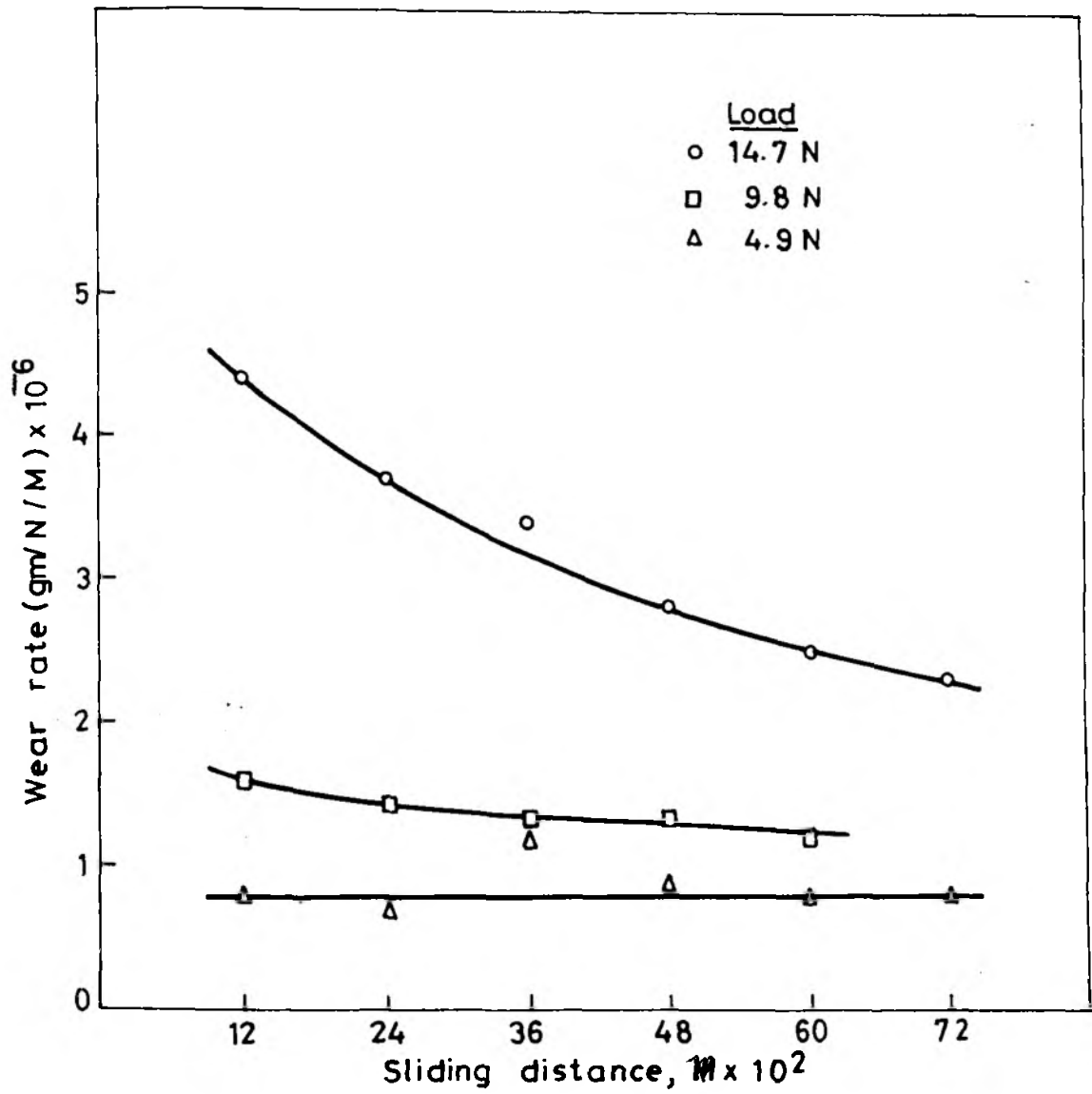


Fig. 4.34. Wear rate versus sliding distance  
[ Sample A<sub>1</sub> ]

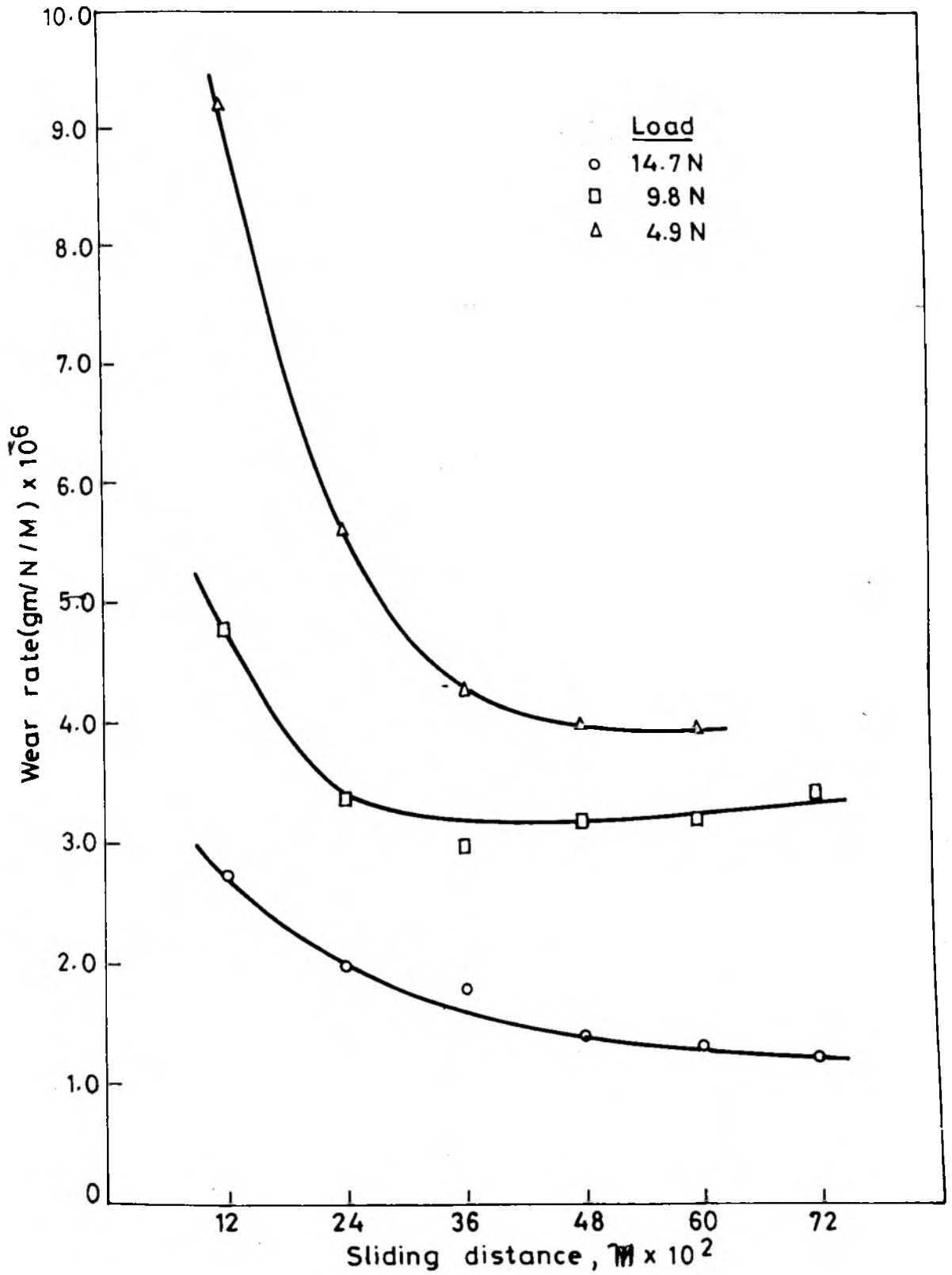


Fig. 4.35. Wear rate versus sliding distance.  
[Sample A<sub>2</sub>]

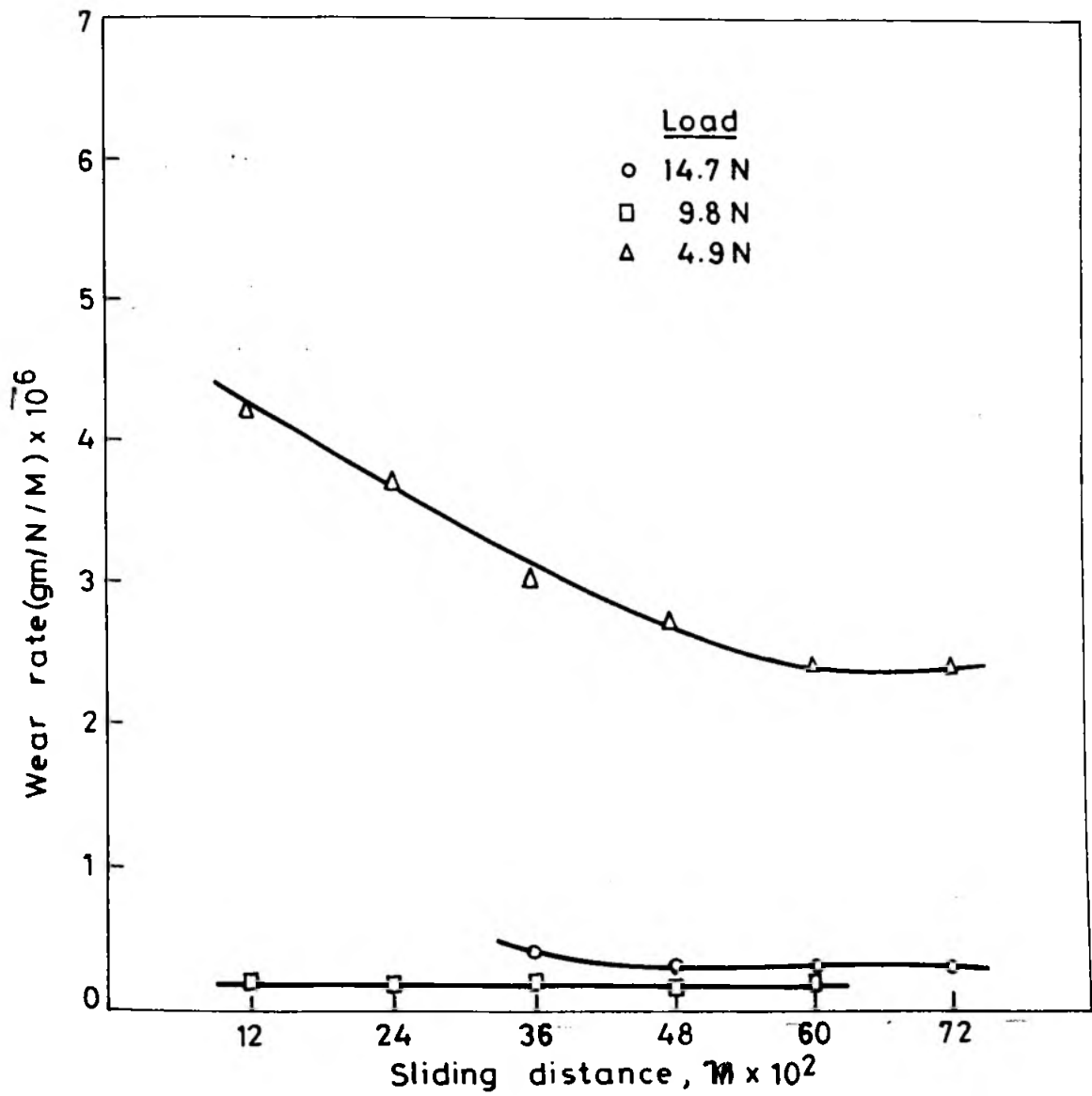


Fig. 4.36. Wear rate versus sliding distance.  
[Sample A<sub>6</sub>]

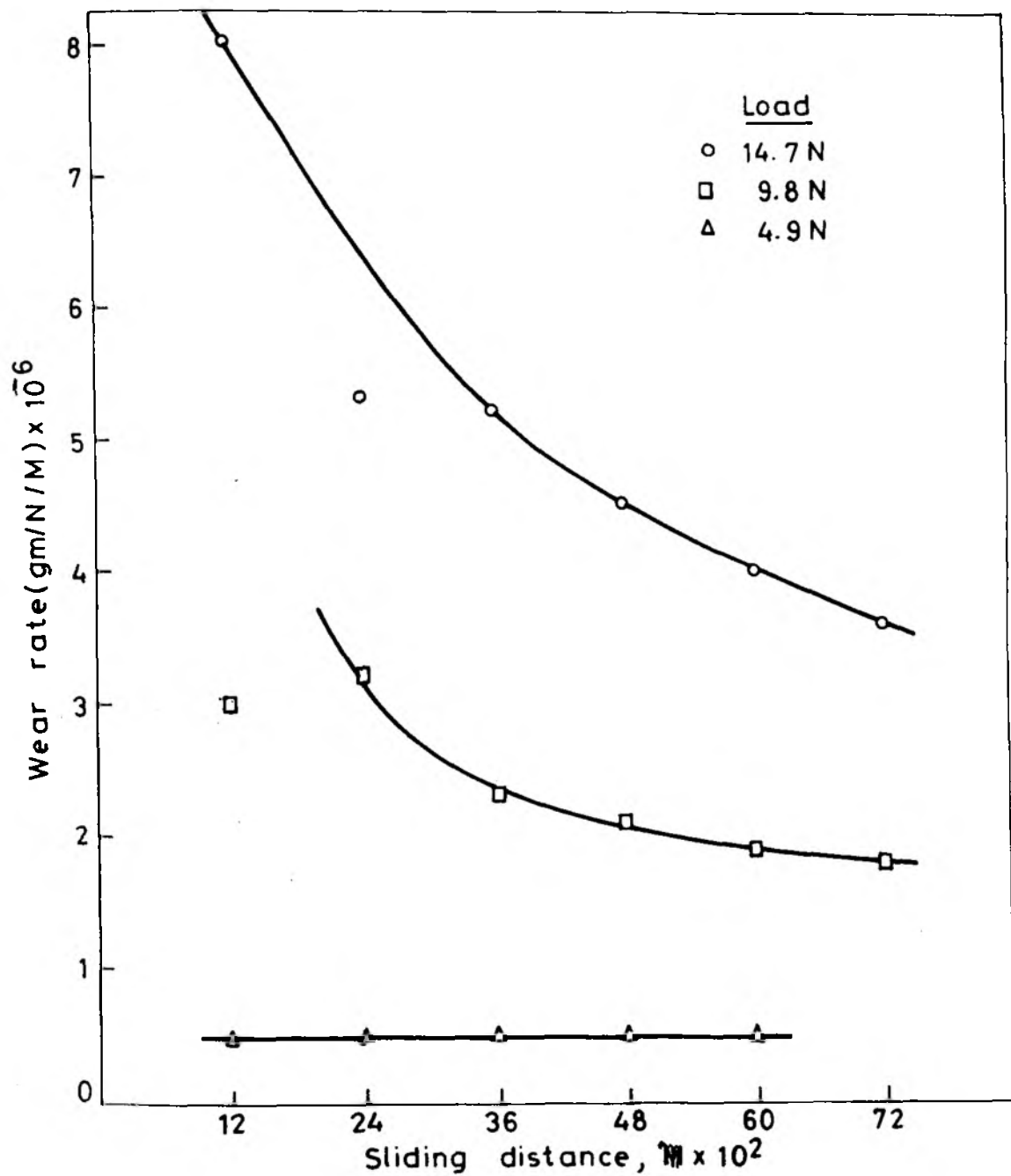


Fig. 4.37. Wear rate versus sliding distance.  
[Sample A7]

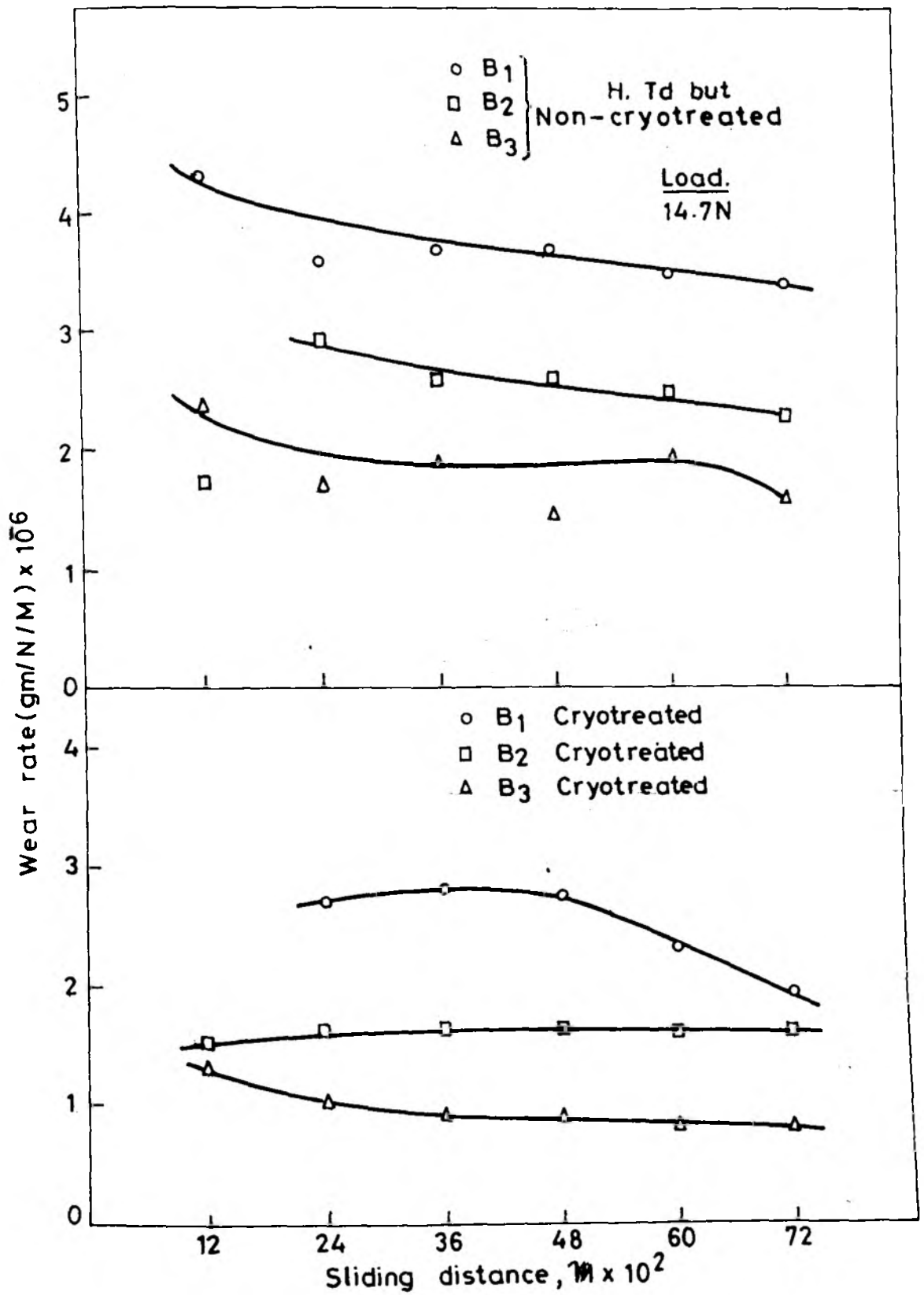


Fig. 4.38. Wear rate versus sliding distance [Samples B<sub>1</sub>, B<sub>2</sub> and B<sub>3</sub>]

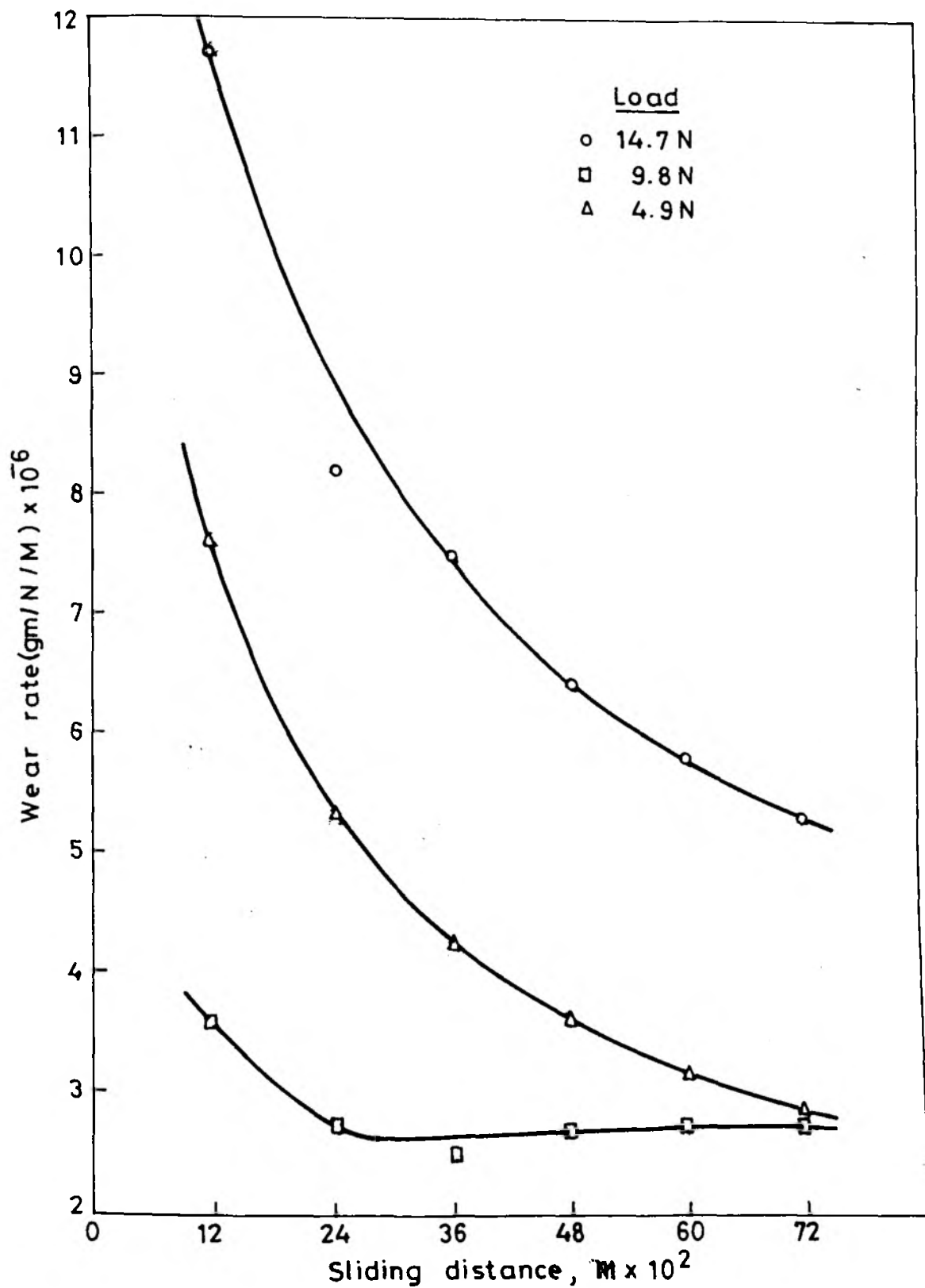


Fig. 4.39. Wear rate versus sliding distance [ Sample C<sub>1</sub> ]

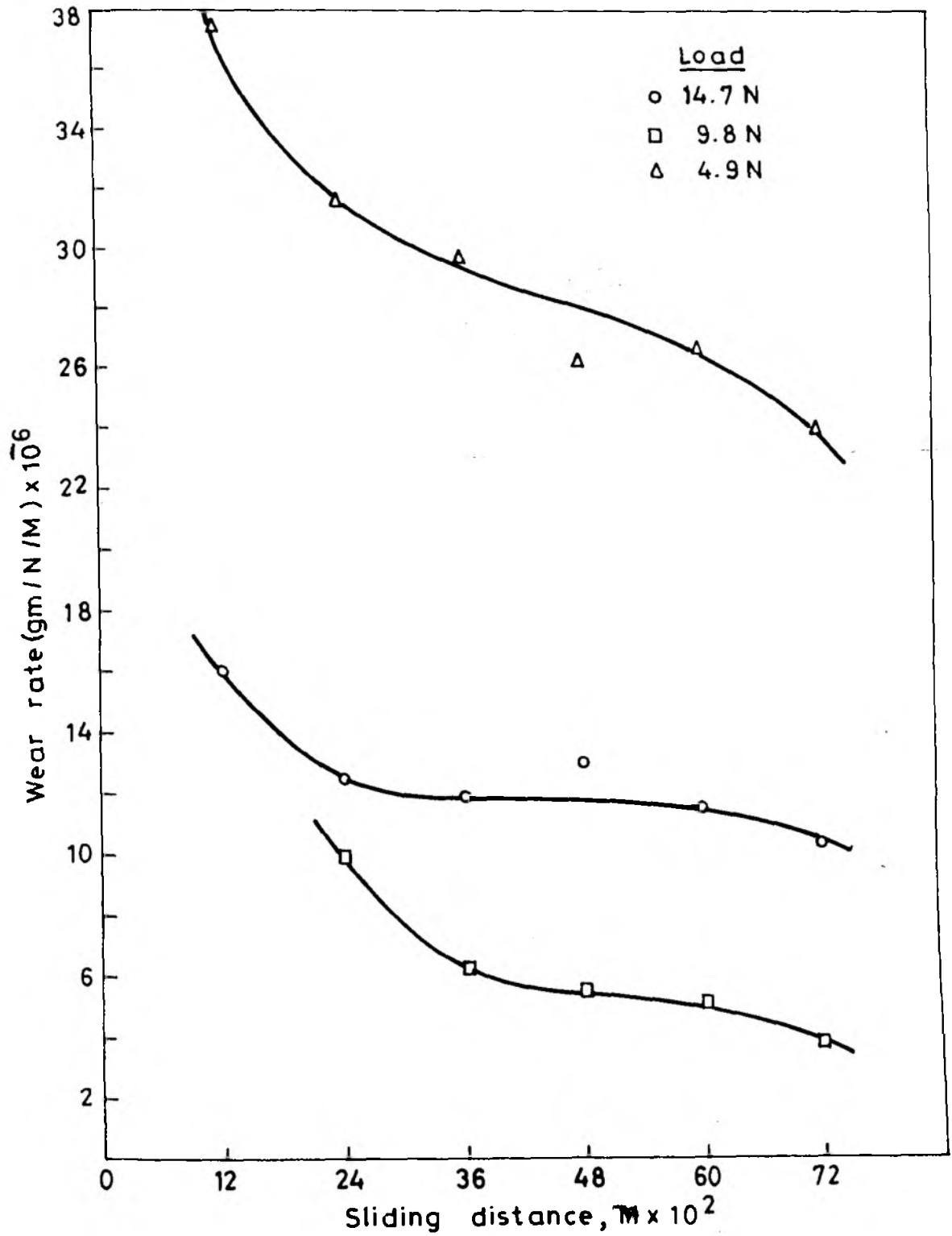
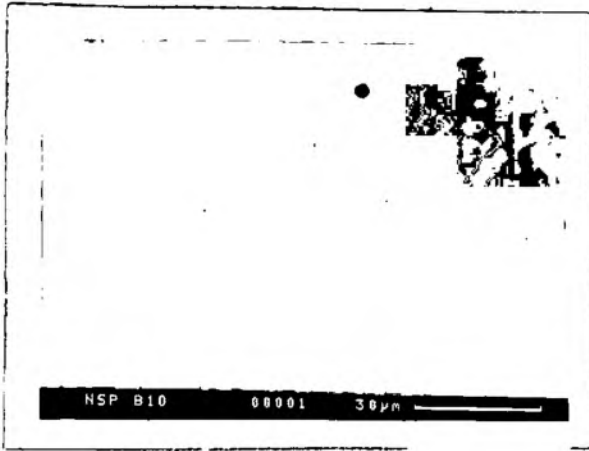
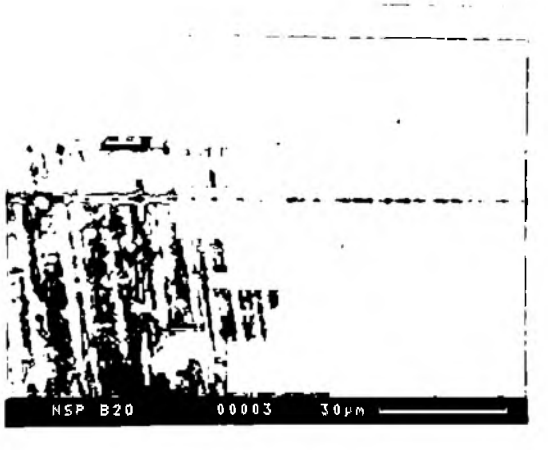


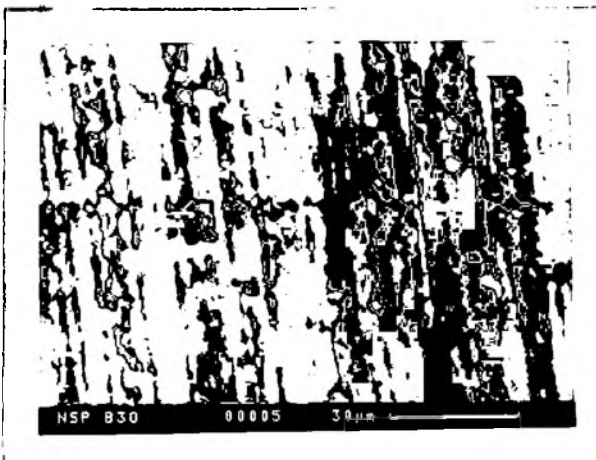
Fig. 4.40. Wear rate versus sliding distance  
[Sample C<sub>2</sub> ]



(a) 600X



(b) 600X



(c) 600X

Fig. 4.41 : SEM view of wear tracks  
 (a)  $B_1$  (b)  $B_2$  and (c)  $B_3$   
 oil quenched and tempered.

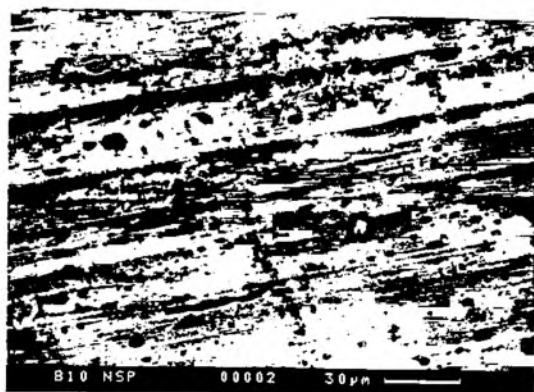


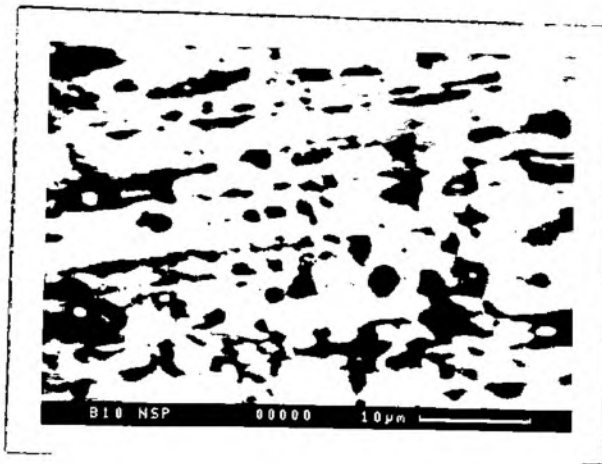
Fig. 4.42 330X



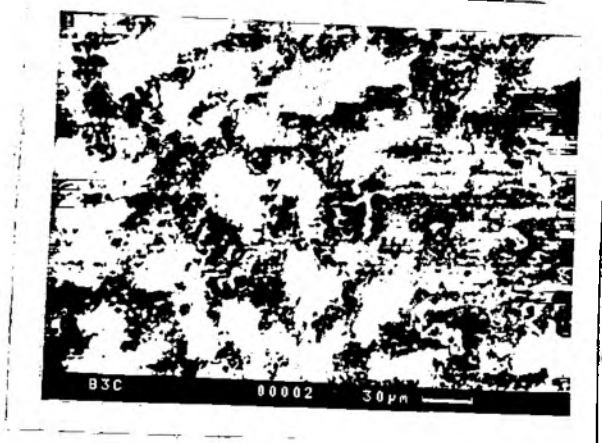
Fig. 4.43 (250X)

Fig.4.42 : Bulging and cracking in the wear surface (SEM)

Fig.4.43 : Deformation and cracking in carbide plates during wear (SEM)



(a) 1500X



(b) 330X

Fig.4.44 : SEM photograph illustrating the wear tracks on both the matrix and the carbide phase. (a)  $T_1$ , (b)  $T_3$

direction. Multiple cracks may also be noted in the carbide plates. Some of the samples were examined after deep etching. In these samples wear tracks were seen to pass through both the matrix and the carbide phase (Fig. 4.44).

#### 4.3 Machining trials with chromium cast iron tools

Chromium cast iron cutting tools prepared from the A series alloys were tested first for turning a mild steel bar in oil quenched and tempered condition. The tools suffered catastrophic failures even at low speeds and feeds. The tools made from the B-series alloys were tested next. The characteristic chips formed during machining with different tools including the reference HSS(Grade BT4 = C 0.75, Cr 4.0, W 18.0, V 1.0, Co 5.0, Hardness Hv 849 and BS 4659:1971) were compared by light and scanning electron micrography. A photograph showing the visual appearance of the chips formed during machining with the B-series tools are given in Fig. 4.45. Fig. 4.45 demonstrates that the chips were more open type at 50m/min speed and 0.16 mm/rev. feed than those produced at lower speed feed combinations. Maximum curling was observed at 40m/min speed and 0.12mm/rev. feed.

SEM photographs of the under surface of the chips formed at 46m/min. speed and 0.12mm/rev. feed are presented in Fig. 4.46 (a-i). Typical optical micrographs of chips formed by chromium cast iron tools and a HSS tool are shown in Fig. 4.47 (a-c). Table 4.6 reports the crack density in the chips determined from the SEM photographs. It is apparent from Table 4.6 and Fig. 4.6 (a-i) that crack density in the chips produced by the B-series tools was higher than that in the HSS tool chip. However, the HSS tool chip appeared to be deformed to a

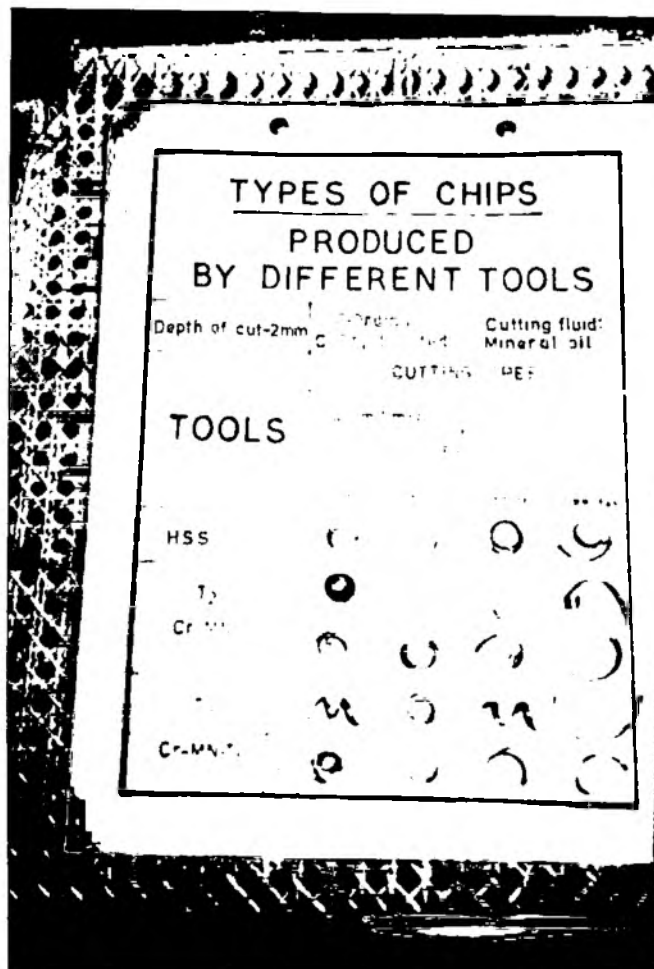
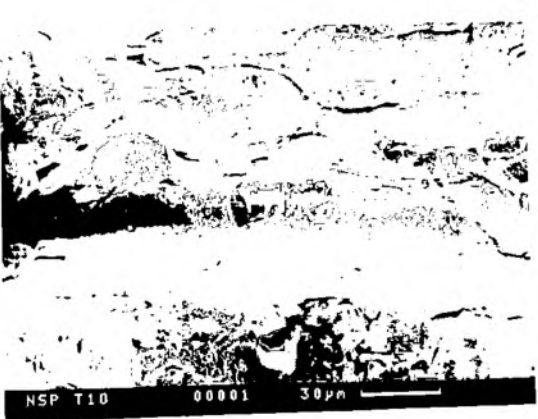
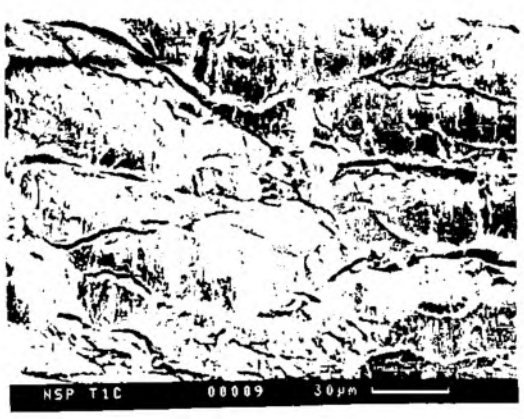


Fig.4.45 : Types of chips produced by different tools (visual appearance).



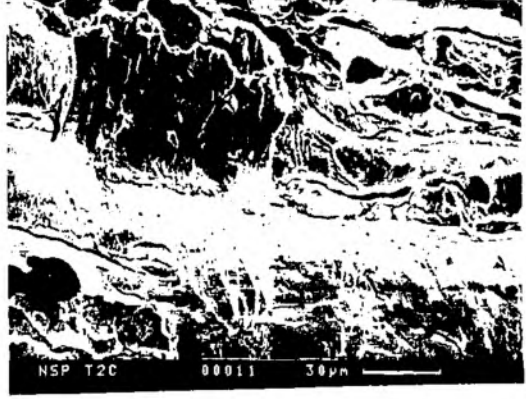
(a) 330X



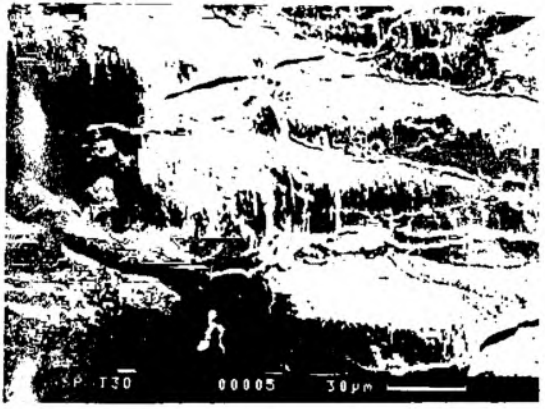
330X



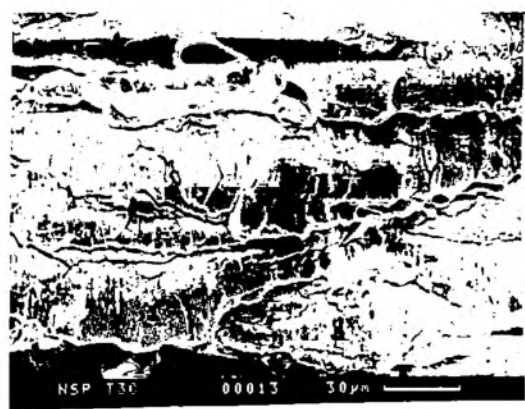
(c) 330X



(d) 330X



(e) 330X

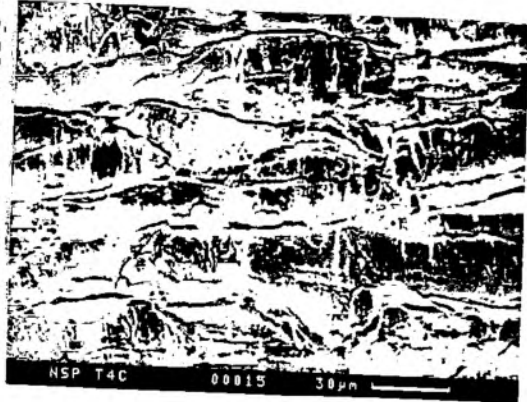


(f) 330X

Fig.4.46 : SEM micrographs of underside of the chips (a-f)



(g) 330X



(h) 330X



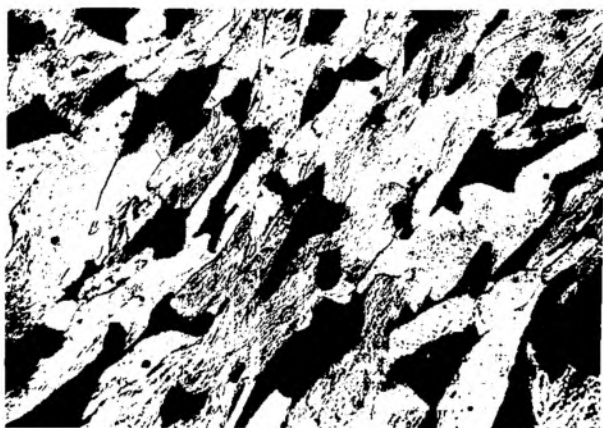
(i) 330X

Fig.4.46 (contd.) : SEM micrographs of undersurface  
of the chips (g-i)

Tool used : (a) B<sub>1</sub> (c) B<sub>2</sub> (e) B<sub>3</sub> (g) B<sub>4</sub>  
 Quenched and tempered  
 (b) B<sub>1</sub> (d) B<sub>2</sub> (f) B<sub>3</sub> (h) B<sub>4</sub>  
 Quenched, cryotreated and tempered  
 (i) HSS tool.



(a)



(b)



(c)

Fig.4.47 : Optical micrographs of the chips, 200X.

(a)  $B_2$  - Ordin. (b)  $B_2$  - cryo-treated (c) HSS

Table 4.6 Crack Density in Chips

Tool sample	Heattreatment	Crack density cms/316 <sup>2</sup> cm <sup>2</sup> on photographic plate (X 366)
B <sub>1</sub>	900°C/2 hrs. A.Q. + 200°C /1 hr.	13
B <sub>2</sub>	-do-	22
B <sub>3</sub>	-do-	24
B <sub>4</sub>	-do-	26
B <sub>1</sub>	900°C/2 hrs. A.Q. cryotreatment in liquid nitrogen +200°C/1 hr.	24
B <sub>2</sub>	-do-	26
B <sub>3</sub>	-do-	30
B <sub>4</sub>	-do-	37
HSS	Quenched & tempered	10

greater extent under the microscope. Among the B-series tools, cryotreated tools induced greater cracking in the chips.

The tools life data in Table 4.7 show that the tools made of B<sub>9</sub> and B<sub>4</sub> alloys recorded reasonable life at a low speed of 40 m/min and a feed of 0.12 mm/rev. At such speed-feed combination, the life of B<sub>9</sub> and B<sub>4</sub> tools were 160 and 200 minutes respectively against 300 minutes life of the HSS tool. With the speed-feed combination of 40m/min and 0.16 mm/rev. the tool life decreased in both HSS and experimental tools. In both B<sub>9</sub> and B<sub>4</sub> the tool life was 30 mins. against 60 mins of the HSS tool. After cryotreatment in liquid nitrogen, the life of B<sub>9</sub> tool increased to 43mins i.e. approximately 75% of the life of a HSS tool. At 50 m/min: speed and 0.12mm/rev. feed, the best tool life (B<sub>9</sub>) was only of the order of 25% of that of the HSS tool. The B series tools suffered catastrophic failure at 50mm speed with 0.16mm/rev. feed. Chips produced by the HSS tool had undergone more plastic deformation and had suffered less cracking than the chips produced by the B-series tools.

A worn out tool of alloy B<sub>9</sub> was examined in SEM before complete failure had occurred. Fig. 4.48 is an SEM photograph of cutting edge of the tool B<sub>4</sub>. In addition to the wear marks the figure shows big cracks nucleated from an interdendritic pores. Complete fracture occurred through propagation of such cracks.

The data on chip reduction coefficient  $\xi$  are presented in Table 4.8. Chip reduction coefficient in general increased on increasing the feed rate from 0.12mm/rev. to 0.16mm/rev. at 40m/min. speed. Thereafter, the variation in

Table 4.7 Tool life data for various tool tested

Depth of cut = 2mm constant Environment = oil

Material : C<sub>25</sub> steel

Tool	Tool life (in mins)			
	speed 40m/min		speed 50m/min	
	Feed 0.12mm/rev	Feed 0.16mm/rev	Feed 0.12mm/rev.	Feed 0.16mm/rev.
HSS	300	60	100	25
B <sub>1</sub> -Ord	12(F) Failed	44(F) Failed	7(F) Failed	1(F) Failed
B <sub>2</sub> -Ord	140	9	24	1.0
B <sub>3</sub> -Ord	160	30	25	1.5
B <sub>4</sub> -Ord	200	30	27	1.0
B <sub>1</sub> -cryo	Failed	2	2	2
B <sub>2</sub> -cryo	Failed	25	3	3
B <sub>3</sub> -cryo	30	43	10	5
B <sub>4</sub> -cryo	30	32	5	5
A <sub>8</sub> chill cast. 900°C/4hrs A.Q+150°/1hr	-	60	32	20
A <sub>8</sub> chill cast 900°C/7hrs. A.Q+150°C/1hr.	-	-	-	40



1300 X

**Fig.4.48** : Cracks appearing on the cutting edge of a worn out tool (SEM).

Table 4.8  $\xi$  (chip reduction coefficient) values of various tools

Tool	Speed		Speed	
	40m/min		50m/min	
	0.12mm/rev.	0.16mm/rev.	0.12mm/rev.	0.16mm/rev.
HSS	$\xi=2.60$	3.17	3.56	3.31
B <sub>1</sub>	O	2.88	3.02	3.27
	C	2.79	2.52	3.17
B <sub>2</sub>	O	2.79	3.24	3.27
	C	3.56	3.02	3.46
B <sub>3</sub>	O	2.69	3.74	3.85
	C	3.46	3.53	3.08
B <sub>4</sub>	O	2.88	3.09	3.46
	C	2.50	3.60	3.85

O = ordinary

C = cryotreated

ORDINARY HEATTREATMENT  
Oil/Air quenched from 900°C,  
and tempered at 200°C for  
one hour

CRYOTREATMENT  
Oil/Air quenched from 900°C  
cryotreated in liquid N<sub>2</sub>  
and tempered at 200°C  
for one hour

chip reduction coefficient with increase in speed and feed was minimal. The axial ( $P_x$ ) and tangential ( $P_z$ ) cutting forces were measured as a function of feed rate at constant speeds for the tools  $B_1$ - $B_4$ . The data are presented in graphical form in figures 4.49 - 4.56. The data indicate that the cutting force required for machining with the HSS tool was lower than that for any of the chromium cast iron tools, at all speed-feed combinations. Among the B-series tools, no systematic variation in cutting force with speed and feed could be noted. However, the difference in the cutting forces required by different tools at any particular cutting condition was not very high.

Tool life of  $A_6$  was comparable to that of the reference HSS tool. This will be clear from Fig. 4.57. Initially the tool was heat treated for 4 hours at  $900^\circ\text{C}$  and then air quenched. The maximum tool life recorded after such heat treatment at 50m/min. speed and 0.16mm/rev. feed was only 20 mins. On adopting a cycle of 7 hours soaking at  $900^\circ\text{C}$  followed by air quenching and tempering at  $150^\circ\text{C}$ , the tool life doubled to 40 mins. at the same speed-feed combination. Under similar cutting condition, the tool life of the reference HSS tool was 35 minutes.

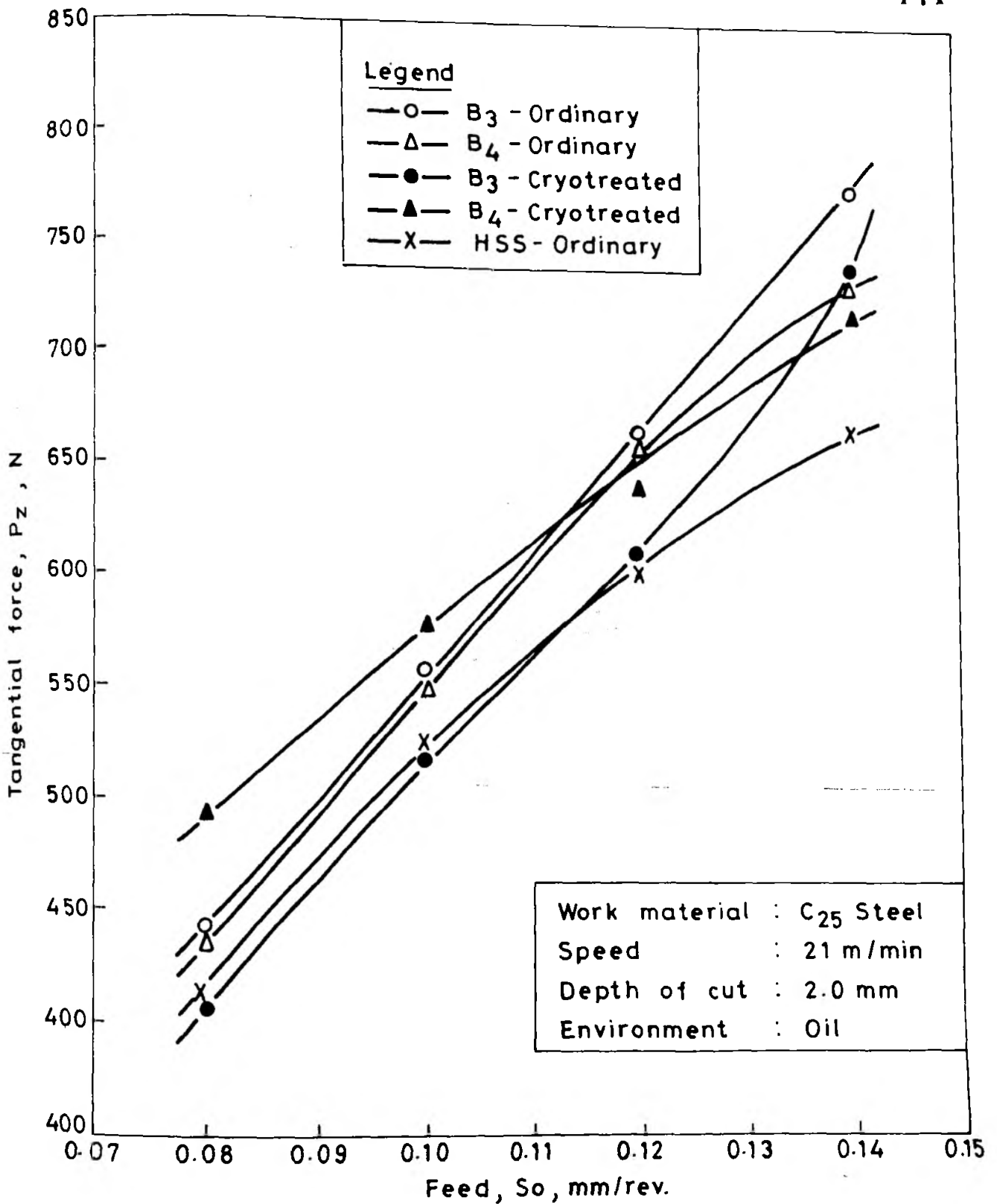


FIG. 4.49. INCREASE IN TANGENTIAL FORCE WITH FEED AT SPEED 21 M/MIN. FOR DIFFERENT TOOLS

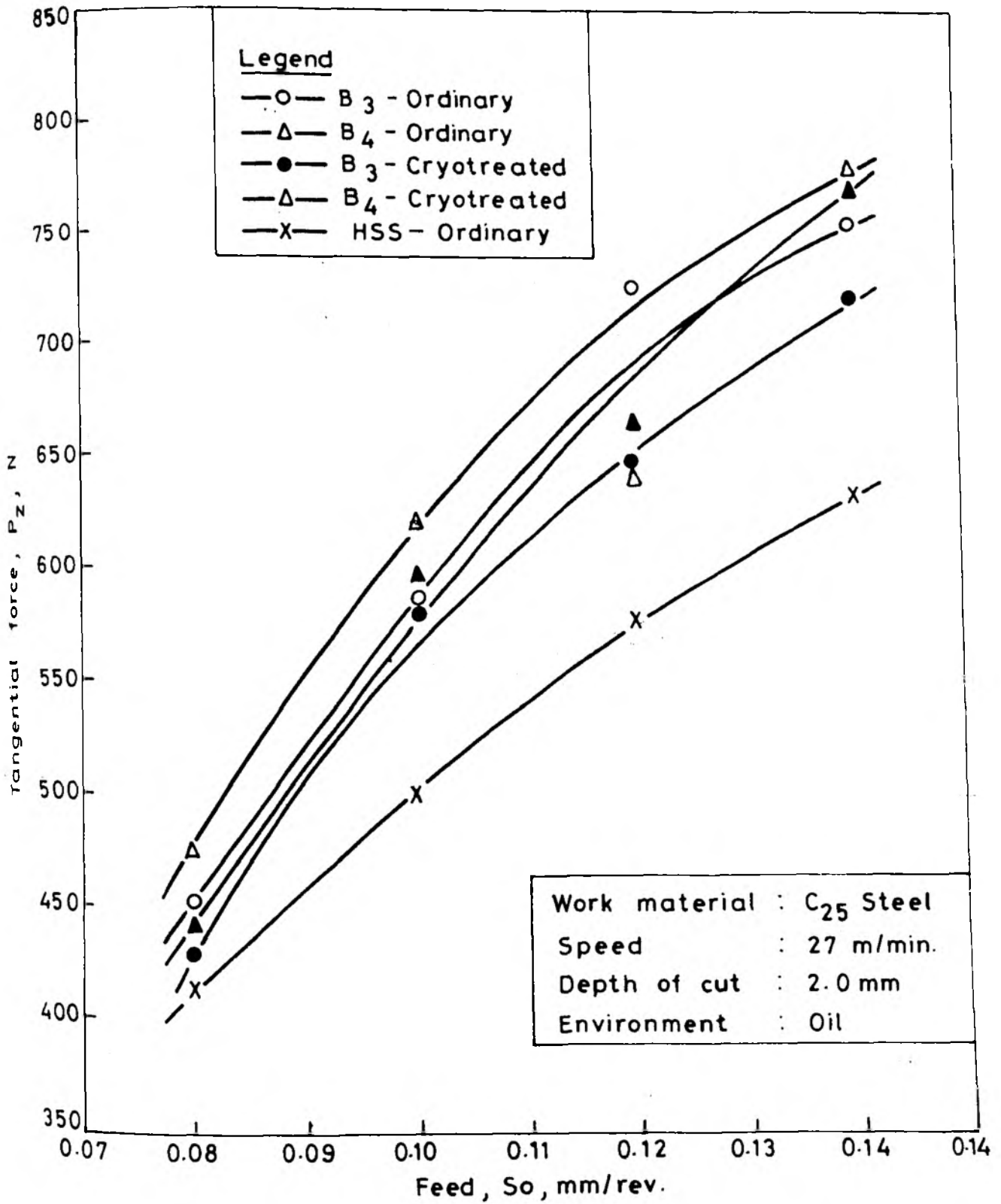


FIG. 4.50. INCREASE IN TANGENTIAL FORCE WITH FEED AT SPEED 27 M/MIN. FOR DIFFERENT TOOLS

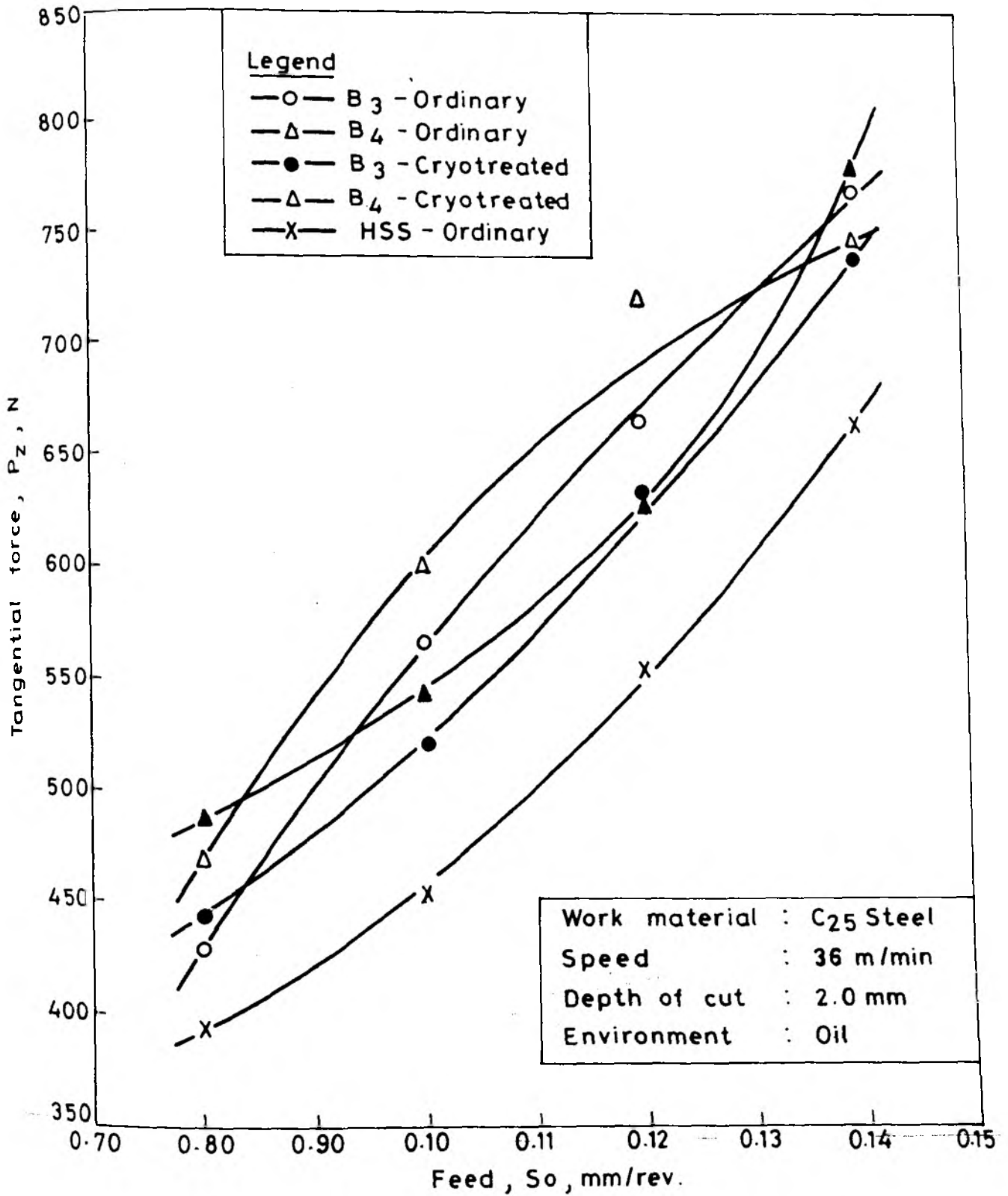


FIG.4.51. INCREASE IN TANGENTIAL FORCE WITH FEED AT SPEED 36 M/MIN. FOR DIFFERENT TOOLS

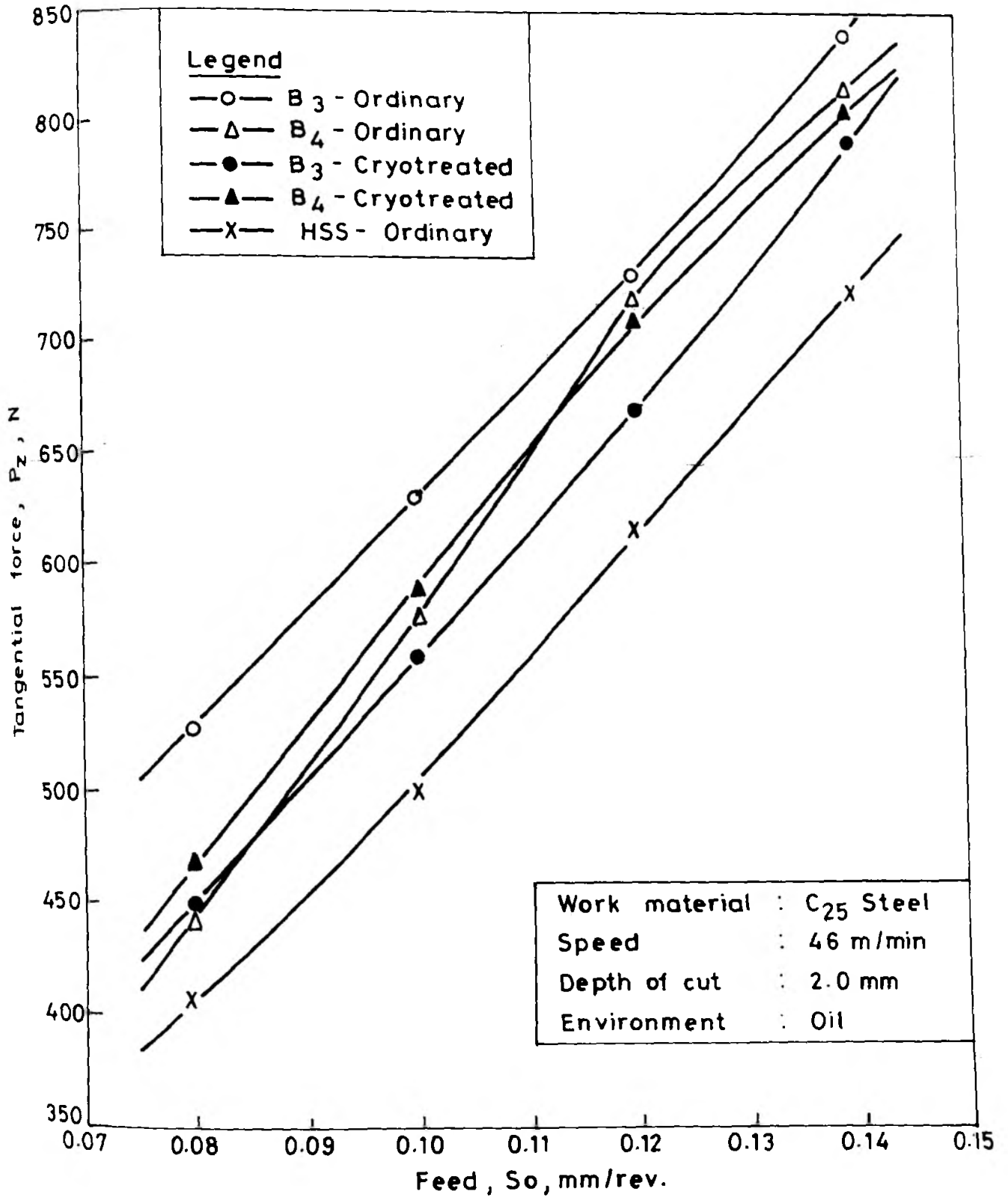


FIG. 4.52. INCREASE IN TANGENTIAL FORCE WITH FEED AT SPEED 46M/MIN FOR DIFFERENT TOOLS

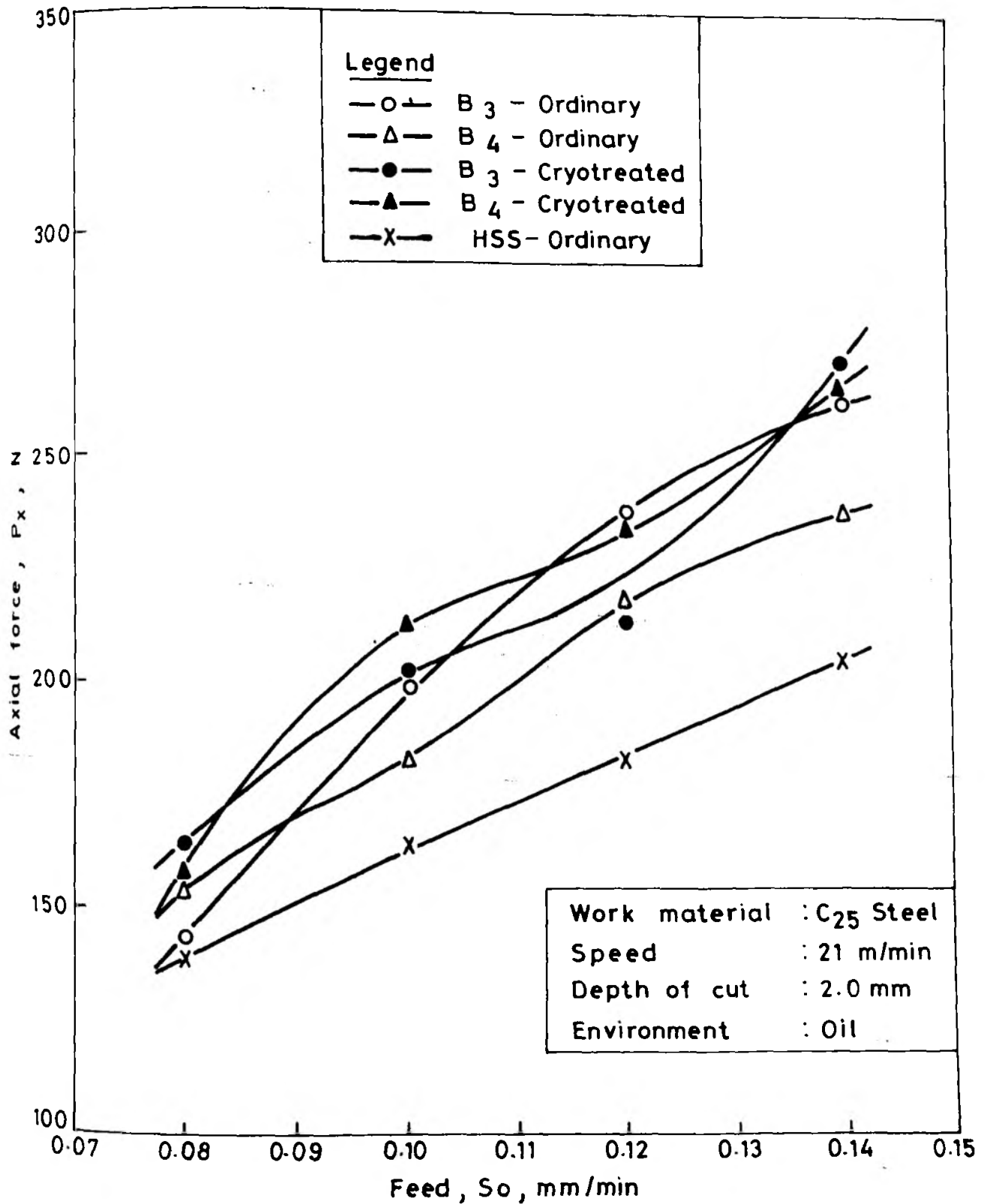


FIG. 4.53. INCREASE IN AXIAL FORCE WITH FEED AT SPEED 21 M/MIN FOR DIFFERENT TOOLS

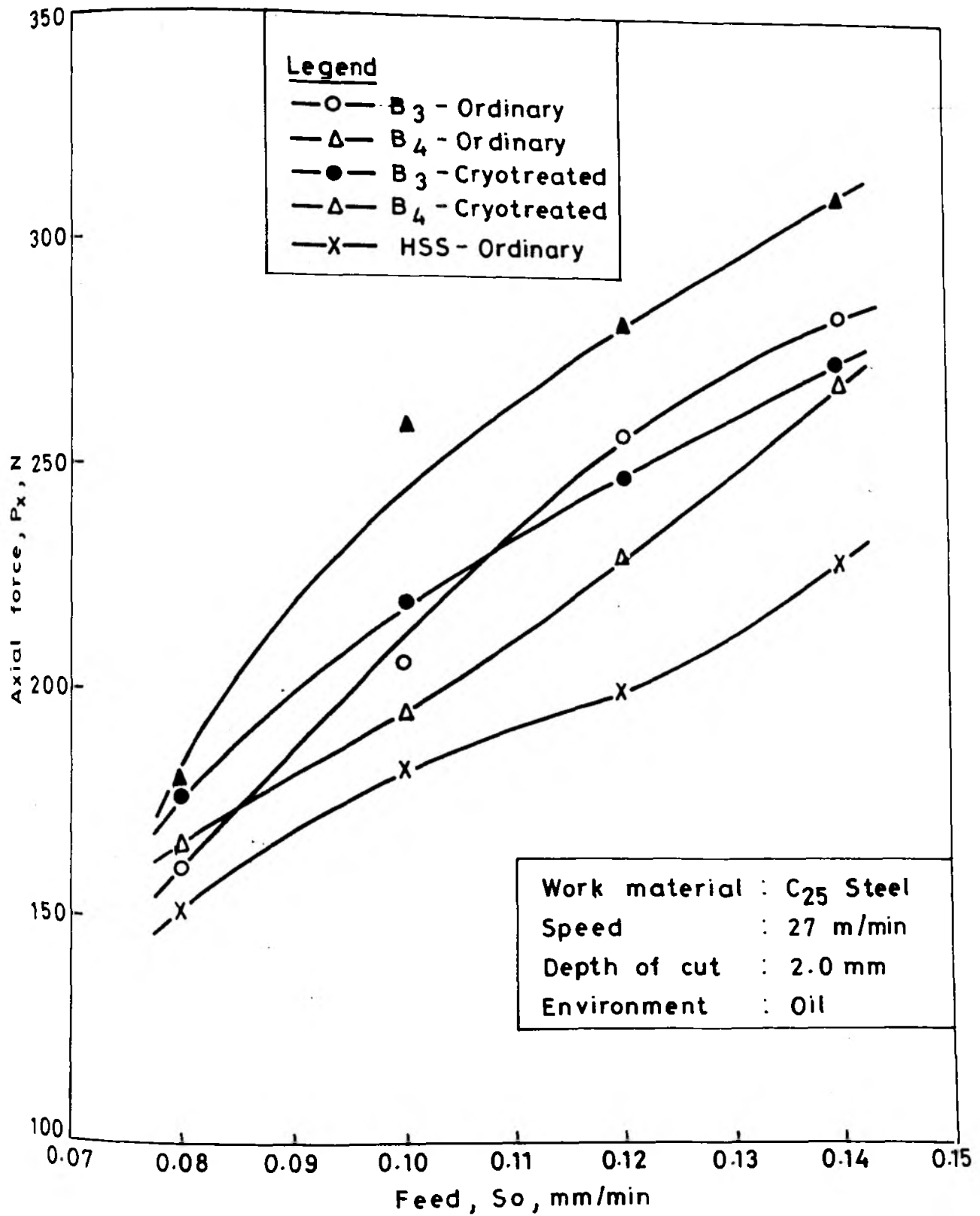


FIG.4.54. INCREASE IN AXIAL FORCE WITH FEED AT SPEED 27 M/MIN FOR DIFFERENT TOOLS

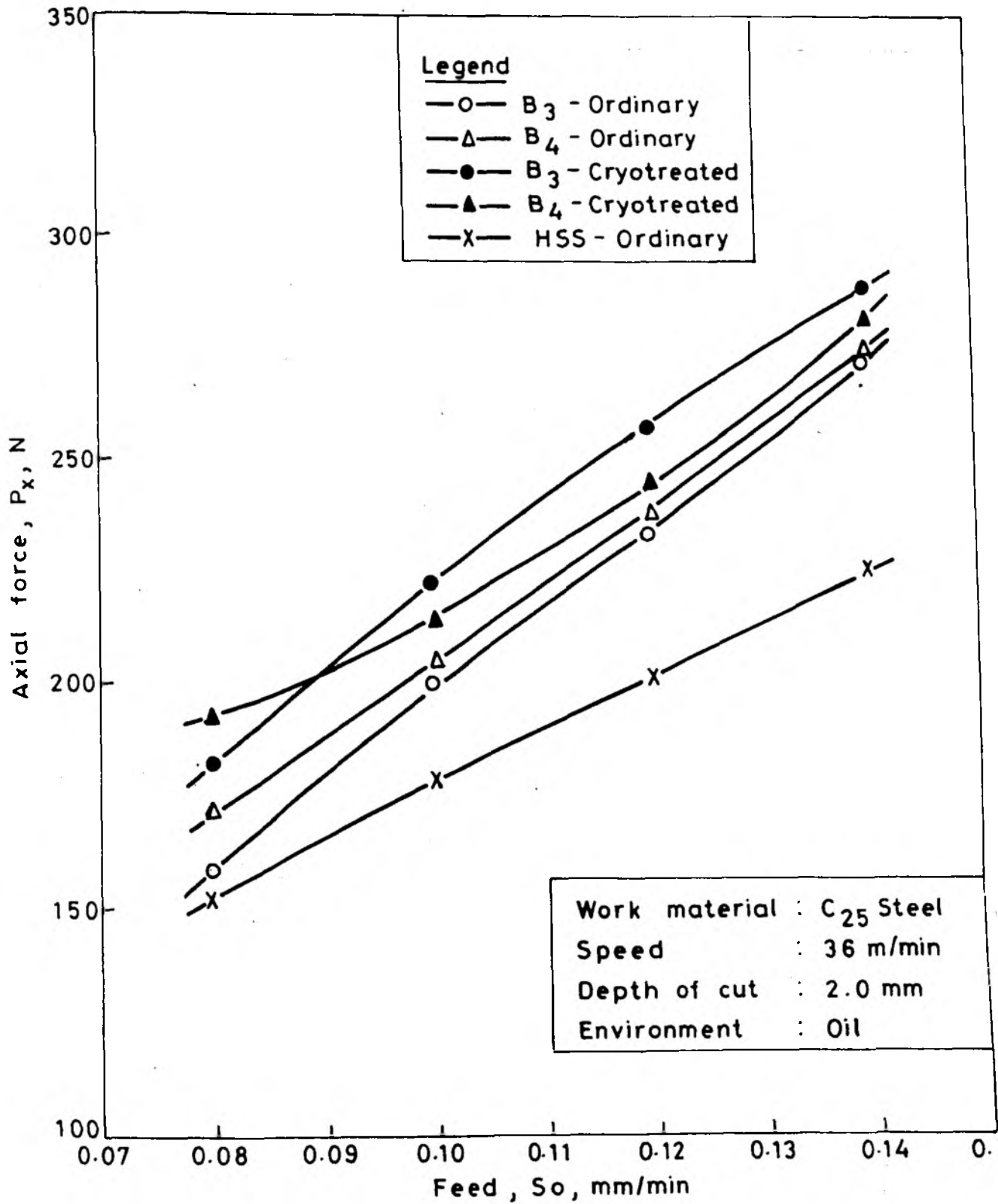


FIG. 4.55. INCREASE IN AXIAL FORCE WITH FEED AT SPEED 36 M/MIN: FOR DIFFERENT TOOLS

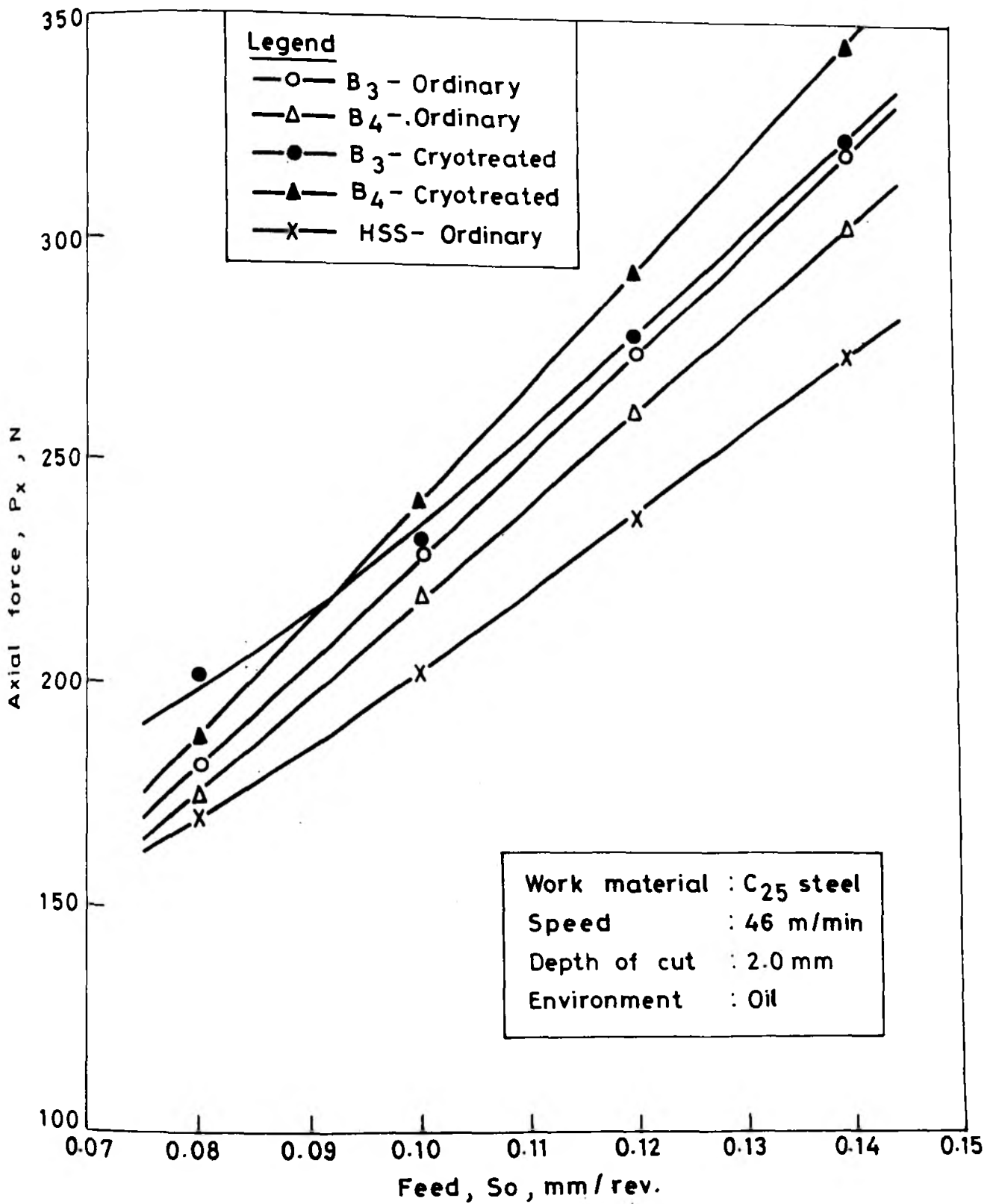


FIG. 4.56. INCREASE IN AXIAL FORCE WITH FEED AT SPEED 46 M/MIN FOR DIFFERENT TOOLS

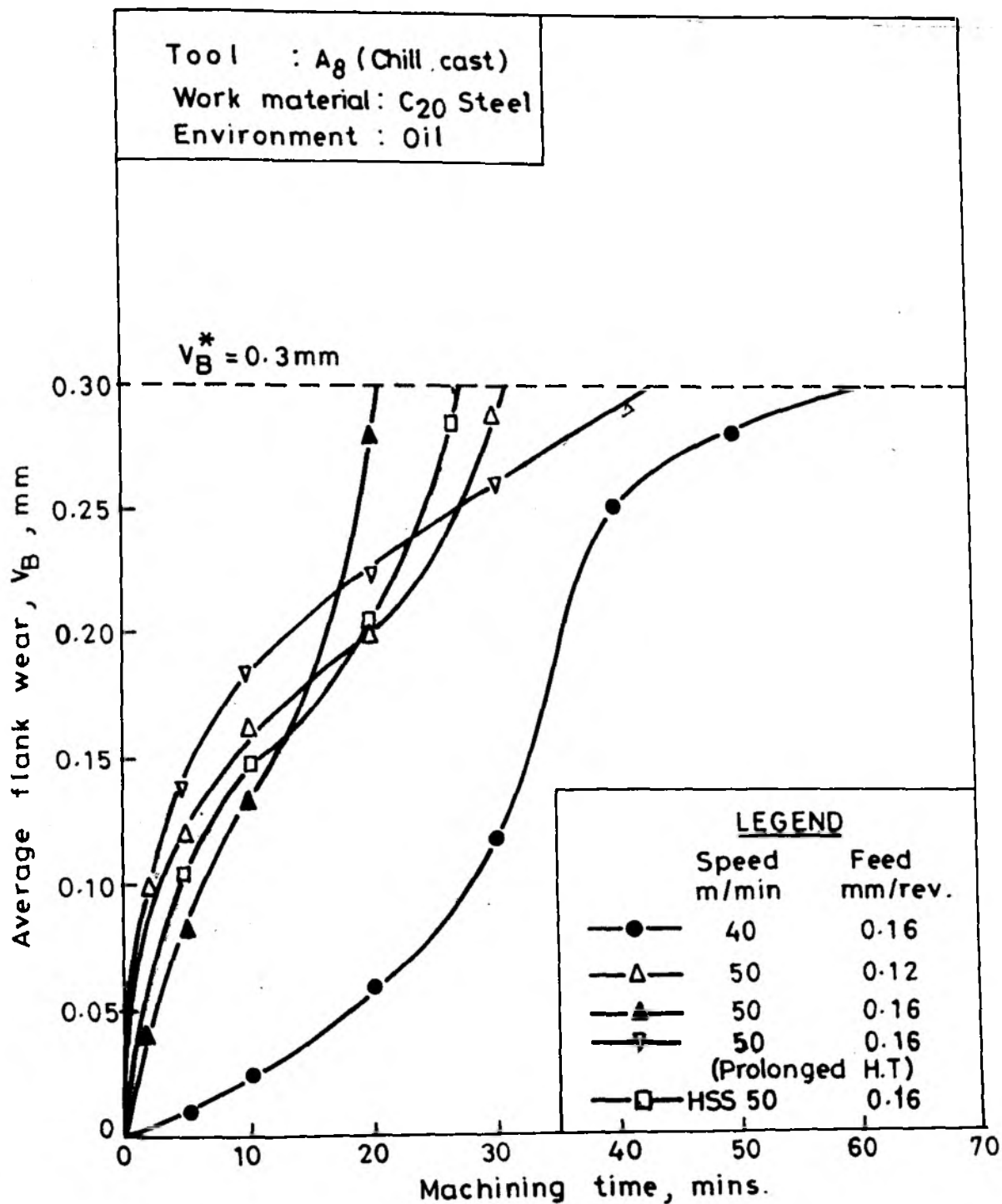


Fig. 4. 57. Growth of flank wear with machining time at different speeds and feeds

## DISCUSSIONS

### 5.1 Metallurgical Aspects

The results presented in the previous section may be discussed under the following broad heads

- (1) As cast structure and carbide morphology
- (2) Response to heat treatment and the associated transformations.

#### 5.1.1 As cast microstructure and carbide morphology

The basic composition of the A series alloys could not be controlled within a narrow range. Extensive segregation of alloying elements, particularly chromium, contributed to further variation of microstructures in the test samples. It is, therefore difficult to characterise the various modes of eutectic solidification reported in Section 4.1.2, in terms of alloy composition. The matrix in each of the alloy in this series was however predominantly pearlitic.

The variety of eutectic morphologies observed in irons of hypoeutectic and near eutectic compositions (Fig. 4.1 (a-f) appears to be a consequence of severe macrosegregation. Representative microanalysis data in Table 4.4 also provide an idea of the severity of macrosegregation possible even in small test pieces (15cm x 15cm cross section). The formation of eutectic colonies have been studied in details by Matsubara et al. The morphological features of the two types of eutectic colonies reported in

Fig. 4.1 generally tallies with those described by Matsubara (25&26). However, unlike that in Matsubara's unidirectionally solidified ~~samples~~<sup>samples</sup>, simultaneous occurrence of two or more types of eutectic carbides have been observed in the samples examined in the present investigation.

The effects of the alloying elements on the phases present in as cast state may be discussed in relation to Cr/C ratio. The A series alloys had a much lower Cr/C ratio than the B series alloys. The retained austenite content in the A series alloys were naturally lower. This is in conformity with the observation of other investigations (47). However, the large vol.% of austenite present in B<sub>3</sub>, B<sub>4</sub>, C<sub>1</sub> and C<sub>2</sub> may be attributed directly to the known influence of manganese and nitrogen as austenite stabilisers. The results further suggest that retained austenite contents in nitrogenated samples of A series alloys was influenced by the level of titanium present. Alloys A<sub>1</sub>, A<sub>2</sub> and A<sub>4</sub> had titanium levels less than 0.1%. When the titanium content was low (0.03%) as in alloy A<sub>1</sub> and A<sub>2</sub>, the retained austenite content increased on addition of nitrided manganese from 21% - 30%. On increasing the titanium level to 0.08% (A<sub>3</sub>) it decreased again to 23%. However, when the titanium levels were higher (0.66% in A<sub>7</sub>), the austenite stabilisation on combined addition of nitrogen and titanium was found to be even less. In fact, the retained austenite content decreased from 20% in alloy A<sub>6</sub> to only 4% in alloy A<sub>7</sub> on raising the titanium level from 0.08 to 0.66%. This trend is only to be expected, because titanium forms refractory carbides and carbonitrides which precipitate out long before the onset of

solidification. The rod like precipitates of cubic cross section observed in the electron micrographs (Fig. 4.24e for example) indeed appear to be a refractory carbide or carbonitride. These precipitates extended over both the dendritic and interdendritic phases confirming that their precipitation occurred before other phases began to form. In XRD also occasionally  $\text{TiC}$  and  $\text{Ti}_2\text{N}$  could be detected even in cast samples (Table 4.2). The consequence of such precipitation is to deplete the matrix in carbon and nitrogen. Hence retained austenite content naturally decreased. In the B-series alloys, apparently an opposite trend was noted. Retained austenite content increased from 8% in alloy  $B_2$  (0.01% Ti) to 16% in alloy  $B_3$  (0.21% Ti) to 30% in alloy  $B_4$  (0.39% Ti). The manganese contents in all the alloys referred to above were more or less same. Apart from the influence of a higher Cr/C ratio, no other explicit cause of such difference is available from the present set of data. This aspect shall require further investigation.

A comparison of the Fig. 4.24b with Fig. 4.24d however clearly illustrates the presence of very fine precipitates in the matrix of sample  $B_3$ . From a combined scrutiny of this information with the data available in Table 4.2, it is likely that these precipitates are various carbides and carbonitrides formed due to alloying with nitrogen and titanium. Electron microprobe analysis results on  $B_4$  (Fig. 4.11b) also reveal precipitation of Ti-N compound. The EPMA photographs however confirms that sufficient nitrogen and titanium remain in solid solution as well.

Titanium has been used as a grain refiner in austenitic stainless steels. It was reported that the addition of titanium and nitrogen together promotes columnar to equiaxed transition in austenitic stainless steels (136). Titanium addition has been quoted to be responsible for grain refinement in cast irons as well (1,48). This aspect has been verified in the present investigation, particularly in the case of B-series alloys. A comparison of the SEM photographs of as cast alloys  $B_1$  -  $B_3$  (Fig. 4.10 (a-c)) reveals a tendency towards dendritic to equiaxed transition. A similar evidence was also obtained in respect of  $C_1$  and  $C_2$ .

Claims were made in the past that titanium addition refined carbide morphology (24). Nitrogen addition has also been observed to be effective in modifying carbide morphology in vanadium containing cast irons (43). In the present investigation, titanium has been added in conjunction with nitrogen. Carbide morphology became partially discontinuous with rod like growth pattern in some of the A series alloys (Fig.4.4). Previously such rod like growth of eutectic carbide were observed in hypereutectic alloys of higher ( 15% Cr) chromium iron only (120). In the B series alloys a typical pattern of dendrite branching with the dendrite arms having well defined crystalline facets have been observed (Fig. 4.9). Hence it appears that nitrogen and titanium do influence carbide morphology, but the extent of modification is influenced also by Cr/C ratio. Future experiments may attempt to characterise the effect of dose of addition of N and Ti in greater details.

### 5.1.2.1 Destabilisation heat treatment

The heat treatment experiments carried out on the present series of alloys have highlighted the distinctive characteristics of chromium cast irons. It is well known that retained austenite in chromium cast irons is destabilised during homogenisation in the temperature range  $900^{\circ}\text{C} - 1100^{\circ}\text{C}$  and the term has been referred to as destabilisation by Maratray(9). The phenomenon of destabilisation has been confirmed in the present series of investigation as well. But simultaneously some new observations have been made. These observations may be summarised as follows:

1. Destabilisation of austenite results in the precipitation of  $\text{Cr}_{23}\text{C}_6$  type carbide.
2. In nitrogen containing alloys, the retained austenite content increases on prolonging the soaking period, although simultaneous precipitation of  $\text{Cr}_{23}\text{C}_6$  type carbide continues. The net increase in hardness initially is positive, but thereafter hardness becomes constant.
3. There is a gradual transformation of the  $\text{Cr}_{23}\text{C}_6$  type eutectic carbide into  $\text{Cr}_7\text{C}_3$  carbide in the nitrogen containing alloys. In one case of prolonged soaking for 7 hours at  $950^{\circ}\text{C}$  (Alloy A<sub>8</sub>),  $\text{Cr}_{23}\text{C}_6$  type carbide was totally eliminated. In the nitrogen containing alloys an actual increase in the retained austenite content occurred on homogenisation at  $900^{\circ}-950^{\circ}\text{C}$  for 3-4 hours.
4. On cryotreatment, the retained austenite is converted to martensite.
5. Addition of nitrogen or nitrogen plus titanium renders the alloys air hardenable. The base 12% Cr cast iron however can

not be hardened only by air quenching. This was established by TMA and actual quenching experiments.

The points mentioned above have been discussed further with reference to specific experimental results. A comparison of the X-ray diffraction patterns of the alloys in the as cast state and after quenching, or quenching and tempering suggest that  $\text{Cr}_2\text{C}_6$  carbide is precipitated during destabilisation. The diffraction patterns of  $A_8$  and  $C_2$  (Fig. 4.15 (a-c), 4.16 (a-b) clearly illustrate this point.  $\text{Cr}_2\text{C}_6$  peaks became stronger on continued heat treatment. The electron micrograph of an as quenched sample of  $A_1$  (Fig. 4.22a) clearly show the precipitation of secondary carbide phase in the matrix. In the sample containing nitrogen and titanium, the precipitates were much finer Fig. 4.22(c-d). The retained austenite data summarised in Table 4.3 show that the retained austenite content in the A series, particularly in  $A_7$  and  $A_8$ , increased on continued soaking in the temperature range 900-950°C. The data in Table 4.3 further report that  $\text{Cr}_{29}\text{C}_6$  carbide in  $A_8$  gradually transformed to  $\text{Cr}_7\text{C}_3$  carbide on prolonging the soaking period to 7 hours at 900°C. It is likely that diffusion of carbon and chromium occurs from the eutectic carbide into austenite during homogenisation treatment. As the austenite gets saturated in these elements, simultaneous precipitation of secondary chromium carbide also occurs. It is further likely that the eutectic  $\text{Cr}_{29}\text{C}_6$  carbide loses chromium and carbon, being depleted and gradually converted into  $\text{Cr}_{17}\text{C}_3$  carbide in 12% chromium cast irons. Enrichment of the matrix with respect to chromium and carbon increases its stability, while

precipitation of secondary carbide decreases it. In the competition between these opposing stabilising and destabilising factors, the most crucial factor is the time of soaking. Transmission electron microscopic evidence of  $\text{Cr}_7\text{C}_3$  -  $\text{Cr}_{23}\text{C}_6$  transition in 30% Cr was presented earlier by Pearce(70). Several replica electron micrographs of the present series of alloys show the presence of a second phase around primary and secondary carbide, as reported in section 4.1.7. The present XRD data however provide evidence of the reverse  $\text{Cr}_{23}\text{C}_6 \rightarrow \text{Cr}_7\text{C}_3$  transition. The initial rise in hardness due to increase in soaking time noted in Fig. 4.12 is actually due to the hardening effect of well dispersed secondary carbide particles in the matrix. It is likely that some of the carbides, nitride and carbonitride particles redissolve in austenite during homogenisation. Nitrogen and manganese are strong austenite stabilisers. Dissolution of nitrogen and manganese in austenite further stabilises it which in turn favours further carbon diffusion. As a result, the retained austenite content rises on continued homogenisation. The effect of homogenisation time on the retained austenite contents in B and C series alloys were not investigated. However, the effect are likely to be identical. Cryotreatment after oil quenching reduced retained austenite content in  $B_1 - B_4$  (Table 4.3).

#### 5.1.2.2 Tempering

Both isothermal and isochronal tempering experiments on as cast and as quenched alloys have indicated a secondary hardening peak at  $600^\circ\text{C}$  in alloys containing N + Ti or N + Al. This part of the investigation was of course

carried out on alloys containing very low levels of Ti or Al. But the conspicuous hardening effect observed in the tempering curves confirm the influence of N + Al or N + Ti combinations on tempering behaviour. XRD data (Table 4.2) point out the possibility of precipitation of AlN or  $Ti_2N$  phases during tempering at  $600^\circ C$ . Basak (47) et al. had reported a hardening peak in their chromium cast iron samples at  $500^\circ C$ . They attributed it to decomposition of retained austenite. In the present series of alloys no such secondary hardening was observed at  $500^\circ C$ .

The two stage electron replica micrographs of the as quenched and tempered specimens, though of limited value in the context of the present level of knowledge of tempering characteristics of Fe-C and Fe-C-N alloys, highlight some basic differences in the tempering behaviour of the base chromium cast iron and the nitrogenated alloys. For example, the martensitic structure in the nitrogenated sample ( $A_4$ ) (Fig. 4.22b) was distinctly different from that of the base alloy  $A_1$  (Fig. 4.22a). After tempering at  $200^\circ C$ , precipitate particles in the nitrogenated samples ( $A_4$  and  $A_7$ ) were observed to be very finer (Fig. 4.22 c-e). The higher magnification electromicrographs illustrate the differences in the precipitate morphology further. Compared to the coarser spheroidal, rod shaped or oblong particles in  $B_1$  (4.25a) the particles in  $B_3$  were of irregular shape and finer dispersion (4.25b). The electromicrographs of samples tempered at  $600^\circ C$  however suggest that chromium cast irons also conform to certain general tempering characteristics of Fe-C alloys irrespective of alloy composition. For example, the

gradual globularisation and coalescence of particles is a common feature of the tempering characteristics of Fe-C alloys (Fig.4.23(a-c)). The precipitation of  $Ti_2N$  or AlN on tempering at  $600^\circ C$ , as detected by XRD in  $A_3$  and  $A_4$  respectively (Table 4.3) could not be identified in two stage replica electron micrographs.

## 5.2 Corrosion Characteristics

High chromium cast irons containing 0.5-2.0%C and 20-28% Cr offer a useful compromise between the resistance to corrosion and abrasion [20]. These irons are cheaper than Ni-hard irons and are often used as moderate to thin section casting such as pump volutes and impellers.

The 12% Cr cast irons though sufficiently abrasion resistant are generally not very attractive for application involving combined erosion and corrosion. Nitrogen additions to austenitic stainless steel casting are reported to improve their corrosion resistance in saline water. In the present investigation, nitrogen addition (as nitrided manganese) had rendered as cast 12% Cr cast irons completely austenitic in the Alloys  $C_1$  and  $C_2$ . Hence it was considered appropriate to assess the corrosion resistance of these irons in the as cast condition. Although evaluation of combined erosive-corrosive wear is essential for potential applications in wet grinding and in slurry transportation systems, as a first step, it was decided to test the corrosion and dry abrasive wear characteristics of these alloys separately. A study of the passivation characteristics of alloys in specific media by means of a potentiostat is a quick and reliable method of evaluation of their corrosion behaviour - particularly

pitting and crevice corrosion characteristics. Therefore the passivity of the base 12% chromium cast iron  $A_1$  and the nitrogenated alloys  $C_1$  and  $C_2$  were compared - all in as cast condition- in 1N HCl and 1M NaCl solutions using a potentiostat.

In 1N HCl solution, the passive region is found to be largest for the  $A_1$  and minimum for alloy  $C_1$  (Fig. 4.26a). Addition of a small amount of titanium in  $C_2$  reduced the current density at which the passive layer formed. The base chromium cast iron  $A_1$  developed passivity at lower current density than  $C_1$  and  $C_2$  but the durability of the passive film was more or less similar (Fig. 4.26b). On the balance, therefore the pitting resistance of the chromium cast irons  $A_1$ ,  $C_1$  and  $C_2$  in 1M NaCl solution are nearly similar.

### 5.3 Wear Behaviour

The abrasive wear behaviour of chromium cast irons has been investigated in various ways by different groups of investigators(3,48,71,78-84). The test procedure adopted in the present investigation is basically a modification of the pin-on-disc process. Instead of the conventional hardened disc, a bonded alumina grinding wheel has been used (142). The grits in the wheel cut into the wearing surface producing a micromachining effect. Under the applied load (0.5 Kg - 1.5 Kg. only), the abrasive alumina particles cut into the specimens producing deep grooves which were clearly visible. Hence, the test condition may be treated as one of high stress abrasion. Since no impact force was applied, the test condition may not be regarded as one of gouging abrasion.

An analysis of the wear test results has clearly established the differences in the behaviour of the plain chromium cast irons from those containing nitrogen alone or nitrogen + titanium together. The principal observations may be grouped as follows:

(1) alloying with nitrogen + titanium contributes to improved wear resistance, when the retained austenite content is maintained at low level (10%). Cryotreatment in liquid nitrogen is beneficial for improving wear resistance.

(2) retained austenite, in itself, may not be always harmful. In certain alloys containing appreciable vol% retained austenite wear resistance actually improved at intermediate loads. At a higher load, of course, the wear resistance deteriorated again. Hence on wear resistance the influence of retained austenite content has to be evaluated with reference to the applied load.

(3) Alloys of the B-series having higher Cr/C ratio had undergone lesser wear than the alloys of A-series having lower Cr/C ratio.

The above observations may be discussed with reference to specific results. From Fig.4.31(a&b) and 4.38 it may be noted, that the cryogenic treatment reduced both total wear and wear rate in the B-series alloys in the order  $B_1$  ---  $B_2$  ---  $B_3$ . The metallurgical variables in the alloys under investigation may be classified as follows:

(1) The A series alloys ( $A_1, A_2, A_6$  and  $A_7$ ) had higher carbon contents and consequently greater vol% carbide than those in B series ( $B_1, B_2, B_3$ ) and C series ( $C_1, C_2$ ) alloys.

(2) The retained austenite contents in  $A_7, C_1$  and  $C_2$  were

appreciably higher than those in other alloys.

(3) Secondary carbide size was finer in alloys containing nitrogen alone or nitrogen + titanium together than that in the base alloys ( $A_1, B_1$ ).

(4) X-ray diffraction analysis had provided evidence of formation of complex carbonitrides and nitrides in some of the quenched and tempered alloys ( $B_3$ , since nitrogen has very little solubility in  $\gamma$ -irons, it is likely that nitrides and carbonitride precipitation had occurred in all the alloys containing nitrogen.

The differences in the wear behaviour of the experimental alloys may be interpreted with reference to the above metallurgical variables.

Bulges appeared on the sample surface. Occasionally cracks also formed. (Fig. 4.42 & 4.43). Transformation of retained austenite to martensite causes volume change and cracking. The bulges and cracks are believed to be the consequence of such martensitic transformation under load. The presence of micro shrinkage forces facilitated initiation of cracks.

However, retained austenite in itself may not be a desirable phase in wear resistant material. The wear data on alloy  $A_6$  and  $C_2$  clearly supports this premise. The heat treated wear test specimen of both these alloys contained a very high vol% (37%) retained austenite. Hence, inspite of a possible martensitic transformation, the total wear as well as the wear rate were high. Except for titanium content (0.09%), both alloys  $C_2$  and  $C_4$  had similar compositions and high retained-austenite contents. In spite of such

similarity,  $C_1$  was found to be more wear resistant than  $C_2$ . In  $C_1$  and  $C_2$  the maximum wear under 14.7N load was as widely different as  $11.00 \times 10^4$  ( $\text{gm/mm}^2$ ) and  $34.00 \times 10^4$  ( $\text{gm/mm}^2$ ) respectively. The reason is not understood at this stage. On the other hand; the total wear decrease after cryotreatment by 20-25% in the B-series alloys due to reduction in retained austenite content. In  $B_2$  nitrogen was added as nitrided manganese. In  $B_3$  nitrided manganese and titanium were added together. The results demonstrate that such additives may improve the wear resistance, when the retained austenite content is not large and the hardness is not lowered significantly. The SEM photographs of the wear cracks in these alloy (Fig.4.41(a-c)) clearly show the wear marks in  $B_1$  and  $B_2$  were deeper than those in  $B_3$ . This is a direct evidence of the superior wear resistance of  $B_3$  to  $B_1$  and  $B_2$ .

The exact influence of retained austenite content on the wear resistance was more explicit in case of A and C series alloys. In the base alloy  $A_1$ , the total wear increased with increasing load. In  $A_2$  it increased initially, on increasing the load from 4.9N to 9.8N, but later it dropped sharply at 14.7N load (Fig.4.35). In  $A_6$  &  $A_7$ , the total wear under 4.9N and 9.8N loads were nearly equal. But the total wear increased again under 14.7N load. In  $A_7$ , the wear rate also increased at this load but in  $A_6$ , the wear rate actually decreased to some extent (Fig.4.36). A nearly similar behaviour was noted in case of alloy  $C_2$  (Fig.4.40). These results suggest that two opposing phenomena are at play simultaneously. On the one hand the softer austenite matrix tends to wear out faster, than a tempered martensite matrix,

on the other hand, greater work hardening of the austenite matrix contributes to improved wear resistance. The hardening of the austenite is most certainly the effect of its strain induced transformation to martensite. Direct TEM evidence of such transformation was reported earlier. Several other authors have also reported such possibility.

The wear rate plots in most cases show a sharp drop after initial sliding. This is the likely effect of work hardening of the matrix. The reported instances of such work hardening was reviewed by Patwardhan (53). In the present experiment, the wearing surfaces was so severely abraded by the alumina wheel, that the worn out surface could not be polished without the risk of removing an appreciable depth of metal. Hence the extent of workhardening could not be measured. The SEM photograph in Fig.4.44 indicate that both the matrix and the carbide phases had worn out during the test. In fact Fig.4.43 suggests that the carbide phase had undergone deformation and fracture as well during the test. But the fractured carbide particles were still held in position by the hard tempered martensitic matrix. Similar instances of bending and fracturing carbide particles during wear test was observed by Pearce(70). Uniform distribution of finer secondary chromium carbide particles and the precipitation of nitride and carbonitride particles in the matrix should normally contribute to improved wear resistance. Except in case of B series of alloys, wear resistance did not improve on alloying with nitrogen alone or nitrogen and titanium together. Both nitrogen and manganese are austenite stabilisers. Possibly the detrimental effect of

retained austenite prevailed over the beneficial effects of nitrogen and titanium in A and C series alloys. The interaction between these contradictory effects needs further indepth study.

#### 5.4 Evaluation of CWCI tools in turning experiments

The results of machining trials reported in section 4.3 may be analysed in the light of following metallurgical factors:

- (1) chemical composition and microstructures
- (2) heattreatment, retained austenite contents and phases present
- (3) wear and failure machanisms in tools (130)
- (4) deformation and cracking in chips (133).

The tools made from A series alloys performed poorly in machining trials. On careful observations of the failure modes, it was found that the tools failed by brittle fracture (Fig.4.48). The cracks initiated from the microshrinkage pores present in the sand cast samples. The chill cast sample A<sub>8</sub> on the other hand performed much better in this case. Very few micropores were present in this tool because of better feeding and faster solidification. In the A series alloys, carbon contents were high - as high as 3.9% in some cases. The Si content also were generally in the higher side. In order to reduce microporosity in sand cast samples, the B series alloys were designed to have lower carbon and silicon contents and a higher Cr/C ratio. In fact, the carbon content in the B series alloys did not exceed 3.0%. A minimum Cr/C ratio of 4.0 was maintained. Si content could not be reduced much because of the higher Si content in the

ferro-chrome itself. However, the C content of 3.0% brought down the Carbon Equivalent value to about 3.3 (compared to 4.2 in A series alloys).

The effect of this compositional change on the tool life of B series alloys was favourable. The sand cast tools prepared from the B-series alloys performed much better than the tools made from A series alloys (Table 4.7). The shorter tool life of the sand cast B series tools compared to that of the standard HSS tool can be attributed to

- (1) the presence of interdendritic micropores and hence lack of adequate toughness
- (2) inadequate hardness
- (3) other possible complex factors like BUE formation tendency, diffusion wear etc.

The cast tools with interdendritic shrinkage pores naturally lacked toughness. Fig. 4.48 a shows how cracks were initiated from micropores. However, chromium cast irons have certain plus points also as tool materials. The high volume of hard eutectic carbide (25-30%) in the cast irons contributed to its wear resistance. In the present experiment, nitrogen and titanium were added as additional alloying elements which in turn contributed to the formation of finely dispersed hard nitride and carbonitride phases (Table 4.2). The presence of finely dispersed particles could be seen even in as cast state on examination under TEM (Fig. 4.24 a&b). The influence of these precipitate phases in improving the abrasive wear resistance of B<sub>2</sub> and B<sub>3</sub> alloys have already been reported in section 5.2. In conformity with the results of abrasive wear tests, the tools made from the

$B_3$  and  $B_4$  performed much better than those made from the plain chromium cast iron ( $B_1$ ) during machining. Cryotreatment to reduce the retained austenite contents affected tool life due possibly to a reduction in shock resistance. A secondary hardening phenomenon associated with the precipitation of  $Ti_2N$  phase during tempering at  $600^\circ C$  has been observed in an alloy containing N and Ti (Fig. 4.19, Table 4.2). However, rapid shortening of the tool life at higher speeds and feeds suggest that no benefit of such a hardening phenomenon could be derived during the cutting trial. The rise in temperature at the cutting tip of the tool therefore merely caused overtempering and consequent softening. The evidence of plastic flow in the cutting edge of tool as revealed in Fig. 4.48 also support such a possibility.

A scrutiny of the tool life data of the A and B series tools further highlights the role of retained austenite contents in determining the tool life. The retained austenite content in tool  $A_8$  increased to a very high level after 4 hours soaking at  $900^\circ C$ . On further extending the soaking period to 7 hours, the retained austenite content decreased to 29%. Such differences in the retained austenite was directly reflected in the service life of the  $A_8$  tool (Fig. 4.57). At 50 m/min. speed and 0.16 mm/rev. feed, tool life increased by 100% on reduction of the retained austenite content. In fact, it superseded the HSS tool in performance. In the B-series tools on the other hand a reduction of retained austenite content to very low levels (2-5%) again reduced tool life in most of the trials. Thus, both very high as well as very low retained austenite contents in chromium

cast iron tools are undesirable. A high retained austenite content reduces tool hardness and probably enhances adhesion and diffusion wear of the tools, while tools having very low retained austenite content lack necessary toughness.

The SEM photographs in Fig. 4.46 (a-i) enable a comparison of the relative plastic flow and microcrack formation tendency in the chips formed by different tools. The influence of microcracks is generally to lower the bulk flow stress of the work material. In the present experiment, the chips formed by the HSS tool had undergone greater deformation and lesser cracking than those generated by the chromium cast iron tools. Among the chromium cast iron tools, the cracking tendency increased in the order  $B_1$ --- $B_2$ --- $B_3$ --- $B_4$ . Cryotreatment to reduce the retained austenite content further increased the cracking tendency (Table 4.6). All these tools had shown a varying tendency for built up edge formation (BUE). Since a detailed study was not done on the BUE formation, it is difficult to correlate the severity of BUE formation with the retained austenite content in the tools.

The adverse effect of BUE formation in promoting attrition wear as investigated by Trent (139). BUE formation observed in most of the tools including HSS is the result of localised seizure at the chip/tool interface. The BUE is a dynamic structure, being constructed of successive layers greatly hardened under extreme strain conditions (139). The BUE are of two types, stable and unstable (140). It has been argued that unstable BUE is detrimental to both the life of the cutting tool and the quality of the machined surface. The

chromium cast iron tools exhibited the tendency of unstable BUE formation. Since the total alloy content in the tools was very high, it is very likely that the seizure of the chip was caused by diffusion of carbon and chromium, specially from the retained austenite. In such a situation it is very likely that the extent of BUE formation is influenced by the volume fraction of retained austenite in the tool material at a particular cutting condition.

A correlation of chip crack density data (Table 4.6) with the data on retained austenite content in tools (Table 4.3) would suggest that the crack density in the chips increased with decrease in retained austenite content in the tools at a particular cutting condition. However, further investigation will be necessary to establish the complex relation among retained austenite content in the tool, BUE formation tendency and microcrack density in carbon steel chips.

## CONCLUSIONS

1. Nitrogen may be conveniently added to chromium cast irons as nitrided manganese (5-6% N), nitrided chromium (5-6% N) and also as  $K_4Fe(CN)_6$ .
2. Nitrogen (added as nitrided manganese or nitrided chromium) and titanium additions to 12% chromium cast irons partially modifies the eutectic carbide morphology to discontinuous rods in sand cast alloys having Cr/C ratio in the range of 2.9 to 3.5. A completely discontinuous mixed rod and blade morphology is obtained on chill casting a nitrogenated alloy of Cr/C ratio 4.1.
3. In sand cast 12% chromium cast irons of chromium /carbon ratio greater than 4.1, the eutectic carbide is primarily of  $Cr_7C_3$  type. When the chromium carbon ratio is in the range of 2.9 to 3.6, both  $Cr_7C_3$  and  $Cr_{23}C_6$  type eutectic carbides precipitate. In addition to  $Cr_7C_3$  and  $Cr_{23}C_6$  types of carbides, the presence of complex carbonitrides have also been detected in as cast nitrogenated samples. TEM studies on two stage replicas also indicate the presence of fine precipitates in the matrix of an alloy containing nitrogen and titanium together.
4. On thermal treatment in the temperature range  $900^\circ C$  to  $950^\circ C$ , secondary carbides of  $Cr_{23}C_6$  composition precipitate due to destabilisation of austenite. In nitrogenated samples, however, the retained austenite content may actually increase after quenching and tempering

- treatment if the soaking period at 900°C to 950°C is unduly prolonged.
5. A  $\text{Cr}_{29}\text{C}_6 \rightarrow \text{Cr}_7\text{C}_3$  type transformation takes place during soaking at 900°C in a nitrogen bearing chill cast sample of Cr/C ratio 4.1.
  6. Secondary carbide and other precipitates are finely dispersed in quenched and tempered (at 200°C) chromium cast irons containing nitrogen alone or nitrogen + titanium together. On tempering at 600°C, coarsening of the precipitates occur. A secondary hardening effect associated with precipitation of TiN or AlN has also been noted in samples containing N+Ti or N+Al respectively upon tempering at 600°C.
  7. Plain 12% Cr cast irons do not transform to martensite on forced air draft quenching from 950°C. Nitrogenated chromium cast irons are however air hardenable.
  8. The corrosion resistance of an as cast pearlitic 12% Cr cast iron in 1N HCl solution and 1M NaCl solution is marginally superior to that of as cast austenitic irons alloyed with nitrided manganese alone or nitrided manganese and titanium together.
  9. The abrasive wear resistance of heat treated chromium cast irons subjected to sliding against a bonded alumina wheel under load improves upon alloying with nitrogen (added as nitrided manganese) and titanium together provided the retained austenite content is maintained around 10% or less. When addition of nitrided manganese stabilises a high percentage of retained austenite (around 40%) both total wear and wear rate increase sharply.

10. Workhardening and strain induced transformation of retained austenite also improves wear resistance. But the actual benefit of this phenomenon depends upon the retained austenite content and the applied load.
11. A chill cast nitrogen bearing chromium cast iron tool may perform better than a standard HSS tool under identical condition of turning a 0.25% C steel bar, provided the retained austenite content in it is maintained around 20% by appropriate heat treatment.
12. Sand cast tools of similar composition as above suffer premature brittle failure during service due to initiation of cracks from microshrinkage pores.
13. The hardness and retained austenite content in chromium cast iron tools directly influence the crack density and the extent of deformation in 0.25% carbon steel chips machined out under identical condition.
14. A strong tendency of built-up-edge (BUE) formation has been observed during machining of 0.25% C steel with chromium cast iron tools. A HSS tool shows lesser tendency of BUE formation under identical machining conditions. The lower hot hardness of chromium cast iron tools is believed to be partially responsible for their enhanced BUE formation tendency.
15. The study has clearly established that nitrogen and titanium are potentially powerful alloying elements for chromium cast irons. The service performance of nitrogenated chromium cast iron components and cutting tools can be further improved by appropriate control of casting defects and heat treatment.

## REFERENCES

1. Roy. Elliott, "Cast Iron Technology" Butterworths, 1988, pp. 31-45.
2. U.S. Patent No. 1,245,552, No. 6, 1917.
3. Laird. G. 11. "Nihard 4 Revisited" AFS Trans. 1988.
4. J. Dodd, "Trends in the Production, Utilisation and Development of Abrasion-resistant alloys in America (Climax Molybdenum CO) and Iron & Steel Engineer, 1982, 59(3), p. 53.
5. R.W. Durman, British Foundryman, 1976, 69(6), p. 141.
6. British patent 727,061, 1952.
7. U.S. Patent, 3,410,682. 1968.
8. L.M. Hogan, "Invited introduction on cast iron" Metals Forum, 3(1) 1980, pp. 1-2.
9. F. Maratray "Improvement of and research into new abrasion resistant materials" Metals Forum 3(1) 1980, pp. 28-36.
10. R.S. Jackson, J. Iron & Steel Inst., 208, 1970, pp 163 - 167.
11. R. S. Jackson, "Metallurgical and Production aspects of high chromium cast irons for abrasion resisting application: British Foundryman, 1974, (Conf. paper) pp. 34-41.
12. T. Srinivasan, A.K. Patwardhan and M.L. Mehta. "Effect of Mn and Cu additions on microstructure of chromium white C.I." AFS, ICM Journal, March 1977, pp. 57-60.
13. A.S. Sudan, M.L. Mehta and A.K. Patwardhan, "Evaluation of the role of Cu as an additive to a CWCI for producing a

- wear resistant microstructure" AFS ICM Jr. March 1980. pp. 42-46.
14. I. Chakraborty and A. Basak, " Structural study of Cr-Mn-Cu white cast irons". Jr. of Mat.Sc.letters, 6, 1987, pp.1399-1402.
  15. I. Chakraborty, A. Basak and U.K.Chatterjee, " Corrosive wear behaviour of CMCu WCI in sand-water slurry media", Wear, 143, 1991, pp. 2-3-220.
  16. R.G.Ward, " An introduction to the physical chemistry of Iron & Steel making, Arnold, 1965, p.177.
  17. G. Hoyle, " High speed steels", Butterworths, 1989.
  18. C. Podrzucki, Wojtysiak, Taber and Wojniak, " Influence of nitrogen on the structure and properties of the chilled layer in the abrasion - resisting iron castings" 4th European Tribo Congress, France, September 1985.
  19. L. Rongde, Y. Jingxiang and Y. Haipeng, " The effects of Nitrogen on solidification process of grey iron". AFS Trans, 1988, pp. 423-430.
  20. G.J.Cox, " Developments in alloy cast irons" British foundryman, 76, September, 1983, pp. 129-144.
  21. H.K.Baik and C.R.Loper, Jr. " The influence of Niobium on the solidification structure of Fe-C-Cr alloys" AFS trans. 80, 1988, pp. 405-411.
  22. J. Dodd, J.L.Parks, " Factors affecting the production and performance of thick-section high Cr-Mo alloy iron castings" Metals Forum, 3(1), 1980, pp. 3-27, and AFS, ICM Journal, September 1980, pp. 47-54 and December 1980, pp. 15-25.
  23. F. Maratray, " Choice of appropriate compositions for

- Cr-Mo white irons". AFS Trans, 17, 1971, pp. 121-124.
24. A. Sawamoto, K. Ogi and K. Matsuda. " Solidification structures of Fe-C-Cr (V-Nb-W) alloys", AFS trans, 72, 1986, pp.403-416.
  25. Y. Matsubara, K.Ogi and K. Matsuda. " Eutectic solidification of high Cr-cast iron-Eutectic structures and their quantitative analysis". AFS trans., 1981, 72, pp. 183-196.
  26. K. Ogi , Y. Matsubara and K. Matsuda, " Eutectic soldification of high chromium cast iron -mechanism of eutectic growth", AFS trans. 1981, 71, pp. 197-204.
  27. W. A. Tiller, " Liquid metals and solidification". ASM, 1958, p. 276.
  28. K. A. Jackson and J.D.Hunt, Trans. Met. Soc. AIME, e36, 1966, pp. 129 and 843.
  29. G. A. Chadwick, " The solidification of Metals" The Iron and Steel Inst. London, p. 138, 1967.
  30. T. E. Norman, A. Soloman and D.V.Doane, AFS Trans, 67, 1959 , p. 242.
  31. D.E.Diesburg and Borik, " Optimising abrasion resistance and toughness in steels and irons for the mining industry" Symposium on Materials for Mining Industry, 1974, Vail, Colorado, U.S.A., p. 15.
  32. G.L.F. Powell, " Morphology of eutectic  $M_9C$  and  $M_7C_3$  in white iron castings" Metals Forum, 3(1), 1980, pp. 37-46.
  33. H.Morrogh and W.J.Williams, J.Iron and steel Inst., 155, 1947, p.121.
  34. W.J.Williams, B.C.I.R.A.J.: 1953, 5, p.132.
  35. J. Rickard and I.C.H.Hughes, B.C.I.R.A.J. 1961, 9, p.11.

36. A. Sawamoto and K. Matsuda, Imono (J.Jpn. Foundrymen's society) 1983, 55(7), pp. 412-418.
37. Japanese patent 47-18223, 1972, Showa.
38. G.X.Sun and C.R.Loper, Jr., "Titanium carbonitrides in cast irons" AFS Trans, 1983, 41, pp. 639-646.
39. Japanese patent, 49-106425, 1974, Showa.
40. W.Day Georgia Instt. of Technology, Diss. Abstr. Inst. B., Aug. 1982, 43(2), pp. 119.
41. U. K. Patent GB 2158462, 1984, GIW Industries Inc. and W.Day.
42. H.S.Young et. al. Q iu.Tie (J.Spheroidal C.I), 1978, (4).
43. Wang Chao Chang, Hus Heng Tsun and Ma Qian "Formation of spheroidal carbide in vandadium WCI by rare earth modification" Mat. Sc. and Tech. 6(9), September, 1990, pp. 905-910.
44. F. Maratray and R.Usseglio - Nanot. "Atlas - transformation characteristics of Cr and Cr-Mo white irons" Climax Molybdenum, S.A.France, 1971.
45. B.M.Hebbar, H.N.Lakshminarasimha and S. Seshan, "Heat treated high Cr. C.I. with superior abrasion resistance, Proceedings of 39th Annual Convention of I.I.F. Calcutta, India, 1990-91, pp. 406-413.
46. W.W.Cias, AFS trans. 1974, 82, p. 317.
47. A.Basak, J. Penning and J.Dilewijns, "Phase transformations om Cr-Mn white cast irons" Mat. Sc. and Technology, January, 1988, 4, pp. 22-33.
48. A.Basak, J. Penning and J. Dilewijhns," Effect of Ti inoculation on the wear resistance and impact strength of

- Cr-Mn alloy white C.I", Metals Technology, 9, September 1982, pp. 381-384.
49. L.S.Zhou, S.F.X.L.Songzhen, F.L.Xing and C.X.Bao, " The cryogenic treatment for tools and dies in fastner industry (in chinese) 1989, pp. 232-239.
  50. Rouns, T.N. Rundman, K.B.and Moore, D.M. " On the structure and properties of austempered ductile iron" AFS Trans., 92, 1984, p.815.
  51. X.H.Fan, L. He and Q.D.Zhou., " A study of high chromium cast iron on abrasion resistance and impact fatigue resistance", Wear, 138, 1990, pp. 47-60.
  52. K.H.Zum Gahr and D.V. Doane, " Optimizing fracture toughness and abrasion resistance in white cast irons", Metal trans. A. 11A. April 1980, pp. 613-620.
  53. A.K.Patwardhan, S.S.Singh and N.C.Jain, " Fundamental considerations in the design of heavy duty abrasion resistant cast irons", Tool and Alloy Steels, Aug, 1987, pp. 305-313.
  54. A. K. Patwardhan, S.S.Singh, and N.C.Jain, " Design conbsideration and applications of abrasion resistant white cast irons", Tool and Alloy Steels, Oct. 1987, pp. 369-377.
  55. T.E.Norman, A. Soloman and D.V.Doane, Modern Casting, 35(4), 1959, pp. 242-256.
  56. R. Bickensderfer, J. Tylezak and J. Dodd, Ed. K.C. Ludema, Proc. Int. Conf. on wear of materials, ASME, Newyork, 1983., pp. 471-476.
  57. R.H.T. Dixon, J. Iron Steel Inst. London, 197, 1961, pp. 40-48.

58. G.J.Cox, Foundry Trade Jr. 6, 1985, pp. 484-486.
59. P.A.Marton, R.B.Gundlach and J. Dodd, " Trans. AFS, 93, 1985, pp. 879-884.
60. D.K.Subramanyam, " Retained austenite measurements in high chromium white iron" AFS trans, . 1985, 117, pp. 763-768.
61. R.L.Miller, " Volume fraction analysis of phases in textured alloys" ASM trans. 61, 1968, pp. 592.
62. C. Kim, " X-ray method of measuring retained austenite in heat treated white cast irons", Heat Treating, 2(3), 1979, pp.43.
63. B. L Averbach and M. Cohen, Trans. AIME, 1948, 176, pp. 401-415.
64. D.F.La Count, " A production technique for measurement of retained austenite in abrasion resistant irons". AFS technical report No. 8001, presented at 84th AFS casting congress, 1980.
65. J. Durnin and K. A. Ridal, " Determination of retained austenite in steel by x-ray diffraction", Jr. of the Iron & Steel Instt., January 1968, pp. 60-67.
66. C. Czichos, " Tribology - a system approach", Verlag, 1968.
67. D.A.Moore, " Principles of Tribology", Elsevier Pub.1976.
68. Rabinowicz. E., " Friction and wear of materials", Wiley, Newyork, 1965.
69. J. D. Watson, P. J. Mutton and I.R.Sare, " Abrasive wear of white cast irons", Metals Forum, 3(1), 1980, pp. 74-88.
70. J.T.H. Pearce, " Structure and wear performance of abrasion resistant chromium white cast irons", AFS trans. 1984, 126, pp. 599-622.

71. J.T.H. Pearce " Abrasive wear behaviour of alloy cast irons". British foundrymen, 78, Sept.1985, pp. 13-23.
72. A.W.J. deGee, " Friction and wear as related to the composition, structure and properties of metals", Int. Metals Review, 1979,(2), pp. 57-67.
73. E.F. Finkin, " Adhesive wear: a general review", Mat. in engg. applications, 1, April 1979, pp. 154-161.
74. W.H.Roberts, " Some current trends in tribology in the UK and Europe", Tribology. Int. 19(6), December 1986, pp. 295-311.
75. K. H. ZumGahr, " How microstructure affects abrasive wear resistance", Metal Progress, September, 1979, pp. 46-52.
76. K. H. Zum Gahr, " Entwicklung und Einsatz verschleissfester Werkstoffe (in German)" Mat. Wiss. u. Werkstofftech.19, 1988, pp. 223-230.
77. E.V.Rozhkova, O.M.Romanov, L. Ya. Kozlov and L. M. Romanov, " The effect of the metal base on the wear resistance of chromium cast iron", Metallov.Termich. Obra. Metallov, 6, June 1986, pp. 30-32, (from Russian).
78. N. S. Poonawala, " Wear of Materials - theories and mechanisms", I.I.T. Bombay, 1981 (unpublished work).
79. F. Borik and W.G. Scholz " Gauging abrasion tests for materials used in ore and rock crushing", Part II, Jr. of Materials, 6, 1971, pp. 590-605.
80. J. Muscara and M.J.Sinnott, " Construction and evaluation of a versatile abrasive wear testing apparatus". metals Engineering Qtrly, 12, 1972, pp. 21-32.
81. F. Borik, " Rubber wheel abrasion test", SAE 700687, Soc.

- of Auto Enggrs, Newyork. 1970.
82. H. S. Avery, " Work hardening in relation to abrasion resistance" Symposium on Materials for mining industry". Climax Molybdenum Co., 1974, pp. 43-77.
  83. J. W.Boyes, " Development and use of abrasion testing at BCIRA", Iron & Steel, 42, 1969, pp. 57-63.
  84. M. A. Moore, " A review of two body abrasive wear", Wear, 27, 1974, pp. 1-17.
  85. R.B.Gundlach and J.L.Parks, Wear, 1978, 46, p. 97.
  86. M. J. Murray, J.D.Watson and P.J.Mutton, Proc. Int. Conf. on the wear of materials, Newyork, 1979, ASME, p. 257.
  87. P. L.Hurricks, Wear, 26, 1973, p. 285.
  88. I. R. Sare, " Abrasion resistance and fracture toughness of white cast irons" Metals Tech. November, 1979, pp. 412-419.
  89. E. Hornbogen, Wear, 33, 1975, p. 251.
  90. W.L.Bradley and M.N. Srinivasan, " Fracture and fracture toughness of cast irons", Int. Mat. Review, 35, (3), 1990, pp. 129-161.
  91. P. N. Crepeau, S. D. Antolovich and G. A. Calboreanu, "Modelling fracture toughness in high Cr white cast iron", AFS trans. 1986, 88, pp. 503-510.
  92. K. H. Zum Gahr and W.G. Sholz, " Fracture toughness of white cast irons", Jr. of Metals, 32, 1980, pp. 38-44.
  93. R.W. Durman, " Fracture toughness of a series of high chromium alloys", Ph.D thesis, Univ. of Aston, England, 1970.
  94. R.W.Durman, " Fractography of high chromium irons", British Foundryman, 74, 1981, pp. 45-55.

95. S. B. Biner " The effects of metallurgical variables on the mechanical properties of high Cr cast irons", Ph.D thesis. Univ. of Aston, England, 1981.
96. D.W.J. Elwell, " The determination of fracture toughness of alloyed white cast iron using the short rod/short bar specimen", Cercle d'Etudes des Metaux Meeting, France, November 1983.
97. M. G. Fontana, "Corrosion Engineering", McGraw Hill, 3rd Edn. 1988, pp. 445.
98. J.B. Andrews, R. A. Buchanan and N. A. Gordon. "Evaluation of the mechanical properties and corrosion resistance of new experimental low Cr stainless steel alloys", AFS trans., 1984, 52, pp. 17-28.
99. N.G.Thompson, " In vitro polarization evaluation of carbon-metal galvanic couples", M.S.E. Thesis, Univ. of Alabama, USA, 1977.
100. A. Koursaris, " Recent developments in cutting and forming tool materials", The South African mechanical engineer., 37, Nov.-Dec. 1987, pp. 553-563.
101. J. Gurland, " New scientific approaches to development of tool materials", Int. Materials Review, 33(3), 1988, pp. 151-166.
102. R. Srinivasan, " Development in cutting tools", Keynote lecture, Proc. of 13th AIMTDR confernce, Nov. 1988, Calcutta (India).
103. M. Chandrasekaran, " Material development and its role in advanced machining situations", Jr. of Metal Working technology, 1988, pp. 117-136.

104. R. P. Bergstorm, "Getting a grip on cutting tools" Manufacturing Engineering, January 1986, pp. 55-59.
105. A. C. Bhattacharya, "Cermets in metal cutting", Ind. Products finder, April 1989, pp. 238-239.
106. E. DowWhitney and P. N. Vaidyanathan, "Microstructural engineering of ceramic cutting tools", Ceramic bulletin, 67(6), 1988, pp. 1010-1014.
107. Y. Shimizu, M. Tobioka, N. Kitagawa and T. Namura, "Development of new 110 A and T 130 A tough cermet", Metal powder report, December 1989, pp. 827-834.
108. L. S. Kremnov, "From steel R 18 to tungstenless low alloy High speed steels", Translated from Metallov Termiche.Obra.Metallov.7 July 1986, pp. 27-30, 35-43.
109. E. A. Smolnikov, T. A. Volosova and L. I. Baranova, "Structure and properties of tungsten free high speed steels, 8M3F3S" translated from Metallov Termich. Obr. Metallov. 7, July 1981, pp. 16-20.
110. R. A. Mandrekar, A. Mandal and A. K. Chakraborty, "Development of white cast iron cutting tool", B.Tech dissertation, May 1979, IIT, Kharagpur.
111. A. Bhattacharyya, "Development of new cutting tool materials", Jr. of Instt. of Enggrs. XLB, (8), July 1968.
112. A. K. Chakraborty, "Development of WCI cutting tool Indian Foundry Journal, September 1981, pp. 9-12.
113. K. J. Babu, A. B. Chattopadhyay and A. K. Chakraborty, "Development and performance evaluation of white cast iron cutting tool" M.Tech thesis, June 1981, I.I.T., Kharagpur.
114. K. J. Rao, "Performance of white cast iron as cutting tool material" M.Tech thesis, May 1983, I.I.T., Kharagpur.

115. B. Mukherjee, A.B. Chattopadhyay and A.K.Chakraborty. " On performance of nitrogenated WCI cutting tool". M.Tech Thesis, June 1984, I.I.T., Kharagpur.
116. A. Das, A. B. Chattopadhyay and A. K. Chakraborty, "Development of an economic cutting tool material for small scale industries", M.Tech thesis. December 1985. I.I.T., Kharagpur.
117. K. Chakraborty, A.B. Chattopadhyay and A. K. Chakraborty, " Further improvement in WCI cutting tool by proper nitrogenation", M.Tech thesis. Dec. 1987, I.I.T., Kharagpur and AFS trans. 1989, 124, pp.637-644.
118. P. Dupin and J.M. Schissler, " Influence of addition of Si, Mo, V and W upon the structural evolution of the as-cast state of a high-Cr cast iron (20% Cr, 2.6% C) AFS trans. 160, 1984, pp. 355-360.
119. D. M. Stefanescu, D. Mitea and S. Craciun, " Structure of 15% Cr C.I.s alloyed with upto 5% Mn or 5% V, a dilatometric and diffractometric study", AFS I.C.M. Journal, June 1976, pp. 19-30.
120. R. W. Durman and D.W.J. Elwell, " Morphology of eutectic carbides in high Cr white irons". British Foundrymen, 78, September 1985, pp. 371-375.
121. Y. Sentarli, N. R. Comins and A. Koursaris. " Suspension casting of a high Cr white iron", British Foundrymen, 78, September 1985, pp. 459-464.
122. A.K. Patwardhan and N. C. Jain, " Modelling of the transformation behaviour of some Fe-Mn-Cr-Cu white-cast irons with martensitic and austenitic matrices". AFS trans. 03, 1988, pp. 329-338.

123. G. I. Sil'man and V. A. Teikh, "Structure and properties of cast iron with alloying elements", (translation from Russian), Metall. Termic. Obrabotka-Metallov. 11, Nov. 1969, pp. 28-31.
124. K. P. Bunin, I. E. Lev, V.M. Snagovskii and Yu. N. Taran, "Structure of Cr. white irons", Russian casting production", 1965, pp. 398-399.
125. M. E. Garber, E. V. Rozhkova and I. I. Tsypin, "Effect of C, Cr, Si and Mo on the hardenability and wear resistance of white cast irons", (Trans. from Metall. Termich. Obra. Metallov. (Russian), May 1969, pp. 11-14.
126. I.E. Kontorovich, E.V. Rozhkova, M.E.Garber and I.I.Tsypin, "The optimal concentration of C and Cr in wear resistant white cast irons" Trans. from (Russian) Metall. Termich. Obra. Metallov. 5, May, 1971, pp. 45-46.
127. J.T.H.Pearce, "The use of Transmission Electron Microscopy to study the effects of abrasive wear on the matrix structure of a high Cr cast iron", Wear, 89, 1983, pp. 333-344.
128. G. Laird II, R. R. Brown and R.L.Nielsen, "Factors affecting eutectic solidification of Cr-Ni (-Si-Mn) white cast irons", Material sci. and tech. July 1991, 7, pp. 631-642.
129. S.H.Avner, "Introduction to Physical Metallurgy", Second edn. McGraw Hill Kogakusha, 1974, pp. 356-357.
130. P.K.Wright and E M Trent, "Metallurgical appraisal of wear mechanisms and processes on high-speed steel cutting tools", Metals Tech. January 1974, pp. 13-23.

131. Li Hong, Wang Youming and C.F. Burdett, " Hot deformation behaviour and ledeburite refinement mechanisms for hypoeutectic low alloy white cast irons", Material Sc. and tech. July 1991, 7, pp. 660-664.
132. G.J.Cox, " Development of abrasion-resistant nickel containing alloy white irons of high hardness", AFS trans. 1989, 62, pp.361-371
133. L.H.S. Luong, " Influence of microcracks on machinability of metals" Metals technology, November 1980, pp. 465-470.
134. S. Katayama and M. Hashimura, " Effect of C,P and N on machined surface and cutting force" ISIJ, Int.30,6,1990,pp. 457-463.
135. N. S. Poonawala, A. B. Chattopadhyay and A.K.Chakraborty, " A metallurgical approach to the design of cutting tool materials", Proc.of 14th AIMTDR Conference. I.I.T., Bombay, 19-21 December, 1990, pp. 385-390.
136. H.T. Hall & W.J.Jackson, " Grain refinement in cast austenitic steels" Symposium of I.S.I., London, 1968 pp. 313-317.
137. D. Cuppini, G.D'Errico and G. Rutelli, " Tool wear monitoring based on cutting power measurement". Wear, Vol.139, No.2, Aug. 1990, pp. 303-311.
138. Yu Geller, " Tool steels" Mir Publishers, Moscow, 1978.
139. E.M.Trent " Metal Cutting" second edition. Butterworths, 1984.
140. B.Mills and A.H.Redford, " Machinability of Engineering Materials", Applied Science Publishers, 1983.
141. J.A.Larson, " New developments in high alloy cast steels". Proceedings of 1981 annual conference, SCRATA.
142. N.F.Piore; J.P.Colye, S.P.Udvardy, T.H.Kosel and W.A.Konnel, " Properties of high speed steels" Int. J. Mach. Tool Des. & Res. 1981, 21, 1-10.